Investigating the Role of SLC24A5 in *Xenopus laevis* Pigmentation Development

Ruth Williams

Supervisor: Dr Grant Wheeler

A thesis submitted for the degree of
Doctor of Philosophy
To the University of East Anglia
Norwich

School of Biological Sciences
University of East Anglia
Norwich

June 2011

Acknowledgements

First and foremost I would like to thank my supervisor Grant Wheeler, for giving me the opportunity to do this PhD and for support and encouragement throughout. Thank you for being approachable and positive!

Thanks also to previous Wheeler lab members, Matt Tomlinson and Jo Mulvaney for teaching me all the tricks of the trade! Thanks to Andrea Munsterberg for helpful discussions and her lab members for guidance in the lab.

Thanks to BBSRC for funding and our collaborators at Unilever for additional funds and useful discussions. Also thanks to the Schnetkamp lab for providing constructs.

To all my lab buddys thanks for enjoyable coffee breaks and some great social outings!

To my supportive family; Mum, Dad, Sally, Josh and Megan, and Greg, thank you for your encouragement and always being there, and tolerating the boring science talk! Thanks to Uncle Steve for his academic help throughout my studies and inspiring me to carry on with science.

My ‘big bro’ and beloved Nanny, I know you would be proud of me.

Contents

List of figures

Abbreviations

FGF.....	Fibroblast growth factor
25HC.....	25 hydroxycholesterol
4C.....	4 cysteine mutant
$6BH_4$.....	6 R-L-erythro 5, 6, 7, 8, tetrahydrobiopterin
ACTH.....	Adrenocortin trophic hormone
AP.....	Adapter primer
APS	Ammonium persulphate
ASIP.....	Agouti signalling protein
AT.....	A111T mutant
ATG	start site of open reading frame
ATPases.....	Adenosine triphosphatase
AUAP.....	Abridge universal amplification primer
BCIP.....	5-Bromo-4-chloro-3-indolyl phosphate
Blast.....	Basic local alignment search tool
BMB	Boehringer Mannheim blocking agent
BMP.....	Bone morphogenic protein
Bp.....	Base pair
BSA.....	Bovine serum albumin
cAMP.....	Cycle adenomonophosphate
cDNA.....	Complementary deoxyribonucleic acid
CH.....	Loop deletion mutant
Chorulon.....	Human Chorionic Gonadotrophin
CIP.....	Calf intestinal phosphatise
CMO.....	Control morpholino
CREB.....	cAMP response element binding protein
cRNA.....	Synthetic capped RNA
DCT.....	Dopachrome tautomerase
DEPC.....	Diethylpyrocarbonate
dH_2O..........	Distilled water
DIG.....	Digoxigenin

DMZ..... Dorsal marginal zone

DN..... D383N mutant

dNTP..... Deoxynucleotide triphosphate

DTT ..... Dithiothreitol

ECM..... Extracellular matrix

Edn..... Endothelin

EdnrB..... Endothelin receptor B

EDTA ..... Ethylenediamine tetraacetate

ER..... Endoplasmic reticulum

ERK..... Extracellular signal activated kinase

ET1..... Endothelin 1

EtOH..... Ethanol

g..... Centrifugal force

GATA ..... GATA-binding transcription factor

GFP..... Green fluorescent protein

HA..... hemagglutinin

HCG..... Human chorionic gonadotropin

HCl…… Hydrogen chloride

Hpf..... hours post fertilisation

Hrs..... Hours

Kb..... Kilobase

KCl..... Potassium chloride

KDa..... Kilo Dalton

KGF..... Keratinocyte growth factor

LB..... Luria broth

L-DOPA..... L-3, 4, dihydroxyphenalanine

LiCl..... Lithium chloride

MAB..... Maleic acid buffer

MAPK..... Mitogen activated protein kinase

MART1..... Melanosome antigen recognised by T cells

MATP..... Membrane associated transport protein

MC1R..... Melanocortin 1 receptor

MEK..... MAP kinase kinase

MEMFA.....	Fix (MEM salts+ formaldehyde)
MeOH	Methanol
$MgCl_2$.....	Magnesium chloride
$MgSO_4$	Magnesium sulphate
Mins.....	Minutes
Mitf.....	Microphthalmia associated transcription factor
MMR.....	Marc´s Modified Ringer
MNT1.....	Constitutatively pigmented melanoma cells
MO.....	Morpholino
mRNA.....	Messenger RNA
NaCl.....	Sodium chloride
NBT.....	nitroblue tetrazolium
NCBI.....	National Centre for Biotechnology Ingomation
NCC.....	Neural crest cells
NCKX.....	Potassium dependent sodium calcium exchanger
NCKX5	Chimera constructs of NCKX5 with cytosolic loop of
cyto2.....	NCXK2
NCKX5	Chimera constructs of NCKX5 with N-terminal region
ntl2.....	of NCXK2
NCX.....	Sodium calcium exchanger
Ng.....	Nanograms
NGF.....	Neuron growth factor
NHM.....	Normal human melanocytes
NI.....	Non injected
nM.....	Nanomolar
nsSNP.....	Non synonymous single nucleotide polymorphism
O/N.....	Overnight
OA.....	Ocular albinism
OCA.....	Oculocutaneous albinism
OD.....	Optical density
P.....	Probability
PAH.....	L-phenylalanine hydroxylase
PAR.....	Protease activated receptors

PBS.....	Phosphate buffered saline
PBST.....	Phosphate buffered saline with Tween 20
PC.....	Prohormone convertase
PCR	Polymerase Chain reaction
pH.....	Concentration of hydrogen ions expressed on the pH scale
PKA.....	Protein kinase A
PMSG.....	Pregnant mare Serum Gonadotrophin
POMC.....	Proopiomelanocortin
PTEN.....	Phosphoinositide phosphatase
PTw	PBS plus Tween-20 (0.01%)
RACE.....	Rapid amplification of cDNA ends
RER.....	Rough endoplasmic reticulum
RNA.....	Ribonucleic Acid
RNAi.....	Ribonucleic Acid interference
RNase.....	Ribonuclease
RPE……..	Retinal pigment epithelial layer
Rpm.....	Revolutions per minute
RT.....	Room temperature
RT PCR.....	Reverse transcriptase Polymerase Chain Reaction
SCF.....	Stem cell factor (Kit)
SDM.....	Site directed mutagenesis
SDS.....	Sodium dodecyl sulphate
SDS PAGE.....	Polyacridamyde Gel electrophoresis- Sodium Dodecyl sulphate
Sec.....	Seconds
SLC24A5.....	Solute carrier family 24 member A5
SP.....	Splice (morpholino)
St……..	Stage
TAE.....	Tris-Acetate-EDTA
TAP.....	Tobacco acid pyrophosphatase
TG……..	Tris-glycine buffer
TGN.....	Trans Golgi network

THI..... Tyrosine hyrdoxylase isoform 1

Tm…… Temperature

TMD..... Transmembrane domain

Tyr..... Tyrosinase

Tyrp1..... Tyrosinase related protein 1

Tyrp2..... Tyrosinase related protein 2 (DCT)

UV…….. Ultraviolet

UVR…… Ultraviolet radiation

V-ATPase..... Vesicular or vacuolar ATPase

VMZ ..... Ventral marginal zone

W/V ..... Weight to volume

WE..... Whole embryo

WISH..... Whole mount *in situ* hybridisation

WT..... Wild type

XL..... *Xenopus laevis*

XT..... *Xenopus tropicalis*

αMSH..... Alpha melanocyte stimulating hormone

Abstract

SLC24A5 has previously been identified as the gene responsible for the hypopigmented golden phenotype seen in zebrafish. A variant allele of human SLC24A5 correlates with lighter skin pigmentation associated with European populations. SLC24A5 encodes a potassium-dependent sodium calcium exchanger of the NCKX family, it is found on an intracellular membrane in pigment cells and partially co-localises with the trans-Golgi network. siRNA knockdown of SLC24A5 in human and murine melanocytes resulted in a significant reduction of pigment production. To further investigate the role of SLC24A5 in pigmentation, we are using *Xenopus laevis* embryos as an *in vivo* model system. We have cloned full length *Xenopus laevis* SLC24A5 and shown it to be expressed from stage 25 in melanophores (pigment cells) and the retinal pigmented epithelium (RPE). To do loss of function studies we have knocked down the SLC24A5 protein using morpholinos (antisense oligonucleotides). We have shown that knockdown of SLC24A5 causes a reduction of pigmentation in the trunk and RPE of stage 38 (4 day old) embryos. The morpholino knockdown phenotype can be rescued by wild type human NCKX5 and some mutated constructs. This suggests that it is not the ion transport function of NCKX5 that is required for its role in pigmentation.

Chapter One:

Introduction

Pigmentation is the natural colouration of animal and plant tissue, it provides camouflage and protection, and offers a means of communication. Pigmentation also has a significant cultural and cosmetic impact. Pigment cells, melanocytes in mammals and birds, melanophores in fish and amphibians, are responsible for producing melanin, the pigment that provides the characteristic pigmentation pattern observed on an animal's skin, hair or fur and eyes. A wide variety of pigment colouring and pattern phenotypes are observed among humans, where the skin, hair and eyes are affected. This variation is a result of numerous genes coordinating their activities in a complex fashion. Pigment phenotypes are hereditary but can be influenced by mutations and environmental factors, namely ultra violet radiation (UVR). Melanin pigmentation is also the main form of protection against UV induced DNA and cellular damage (Brenner and Hearing, 2008). Many pathologies are associated with defects in pigmentation pathways including; vitiligo, albinism and melanoma. As such, a large volume of research has been conducted over the years, revealing in excess of 120 genes involved in pigmentation, many of which have not been fully characterised, including SLC24A5. Melanoma is a particularly aggressive cancer, incidence of which has increased more than any other cancer in last 10 years. Once diagnosed with malignant melanoma less than 10% of patients survive for more than 5 years (Kuphal and Bosserhoff, 2009). With this in mind it is important to further understand the mechanisms underlying pigment cell function and behaviour.

SLC24A5 was originally identified as the gene responsible for a hypopigmented 'golden' phenotype observed in zebrafish. Its role in human pigmentation has been highlighted by the presence of a non synonymous single nucleotide polymorphism (nsSNP) which correlates with lighter skin colour at a population level (Lamason et al., 2005). Studies so far have shown SLC24A5 to be partially co-localised to the trans Golgi network and knockdown results in a decrease in pigmentation (Ginger et al., 2008). SLC24A5 has been shown to encode NCKX5, a potassium dependent sodium calcium exchanger. However, the role for such a protein in melanogenesis is not clear. The work here presents an in vivo study of SLC24A5 and aims to further elucidate the function of this gene in pigmentation.

X.laevis (*Xenopus laevis*) is an ideal model organism for developmental biology due to the ease at which embryos can be acquired and manipulated, and their fast development time. At stage 38 (Nieuwkoop and Faber, 1994), 53 hours post fertilisation (hpf), *X.laevis* tadpoles have a distinct pigmentation pattern, thus perturbations in pigmentation are easily detected by microscopic analyses. As a derivative of the neural crest population, pigment cells also provide a good system in which to study cellular migration and differentiation.

Mice have also proved to be an invaluable tool for pigment research, thanks to the identification of many different coat colour strains. Many mutant lines are available and also many pigment genes have a knock out mouse (Steingrimsson et al., 2006). It is also relatively easy to conduct human studies, due to the ease at which phenotypes can be determined, in a non invasive manner. Samples are easy to take of healthy or diseased skin. Pigmentation is also studied at an evolutionary level as it holds many clues to our development over long time scales and can also indicate dietary habits, environment etc (Jablonski and Chaplin, 2000). Thus pigmentation is an important area to study for its physiological role and as an evolutionary trait and this can be accomplished by the combination of techniques using many different model organisms.

1.1 Pigmentation

Pigmentation results from the production of melanin. This takes place in melanosomes found in melanocytes. The amount, type and distribution of melanin determines the pigmentation phenotype. As well as providing the obvious pigmentation pattern for an organism, melanin also serves to protect DNA from UV induced damage, and acts as a free radical sponge to protect the cell from oxidative damage (Parra, 2007).

Melanocytes are found in the basal epidermal layer of skin, they form epidermal melanin unit's by contacting up to 30 surrounding keratinocytes via their long dendritic processes (figure 1), to which they pass packages of melanin. Melanocytes are also found at significant levels in hair follicles and the retinal pigmented epithelium (RPE), iris and choroid structures of the eye and at lower levels in structures of the brain including, the medulla, adrenal gland and brainstem. Melanin is derived from tyrosine and is present in two main forms, eumelanin and pheomelanin (Le Pape et al., 2008). Melanin is produced in melanocytes which contain specialised organelles – melanosomes which synthesize melanin. Melanosomes are translocated from melanocytes to surrounding keratinocytes where they accumulate around the nucleus, as depicted in figure 1.

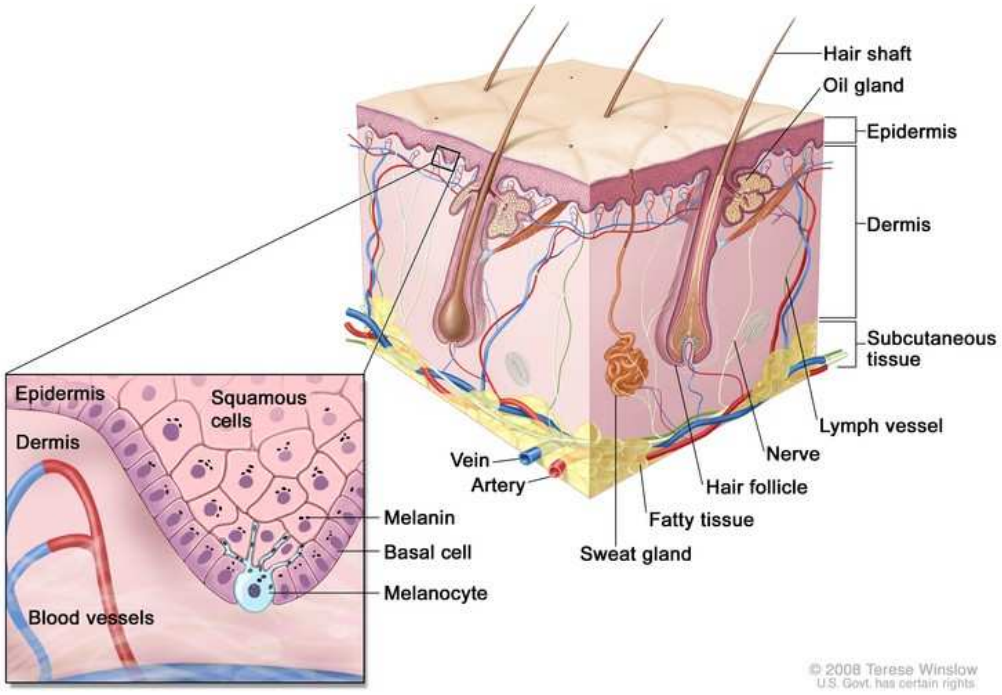

Figure 1
A cartoon cross section of human skin.
Melanocytes are found in the epidermis of the skin. Melanin producing melanosomes are synthesized in melanocytes and transported to neighbouring keratinocytes (squamous cells), where they localise to the supranuclear region.

Melanocytes arise from the neural crest and migrate to their final positions around the embryo during embryogenesis (Silver et al., 2006). During their migration they encounter a number of factors which leads them to their terminal differentiation as a pigment cell (Thomas and Erickson, 2008). Once migrated and differentiated, melanocytes respond to UV light and other cues to interact with the surrounding keratinocytes to provide a photoprotective layer (Park et al., 2009).

1.2 Melanocytes are derived from the neural crest

The protective pigment, melanin is synthesised in melanocytes. Melanocytes of the epidermis are derived from the neural crest and migrate to the epidermis during embryogenesis (Goding, 2007). Melanocytes of the RPE are not derived from the neural crest (Thomas and Erickson, 2008).

1.2.1 The neural crest

The neural crest is a transient population of pluripotent cells unique to vertebrates. Originating from the border between the dorsal neural tube and overlying ectoderm, neural crest cells (NCC) appear following closure of the neural tube during neurulation. Induction of the neural crest population requires the actions of several transcription factors including; Msx1, Pax3, FoxD3, Zic1, Snail2, AP-2 and Sox10 (Steventon et al., 2005). Expression of these factors is in turn regulated by Wnt and BMP signalling (Abu-Elmagd et al., 2006; Thomas and Erickson, 2008).

NCC initially undergo an epithelial to mesenchymal transition to delaminate from the neural tube, after which are discernible as discrete cells. The NCC then migrate along defined paths to various areas of the embryo, differentiating as they go. NCC give rise to a number of different cell types including ectodermal cells such as; neurons and glia of the peripheral nervous system, endocrine cells specifically those of the adrenal medulla, and melanocytes. NCC are also precursors to mesodermal tissues including; craniofacial bones, cartilage and connective tissue, and some cardiac tissues such as the septum and semilunar valves (figure 2) (Le Douarin and Dupin, 2003), (Jessell et al 2007).

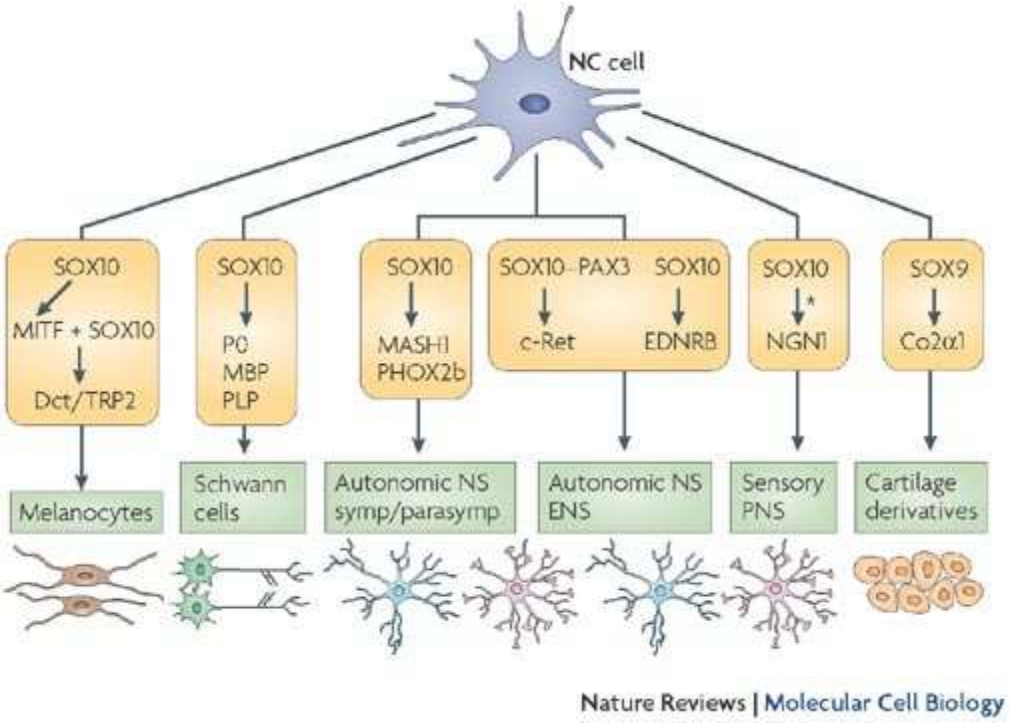

Figure 2
Neural crest lineages. This figure shows a simplistic view of signalling processes during neural crest specification and differentiation, and the cell types which arise from the neural crest.

Neural crest cells migrate extensively around the embryo, during which they differentiate into specialised cell types.

1.2.2 Neural crest migration

The fate of NCC is determined by their original position along the anterior-posterior axis of the neural tube and the migration pathway they undertake. NCC of the mid/hind brain region will give rise to cranial structures and neurons, whereas NCC of the trunk region will give rise to adrenal cell, peripheral ganglia and melanocytes (Baker et al., 1997). Neural crest cells are transient in nature and migrate from their origin across the embryo via two distinct pathways, dorso-laterally or ventrally (figure 3).

Before migration, NCC have to undergo an epithelial to mesenchymal transition to allow them to migrate away from their origin. This process requires expression of transcription factors of the Slug/Snail family, which repress E-cadherin and thus allow the cells to move. This expression is lost when the cells complete their migration (Cano et al., 2000). Slug expression is positively regulated by Sox10 (Uong and Zon, 2010).

Pigment cells arise from dorso-laterally migrating NCC while ventrally migrating NCC become cells of the peripheral and enteric nervous system and other tissues including bone, tendon, connective and adipose (Erickson, 1993; Silver et al., 2006; Thomas and Erickson, 2008). As depicted in figure 3, dorso-laterally migrating cells move over the somite, or more specifically the dermatome, close to the overlying ectoderm, they then invade the ectoderm and complete the differentiation process to become melanocytes of the epidermis. Ventrally migrating cells move between the somite and neural tube. The ventral migration pathway is initiated about a day before the dorso-lateral path. During this time the later 'born' NCC, including melanoblasts (prospective melanocytes) accumulate in a migration staging area (Wehrle-Haller and Weston, 1997), (figure 3), before they embark on their migration route through the mesenchyme to the epidermis (Dupin and Le Douarin, 2003). In the migration staging area melanoblasts express the receptor tyrosine kinase Kit, and require its ligand Kitl for survival and differentiation, Kitl is expressed early along the dorso-lateral pathway by dermatome cells (Wehrle-Haller and Weston, 1995) (Wehrle-Haller et al., 2001) it is possible that Kitl acts as a cue for the cells to migrate (Silver et al., 2006)

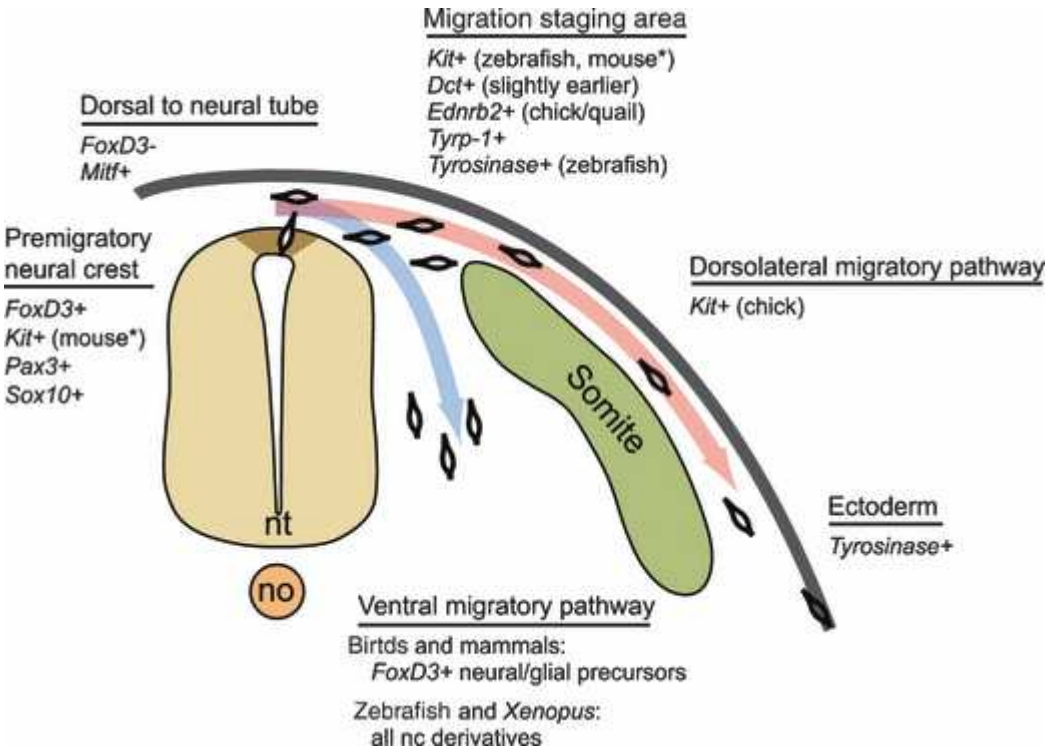

Figure 3
Neural crest migration pathways and gene expression.
Following delamination from the dorsal neural tube, NCC migrate ventrally (blue) or dorsolaterally (pink). Cells destined to become melanocytes take the dorsolateral route after a short pause in the migration staging area, (taken from Thomas and Erickson 2008).

Endothelins and their respective receptors have also been shown to be important for melanoblast migration (Uong and Zon, 2010). This has been demonstrated in Endothelin receptor B (EdnrB) and endothelin 3 (Edn3) mutant mice, which have a disrupted pigmentation pattern (Dupin and Le Douarin, 2003). EndrB is expressed as the cells reach the migrating staging area, and is not required before then, indicating that endothelin signalling is not important to neural crest induction (Saldana-Caboverde and Kos, 2010). Furthermore, in conjunction with Kit and Kitl, Edn3 and EdnrB have been shown to be crucial for melanocyte differentiation and proliferation. Edn3 and Kitl have a symbiotic relationship whereby without Edn3/EdnrB signalling, melanocytes cannot fully proliferate, yet Edn3/EndrB signalling is dependent on previous Kit/Kitl stimulation (Ono et al., 1998).

Like any other cell migratory behaviour, neural crest migration is dependent on interactions between the cells and the extra cellular matrix (ECM). Melanoblasts express a profile of integrins which respond to components of the ECM. These interactions allow the migrating melanoblasts to interpret their surrounding environment and respond accordingly, this is crucial for melanocyte survival and homeostasis (Pinon and Wehrle-Haller, 2011). Developing and mature melanocytes also express a repertoire of cadherins which are important to cell migration, as well as induction and differentiation. In particular N-cadherin, which is expressed in the neural plate, is involved in epithelial to mesenchymal transition and subsequent migration. (Taneyhill, 2008). N-cadherin is negatively regulated by BMP signalling (Burstyn-Cohen et al., 2004). Once migrated to the epidermis melanocytes continue to express N-cadherin, here it is thought to facilitate contacts with the surrounding keratinocytes and fibroblasts (Derycke and Bracke, 2004). Cadherin 6B is expressed in the dorsal most region of the neural folds and remains in this region following neural tube closure. This differential expression of these cadherins is thought to assist separation of different cells at this early stage of neural crest development (Taneyhill, 2008).

1.2.3 Melanocyte specification

Melanocytes are specified prior to migration, however melanin is not synthesised until after migration (Kumasaka et al., 2003). As NCC migrate dorso-laterally some of them gradually become determined to a melanocytic fate. Melanocyte precursor cells (melanoblasts) are specified by a combination of Wnt and BMP signalling, and other intrinsic and extrinsic factors including Kit and Kitl interactions (figure 3) (Jessell et al 2007) (Kanzler et al., 2000).

The canonical Wnt signalling pathway is initiated by the binding of an extracellular Wnt molecule to a Frizzled receptor which results in the cytoplasmic accumulation of β-catenin. Some β-catenin translocates to the nucleus where it interacts with Tcf/Lef sites in Wnt target genes and thus triggers transcription. The master melanocyte transcription factor, microphthalmia-associated transcription factor (Mitf) contains such a Tcf/Lef site and is thus thought to be a target of Wnt signalling (Yasumoto et al., 2002). This is supported by some experimental observations. In Xenopus and zebrafish,

over expression of canconical Wnt signalling has been shown to increase expression of neural crest markers at the expense of neural markers (Le Douarin and Dupin, 2003), conversely inhibition of Wnt signalling down regulates neural crest markers. Double knockout of Wnt1 and Wnt3a in mice results in a decrease of melanocyte markers (Ikeya et al., 1997; Silver et al., 2006). As well as promoting a melanocytic fate, Wnt signalling is also proposed to inhibit a neurogenic fate, as increasing the amount of β-catenin is inhibitory to neurogenesis. Thus Wnt signalling can be considered as the switch between neural and melanogenic specification (Dorsky et al., 1998).

Once initially activated, by Wnt signalling, Mitf interacts with Lef1 to transactivate its own promoter (Saito et al., 2002; Uong and Zon, 2010). Mitf acts as a master switch to drive NCC to a melanocytic fate. Mitf positive cells are first seen as developing melanoblasts just after migration from the neural tube, and before they enter the dorso-lateral pathway. This expression timing is coincident with lineage specification. Mitf is essential for specification and survival of melanoblasts, this is achieved by up regulation of Tbx2 and Bcl2, which are important for cell identity, growth and survival respectively. Mitf is a basic-helix-loop-helix leucine zipper transcription factor, it is the earliest marker of the melanocytic lineage. Mitf is responsible for activating expression of various key pigmentation enzymes. Mutations in Mitf cause various pigmentation defects across many species, indicating its conservation. The human pigment and hearing condition, Waardenburg syndrome 2A is caused by mutations in Mitf. In the absence of Mitfa, zebrafish do not develop normal pigmentation and also suffer loss of hearing, however RPE development and function appear normal, unlike similar mammalian mutants. It is thought that a secondary Mitf gene, Mitfb is able to compensate in the fish (Lister et al., 1999). Mitf is also dynamically involved in the progression of melanoma (Hoek, 2010). Naturally Mitf is not solely regulated by Wnt signalling; Sox10 and Pax3 are also involved. These proteins can work individually or together to activate Mitf expression. Mutations in Sox10 and Pax3 can also lead to defects in pigmentation as seen in Waardenburg syndrome (Bondurand et al., 2000; Saito et al., 2002). Sox10 and Pax3 are expressed in the dorsal neural tube before neural crest formation and knockout studies suggest they have an important role in neural crest differentiation. Sox10 and Pax3 are thought to activate Mitf expression, by targeting the Mitf promoter, but Pax3 has another interesting role.

Pax3 also binds to the promoter region of DCT (dopachrome tautomerase), a key pigment gene, and thus is a competitor for Mitf binding to the same site. In this way Pax3 is repressive to the expression of DCT. Such repression is alleviated by Wnt signalling, where β-catenin removes Pax3, and indeed the ubiquitous Wnt repressor groucho, allowing the accumulated Mitf to activate DCT expression (Lang et al., 2005). DCT expression cannot be activated by Mitf alone, Sox10 is required here as a transactivator (Passeron et al., 2007). In conjunction with Sox10 and Pax3, Mitf is responsible for conferring a melanocytic fate.

BMP signalling has been suggested to play an inhibitory role in melanocyte formation. When BMP4 or BMP2 plus FGF2 are added to chick neural crest cultures melanocyte numbers are reduced, whereas neurogenic neural crest derivatives are increased (Silver et al., 2006). FoxD3 is expressed in early NCC, several studies indicate that FoxD3 is repressive to melanogenesis. FoxD3 is a transcriptional repressor and targets Mitf (Thomas and Erickson, 2008).

These and other genes compile the genetic profile of a specified melanocyte, their expression and function often continues throughout differentiation (Thomas and Erickson, 2008).

1.2.4 Melanocyte differentiation

Expression and regulation of many of the genes discussed above continues after specification, for example Mitf expression is continued and this activates expression of other key genes for pigment cell function, thus defining the melanocyte lineage. Additional genes are also expressed to activate other genetic pathways involved in differentiation and function of the melanocytes, for example MC1R, which is an important receptor for endogenous signals (discussed later 1.3.5). It is also thought that post translational mechanisms are required to promote specificity and maintain the differentiated state. Differentiated melanocytes are characterised by the presence of melanin (visibly dark), melanosome transport to surrounding keratinocytes and dendritic morphology.

Each of the defining characteristics of the melanocyte requires the expression, function and regulation of another set of genes, many of which are activated by Mitf. The melanin synthesising enzymes; tyrosinase (Tyr), tyrosinase related protein 1 (Tyrp1) and tyrosinase related protein 2 (Tryp2, also known as dopachrome tautomerase, DCT) are expressed early in differentiation by the actions of Mitf. These enzymes interact to regulate each other's activities (Kobayashi and Hearing, 2007). In order to achieve pigmentation, the melanin containing organelles, melanosomes must be transported out of the melanocyte to surrounding keratinocytes. Several cytoskeletal related proteins are important for this process; Rab27a, melanophilin and myosinVa. Mutations in any of these leads to lighter pigmentation phenotypes in mice (Hammer and Wu, 2007). The dendritic nature of melanocytes is crucial to its role in pigmentation. Once differentiated, melanocytes form many dendritic processes to interact with multiple keratinocytes. Adhesion proteins such as CCN3 (Cooper and Raible, 2009) and N-cadherin (Derycke and Bracke, 2004) are vital for this process.

Another important gene for melanoblast differentiation is Kit and its ligand Kitl or SCF (stem cell factor, also called steel). Kit activation leads to phosphorylation of Mitf via the MAPK pathway, and subsequently an increase in Mitf activity and therefore an increase in expression of melanogenic genes (Thomas and Erickson 2008). As a target of Mitf, anti apoptotic Bcl2 expression is increased indirectly by Kit activation, this promotes melanocyte survival. Mutations in Kit or Kitl loci (*w* and *sl*, respectively) result in pigmentation disorders, as demonstrated in the *white dominant spotting (w)* and *steel (sl*) mutant mice. These mutations are homozygous lethal, but heterozygotes show abnormal pigmentation, as well as hematopoietic and germ cell defects (Williams et al., 1992).

Wnt signalling continues to play a role in melanocyte differentiation (Dunn et al., 2000). As described earlier, Wnt signalling is crucial to remove Pax3 from the DCT promoter site, allowing Mitf to access this region and activate DCT transcription and thus keep the drive to differentiation going (Cooper and Raible, 2009). Sox10 has also been shown to be a vital transactivator of DCT (Potterf et al., 2001). Mitf has also been shown to interact directly with β-catenin and as such can tweak the Wnt signalling target towards melanogenic genes (Schepsky et al., 2006) .

Factors secreted from surrounding keratinocytes also play a role in melanocyte differentiation, as well as proliferation and dendrite formation. Melanocyte stimulating hormone (αMSH) , adrenocortin trophic hormone (ACTH), neuron growth factor (NGF), endothelin-1, bFGF and Kitl are just some of the factors produced in and secreted from keratinocytes (Hirobe, 2005).

Once differentiated, melanocytes are maintained by the signalling pathways described above, as well as extrinsic environmental signals. For example, isolated chick melanocytes have been shown to respond to external endothelin 3, which binds the endothelin B2 receptor causing proliferation of the melanocytes (Lahav et al., 1998). In mice it has been shown that surrounding epithelial cells can also alter the behaviour of melanocytes (Weiner et al., 2007). The melanocytes also have to be renewed from time to time. Studies in the hair follicles, of humans and mice, have shown there to be a population of melanocyte stem cells in the bulge region of the follicle (discussed further in section 1.5). These cells have the potential to differentiate into mature melanocytes in the presence of appropriate transcription factors such as Pax3, Sox10 and Mitf (Nishimura et al., 2005). Bcl2 activity also plays a role here (McGill et al., 2002).

Once specified, differentiated and migrated to the appropriate location melanocytes can start to produce melanin in order to fulfil their pigmentary and photoprotective role.

1.3 Melanogenesis

The process of melanogenesis begins with the progressive synthesis of melanosomes, within the melanocyte, which then produce melanin. Mature melanin rich melanosomes are then moved out of the melanocyte into neighbouring keratinocytes.

1.3.1 Melanosomes

Melanin is synthesized in specialised organelles termed melanosomes. Melanosomes are membrane bound lysosome-like organelles and are made

solely within melanocytes following a four stage biosynthetic programme (Hearing, 2005), summarised in figure 4 and 5. Melanosomes are tailored to produce either eumelanin or pheomelanin. Eumelanosomes tend to be larger and ellipsoidal in shape, whereas pheomelanosomes are small and spherical (Hirobe and Abe, 2006; Hirobe et al., 2006).

Broadly speaking melanosome biogenesis can be divided into 4 stages (Sturm, 2006), which are described below.

Melanosome synthesis starts with the budding of empty vacuoles from the endoplasmic reticulum (Scherer and Kumar, 2010). These stage I melanosomes have a round morphology and contain scaffolding proteins such as Pmel17, which are involved in creating a proteinaceous fibrillar matrix structure in the melanosome (Schiaffino, 2010). Mutations in Pmel17 (also known as silver and gp100) lead to defects in pigmentation, due to the loss of the fibrillar structure within melanosomes (Theos et al., 2006). Pmel17 is synthesized within the melanocyte and following processing in the trans-Golgi network is transported into melanosomes (Leonhardt et al., 2010). During transportation into the melanosome, Pmel17 is cleaved by a proprotein convertase, into a large N terminal fragment and a smaller C terminal fragment, which form the fibrillar matrix (Raposo and Marks, 2007). This cleavage has been shown to be vital for Pmel17's role in fibrillogenesis (Berson et al., 2003). Expression, stability, processing and trafficking of Pmel17 is highly dependent on another melanogenic protein – MART1 (melanoma antigen recognised by T cells) (Hoashi et al., 2005).

MART1 is a type III transmembrane protein and is expressed in the endoplasmic reticulum (ER), trans-Golgi network (TGN) and melanosomes (De Maziere et al., 2002).

The importance of the fibrillar network becomes clear as the melanosomes progress to stage II. During this process the fibrillar network becomes visible and these organelles elongate (figures 4 and 5). The fibrillar scaffold is also important for melanin depositition. At stage II, the first melanogenic enzyme, tyrosinase (TYR) is expressed, closely followed by tyrosinase related protein 1 (TYRP1) and DCT, also known as tyrosinase related protein 2 (Chi et al., 2006). These proteins catalyse the synthesis of melanin, which is deposited on the matrix structure making the melanosome visibly darker (figures 4 and 5), leading to the next stage of melanosome maturation. By the final stage of melanosome

biogenesis the matrix is so densely packed with melanin it is indistinguishable and the melanosome is very dark (figures 4 and 5). At this final stage the melanosomes are considered mature, and are transported out of the melanocyte to the surrounding keratinocytes, here they cluster around the nucleus to the protect the DNA, the pigmented keratinocytes then in turn protect the underlying melanocytes, as shown in figure 1 (Aspengren et al., 2006).

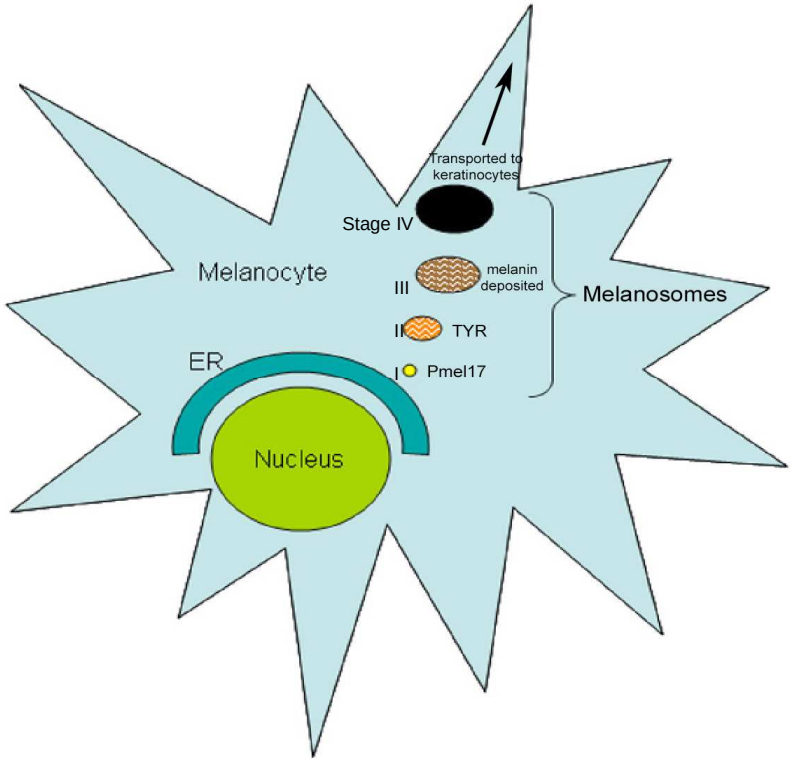

Figure 4
Schematic representation of melanosome formation within the melanocyte.
The small round early melanosomes bud off the ER, initially as endosomes, but develop into melanosomes. Pmel17 forms a scaffold structure (stage I). Tyrosinase and related proteins synthesise melanin and deposit it on the scaffold structure (stage II). Melanin synthesis and deposition continues (stage III). Mature, melanin dense, stage IV melanosomes are transported to keratinocytes.

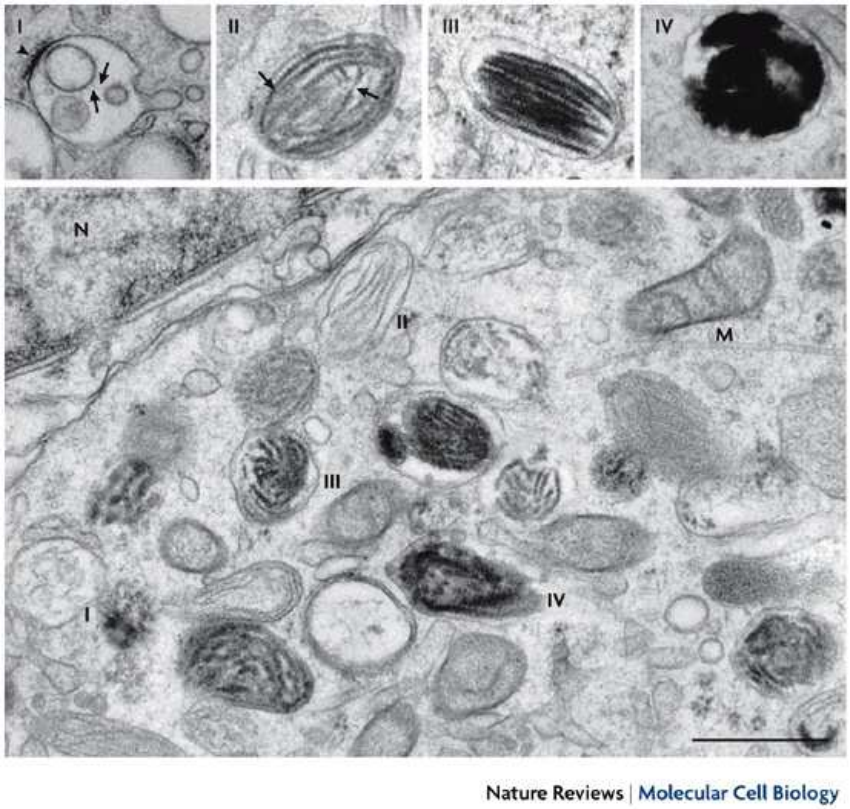

Figure 5
Transmission electron micrograph (TEM) of developing melanosomes.
The top panels show the different stages of melanosome synthesis. Note stage I melansomes round shape and intralumenal vesicles. Stage II melanosomes are clearly elongated and show the developing fibrillar scaffold. In stage III melanosomes melanin can be seen. Stage IV melanosomes are dense with melanin, such that the fibrillar structure is no longer distinguishable (Raposo and Marks, 2007).

1.3.2 Melanosome motility

Upon maturation to stage IV, melanin rich melansomes are transported from the perinuclear region to the cell periphery and along the dendrites of the melanosome to be transferred to surrounding keratinocytes. This is accomplished by a combination of microtubule and actin filament activity. Mature melanosomes interact with microtubules via kinesin or dynein molecules which move the melanosomes in an anterograde/reterograde direction respectively (figure 6) (Byers et al., 2000; Hara et al., 2000). Kinesin and dynein are motor proteins which use ATP to 'walk' along the microtubules with their cargo (Gennerich and Vale, 2009). They are comprised of a globular domain

which attaches to the microtubules by two heavy chain subunits, and several light chains which attach to the melanosome (Hara et al., 2000). Kinesin molecules are responsible for moving the melanosome from the perinuclear area to the cell periphery where the melanosome is taken on by the actin filaments (Barral and Seabra, 2004). Actin filaments are particularly important for dispersal of melanosomes. Melanosomes engage with actin filaments via a complex of proteins; Rab27a, melanophilin and myosinVa. Mutations in these proteins lead to various forms of Griscelli syndrome in humans (characterised by perinuclear accumulation of melanosomes), and have also been characterised by mouse mutants. Ashen, leaden and dilute are mouse coat colour phenotypes associated with mutations in Rab27a, melanophilin and myosinVa respectively (Wilson et al., 2000). In these mutants melanosomes are seen to cluster around the melanocyte nucleus, this is due to the imbalance of microtubule/actin filaments and an overriding dynein activity versus kinesin activity (Barral and Seabra, 2004). Rab27a provides the direct linkage between melanosomes and the complex, and is independent of melanophilin and myosinVa (Hume et al., 2001). Melanophilin is recruited to the complex by Rab27a-GTP, and binds to Rab27a by its N terminal domain and to actin via its C terminus. Interaction between melanophilin and myosinVa is via a coiled coil domain (Strom et al., 2002). MyosinVa colocalises with actin and is thought to be crucial for capturing the melansome at the cell periphery (Barral and Seabra, 2004). The process of melanosome movement around the melanocyte is depicted in figure 6.

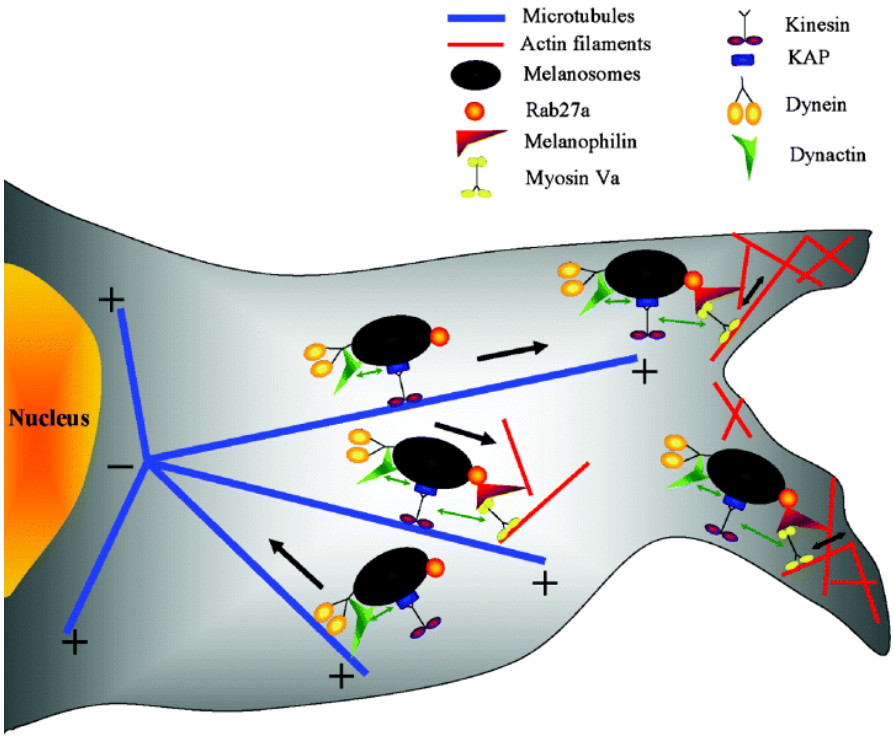

Figure 6
Melanosome movement from the perinuclear region to the cell periphery. Schematic representation of the components involved in translocating melanosomes. Microtubules govern melanosome movement to and from the nuclear region towards the cell periphery. At the cell periphery actin filaments take on the melanosomes in preparation for transfer to surrounding keratinocytes (Barral and Seabra, 2004).

1.3.3 Melanosome transport to keratinocytes

The process by which melanin is transferred from melansomes to keratinocytes is not fully understood, despite many years of research in this area (Yamaguchi and Hearing, 2009). Several mechanisms have been suggested based on experimental evidence, these include; exocytosis/phagocytosis, membrane fusion and cytophagocytosis (Park et al., 2009). Exocytosis is a highly regulated process, involved in many cellular situations. Electron microscopy analysis shows the melanosome membrane fuses to the melanocyte membrane and consequently unbound melanin is released into the intracellular space, this 'naked' melanin is then phagocytosed by keratinocytes (Yamamoto and Bhawan, 1994). This process is likely regulated by SNARES and Rab-GTPases

expressed on melanocytes. Keratinocytes take up the melanin via clathrin coated pits. Once in the keratinocyte melanin can be seen as aggregates of small granules of individual larger granules (Van Den Bossche et al., 2006). Direct plasma membrane fusion between melanocytes and keratinocytes has also been observed by electron microscopy. This forms a tunnel for melanosomes to move through (Scott et al., 2002). Electron microscopy has also provided evidence for keratinocytes engulfing the dendritic tips of melanocytes and taking them up by cytophagocytosis (Park et al., 2009). During this process the dendrite tip of the melanocyte contacts the keratinocyte which stimulates membrane ruffling and subsequent engulfment of the dendrite tip. Which is then pinched off and invaginates into the keratinocytes as a phagolysosome, the contents of which are dispersed following catabolises of the lysosome type structure (Van Den Bossche et al., 2006). This phenomenon is also observed by time lapse video microscopy. However, all the experimental data for this type of melanin transfer could be considered somewhat dated (Klaus, 1969; Mottaz and Zelickson, 1967) and as such should be examined with more advanced techniques to ensure accurate interpretation. Another proposed method by which melanin reaches the keratinocytes employs membrane vesicles. Here melanosomes are enclosed in membrane bound vesicles which are secreted from the melanocytes and taken up by keratinocytes, or fibroblasts (Aspengren et al., 2006). Despite the evidence available, so far none of these methods of melanin transfer have been conclusively accepted within the field. Perhaps all these methods occur in response to different stimuli or environmental cues (Virador et al., 2002).

One component that has been shown to be involved in all proposed methods of melanin transfer is PAR2. This is a G protein coupled receptor, expressed in keratinocytes and not melanocytes. PAR2 comes from a family of PAR proteins (1-4), these are protease activated receptors. They are activated by serine proteases, in an autocrine fashion. The serine protease cleaves the extracellular domain of the PAR2 receptor, the resulting amino terminus acts as a bound ligand to the receptor. PAR2 activity can also be triggered by UV. Activated PAR2 has been shown to increase phagocytosis. (Seiberg, 2001; Van Den Bossche et al., 2006). PAR2 functions via Rho-GTP which is involved in cytoskeletal remodelling during phagocytosis (Scott et al., 2003). As PAR2 is involved in all melanin transfer mechanisms it is assumed that phagocytosis is a crucial element in this process. Moreover, loss of function studies indicate

possible redundancy of PAR2 function, this is thought to come from keratinocyte growth factor (KGF) and keratinocyte growth factor receptor (KGFR) signalling (Cardinali et al., 2005).

1.3.4 Melanin synthesis

The pigment melanin is derived from the amino acid tyrosine and is found in two forms. Eumelanin is the most prevalent form; this is an insoluble polymer of dihyrdroxyindole carboxylic acids, (figure 7) and gives a black/brown colour. Pheomelanin gives a yellow/red/brown colouration and is synthesised from benzothiazine intermediates (figure 7). The balance of eumelanin-pheomelanin provides some of the variation of pigment phenotypes. Individual melanosomes will only make one kind of melanin, depending on the internal environment, particularly the level of cAMP and presence of cysteine (Tully, 2007). Tyrosinase is an essential enzyme for the synthesis of both types of melanin (Park et al., 2009). Tyrosinase is a membrane bound glycoprotein, found in melanosomes. The N terminal catalytic portion of the protein is found within the melanosome where it interacts with copper ions which are required for its stability. These copper ions are removed by L-DOPA in order to activate tyrosinase. The C terminal domain which protrudes into the melanocyte cytosol, contains two serine residues which are phosphorylated by PKC, this activates tyrosinase (Park et al., 1999). Tyrosinase colocalises with its related proteins, they form a stable catalytic complex (Olivares and Solano, 2009). Tyrosinase conducts the first reaction in the synthesis of melanin which is the hydroxylation of L-tyrosine to L-3,4-dihydroxyphenylalanine (L-DOPA). L-DOPA is also a substrate for tyrosinase. L-DOPA can also be formed by tyrosine hydroxylase isoform 1 (THI), an enzyme which resides close to tyrosinase in the melansome membrane. Tyrosinase and THI compete for their substrate, L-tyrosine, which itself is generated from L-phenylalanine by phenylalanine hydroxylase (PAH). PAH is found in the melanocyte cytosol, thus the resulting tyrosine must be transported into the melanosome by facilitated diffusion (Schallreuter et al., 2007). L-DOPA is a transient intermediate and is quickly converted to L-dopaquinone (Olivares and Solano, 2009). In the absence of thiol compounds, i.e. cysteine, L-dopaquinone undergoes cyclisation to generate dopachrome (Lamoreux et al., 2001). Dopachrome is then converted to 5,6,dihydroxyindole-2-carboxylic acid (DHICA), this reaction is catalysed by DCT (Ito et al., 2000).

DHICA is then oxidised to form polymers by DCT, some dopachrome becomes 5,6,dihydroxyindole (DHI), which is oxidised by tyrosinase to form polymers (Ito et al., 2000). This sequence of catalysis leads to the production of eumelanin. When thiol compounds are present, dopaquinone becomes cysteinyldopas, which, following cyclisation and polymerisation become pheomelanin polymers (Kobayashi et al., 1995).

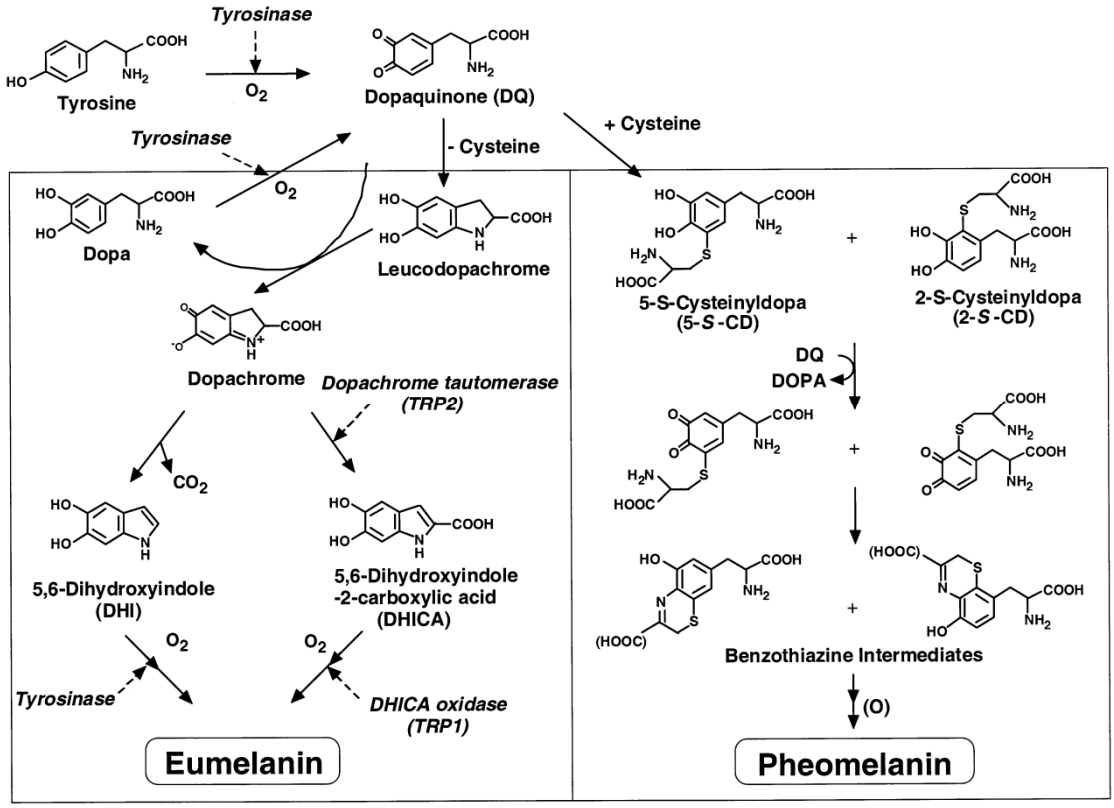

Figure 7
Melanin synthesis.
The pathways to melanin production (Lamoreux et al., 2001).

1.3.5 Regulation of melanogenesis

As with any cellular process, tight regulation of melanogenesis is important. This ensures timely and appropriate production of the protective pigment. Mis-regulation of melanogenesis can have pathological consequences. If too little pigment is made the DNA is not sufficiently protected from UV induced damage and is thus susceptible to mutations which in turn could have disastrous consequences for the cell and surrounding tissue, such as induction of various skin cancers. If too much pigment is made it can prove toxic to the cell causing apoptosis, and can also prevent synthesis of vital molecules such as vitamin D and folate. The various factors regulating melanogenesis will now be discussed.

As previously discussed, Mitf is considered the master regulator of melanocyte specification and differentiation. This is because it is a key element in the activation of transcription of many melanogenic genes, including tyrosinase and related proteins, as such Mitf is also considered a master regulator of melanogenesis.

There are four different isoforms of Mitf, A,C,H and M, which differ in their N terminal domain and expression pattern (Shibahara et al., 2001). Mitf-A is the longest isoform and is found in many types of cultured cells including RPE, Mitf-C is also found in many cultured cells, but has not been detected in melanocytes, Mitf-H is found primarily in heart tissue, Mitf-M is exclusively found in the melanocytes, and controls the expression of tyrosinase (Tachibana, 2000). The Mitf-M isoform contains a Lef promoter site which is targeted by Wnt signalling (Shibahara et al., 2001).

As well as tyrosinase, Mitf also regulates the transcription of Pmel17, the structural component of melanosomes, and Rab27a, important for melanosome movement (Chiaverini et al., 2008; Du et al., 2003). Mitf itself is regulated by phosphorylation. Phosphorylation of Mitf is accomplished by MAPK signalling, whereby Erk-2 is most likely responsible for phosporylation of S73 in the N terminal region, which activates Mitf. MAPK signalling is induced by Kit/Kitl signalling (Hemesath et al., 1998). However, Kit induced phosphorylation of Mitf also leads to its degradation by the proteosome (Wu et al., 2000). Mitf is also stimulated by αMSH which activates Mitf for a prolonged period of several hours by increasing cAMP (Price et al., 1998).

So a careful balance of short term Mitf activation by Kit/MAPK signalling and long term Mitf activation by αMSH must be maintained to ensure appropriate melanocyte behaviour.

αMSH triggers melanogenesis by binding to the melanocortin 1 receptor (MC1R) found on the melanocyte plasma membrane. MC1R is a G protein coupled receptor, which activates Gαs proteins to stimulate cAMP production via adenylate cyclase. Increased cAMP activates PKA (protein kinase A) by binding to its regulatory subunit which activates the catalytic subunit. PKA in turn phosphorylates and activates CREB (cAMP response element binding protein) this then activates Mitf by binding to its CRE motif in the promoter region. Mitf is a basic helix loop helix transcription factor with a leucine zipper domain, it binds to the E and M box motifs in the promoter region of its target genes, including tyrosinase etc, thus stimulating melanin synthesis (Busca and Ballotti, 2000; Newton et al., 2007; Park et al., 2009). As well as inducing Mitf expression, cAMP signalling is also important for regulating PAH and THI by phosphorylation and as such regulating their behaviour and subsequent production and activity of tyrosine and tyrosinase respectively (Schallreuter et al., 2007). cAMP signalling is also induced by other receptor/ligand complexes on the melanocyte including; β2-adrenoceptor, muscarinic receptors, α and β estrogen receptors and corticotrophin releasing hormone (CRH) receptor. These are responsible for initiating other synthetic pathways such as; catecholamine, acetylcholine and oestrogen synthesis in melanocytes (Gillbro et al., 2004). CRH signalling however leads to POMC (proopiomelanocortin) expression and thus subsequent αMSH and ACTH (adrenocortico trophin hormone) production (Slominski et al., 2006). Signalling via MC1R can also initiate Ras/Raf interactions and subsequently trigger the cascade of kinase reactions involving MEK, MAPK and ERK proteins, resulting in ERK translocation to the nucleus where it regulates gene expression to control proliferation and differentiation. (Busca et al., 2000). This signalling pathway is more commonly activated by receptor tyrosine kinases such as Kit, as mentioned earlier.

In contrast to αMSH binding, when the agouti signalling protein (ASIP) binds to MC1R, eumelanogenesis is inhibited whereas pheomelanogenesis is enhanced, due to the decreased transcription of tyrosinase related proteins. ASIP is a paracrine agent, released from nearby dermal papillae cells (Gantz and Fong,

2003). ASIP is a competitive ligand for αMSH, ASIP antagonism is also thought to play a negative role in melanocyte differentiation (Le Pape et al., 2008). In birds, mutation of ASIP has been shown to reduce the expression of SLC24A5, implying that ASIP positively regulates SLC24A5 (Nadeau et al., 2008). ASIP is in turn regulated by mahogany (Gunn et al., 1999). Mahogany is a trans-membrane protein and despite having a relatively low affinity for ASIP, is able to rescue ASIP mutant phenotypes (Gantz and Fong, 2003).
MC1R is a highly polymorphic gene and therefore is highly influential for the great variety of pigmentation phenotypes, as well as dictating susceptibility to melanoma. In contrast αMSH and ASIP are less polymorphic, therefore their role is more dependent on the type of MC1R present (Le Pape et al., 2009).

ACTH is also a stimulating ligand for MC1R, αMSH and ACTH are both derived from POMC. POMC is a large precursor polypeptide of 241 amino acids, it is ubiquitously expressed but is cell specifically cleaved into smaller peptide hormones by prohormone convertases (PC) (Gantz and Fong, 2003; Peters et al., 2000). POMC is expressed and processed in melanocytes and keratinocytes, this is enhanced by UV (Cui et al., 2007).

αMSH is just one of several paracrine agents secreted from keratinocytes and fibroblasts that act upon melanocytes, these include; Kitl, endothelin 1 (ET1), keratinocyte growth factor (KGF) and bFGF, all of which are increased by UV exposure (figure 8). Kitl has already been discussed here. ET1 activates tyrosinase and tyrp1 expression and has also been show to stimulate melanocyte proliferation and dendrite formation (Imokawa et al., 1992). KGF (FGF7) has been shown to promote melanosome transfer to keratinocytes by increasing phagocytosis. KGF receptor is expressed on the recipient keratinocyte, KGF is secreted from keratinocytes, thus establishing an autocrine signalling loop (Cardinali et al., 2005). bFGF isn't actually secreted from keratinocytes, it remains embedded in the membrane and activates receptor tyrosine kinases in the presence of cAMP to promote melanocyte survival and proliferation (Halaban et al., 1988). cAMP also regulates the expression of THI via its CRE, and, the phosphorylation of PAH via PKA.
The enzymes; tyrosinase, THI and PAH are also heavily regulated by (6R) –L-erythro-5, 6, 7, 8-tetrahydrobiopterin ($6BH_4$). This cofactor is an essential electron donor to PAH and THI, whilst also acting as an inhibitor of tyrosinase.

$6BH_4$ itself is synthesised and recycled by keratinocytes and melanocytes in an autocrine fashion (Schallreuter et al., 2007). αMSH can bind $6BH_4$ and thus alleviate the inhibition of tyrosinase, this little loop provides positive feedback (Moore et al., 1999).

Melansome pH can also be considered as a regulating factor for melanogenesis. Indeed tyrosinase activity is sensitive to fluctuations in pH. However, there has been some controversy regarding optimal melanosomal pH over the past decade and the experimental data is conflicting. It is generally acknowledged that melanosomes can be acidic (Bhatnagar et al., 1993), however the benefits of an acidic environment to melanogenesis are debated, as is the role of particular proteins (Ancans et al., 2001a; Chi et al., 2006; Puri et al., 2000). Reviewing the work over the last decade it can be observed that while some tyrosinase activity occurs at an acidic pH, more activity can be seen at a more neutral pH (6.5-7.0), thus this is optimal for tyrosinase activity. Also the observed acidic organelles may be early or precursor melanosomes and perhaps there is a change in pH during melanosome maturation (Schallreuter et al., 2007). It should also be noted that melanosomes from black melanocytes tend to have a more neutral pH than those of white melanocytes (Fuller et al., 2001). As black melanosomes contain more pigment this indicates tyrosinase functions better at neutral pH, this has also been shown experimentally (Smith et al., 2004). The P protein has caused much controversy over its role in melanosomal pH. The P protein is encoded by the OCAII gene and when mutated causes oculocutaneous albinism type II. As a relative of the SLC13 sodium/sulphate transporter family, the P protein was originally thought to move tyrosine, however this was shown not to be the case in pink eyed dilution mice which have a mutated P protein but can still transport tyrosine (Puri et al., 2000).

The P protein has been speculated to be involved in pH due to the less acidic nature of the pink eyed melanosomes, which is unfavourable for melanin synthesis (Puri et al., 2000). Moreover, this concurs with the general consensus that factors that increase melanosomal pH are favourable to melanogenesis (Ancans et al., 2001b; Brilliant, 2001; Hirobe et al., 2011).
Melanosomal pH is thought to be regulated by sodium proton exchangers (NHE) (Smith et al., 2004). Studies have shown that acidifying melansomes in vitro causes a reduction in tyrosinase processing and trafficking as well as catalytic

activity (Watabe et al., 2004). Conversely neutralisation of acidic melanosomes leads to an increase in tyrosinase activity and subsequent pigmentation (Ancans et al., 2001b).

αMSH and cAMP have recently been shown to play a role in regulating melanosomal pH. In vitro, increased αMSH leads to an increase in melanosomal pH, the same result is observed following forskolin treatment, forskolin is a known cAMP elevating agent, so this suggests αMSH is acting via cAMP signalling. In the same study cAMP was also shown to effect the expression of several ion transporters, thus indicating a mechanism for the alkanisation of the melanosome (Cheli et al., 2009). One of the transporters they found to be upregulated by cAMP was SLC24A5, which is of interest to this project.

The vesicular ATPase (V-ATPase) has been shown to be expressed in melanosomes and is thought to play a role in melanosome pH regulation. This has been demonstrated using a specific inhibitor (Basrur et al., 2003). Cheli et al (2009) showed that cAMP up regulates V-ATPase, this should cause a decrease in the melanosomal pH and subsequently inhibit melanogenesis, however this remains to be confirmed experimentally. The electrochemical equilibrium contributes to the regulation of pH. cAMP up regulates the expression of several solute carriers, including SLC24A5, SLC24A4 and SLC45A2 (also known as membrane associated transport protein, MATP) (Cheli et al., 2009), all of which are thought to play a role in pigmentation. This promotes the idea that solute carriers can be coupled to V-ATPases to establish electrochemical gradients (Lamason et al., 2005).

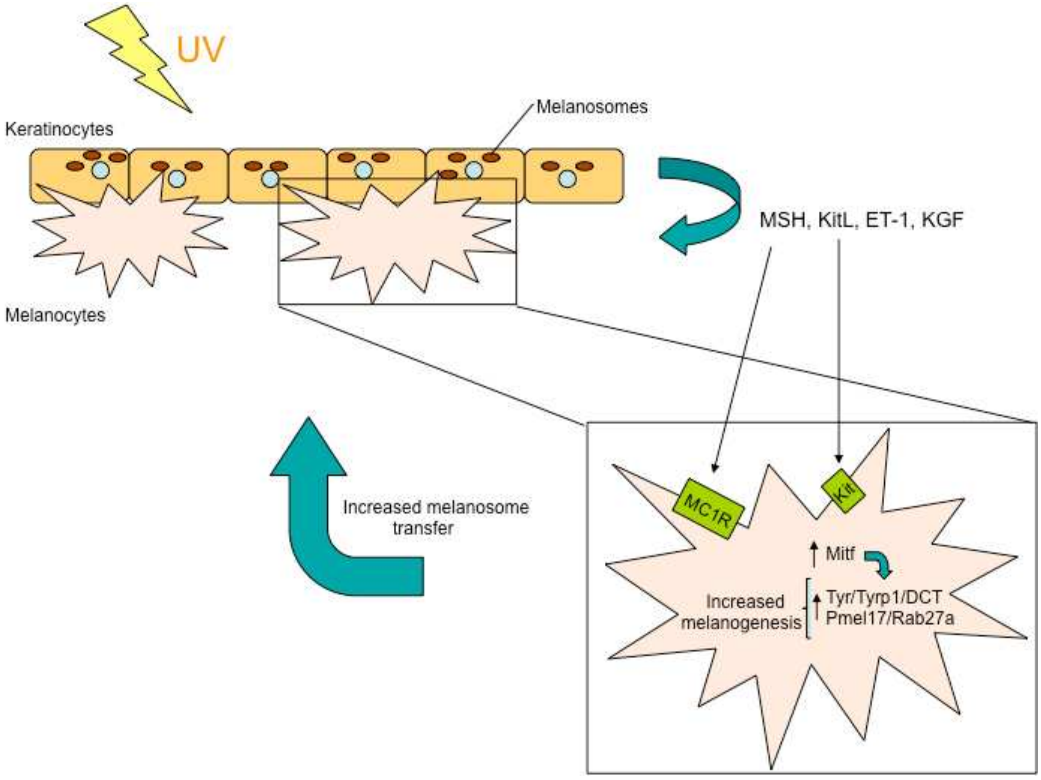

Figure 8
Signalling interaction between keratinocytes and melanocytes.
Secreted factors from keratinocytes induce expression of melanogenic genes in melanocytes and thus increase pigment production and melanosome transfer.

1.3.6 Calcium signalling and melanogenesis

Calcium signalling is involved in many physiological processes including; fertilisation, neuronal synapses and muscle contraction. Calcium ions are ubiquitous intracellular second messenger molecules. Therefore it is not surprising to find calcium plays a role in melanogenesis, however, in other processes calcium signalling tends to come about in the form of fluxes of intracellular Ca^{2+} concentration from low levels to relatively high, which tend to be observed in excitable tissues. So in this context a role in melanogenesis is surprising, but nonetheless there is substantial evidence for a role of calcium in pigment production.

Calcium signalling within melanocytes is initiated by the binding of ACTH to MC1R (Schallreuter et al., 2007). This activates phospholipase C (PLC), which cleaves phosphatidylinositol 4, 5-bisphosphate (PIP_2) into inositol 4,5-trisphosphate (IP_3) and diacyl glycerol (DAG). IP_3 then binds to IP_3 receptors (IP_3R) on the ER membrane; this allows Ca^{2+} to be released from the ER into the cytosol. Whereas, DAG remains associated with the plasma membrane but in conjunction with the increased Ca^{2+}, activates protein kinase C (PKC), which in turn activates tyrosinase by phosphorylating it at two serine residues in its C terminal domain (Park et al., 1999).

Calcium has been suggested to be important for the active transport of the melanin precursor L-phenylalanine, into melanocytes. This is an important step for melanogenesis as without imported L-phenylalanine there is not enough L-tyrosine to produce adequate amounts of melanin. This same work showed that L-tyrosine uptake is much slower than that of phenylalanine and is not calcium dependent (Schallreuter and Wood, 1999).

Melanin is able to bind calcium at high affinity. This has been proposed to be important for protecting the melanocyte from oxidative damage by H_2O_2 (Hoogduijn et al., 2004). As more melanin is synthesised more Ca^{2+} will be bound, therefore the amount of free Ca^{2+} available to assist L-phenylalanine transport is reduced, in this sense Ca^{2+} provides a negative feedback loop

POMC processing is also heavily dependent on Ca^{2+} concentration. POMC is cell specifically cleaved into smaller peptide hormones by prohormone convertases (PC). αMSH and ACTH are both derived from POMC, several prohormone convertases are required to yield αMSH and ACTH, including PC1 and PC2, all of which are found within the melanocyte and are calcium dependent (Peters et al., 2000). Another aspect of melanogenesis that is Ca^{2+} dependent is the processing of the melanosomal structural protein Pmel17. This involves a furin- like proprotein convertase (Berson et al., 2003) which is calcium dependent (Thomas, 2002).

1.3.7 Protecting DNA from UV

The UV spectrum can be arbitarily broken down into UVA (320-400nm), UVB (280-320nm) and UVC (100-280nm) radiation. UVC does not make it through the earth's ozone layer. UVB, having a shorter wavelength, is more energetic than UVA and is thus the most damaging UV radiation, as its wavelength is absorbed best by DNA, therefore directly causing DNA base mutations. However, UVA can penetrate through to the dermal skin layer and is thought to cause accumulation of reactive oxygen species which cause single strand DNA breaks (Fisher et al., 2002). UV damage can be visualised by sun burn (erythema), tanning and photoageing, non visible damage can also occur, such as immunosuppression and genetic mutations. UV can damage DNA in a number of ways including; pyrimidine dimer formation and oxidative damage (Abdel-Malek et al., 2010). Cells have a number of ways of handling such damage, including DNA repair mechanisms, apoptosis, and pigmentation (Brenner and Hearing, 2008). It is well documented that melanin is the main photoprotective agent in the skin. This observation comes from epidemiologic evidence, which shows an inverse correlation between skin cancer incidence and density of melanin pigmentation (Brenner and Hearing, 2008). Melanin pigments absorb and reflect/scatter UV waves and convert them into harmless heat (Park et al., 2009) they also have antioxidant and free radical scavenging properties.

Many melanogenic genes are upregulated in response to UV exposure, including Mitf and therefore its target genes. The catalytic activity of tyrosinase, PAH and THI also increases.

Paracrine agents, αMSH and ET-1 have been shown to have additional roles in protecting against DNA damage. αMSH has been shown to enhance the nucleotide excision repair pathway and inhibit the production of reactive oxygen species, by increasing the amount of the enzyme catalase which reduces the amount of hydrogen peroxide. This also highlights the importance of MC1R in UV protection, as αMSH cannot provide such protective measures in the presence of mutated MC1R (Kadekaro et al., 2005; Song et al., 2009). It has also been shown that MC1R expression is up regulated by αMSH, ET-1 and bFGF and MC1R dependent UV responsive genes are generally cell cycle or oncogenesis related (April and Barsh, 2007). Activation of adenylate cyclase by forskolin and subsequent increase in cAMP has the same effect on photo protection as αMSH, thus supporting the role of αMSH and the cAMP pathway in DNA damage response (Passeron et al., 2009).

Thus the mechanisms involved in producing constitutive pigmentation are also employed to increase pigmentation in response to the environment, namely UV radiation.

1.4 Pigment pathologies

There are many diseases associated with malfunctions in pigmentation. The most dangerous of which is skin cancer, which results from mis-guided behaviour of melanocytes or keratinocytes. Other diseases are less lethal but still pose a health risk. Pigmentation diseases are easy to detect and relatively easy to diagnose. Some diseases are the result of direct genetic mutations of the pigmentary system others are caused by mis-placed autoimmune responses. Either way pigmentation diseases can be divided into two categories; hypopigmentation or hyperpigmentation.

The most common pigmentation related diseases will be discussed below.

1.4.1 Melanoma

Melanoma is cancer of melanocytes. It is the least common but most lethal form of skin cancer. Other, more common skin cancers include; basal cell carcinoma (BCC) and squamous cell carcinoma (SCC), both neoplasms of the keratinocytes, but vary depending on their location in the skin. Skin cancers are caused by genetic and environmental factors. A genetic predisposition to skin cancer can be caused by mutation(s) in any number of different genes; such a predisposition makes one more susceptible to the effect of carcinogenic environmental contributors, principally UV exposure (Scherer and Kumar, 2010). Skin phenotypes such as fair skin and light hair and freckled skin and red hair are known risk associated phenotypes, these are often associated with mutations in MC1R. Incidence and mortality of melanoma has increased more than any other cancer in the last 10 years. Malignant melanoma is a particularly tricky cancer to treat successfully this is partly due to its highly aggressive nature, but also as not enough is known about the molecular interactions involved in its development and progression (Levy et al., 2006). Arising from the neural crest, melanocytes have a naturally high motility and survival rate, and have a reduced self afflicted apoptosis record (Gray-Schopfer et al., 2007). Melanocytes are also highly resistant to apoptosis, which is thought to be due partly to their resistance to the toxins accumulated during the melanin synthesis but also because they are not a renewable population, unlike keratinocytes which are replaced following damage, melanocytes have to be able to withstand such damage without conceding to apoptosis.
Whilst this behaviour is advantageous to the protective role of melanocytes, it also makes neoplasm of these cells difficult to treat, as many available treatments are based on apoptosis (Robinson and Fisher, 2009).

Many of the genes involved in melanocyte development and function are also implicated in the development and progression of melanoma. Many genome wide association studies have been conducted which reveal particular variants of genes that are associated with an increased risk of developing melanoma.

MC1R is a highly polymorphic gene and is associated with various pigment phenotypes and correlating cancer risk, including melanoma. Different variants of MC1R are associated with different pigmentation phenotypes and aspects of

disease susceptibility and this varies between populations, for instance the V60L mutant is a major risk contributor in Spanish populations whereas red hair colour (RHC) mutants are the greater risk factor in German populations (Scherer et al., 2009). The V60L mutant was one of several found to show decreased cell surface expression and subsequent loss of cAMP signalling. Other mutants had normal cell surface expression but demonstrated a lack of G protein coupled signalling, while others showed impaired ligand binding or dominant negative effects (Beaumont et al., 2007).

ASIP is a ligand for MC1R and is reported to be involved in various pigment phenotypes. ASIP is inhibitory to eumelanogenesis thus pheomelanogenesis is favoured following ASIP signalling, leading to lighter skin/hair and red hair colour phenotypes. A polymorphism has been identified in ASIP which causes a down regulation of ASIP mRNA and therefore alleviates its inhibitory effects leading to production of darker eumelanin. However this polymorphism has not been shown to correlate with any increased risk of melanoma (Voisey et al., 2006). More recently a two SNP haplotype was discovered in ASIP which does strongly correlate to increased melanoma risk (Gudbjartsson et al., 2008).

Tyrosinase, as previously discussed, is the key enzyme in melanin synthesis; therefore it is not surprising that variants of tyrosinase lead to different pigmentation phenotypes. However, the correlation of tyrosinase variants with melanoma is not clear and this has caused some controversy (Duffy et al., 2007; Gudbjartsson et al., 2008; Nan et al., 2009). Tyrosinase does not regulate melanocyte behaviour and therefore seems unlikely to play a role in melanoma. Over-active tyrosinase may be detrimental to the cell by way of producing excessive amount of toxic free radicals during melanin synthesis, this process is also energetically demanding for the cell. Tyrosinase seems more likely to have a contributory rather than a causative role in melanoma. Mutations in tyrosinase are more commonly associated with oculocutaneous albinism (Scherer and Kumar, 2010). The TYRP1 enzyme, involved in eumelanogenesis, also has variants which are associated with mild oculocutaneous albinism, but one particular variant has also been found to correlate with melanoma (Duffy et al., 2007).

Mutations in proteins involved in signalling pathways can lead to mis-regulation of melanocyte growth, survival and proliferation. Ras/Raf/MAPK/ERK signalling is important for normal melanocyte behaviour (Busca et al., 2000), when components of this pathway are mutated it can lead to uncontrolled cell growth and/or proliferation/survival (Gray-Schopfer et al., 2007). Common mutations of this pathway include; ERK hyperactivation (seen in 90% of melanomas) (Cohen et al., 2002), Ras gain of function (15% - 30% of melanomas) (Chin et al., 1999), and BRAF (~66% melanomas) (Davies et al., 2002). In particular, the V599E-BRAF mutant which stimulates constitutive ERK signalling and consequently hyperproliferation and survival of tumour cells. Mitf is a target of V599E-BRAF (Gray-Schopfer et al., 2007).

Another signalling pathway found to be equally significant in melanoma is the PI3K pathway (phosphoinositide-3-OH kinase). This pathway utilises lipid second messengers, which are activated by PI3K, these lipid molecules regulate cell proliferation, survival, growth and motility. PI3K signalling is over active in 5-20% of melanomas, this is often due to mutations in PTEN. PTEN (phosphate and tensin homologue found on chromosome ten) is a lipid and protein phosphatase, it is a negative regulator of PI3K signalling (Wu et al., 2003). In vitro analyses of PTEN have revealed it to be a key tumour suppressor in melanoma.

In PTEN deficient melanoma cells addition of exogenous PTEN reduced melanoma progression. In vivo, PTEN+/- heterozygous mice show increased development of many cancers, including melanoma (homozygous knockout was embryonic lethal). These animals also demonstrated a reduced sensitivity to agonist induced apoptosis. This strongly indicates PTEN is crucial for controlling cell cycle progression and cell death (Di Cristofano et al., 1998; Podsypanina et al., 1999; Stambolic et al., 1998). PTEN can dephosphorylate lipids, particularly PIP3, which is a product of PI3K activity. Active PIP3 activates Akt. Akt is a serine threonine kinase with a plethora of different targets, many of which are involved in cell proliferation, survival and migration. Protein targets of PTEN include MAPK (Wu et al., 2003). By de-phosphorylation, PTEN de-activates its targets and consequently inhibits further downstream signalling thus providing a restraining mechanism on cell survival, proliferation and migration. So when mutated or absent, alleviation of PTEN

inhibition allows uncontrolled cell growth and proliferation to proceed, leading to tumour development.

The role of Mitf as a key player in melanocyte development and melanogenesis has been covered earlier. It is therefore not surprising that Mitf has a role in melanoma. Mitf has been shown to be over expressed in 10-20% of primary melanoma tissue, this correlates with the 5 years or less survival rate associated with metastatic melanoma (Garraway et al., 2005). Having said this, the levels of Mitf expression are variable across specimens, and display little consistency. Having many targets, variability in Mitf expression has numerous consequences, promotion of cell survival and proliferation is typical but apoptosis and differentiation are also likely. Thus Mitf can be proliferative or inhibitory to melanoma development and progression. It is not understood how different melanomas express different levels of Mitf, with no consistent pattern. It is thought that perhaps the different classes of melanoma have different responses to Mitf levels (Levy et al., 2006). It would also be beneficial to determine what is causing the mis-regulation of Mitf and therefore how this could be corrected therapeutically.

Remarkably mutations in p53 are rarely detected in malignant melanoma, despite the well established role of p53 mutants in other malignancies. This is also surprising as melanomas are particularly resistant to apoptotic therapies, as a pro apoptotic protein, p53 is often the cause of such resistance (Soengas and Lowe, 2003).

1.4.2 Vitiligo

Vitiligo is an acquired condition characterised by localised skin hypopigmentation. It is thought to be caused by a combination of factors including genetic mutations in melanogenic genes but also immune system defects, which result in the body targeting melanocytes for destruction, and environmental factors. Furthermore, vitiligo is due to a lack of melanocytes as opposed to a lack of melanin synthesis within melanocytes. It is not a serious life threatening disorder; however it can have a significant psychological effect on sufferers. There are limited treatments available, none of which are suitably

effective. More often individuals tend to manage the condition using cosmetic approaches. Vitiligo is relatively common, effecting ~1:200 people.(Fistarol and Itin, 2010) (Boissy and Nordlund, 2011).

1.4.3 Albinism

There are two forms of albinism, OCA (oculocutaneous albinism) which is characterised by the lack of melanin pigment in the skin, hair and eyes. OA (ocular albinism) just affects the eye. OCA causes an increased susceptibility to UV damage and skin cancer. In both disorders the lack of eye pigment causes a reduction in visual acuity (Oetting and King, 1999). There are three different categories of OCA; OCA1 is the most severe, this is caused by mutation of the tyrosinase gene leading to an inactive enzyme. OCA1 patients have no pigment from birth and do not develop any throughout their life span (King, 1993). OCA2 is caused by mutation of the OCA2 (or P gene) gene, these patients are born with a little hair pigment, but do not develop any more, this is the most common form of albinism (Rinchik et al., 1993). Mutations in Tyrp1 gene cause OCA3, these individuals have minimal pigment from birth and do develop more over time (Boissy et al., 1996).

OA1 hypopigmentation is caused by mutation of a melanosomal membrane GPCR called OA1 (Schiaffino et al., 1996). The exact role of OA1 in eye pigmentation is not known, OA1 mutations cause a number of visual defects including; optic misrouting, nystagmus, strabismus and loss of stereoscopic vision. Several types of mutations have been found in patients with OA, all of which lead to a non functional protein. The melanosomal membrane localisation of the OA1 protein suggests it is involved in melanosome biogenesis as opposed to directly affecting tyrosinase function (Schiaffino, 2010).

1.4.4 Other syndromes

Hermansky-Padlat syndrome is a diseased caused by abnormal lysosome and melanosome biosynthesis. This leads to UV sensitivity and an increased risk of developing skin cancers, and increased bleeding, due to lack of lysosome related bodies in the thrombocytes.

Chediak-Higashi syndrome is also caused by abnormal melanosome biogenesis, it is characterised by partial OCA and immune deficiency. This disease is caused by a mutation in LYST, a lysosomal trafficking regulator (Fistarol and Itin, 2010; Hershkovitz and Sprecher, 2008).

Piebaldism and Waardenburg syndrome are related hypopigmentation diseases associated with defective migration of melanoblasts to the epidermis from the neuroectoderm. This presents in localised hypopigmentation particularly of the face. Waardenburg syndrome is associated with defects in Mitf (Price et al., 1998)

Griscelli syndrome is another hypopigmentation disorder, in which melanosomes cannot be transferred to keratinocytes. Patients with this disease also have neurological and immunological issues.

Phenylketonuria is a relatively common skin complaint, in which PAH levels are reduced thus inhibiting tyrosine synthesis and melanogenesis. This results in fair skin, blue eyes phenotype with a tendency to develop eczema. Due to role of tyrosine in other physiological processes this disease also presents other more severe effects such as; motor and mental retardation, microcephaly and seizures (Baxter et al., 2009; Fistarol and Itin, 2010; Hershkovitz and Sprecher, 2008). However it can be easily treated using diet restrictions.

1.5 Pigmentation of hair

Melanocytes of the hair follicle are also derived from the neural crest. A subset of migrating melanoblasts leave the epidermis and localise to the hair follicle, here they can reside in one of two areas; the bulge region and hair bulb (figure 9). The bulge region tends to be occupied by melanocyte stem cells (melanoblasts), whereas differentiated melanocytes tend to occupy the hair bulb, where they transfer melanin to the growing hair fibre. This is the only site of active melanogenesis and hair pigmentation (Peters et al., 2002). Melanocytes of the hair follicle tend to be larger than their epidermal counterparts, they also have more dendrites, more extensive Golgi and RER networks and produce larger melanosomes (Tobin and Bystryn, 1996). Follicular melanocytes are regulated by the hair growth cycle. They only produce pigment during the anagen phase where the hair is growing (Slominski et al., 1994). This is in contrast to the constitutively active melanocytes of the skin.

The anagen phase can last for several years in human head hair. The hair cycle ends with catagen, during this phase the hair bulb structure is lost and the melanocytes undergo apoptosis (Robinson and Fisher, 2009). This is of particular significance because epidermal melanocytes are highly resistant to apoptosis, as discussed above. More melanocytes are produced during telogen, the resting phase between catagen and the next anagen, these are thought to arise from a population of melanocyte stem cells present in the hair bulge (Steingrimsson et al., 2005). This stem cell niche is continuing to provide researchers with a model to understand stem cell behaviour, understanding of which could lead to exploitation of stem cells in a therapeutic manner.

Like skin melanocytes, hair follicle melanocytes are regulated by many factors, such as growth factors, cytokines and hormones. These are associated with the individual phenotype, such as gender, race, age and genetic background. These regulatory factors can operate via autocrine, paracrine and endocrine systems. Also hair melanocytes are not affected by UV (Tobin, 2008). Follicular melanocytes are lost over time, this is demonstrated by hair greying in mature years (Tobin, 2009).

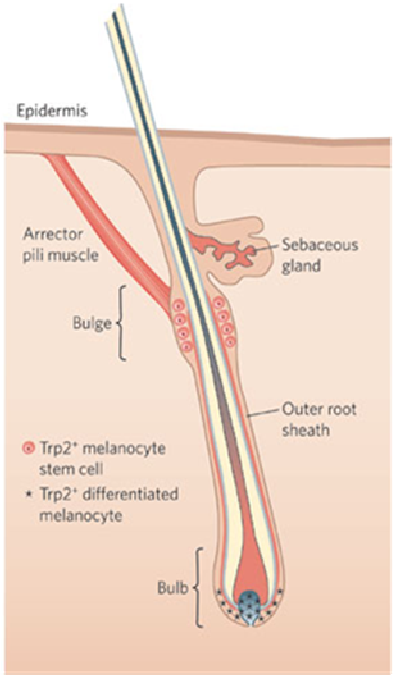

Figure 9
The hair follicle. Melanocyte stem cells reside in the hair bulge whereas differentiated functional melanocytes are found in the hair bulb, where they pass their melanosomes to the keratinocytes (Lin and Fisher, 2007).

1.6 Pigmentation of the Eye

Melanin pigments are the key factor that allow light reception in the eye and thus provide the sense of sight. The majority of pigment in the eye comes from the retinal pigmented epithelium (RPE) cells, these cells are supported by choroidal melanocytes and there are also iris pigmented epithelium (IPE) cells (Aoki et al., 2008).

In contrast to skin and hair melanocytes, RPE cells are not derived from the neural crest, they arise from the multi potent optic neuroepithelium during eye development (Fuhrmann, 2010). They are non migratory cells and thus remain embedded in the local environment (Bharti et al., 2006). They are initially present in the posterior portion of the optic vesicle, but as the optic cup and eventual eye develop their domain spreads to encompass the retina, lens and cilary marginal zone (figure 10), (Fuhrmann et al., 2000). Posteriorly the RPE is boarded by Bruch's membrane, which separates the RPE from the choroid structure, which also contains pigment cells. This sets up the blood-retinal barrier (Bharti et al., 2006).

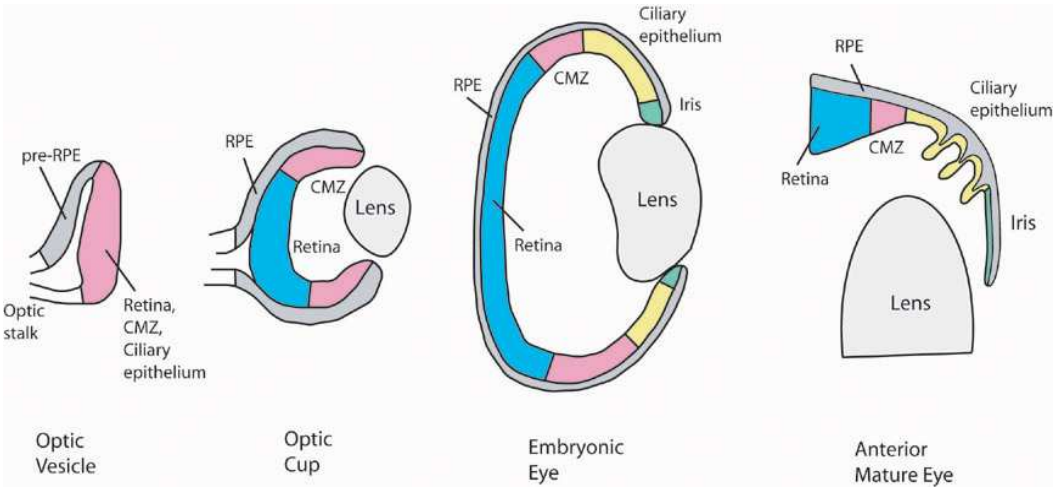

Figure 10
Schematic representation of embryonic eye development.
The RPE monolayer remains posterior to the multi layered retina. RPE cells eventually cover the ciliary marginal zone (CMZ), as they become iris pigmented epithelium cells (IPE) they partially cover the lens. The anterior portion of the eye is in turn covered and protected by the cornea (not shown). Posterior is to the left. (Fuhrmann et al., 2000).

The most notable role of the RPE is to absorb the light energy focussed by the lens onto the retina (Boulton and Dayhaw-Barker, 2001). Another important role of RPE cells is to re-isomerize retinal. Following photon absorption in the photoreceptors, all-trans-retinal is transported to RPE cells, which isomerize it to 11-cis-retinal and pass it back to the photoreceptors. This cycle is key to maintain the excitability of the photoreceptors.

As well as providing visual acuity, RPE cells are also important for various aspects of eye development and maintenance of the surrounding photoreceptor cells (Strauss, 2005). RPE cells are not dendritic like skin melanocytes, they are however ciliated on their apical aspect, this is to facilitate ion exchange and transport of other factors including retinal, and also uptake of pieces of degraded retina cells, to keep the environment clear of debris (Bharti et al., 2006). Like epidermal melanocytes, RPE cells express Mitf and thus many of its targets. RPE cells and epidermal melanocytes also share the common feature of melanosomes, where the melanin pigments are synthesized in much the same manner (Martinez-Morales et al., 2004). However, RPE cells do not transport their melanosomes out of the cell (Futter, 2006). Another significant difference between RPE and epidermal pigment cells is their interaction with their surrounding environment. Epidermal melanocytes function independently of each other and respond to dynamic environmental cues, whereas RPE cells work together more a like a tissue and have limited responses from other cells of their relatively static environment.

The loss of a functional tyrosinase gene in the RPE, as seen in albinism, causes abnormal development of the retina and inappropriate crossing of retinal axons leading to incorrect cerebral innervations and consequently defects in visual acuity (Jeffery, 1997)

1.7 Evolution of Human Pigmentation

Pigmentation phenotypes can be unique to individuals, but general phenotypes among populations have emerged through evolution by natural selection. This is largely due to UVR incidence (Chaplin, 2004; Jablonski and Chaplin, 2000). Figure 11 describes the distribution of pigmentation phenotypes, measured by skin reflectance, across the world, of indigenous populations. Reduced skin reflectance (i.e. darker skin) is shown to correlate with higher UVR intensity (Chaplin, 2004).

Lighter skin pigmentation phenotypes are thought to have evolved as populations emigrated out of Africa. This equatorial ancestral continent is exposed to high levels of UVR, therefore the presence of a dense layer of photoprotective pigment is advantageous and selected for over lighter more damage prone skin. In regions of lower UVR exposure such density of photo protection is unnecessary and hinders vitamin D synthesis.

The damaging effects of UVR exposure on unprotected skin are well established. Symptoms initially present as sunburn, extreme sunburn can cause damage to sweat glands leading to disruption of thermoregulation and greater risk of infections. Prolonged exposure to UVR is associated with skin cancer. However, such damage is progressive and doesn't present until later life, i.e. post reproduction, therefore it cannot be a selective trait (Parra, 2007). Other UVR related factors have to be considered. More vitamin D is synthesised in response to UVR than is consumed by diet. Vitamin D is essential for many physiological processes including; bone metabolism, immunoregulation and calcium homeostasis (Parra, 2007). In regions of high UVR, vitamin D synthesis is easily stimulated even with heavily pigmented skin. However, populations living in lower UVR regions have evolved lighter skin to facilitate maximum absorption of UVR to stimulate vitamin D synthesis, as lack of vitamin D can result is disorders such as osteomalacia. Darker skin individuals living in lower UVR areas are prone to vitamin D deficiency related disorders due to the lack of UVR stimulus (Parra, 2007).

Another victim of UVR damage is folate. Folate is essential for DNA synthesis and repair, folate deficiency is known to cause numerous birth defects, and as such pregnant women are encouraged to supplement their diet with folic acid. UVR has been shown to significantly reduce the concentration of plasma folate in light skin populations in high UVR areas. Due to the necessity of optimal folate levels, particularly during early life, selective influences are likely to apply here (Parra, 2007).

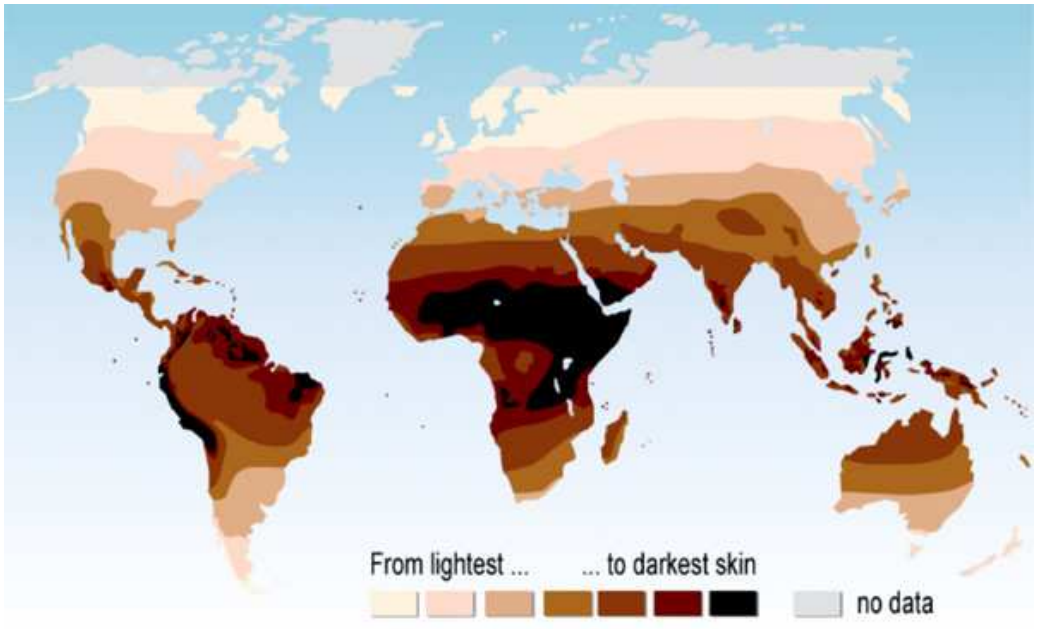

Figure 11
The distribution of global skin pigmentation phenotypes. Greater exposure to UVR correlates to increased pigmentation (Chaplin, 2004).

Changes in human skin colour over evolutionary time scales can be associated with human migration and changes in diet, as well as environmental changes. According to natural selection, individuals with the best adaptive mechanism will have a survival advantage, and therefore their genetic adaptation will be carried on throughout generations (Juzeniene et al., 2009).

Many genes are associated with variations in pigmentation. For example, the previously mentioned MC1R is highly polymorphic and mutations in this gene are associated with red hair and freckles. The high polymorphism rate in this

gene is thought to be a response to selective pressures (Harding et al., 2000). Wild type MC1R is associated with dark skin colouration (Rees, 2000), as this receptor leads to eumelanin production. There are also reports that SNP's in MATP (membrane associated transport protein), also known as SLC45A2, correlate with pigment variations between populations, this is interesting as the role of MATP in pigmentation is not yet clear (Graf et al., 2005). Some allelic changes in MATP are conserved among European populations whereas some are shared between European and East Asian populations (Lao et al., 2007).
The related gene SLC24A5 also has a significant SNP which correlates with European population and thus is heavily associated with evolutionary skin lightening (Soejima and Koda, 2007)

1.8 NCKX family

NCKX's (potassium dependent sodium calcium exchangers) are members of the Ca^{2+} cation (CaCA) antiporter superfamily. This superfamily plays key roles in mediating Ca^{2+} movement over the plasma, or intracellular membrane. The superfamily can be broken down into 5 sub-families; CCX, Ca^{2+}/cation exchangers, CAX, Ca^{2+}/anion exchangers, YRBG (uncharacterised E.coli membrane transporter), NCX, Na^{+}/Ca^{2+} exchangers and NCKX (Lytton, 2007).

The NCKX protein family has five members, (NCKX1-5, SLC24A5 encodes NCKX5). NCKX 1-4 extrude calcium across the plasma membrane using the sodium/potassium gradient (Altimimi and Schnetkamp, 2007b). Lamason et al (2005) showed that NCKX5 is found intracellularly (figure17), not restricted to the plasma membrane, and is therefore likely to be found in an organelle membrane. This has been further analysed by Ginger et al (2008) (see section 1.9.2).

Calcium is an important signalling molecule and is involved in many physiological functions. The extracellular calcium concentration is much higher than cytosolic calcium concentration; calcium is also stored in some organelles, such as endoplasmic reticulum, Golgi and mitochondria. Small increases in cytosolic calcium can bring about dramatic effects, thus movement of calcium into and out of the cytosol must be carefully regulated. This is achieved though

the behaviour of many ion channels and transporter proteins that move Ca^{2+} across membranes (Lytton, 2007).

Na^{+}/Ca^{2+} exchange has been studied since the 1960's, but K^{+} dependent Na^{+}/Ca^{2+} exchange was not described until the 1980's in retinal rod outer segments. The potassium dependent sodium calcium exchanger (NCKX) family comprises 5 distinct gene products, making it the most numerous calcium transport family (Altimimi and Schnetkamp 2007).

NCKX proteins are found in various excitable tissues. NCKX1 was the first to be described and this is found in the outer segments of bovine retinal rod cells (Reilander et al., 1992). Here NCKX1 is the only calcium extrusion pathway, which is accomplished by interaction with the cGMP-gated channels (Krizaj and Copenhagen, 1998; Schnetkamp et al., 1991). NCXK1 was then cloned from human and other species and soon found to be the first member of a new family of proteins, NCKX, encoded by the SLC24 gene family (Schnetkamp, 2004). NCKX2 was identified in 1998 (Tsoi et al., 1998) and is found in various areas of rat brain, particularly the cerebellum, midbrain and hippocampus. NCKX2 is also detected at lower levels in the eye, this was later shown to be specific to the cone photoreceptor cells (Prinsen et al., 2000). NCKX3 is also widely expressed in the brain, although this is also found in smooth muscle tissues (Kraev et al., 2001). NCKX4 is also detected in the brain, particularly the hippocampus as well as other tissues including heart, stomach and kidney (Li et al., 2002). NCKX5 is expressed in pigment producing cells of the skin and eye (Lytton, 2007). A sixth NCKX, NCKX6, was found in mice. Here it is widely expressed in the brain, lung, heart and kidney (Cai and Lytton, 2004)

SLC24 family genes have been cloned from many mammalian species such as human, mouse and rat and lower animals including; sea urchins (Su and Vacquier, 2002), drosophila (Haug-Collet et al., 1999; Webel et al., 2002) and the nematode C.elegans (Szerencsei et al., 2000), and even in some prokaryotes (Schnetkamp, 2004) and this suggests an evolutionarily conserved role for these genes.

Due to their cerebral expression NCKX proteins have attracted interest as potential targets for drugs to treat conditions such as ischaemia and stroke (Cuomo et al., 2008; Kiedrowski, 2007)

So far most experimental work has been conducted on NCKX1 (Cooper et al., 1999; Poon et al., 2000)and NCKX2 (Kinjo et al., 2007; Kinjo et al., 2003; Li et al., 2006) . Such studies suggest the overall topology of NCKX family members is identical; figure 12 describes the structure of NCKX2. NCKX structure comprises an N terminal signal peptide, followed by an extracellular loop, which leads to a cluster of 5 hydrophobic transmembrane domains. This cluster is separated from another cluster of 5 hydrophobic domains by a large cytosolic loop. The C terminus is found on the cytosolic side of the membrane. All 5 members of the NCKX family contain two alpha repeats, alpha 1 and alpha 2, these are thought to have arisen from a gene duplication event and contain several conserved residues which are important for $Na^+/Ca^{2+}/K^+$ exchange (Kinjo et al., 2003). Much work has been done to establish the essential residues for NCKX function. By substituting candidate residues in the transmembrane domains of NCKX2, Kang et al (2005), showed that charge conserved substitution of Glu188 (E188D) and Asp548 (D548E) resulted in reduced K^+ and Ca^{2+} dependencies compared to wild type NCKX2. This suggests that Glu188 and Asp548 are important residues for the binding of K^+ and Ca^{2+} at the binding pocket of NCKX2 (Kang et al., 2005a). In a similar study, Asp575 was found to be essential for the K^+ dependence of NCKX2. When Asp 575 was substituted to asparagine or cysteine (charge removal), NCKX2 was found to transport Ca^{2+} independently of K^+. Charge conservative substitution of Asp575 rendered the protein non functional (Kang et al., 2005b). Site directed disulphide mapping was used to demonstrate that the alpha repeat domains of NCKX2 are close together in 3 dimensional space, and this in turn shows that the key residues (Glu188 and Asp548) previously identified for Ca^{2+}/K^+ transport are also in close proximity (Kinjo et al., 2005).

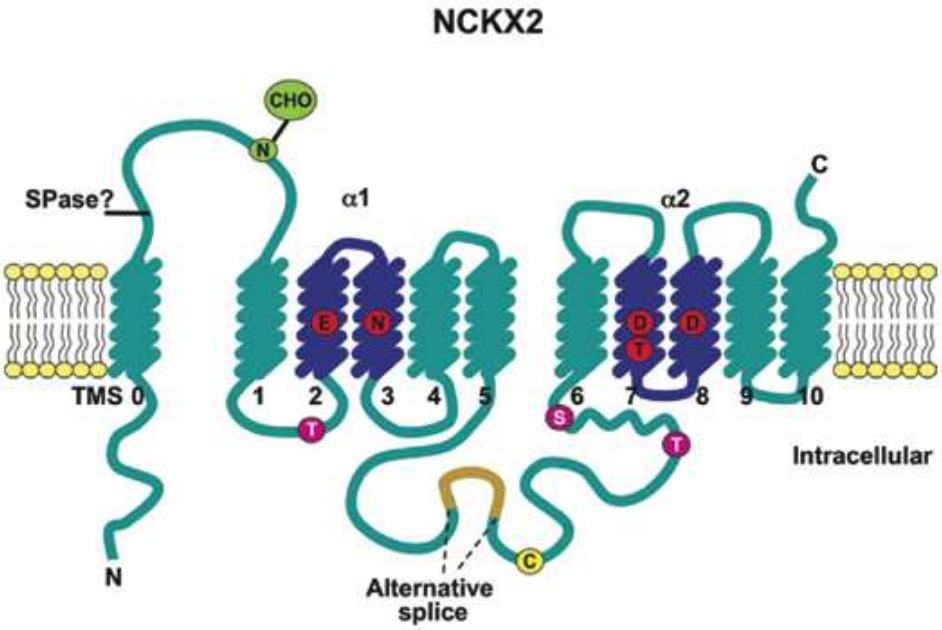

Figure 12
NCKX2 structure based on experimental findings. TMS 0 is the signal peptide, which is cleaved at the SPase site. N-CHO is the single glycosylation site. Alpha repeats are highlighted in dark blue and essential residues are highlighted red. The alternative splicing sites of the cytosolic loop are indicated, T and S labels on the loop represent phosphorylation sites and the C is thought to be important for redox. Phosphorylation and redox are thought to be important for regulation of NCKX2 function – not discussed here. (TMS, transmembrane segment), (Lytton, 2007).

NCKX proteins use the Na^+ gradient across the membrane to transport other substrates. NCKX proteins are thought to function by the alternating access model. This model suggests the binding sites on the protein of different ions can alternate from one side of the membrane to the other by conformational change(s). As such these proteins are assumed to be bidirectional depending on the Na^+ gradient. NCKX5 mediated Ca^{2+} transport is activated by Na^+ it is thought $4Na^+$ ions are transported to $1Ca^{2+}$ and $1K^+$.

Physiologically, NCKX1 is the only NCKX protein to be fully characterised. NCKX1 is the main Ca^{2+} transporter in retinal rod outer segments. In the dark cGMP-gated channels are open, which causes Na^+ entry by depolarization, this also causes Ca^{2+} influx, but this is balanced by NCKX1 Ca^{2+} efflux. In the light, cGMP-gated channels close, this stimulates NCKX1 to remove the excess Ca^{2+}, this in turn results in an increase in cGMP synthesis and re-opening of the

cGMP channels. NCKX2 is thought to play a similar role in cone photoreceptors (Lytton, 2007).

NCKX2 has been successfully knocked out in mice. These animals were found to have a clear reduction in Ca^{2+} flow in cortical neurons, a loss of long term potentiation and an increase in long term depression at hippocampal Schaffer/CA1 synapses. Lack of motor learning and working memory was also detected by specific tests (Li et al., 2006). The authors were surprised not to find any defects in the cone photoreceptors.

More recently NCKX5 knockout mice have been developed. These mice were viable, fertile, displayed normal behaviour, and had indistinguishable coat colour, from wild-type and heterozygous animals. However, opthalmoscopic and histologic inspection found significant hypopigmentation of the retinal pigment epithelium, iris pigment epithelium and ciliary body. Hypopigmentation was also identified in melanocytes of the ears and nose of the NCKX5 null mice. The authors conclude NCKX5 is important for normal melanin pigmentation in all pigmented cells, but most especially in the pigmented cells of the eye (Vogel et al., 2008).

1.9 SLC24A5

SLC24A5 was first identified in the zebrafish as the gene responsible for the golden pigmentation phenotype (figure13). A non-synonymous SNP (single nucleotide polymorphism), identified in the human gene (Tanaka, 2005), encodes an amino acid switch (alanine to threonine) at position 111 of the protein. The two different alleles have been shown to be population specific. Alanine is found at 93–100% in African, East Asian and indigenous American populations, whereas threonine is found in 98.7– 100% of European and American populations (Lamason et al., 2005; Stokowski et al., 2007).

Unilever Discover have conducted extensive cell based analysis of SLC24A5 (Ginger et al., 2008). More recent work has involved genome wide micro array analysis following repression of SLC24A5. This has provided clues as to the role of SLC24A5 in pigmentation. This work is as yet unpublished and will therefore be referred to as Wilson et al unpublished data in this thesis, and is referenced in the bibliography.

1.9.1 Golden zebrafish

The golden mutant is a well known strain of zebrafish, and is used as a background model for many different areas of research (Denvir et al., 2008; Hattori et al., 2011; Liao and Essner; Moore et al., 2006). The golden phenotype is characterised by the delayed expression of fewer, smaller and less dense melanophores, and thus a hypopigmented appearance (figures 13 and 14). This is comparable to lighter skin humans, such as European populations, which make it of interest to understanding human melanogenesis. The golden phenotype can be observed in developing zebrafish larvae, but is particularly prominent in the adult animal where the 'golden' colour can be seen (figure 14).

Figure 13
Golden zebrafish larvae.
D and E wild type larvae, F and G golden larvae. D and F lateral views of eyes. E and G dorsal views of head. Golden larvae clearly show reduced pigmentation in the head and eye pigment cells (Lamason et al., 2005).

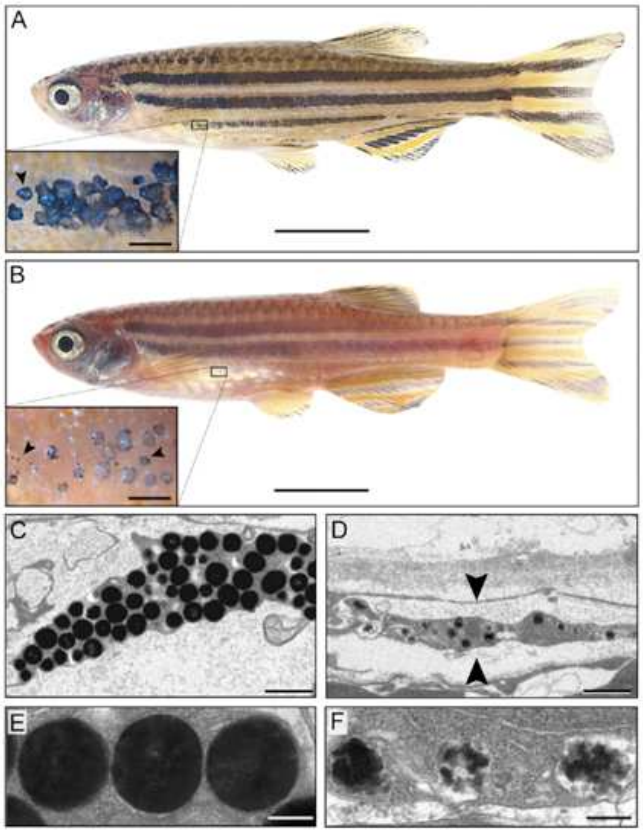

Figure 14
Golden pigmentation phenotype in zebrafish.
A, wild type adult. B, golden mutant adult. Boxes show close up of melanophores. C, E, transmission electron micrograph of skin melanophores of wild type 55hpf embryos. D, F, TEM of skin melanophores from golden 55hpf embryos, arrow heads indicate edge of melanophore. (Lamason et al 2005).

Lamason et al (2005) used a combination of linkage analysis, PCR and screening a zebrafish genomic library to identify satellite markers and a clone in which they reside. They then used shotgun sequencing, contig assembly and gene prediction to identify the genes within this clone. Morpholinos targeted to the potential targets were then used to see if they could phenocopy the golden phenotype. Only the morpholino to SLC24A5 did, and this was confirmed by rescue experiments (Lamason et al 2005). The mutation responsible for golden pigmentation was found at position 208 of the SLC24A5 protein. Here there is a C to A nucleotide switch, which converts a tyrosine residue to a stop codon, thus prematurely truncating the protein, reducing it to 40% of its normal size. This truncation includes loss of the cytosolic loop and C terminal transmembrane domains (Lamason et al., 2005)

1.9.2 Expression of SLC24A5

In situ hybridisation was used to detect expression of SLC24A5 in wild type and golden zebrafish. Expression was seen in melanophores and RPE of 24hpf wild type larvae (figure 15). Expression was not detectable in golden embryos (figure 15); this is likely due to nonsense mediated decay of the truncated transcript. RT PCR was also used for expression analysis in normal mouse tissues and B16 melanoma cells, this showed 10 fold greater expression of SLC24A5 in skin and eye tissues and melanoma cells compared to non melanin producing tissues (figure 16) (Lamason et al 2005).

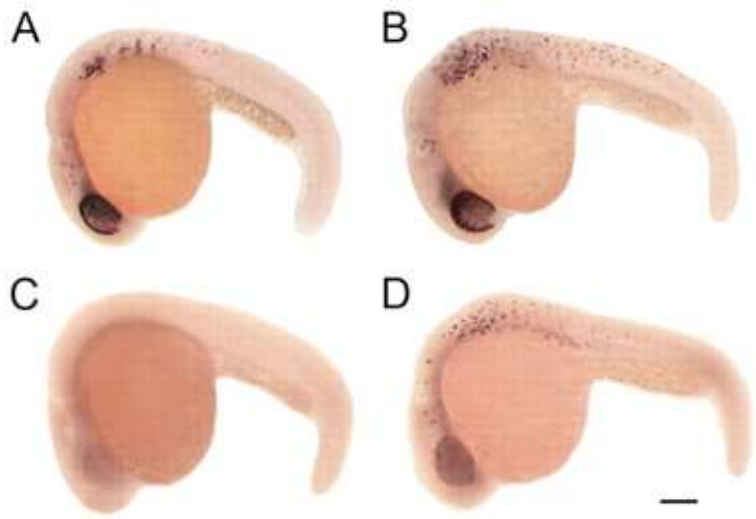

Figure 15
SLC24A5 and DCT expression in 24hpf zebrafish embryos.
A, SLC24A5 expression in wild type embryos. B, DCT expression in wild type embryos. C, SLC24A5 expression in golden embryos and D, DCT expression in golden embryos (Lamason et al., 2005)

As well as its obvious expression in the pigment cells, SLC24A5 transcript was also detected in other tissues, including heart and muscle (figure 16). Of particular interest is the increased expression level in B16 melanoma cells (figure 16), indicating this gene is upregulated during melanoma development. Determining the role of SLC24A5 could therefore provide additional information on the genes and functions involved in melanoma development and progression.

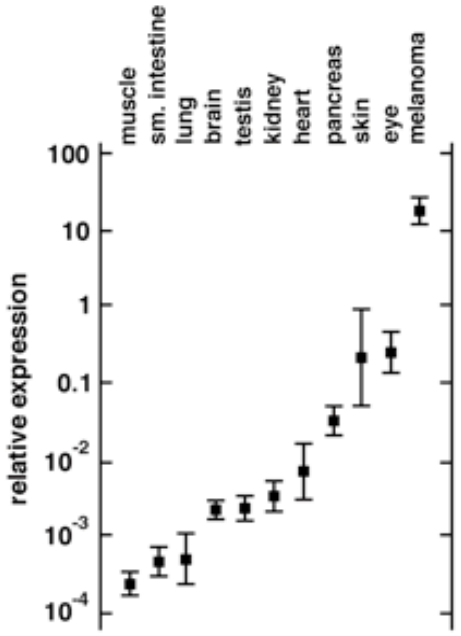

Figure 16
Relative expression of SLC24A5 in various tissues as analysed by RT-PCR (Lamason et al., 2005)

Lamason et al (2005) used confocal microscopy to detect GFP and HA tagged SLC24A5 proteins in MNT1 cells (constitutively pigmented human melanoma cell line), to analyse the intracellular expression pattern (figure 17).

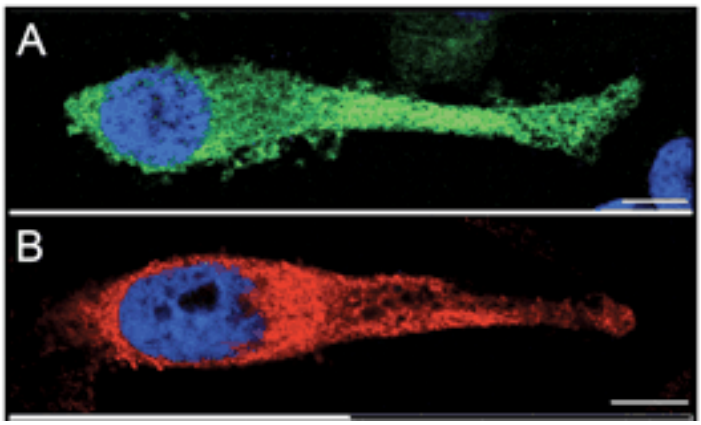

Figure 17
Intracellular localisation SLC24A5 following over expression in MNT1 cells.
A, GFP tagged SLC24A5. B, HA tagged SLC24A5 transfected into MNT1 cells (constitutively pigmented melanoma cells (Lamason et al., 2005).

As shown in figure 17 SLC24A5 is expressed throughout the cell, excluding the nucleus, showing no restriction to the plasma membrane. This is in contrast to other NCKX proteins which are found within the plasma membrane (figure 18).

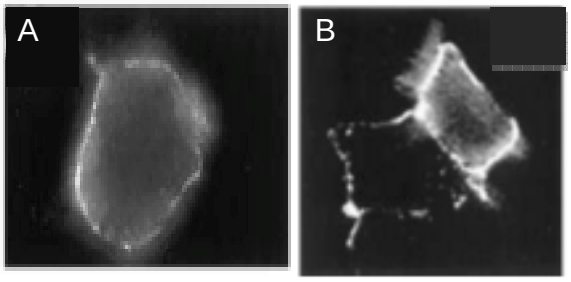

Figure 18
Localisation of NCXK1 (A) and NCKX2 (B) in HEK293 cells. These proteins are predominantly expressed in the plasma membrane (Kang and Schnetkamp, 2003; Poon et al., 2000).

Human SLC24A5 has since been shown to be partially localised to the trans-Golgi network (TGN) in human melanocytes, (figure 19). This fits with the TGN role as a calcium store and processing department for secretory and membrane proteins, which is sensitive to calcium fluctuations (Ginger et al 2008).

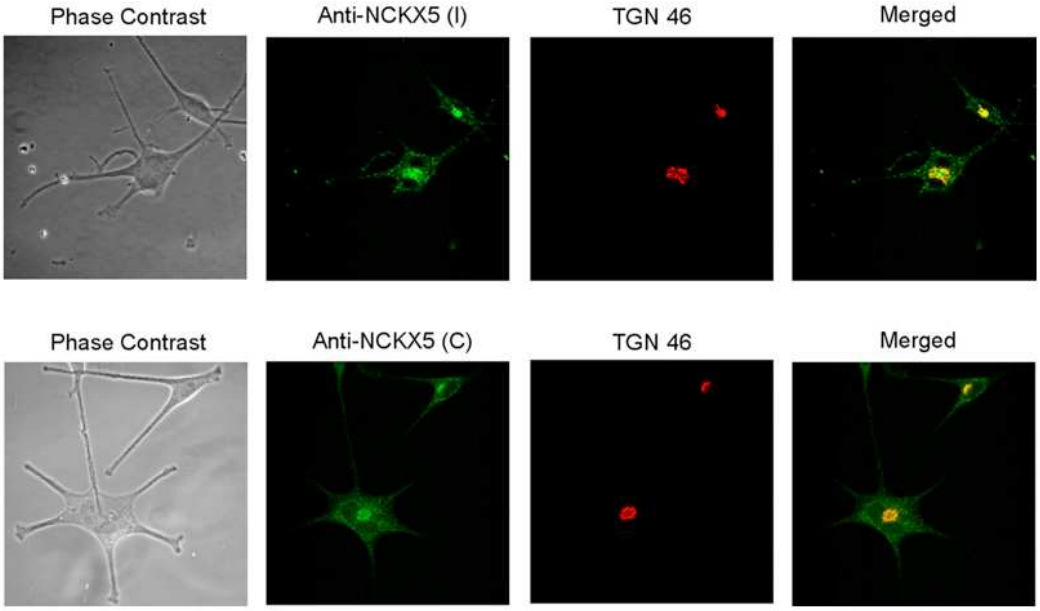

Figure 19
NCKX5 partially colocalises with the TGN.
Untreated normal human melanocytes (NHM) were probed with anti-NCKX5 (I antibody raised against the cytoplasmic loop or C antibody raised against the carboxyl terminal peptide) (green) or anti-TGN (red). Yellow staining in merged images indicates colocalisation (Ginger et al 2008).

1.9.3 Knockdown of SLC24A5

To confirm SLC24A5 was the gene responsible for the golden phenotype, Lamason et al (2005) used morpholinos to phenocopy the golden phenotype in zebrafish embryos. Figure 20 clearly shows morpholino knockdown of SLC24A5 results in the same phenotype as the golden mutant, where pigmentation is lost on the body as well as in the eye.

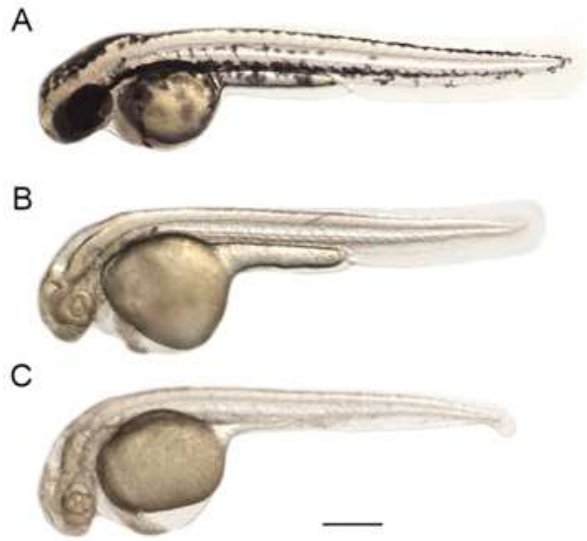

Figure 20
Morpholino knockdown of SLC24A5 in zebrafish embryos phenocopies the golden phenotype. A, wild type 48hpf zebrafish embryo. B, golden 48hpf zebrafish embryo. C wild type 48hpf embryo injected with morpholino targeted to SLC24A5 (Lamason et al., 2005).

SLC24A5 can also be knocked down by siRNA, this results in a marked reduction in melanin production (figure 21), and demonstrates a role for SLC24A5 in melanogenesis in human melanocytes (Ginger et al., 2008).

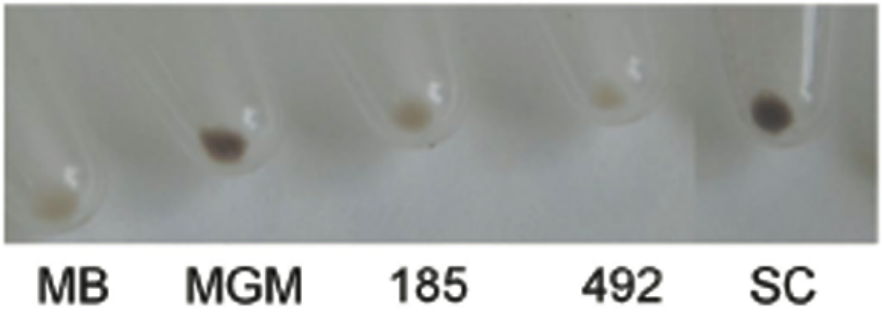

Figure 21
siRNA knockdown of SLC24A5 in NHM.
Light NHM were transfected with siRNA 185, siRNA 492, scrambled control (SC) or untransfected (MGM) and left to grow in MGM (M254 medium supplemented with human melanocyte growth supplement) or melanoblast media (MB) for five days. A clear reduction in pigmentation can be seen in the siRNA transfected cells, compared with the SC or untransfected samples. MB remain melanoblasts and therefore do not produce pigment (Ginger et al 2008).

Knockdown of SLC24A5 resulted in reduced protein levels of Pmel17, MART1, Tyr and Tyrp1, and increased levels of the lysosome associated protein Lamp1. Indicating that NCKX5 plays an early role in melanosome biogenesis and this is linked to lysosome biogenesis. However the mRNA levels were not affected. Therefore it is thought that NCKX5 may be involved in post transcriptional regulation of these proteins, most likely in the Golgi network as ER trafficking has been assessed by EndoH and PHGaseF treatment (Ginger et al., 2008; Wilson S., unpublished data).

SLC24A5 knockdown also effected the expression of several genes involved cholesterol and sterol homeostasis, including ATP-binding cassette transporter A1 and the low density lipoprotein receptor. This led to an increase in cytosolic cholesterol and esters. SLC24A5 has therefore been proposed to play a role in cholesterol homeostasis, (Wilson et al unpublished data). Reduced melanin pigmentation following SLC24A5 RNAi knockdown has also been observed in chicken RPE cells (Liu et al., 2011).

1.9.4 SLC24A5 encodes NCKX5

Sequence homology suggested that SLC24A5 encoded a member of the NCKX (potassium dependant sodium calcium exchanger) protein family – NCKX5, (Lamason et al 2005). This has been determined experimentally using a high five insect cell expression system (Ginger et al. 2008). In this assay the cells are transfected with human NKCX5 and loaded with sodium, this reverses the ion exchange direction and therefore allows radioactive calcium uptake to be measured. The A111T mutant protein was also assessed and showed less activity than the wild type.

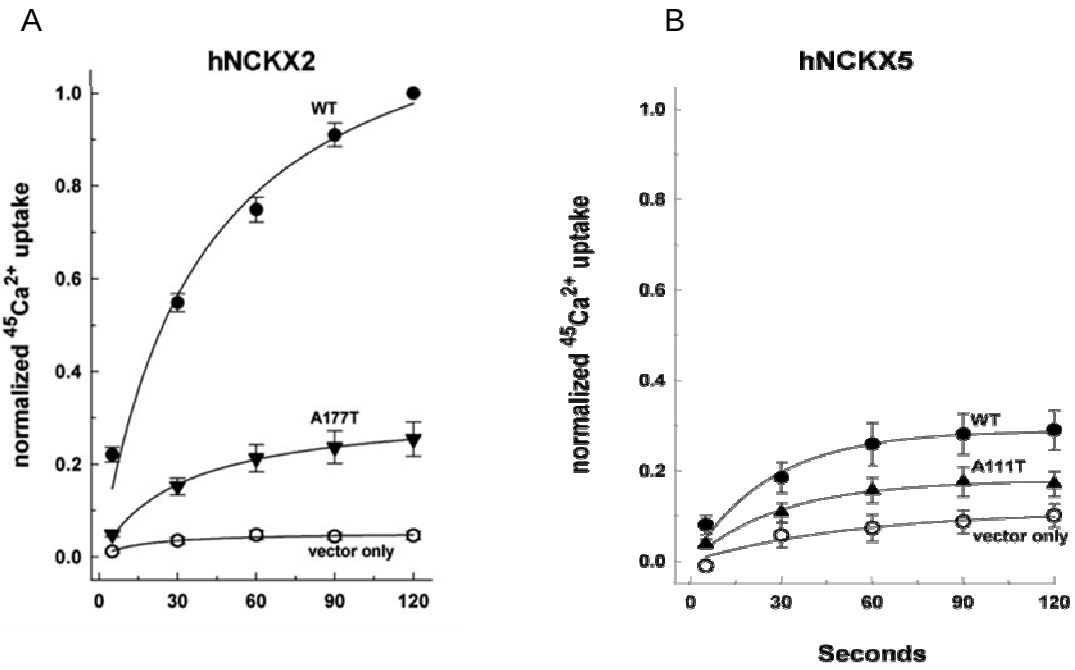

Figure 22
NCKX5 activity was determined using a heterologous expression system (Ginger et al., 2008). NCKX2 and NCKX5 were transfected into insect high five cells, which were loaded with Na^+ to reverse the direction of ion exchange. $45Ca^{2+}$ uptake was recorded.

As an ion exchanger, NCKX5 was initially assumed to reside in the plasma membrane, however as the expression analysis in MNT1 cells shows (figure 17), it is not restricted to the plasma membrane. Thus it is thought to reside in an internal organelle membrane, possibly the melanosome membrane although colocalisation studies suggest it is more likely to be in the TGN membrane (figure 19). An internal localisation of NCKX5 is also consistent with the functional data in figure 22. NCKX2 is a plasma membrane protein and shows much greater activity than NCKX5 in the same assay, also NCKX5 has to be over expressed in this assay to detect any function, this thought to be due to its being trafficked to and organelle membrane.

1.10 Pigmentation in *X.laevis*

X. laevis is an ideal developmental model organism in many respects. The adult animals are easy and cheap to keep, large numbers of eggs are easily obtained from the female by simple hormone injection and *in vitro* translation (IVF) can be performed using testes extracted from a euthanized male. The embryos are large and robust and thus amenable to microinjection and surgical manipulation.
In particular *X. laevis* tadpoles are suitable for pigmentation studies due to their distinct pigmentation pattern (figure 23). By stage 38 (Nieuwkoop and Faber, 1994) (~4 days post fertilisation) pigment cells (melanophores in lower vertebrates) can be clearly seen around the head, neural tube and along the lateral area. The retinal pigment epithelium (RPE) and cement gland is also very clear. *X.laevis* also have xanthophores and iridophores, these provide yellow pigmentation and reflective iridescent colouration respectively. They are also neural crest derived (Akira and Ide, 1987). However, as their function is distinct from melanophores they will not be discussed further here.
The distinct pattern of melanophores makes it very easy to observe pigmentation phenotypes in response to gain of function and loss of function experiments, especially since affecting pigmentation is rarely lethal. A previous chemical genomic screen identified several compounds that effect pigmentation, including migration and pigment production (Tomlinson et al., 2005; Tomlinson et al., 2009a; Tomlinson et al., 2009b; White et al., 2011).

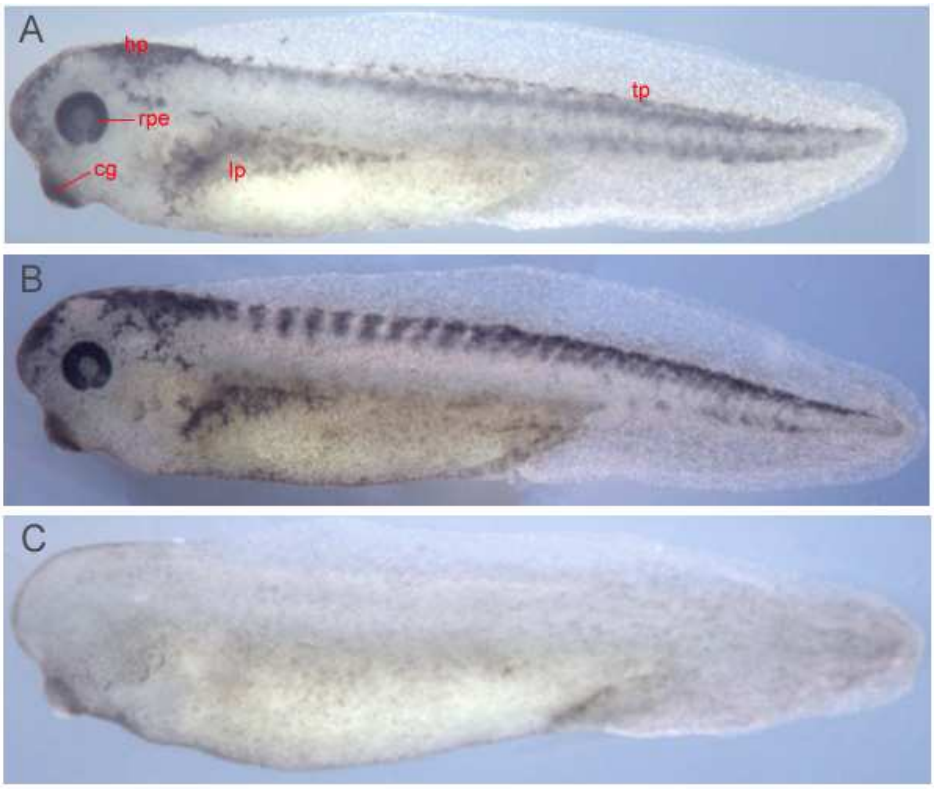

Figure 23
Pigmentation in *X.laevis* tadpoles. A, wild type stage 38 tadpole, hp; head pigmentation, rpe; retinal pigmented epithelium, cg; cement gland, lp; lateral pigmentation and tp; tail pigmentation. B, compound NCS 84093 from the Diversity Set, National Cancer Institute, caused a segmented pattern in the pigment cells and was found to be an matrix metalloproteinase (MMP) inhibitor. C, compound NSC 86153, also from the Diversity Set, caused a complete loss of pigmentation and was found to be a tyrosinase inhibitor (Tomlinson et al., 2009b)

Aims and Approaches

The aim of this project is to further characterise the role of SLC24A5 in *X.laevis* pigmentation development. This is part of an ongoing project coordinated by Unilever Discover. Bringing together a number of different labs with expertise in biochemical, computer modelling, cell based assay development and developmental biology. To look at SLC24A5 in greater detail in order to determine if it could be used as a target for manipulating pigmentation in humans.

Approaches will include PCR and cloning of *X.laevis* SLC24A5; whole mount *in situ* hybridisation to determine the expression pattern of SLC24A5 in *X.laevis* tadpoles. Morpholinos will be used to knock down expression of SLC24A5 in developing tadpoles. To begin to understand the biochemistry of SLC24A5 we will rescue the resulting phenotypes using mutant constructs of human SLC24A5. The effect of knocked down SLC24A5 on other melanogenic genes will also be analysed. Over expression analysis of SLC24A5 will also be conducted.

Chapter Two:

Materials and Methods

2.1 Frog housing and care

Animals were housed in large plastic tanks (approximately 1m x 1m), in 40L water. They were kept at 18℃ in 12 hour cycles of light and dark, the water was changed weekly. The diet of dried trout pellets was biweekly, and supplemented with live maggots. During egg collection females were squeezed once per hour for a maximum of 6 squeezes. After use females were rested for at least 3 months. The dissection of the males for testes was carried out following the legislation in the Animals (Scientific Procedures) Act 1986. Males were euthanized by immersion in a solution of 0.5g Ethyl 3-aminobenzoate methanesulfonate salt (sigma) in 300ml water for 1hr at 4ºC. To ensure the animal was dead the digits were nipped with forceps and the gag reflex tested. The testes were then dissected, any remaining blood vessels or other tissue was removed and the testes were stored in 100% goat serum at 4℃.

2.2 Obtaining embryos

To induce ovulation adult female *X.laevis* frogs were primed by sub cutaneous injection with 100U of Pregnant Mare Serum Gonadotropin (PMSG) into the dorsal lymph sac. The frogs were then kept at 18^{o}C for 4-7 days without feeding. 14 hours before the eggs were required the primed frogs were induced with 500U of Human chorionic gonadotropin (HCG) and placed at 18^{o}C. Eggs were obtained by manually squeezing female frogs over 9cm Petri dishes. IVF (in vitro translation) was conducted using testes isolated from a euthanized male frog. A small piece of testes was masticated and dragged with forceps over the freshly laid eggs, the piece of testes was then placed in an eppendorf tube with 1ml 1XMMR and further crushed using small plastic pestle. The testis/1XMMR

solution was then evenly distributed over the eggs, by pipette and left at 18^{o}C for 5 minutes. The eggs were then covered with 0.1XMMR for 20 minutes at 18^{o}C. Eggs can then be visually assayed for cortical rotation, an indication of successful fertilisation. Once fertilised, the jelly coating around the eggs is removed. The eggs are covered in 2% cysteine (pH 8) dissolved in 1XMMR and transferred to a 250ml glass beaker. Eggs are then gently swirled until de-jellying is complete, tight packing of the eggs is taken as an indication of jelly coat removal. The eggs are then immediately washed several times in 1XMMR then 0.1XMMR to remove trace amounts of cysteine. The eggs are now ready for experimental use and can be left at varying temperatures to influence developmental timing, embryos were staged according to Nieuwkoop and Faber (1994).

Solutions

0.1XMMR: 10mM NaCl, 0.2mM KCl, 0.1mM $MgCl_2$,0.2mM $CaCl_2$, 0.5mM HEPES (pH 7.5).

1XMMR: 100mM NaCl, 2mM KCl, 1mM $MgCl_2$, 2mM $CaCl_2$, 5mM HEPES (pH 7.5).

Cysteine: 5g L-cysteine (Sigma), 250ml 1XMMR, pH 8 by addition of ~1ml 10M NaOH

2.3 Generating cDNA from embryos

Total RNA was extracted from 10 stage 38 embryos using a Qiagen RNeasy mini kit, the protocol provided was followed. Reverse transcription from extracted total RNA was set up as follows on ice; 9.9µl dH_20, 6µl M-MLV RT 5x Buffer, 1µl DTT (100mM), 1µl dNTP mix-10mM, 1µl random hexamer, 200mg/ml, 1µl RNasin, 1µl (200U) reverse transcriptase, 10µl RNA template (1-3µg). Incubated at 42^{o}C for 1 hour.

2.4 Bioinfomatical sequence analysis

NCBI BLAST and Ensembl searches were conducted to find the sequence of SLC24A5 in several different species; human, mouse, zebrafish and *X.tropicalis*. These were aligned using DNAstar software, using the Clustral W method. From this sequence homology between species could be analysed with a view to designing primers for PCR to generate *X.laevis* SLC24A5.

2.5 PCR/RACE PCR

As the sequence for *X.laevis* SLC24A5 was unknown, PCR primers were designed from the closely related X.*tropicalis* sequence (www.xenbase.org), (see appendix). Reactions were conducted using a thermocycler. Each 50µl reaction contained; 1X PCR buffer, 2.5mM $MgCl_2$, 0.2µM of each primer, 0.25mM dNTPs, 1µl cDNA template and 1 unit Taq polymerase and up to final volume of 50µl with dH_2O. The conditions were; initial denaturation step of 94°C for 3 minutes, followed by 30 cycles of 94°C 30 seconds, 50°C 45 seconds, 72°C 1 minute, the reaction was finished with a 10 minute 72°C step. 5µl of each reaction was analysed by 1% agarose gel electrophoresis using ethidium bromide to visualise the DNA. This yielded an internal 800 base pair fragment of *X. laevis* SLC24A5, using primers I.P1F and I.P2R (see appendix). To obtain the 5' and 3' ends RACE (rapid amplification of cDNA ends) PCR had to be implemented.

2.5.1 5' RACE

RACE was conducted using Invitrogen GeneRacer™ kit.

3µg of total RNA was treated with 10U of calf intestinal phosphatase (CIP) in a reaction containing; 1X CIP buffer, 40U RNaseOut™ and made up to a final volume of 10µl with DEPC treated water, to dephosphorylate the mRNA , this was left at 50°C for 1 hour. The RNA was then extracted from the reaction by phenol chloroform and ethanol precipitation. Here 100µl of phenol:chloroform and 90µl of DEPC H_2O are added to the reaction, this is vortexed for 30

seconds. The sample is then centrifuged at full speed for 5 minutes. The top aqueous phase is removed and placed in a new tube. 2µl of 10mg/ml mussel glycogen, 10µl of 3M sodium acetate, pH 5.2, are added and the sample is mixed before 220µl of 95% ethanol is then added and this is vortexed briefly. The sample is then frozen on dry ice for at least 10 minutes. To pellet the RNA the sample is centrifuged at full speed for 20 minutes at 4°C. The supernatant is then discarded and 500µl of 70% ethanol is added, this is mixed and vortexed briefly followed by full speed centrifugation for 2 minutes at 4°C. The ethanol supernatant is removed and the sample is spun again and the residual ethanol is removed by pipette. The sample is then air dried for 10 minutes at room temperature. The dry RNA pellet is resuspended in 7µl of DEPC H_2O and stored at -20°C. The RNA was then treated with 0.5U of tobacco acid pyrophosphatase (TAP), to remove the 5' cap structure, this reaction contained 7µl dephosphorylated RNA, 1X TAP buffer, 40U RNaseOut™ in a final volume of 10µl, this was incubated at 37℃ for 1 hour, then the RNA was extracted using phenol chloroform and precipitated with ethanol, as described earlier. The GeneRacer™ RNA oligo was then ligated to the 5' ends of RNA. The oligo is specifically designed to ligate to decapped mRNA and contains priming sites for the GeneRacer™ 5' primers, supplied. The ligation reaction contained 1X ligase buffer, 1µl 10mM ATP, 40U RNaseOut™ and 5U T4 RNA ligase in a final volume of 10µl, this reaction was incubated at 37°C for 1 hour. After the ligation reaction the RNA is again extracted and precipitated using phenol chloroform and ethanol. The RNA is now ready to be reverse transcribed to cDNA to use as the template in the PCR. Reverse transcription was carried out using SuperScript™ III RT. For this reaction 1µl of GeneRacer ™ oligo dT, 1µl of a gene specific primer (RACE 1*), 1µl of dNTP mix and 6µl of dH_2O was added to 5µl of the ligated RNA, this was incubated at 65°C for 5 minutes to remove any RNA secondary structure. After this incubation the following components were added, 1X first strand buffer, 1µl 0.1M DTT, 40U RNaseOut ™ and 200U SuperScript ™ III RT, this reaction was incubated at 55°C for 1 hour then inactivated at 70°C for 15 minutes. 1µl of RNase H (2U) was added to the reaction mix and incubated at 37°C for 20 minutes. 1µl of this RACE ready cDNA was then used in a 50µl PCR with 1X buffer, 2.5mM $MgCl_2$, 0.2µM of each primer (Generacer™ 5' and RACE 1*), 0.25mM dNTPs, IU Taq polymerase and made up to 50µl with dH_2O. Touchdown conditions were used,

94℃ for 3 minutes, followed by 5 cycles of 94 °C for 30 seconds and 72°C for 1 minute, then 5 cycles of 94°C for 30 seconds and 70°C for 1 minute, then 25 cycles of 94°C for 30 seconds, 66°C for 30 seconds and 70°C for 1 minute, the reaction was completed with 70°C for 10 minutes. The products of this reaction were then used in a nested PCR, the reaction was assembled as described above, only with the previous PCR product as template and the GeneRacer 5' Nested primer, and the same touchdown conditions were used again.

2.5.2 3' RACE

3' RACE was carried out using Invitrogen 3' RACE system.

3µg of total RNA extracted from 10 stage 38 embryos was used in the first strand cDNA synthesis reaction, to this, DEPC treated water was added to a final volume of 11µl plus 1µl AP (adapter primer), solution, these were heated to 70°C for 10 minutes. The AP provided in the kit is designed to target the natural poly A tail of mRNA and contains several restriction enzyme sites as well as the priming site for the adapter primer. After the 10 minute incubation the following components were added to the reaction; 1XPCR buffer, 2µl 25mM MgCl2, 1µl 10mM dNTP mix and 2µl 0.1M DTT, this mixture was equilibrilated to 42°C for 5 minutes, after which time 1µl of SuperScript ^{TM} II RT was added and the reaction was incubated at 42°C for 50 minutes. The reaction was inactivated at 70°C for 15 minutes before being briefly chilled on ice, 1µl RNase H was then added and incubated for 20 minutes at 37°C. the cDNA is now ready to be used in PCR. The PCR contained; 1XPCR buffer, 2.5mM $MgCl_2$, 0.2µM of each primer (AUAP, abridged universal amplification primer, provided in kit, recommended for T4 DNA polymerase cloning and 3'RACE 2), 0.25mM dNTPs, 2µl cDNA, IU Taq polymerase and made up to 50µl with dH_2O. The conditions used were as follows; 94°C for 3 minutes, then 30 cycles of 94°C for 30 seconds, 58°C for 45 seconds and 72°C for 2 minutes, and completed with 72°C for 10 minutes. The product of this reaction was then used as the template in a nested primer reaction, the same recipe and conditions were used, only using the 3'RACE 3 nested primer.

2.5.3 Full Length PCR

Primers were designed from the 5' and 3' RACE products and used to generate the full sequence of SLC24A5. Stage 38 cDNA was used as the template, 12.5µl of BioTaq Premix was used with 1µl template, 0.2µM of each primer (FL 5'* and FL3'3*) and made up to 25µl with water. The reaction conditions were 94°C for 3 minutes, then 35 cycles of 95°C for 30 seconds, 64°C for 1 minute, 72°C for 2 minutes, and finished with 72°C for 10 minutes. This PCR product was cloned and sequenced.

2.5.4 Semi quantitative RT PCR

Primers XLF and XLR (see appendix) were used in PCR across a range of embryo stages to detect expression. Primers for DCT were used at the same stages to provide a comparison and Histone H4 primers were used as a loading control. The PCR contained; 1X PCR buffer, 2.5mM $MgCl_2$, 0.2µM of each primer, 0.25mM dNTPs, 1µl cDNA template and 1 unit Taq polymerase and up to final volume of 50µl with dH_2O. The conditions were; initial denaturation step of 94°C for 3 minutes, followed by 30 cycles of 94°C 30 seconds, 50°C (58°C for H4 and DCT primers) 45 seconds, 72°C 1 minute, the reaction was finished with a 10 minute 72°C step. Reactions were analysed by 1% agarose gel electrophoresis using ethidium bromide to visualise the DNA.

2.5.5 Intron/exon boundary PCR

PCR was also used to obtain sequence data over an intron/exon boundary such that a splice junction could be targeted by morpholino mediated knockdown. X.*tropicalis* intronic and exonic sequence data was determined bioinfomatically, this was then translated to the *X.laevis* sequence, obtained in this work. This revealed close homology over exons 9 and 10, (10 being the last exon).

To extract genomic DNA 10 stage 38 embryos were lysed in 1ml lysis buffer (50mM tris pH8.8, 1mM EDTA, 0.5% tween20, 200µg/ml proteinase K) and incubated at 56℃ for 4 hours, this was then used in PCR as follows. Primers SLC frameshift 1 and FL 3' 3* were used. PCR was carried out using Bioline taq

premix as previously described. Following initial denaturation at 95℃ for 3 minutes, 35 cycles of 95℃ 30 seconds, 66℃ 90 seco nds, 72℃ 150 seconds and a final elongation step of 72℃ 10 minutes. The resulting products were purified and cloned into pGEM and sequenced.

2.6 TA cloning

All PCR products were cloned directly into pGEM® T easy vector system from Promega. Taq polymerase adds a single A to the 3' end of PCR products, pGEM has a single T at the 3' end, thus Taq synthesized PCR products can be easily ligated into pGEM. PCR products were extracted from a 1% TAE agarose gel, following visualisation with ethidium bromide. Gel extractions were performed using a Qiagen gel extraction kit, manufacturers instructions were followed. Ligation reactions were assembled as follows; 1µl of pGEM vector, 1µl of 10X ligation buffer, 1µl Ligase, 4µl of PCR product, dH_20 to a final volume of 10µl and left at 16°C overnight. The ligation reactions were then transformed into DH5α competent E.coli cells. The ligation product was added to 100µl cells and incubated on ice for 30 minutes, the cells were then heatshocked at 42°C for 90 seconds then returned to ice for 2 minutes. 300µl of SOC media was then added and the cells were incubated at 37°C with shaking for 1 hour. After this incubation 150µl of the cells was spread onto pre-warmed, LB(Luria broth)/carbicillin plates along with 4µl IPTG ad 40µl Xgal, to allow for blue/white colony selection, the plates were left inverted at 37°C overnight. 12 white colonies were selected from each sample and grown overnight at 37°C in 5ml LB media, inoculated with carbicillin.

Solutions

LB, (Luria Broth) 1L: Tryptone 10g, Yeast extract 5g, Sodium Chloride 10, up to 1L with dH_2O autoclave to sterilise

SOC (super optimal broth with catabolite repression) media: 2% w/v bacto-tryptone (20 g), 0.5% w/v bacto-yeast extract (5 g) 8.56mM NaCl (0.5 g), 2.5mM KCl (0.186 g), $_{dd}H_2O$ to 1000 ml, 10mM $MgCl_2$ (0.952 g) or 20mM $MgSO_4$ (2.408 g), 20mM glucose (3.603 g)

2.6.1 Mini Prep isolation of plasmid DNA

To isolate the plasmid DNA from the E.coli culture alkaline lysis was used, using Qiagen kit buffers. 1.5ml of each culture was transferred to an eppendorf tube and centrifuged for 5 minutes at maximum speed. The supernatant was discarded and the cell pellet was resuspended by vortexing in 100µl buffer P1 (resuspension buffer, 50mM Tris-Cl pH 8.0, 10mM EDTA, 100µg/ml RNase A). 200µl of buffer P2 (alkaline lysis buffer, 200mM NaOH, 1% SDS) was added, mixed by inverting 6 times and left on ice for 5 minutes. 100µl ice cold buffer P3 (neutralisation buffer, 3.0M potassium acetate pH 5.5) was added next and mixed by inverting, this was centrifuged for 10 minutes at maximum speed. The supernatant was, discarded and the pellet was washed with 100% ethanol, air dried and resuspended in 30µl water. Mini prep samples were then analysed by restriction digests. 1µg of DNA was added to 1µl 10X buffer, 1µl appropriate restriction enzyme and up to 10µl H_2O, the digests were left at 37°C for 1 hour. For pGEM diagnostic digests were performed using EcoR1 as this cuts either side of the cloning site, thus dropping out the insert.

2.6.2 Midi prep isolation of plasmid DNA

Following mini prep and restriction digest analyses, 2 colonies of each sample were grown up in 50ml LB/carb media, overnight at 37°C with shaking. Plasmid DNA was then isolated from these cultures using the Qiagen Compact Midi prep kit, manufacturers instructions were followed. DNA concentrations from midi preps were determined by gel electrophoresis, using a quantative DNA ladder and nanodrop OD readings, and the appropriate amount sent for sequencing.

2.6.3 Sequencing

All sequencing analyses was conducted by Unilever Discover at Colworth Park, Bedfordshire. Using plasmid primers T7 and SP6 and gene specific primers.

2.7 Whole mount In Situ Hybridisation

2.7.1 Probe synthesis

Plasmids containing cDNAs to be tested were first linearised by restriction enzyme digestion (according to manufactures guidelines; Roche), using an appropriate downstream restriction enzyme site. Probe synthesis with a promoter specific RNA polymerase, used the following reaction conditions; 2µl linearised DNA template, 2µl DTT, 1µl DIG labelled UTPs, 1µl RNase inhibitor, 2µl (40U) RNA polymerase, 4µl transcription buffer, dH_2O to a final volume of 20µl. This was incubated at 37^{o}C for 3hrs. The reaction was stopped and diluted to 50µl with Sigma H_2O. Unincorporated UTPs were removed by G50 column centrifugation, according to the manufacturers protocol. Probe quality and transcription efficiency was checked by agarose gel electrophoresis. 5µl of the purified probe was mixed with 1ml of Hybridisation buffer for long term storage at –20^{o}C. Under normal conditions sufficient probe was generated to make 15mls of probe:Hyb buffer mix.

2.7.2 In situ protocol

Following egg collection and fertilisation, embryos can be fixed at the desired stage by a 1 hour wash in MEMFA, after which they are rinsed in DEPC PBST and can be stored in 100% EtOH at -20ºC, or processed immediately for *in situ* analysis. Whole mount *in situs* were done according to (Harland, 1991). Embryos were re-hydrated after storage in 100% EtOH using 100%, 75%, 50% and 25% methanol/phosphate buffered saline with 0.1% Tween 20 (PBST) 5 minutes each and finally 2 washes of DEPC PBST. The embryos were then treated with 10µg/ml Proteinase K for 5 minutes for stage 20-25 embryos and 8 minutes for stage 38-40 embryos. Washed twice with a 0.1M triethanolamine solution (pH 7.8) at RT for 5 minutes each, then 2.5µl of acetic anhydride was added. Embryos were allowed to wash in this solution for 5 minutes at RT before another 2.5µl of acetic anhydride was added. Embryos were then transferred into DEPC PBST twice for 5 minutes each and then incubated in 3.7% formaldehyde/DEPC PBST for 20 minutes at room temperature with rocking.

Embryos were washed three times in PTw, 5 minutes each, then transferred into hybridisation buffer for 2-6hrs at 60ºC.

After the embryos are adjusted to the hybridisation buffer they were then incubated overnight in hybridisation buffer plus probe at 60^{o}C with rocking. Probe was replaced with fresh hybridisation buffer for 10 minutes, 3 washes of 2x Sodium Chloride and sodium Citrate solution at pH 7 (2XSSC) for 20 minutes each and 2 washes of 0.2X SSC (pH 7) for 30 minutes each, all at 60ºC. The probe can then be stored at -20°C and reused up to ten times. The embryos were then washed twice with 1xMAB (Maleic acid buffer) for 5 minutes at room temperature and blocked in 2% BMB/1xMAB for 1 hour.

Embryos were then incubated over night (15-16 hours) with anti-digoxigenin (1:1000) in 2%BMB/20% Goat serum/ 1XMAB at 4^{o}C. The antibody solution was replaced with 1XMAB and washed by five further washes of 1XMAB at pH 7.5, 30 minutes each at room temperature the final wash was allowed to incubate over night at 4ºC.

The colour reaction was performed after washing the embryos in freshly prepared alkaline phosphate buffer twice for 5 minutes at room temperature. Detection of the probe was performed by using NBT/BCIP in alkaline phosphate buffer, keeping the embryos in the dark. Whole mount embryos were photographed using a Ziess stemi SV 6 stereo dissection microscope and Qcapture software.

<u>Solutions</u>

MEMFA: 10% MEM salts, 10% formaldehyde

MEM salts: 0.1M MOPS, 2mM EGTA, 1mM $MgSO_4$, pH7.4

PBS 10X: 2.5g $NaH_2PO_4.H_2O$, 11.94g $NaHPO_4.H_2O$, 102.2g NaCl, 400ml DEPC dH_2O. pH adjusted to 7.4 and volume to 1 litre.

PBST: 1XPBS, 0.1%Tween 20.

Proteinase K (10μg/ml): 1μl proteinase K, 1ml PBST.

Triethanolamine (0.1M), pH 7.5: 1.86g triethanolamine, 90ml DEPC H_2O, pH was adjusted to 7.8 and volume to 100ml with DEPC H_2O.

Hybridisation buffer: 50% formamide, 5XSSC, 1mg/ml Torula RNA, 100μg/ml Heparin, 1X Denharts solution, 0.1% Tween 20, 0.1% CHAPS, 10mM EDTA.

SSC 20X: 175.3g NaCL, 88.2g Sodium citrate. pH adjusted to 7.0 and volume to 1 litre with DEPC H_2O.

MAB 1X (Maleic Acid Buffer): 100mM Maleic acid; 150mM NaCL (pH 7.5).

Blocking solution: 2% BMB in 1X MAB.

BMB (Boehringer Mannheim Blocking agent) 10%: 10% (w/v) in BMB preheated (50^{o}C) 1XMAB, stirred until dissolved and then autoclaved, aliquoted and stored at –20^{o}C.

Antibody solution: 2% BMB, 20% goat serum, anti-DIG Fab fragment, (1:2000 dilution) in 1X MAB.

Alkaline Phosphatase Buffer: 100mM Tris (pH 9.5), 50mM $MgCl_2$, 100mM NaCl, 0.1% Tween 20.

BCIP: 50mg/ml in 100% DMF.

NBT (Nitro Blue tetrazolium): 75mg/ml in 70% dimethylformamide (DMF).

2.7.3 Bleaching embryos

Following in situ hybridisation some stage 38 embryos were bleached to remove the naturally occurring pigment, to better observe the in situ colour. To achieve this, embryos were submerged in bleach solution in a multi well dish, placed on a fluorescent light box and covered in foil for approximately 10 minutes, inspecting the reaction every 2 minutes. When the desired affect was achieved the embryos were rinsed twice in PBST for 5 minutes before fixing in MEMFA overnight at 4°C.

Bleach solution

10% H_2O_2, 5% formamide, 0.5XSSC, up to final volume with dH_2O.

2.7.4 Histology

To further analyse embryos after in situ hybridisation or to inspect the morpholino mediated disruption of the natural pigment pattern, embryos were processed for cyrosectioning. Embryos were fixed in MEMFA overnight at 4°C. Following two 5 minute PBS washes the embryos were incubated overnight in 30% sucrose (in PBS) at 4°C. The embryos were then embedded in OCT (TissueTek). A labelled cyro mould (10mm x 10mm x 5mm) was filled with OCT, using forceps the embryo was gently placed into the cryo mould and using a dissecting microscope the embryo was vertically aligned. These where then snap frozen on dry ice and kept at -20°C until sectioned. Sectioning was performed using a Leica cyrostat CM1950.

2.8 Microinjection of embryos

Microinjection was into a single blastomere at the two cell stage, or other targets as discussed later. Needles were calibrated to inject 10nl/injection using Harvard Apparatus Pli100 set to P_{out}= 16, $P_{balance=}$ 0.6 and P_{inject}=85. Injections were carried out in 3% ficol in 1XMMR. To perfect the injection technique lacZ cRNA was injected and its expression analysed by detecting β-galactosidase activity as follows; embryos were rinsed in DEPC PBS 3 times for 10 minutes before fixation in MEMFA for 1 hour at room temperature (no longer as this could impair β-galactosidase activity). They were then rinsed again in DEPC PBS 3 times for 10 minutes before being transferred in the Red Gal colour mix, which comprises; 5mM $K_3Fe(Cn)_6$, 5mM $K_4Fe(Cn)_6$, 1mg/ml Red Gal* and 2mM $MgCl_2$.

After complete development, 1-2 hours, embryos were rinsed in DEPC PBS 3 times for 10 minutes and re-fixed in MEMFA for 1 hour at room temperature. MEMFA was then replaced with 100% MeOH and the embryos were stored at -20ºC.

*Red Gal (Apollo Scientific, cat No. 1026) 1g was dissolved in 50ml DMF to make a 20mg/ml stock, and aliqutoted and stored at -20ºC.

2.9 Using Morpholino to manipulate gene expression

Morpholinos are used to repress translation of the target gene. The morpholinos were designed by Gene Tools (Oregon, USA) based on supplied sequence of *X.laevis* SLC24A5. Morpholinos were re-suspended in 300µl RNase free water to make a 1mM stock, which was aliquoted and stored at -20°C, after thawing they were heated to 65°C for 10 minutes prior to use, morpholinos were kept at room temperature during use. Morpholino was delivered to a single blastomere at the two cell stage by microinjection. Embryos were then left in 3% ficoll/1XMMR at 23°C, to activate the morpholino and accelerate embryo development.

Morpholino efficacy was tested using the Promega TNT in vitro translation kit, L4600. Manufacturers protocol was followed, using S35-methionine. Samples were not boiled prior to SDS PAGE on a 10% gel. Photograph film was exposed overnight.

2.9.1 Rescuing the morpholino knockdown

Human SLC24A5 was used to rescue the morpholino knockdown phenotype. cRNA was synthesised from wild type and mutant human SLC24A5 in pCS2+ and co-injected with 100ng morpholino, injections were performed as above. cRNA was synthesized using the mMESSAGE mMACHINE kit from Ambion, the manufacturers instructions were followed.

2.9.2 Statistical analysis

Statistical analysis was undertaken to determine the significance of the rescues. The Kruskal Wallis test was used to compare the difference between the percentage of phenotypes seen in the rescue data and the morpholino alone data. $P < 0.05$ indicates statistical significance. This in indicated at the top of the graphs.

2.9.3 Mutating *X. laevis* SLC24A5

In order to rescue the morpholino phenotype with *X. laevis* SLC24A5 it had to be mutated such that the morpholino wouldn't recognise it, it also had a myc tag incorporated so it could be detected by western blot. A primer was designed over the morpholino target sequence with two base pair changes, this conveniently gave a BamH1 site (SDM of SLC, see appendix). This primer was used in a PCR reaction with the FL 3*2 primer (see appendix), the reaction was assembled as follows; 12.5µl Bioline Taq pre mix, 2.0µl primers (20µM), 1.0µl template cDNA, 1.0µl phusion, 6.5µl H_2O, the conditions for the reaction were; 95°C 3 minutes, followed by 35 cycles of 95°C 30 seconds, 62°C 1 minute, 72°C 2 minutes and finished with 10 minutes at 72°C. 1µl of taq was added for 15 minutes at 72℃. The product was gel purified and cloned into pGEM as previously described, this clone is pRW07.

2.9.4 Adding the myc tag

To facilitate incorporation of a myc tag into pRW07, an EcoR1 site was inserted at position 93 of the amino acid sequence. PCR using primers 5' Xho1 and EcoR1R, and EcoR1F and 3'Xba1** yielded two products each with an EcoR1 site. These products were gel purified and ligated together using T4 ligase, and cloned into pGEM. This clone is pRW08.

Separately, PCR was performed using pRW07 as template again, and primers including the myc tag sequence and another EcoR1 site (5' Xho1 and mycR). This yielded a 300bp fragment of the 5' end of the gene with the myc tag sequence and EcoR1 site at the 3' end. This was also purified, cloned and named pRW09.

Both pRW08 and pRW09 were digested with EcoR1 and re-ligated together to give a full length clone containing a myc tag and mutation at the morpholino target sequence. This clone was sub cloned into pCS2+ using Xho1 and Xba1, previously included in the PCR primers, and named pRW11.

2.10 Western blotting

Western blotting was used to detect the myc tagged constructs after injection into the embryo.

2.10.1 Preparing embryos

At stage 11, 10 embryos from each injection were lysed in 100µl NP40 containing protease inhibitors and left on ice for 10 minutes. To extract the proteins 300µl of Freon was added, the mixture was vortexed thoroughly then spun at 4℃, at full speed for 15 minutes. After centrifugation the top layer of the mixture was removed and stored at -20℃.

2.10.2 Determining protein concentration

Total protein concentrations were determined by the Bradford assay. Individual samples were compared to a standard curve constructed of known bovine serum albumin protein concentrations (BSA 0-10mg/ml), 1 µl of sample was added to 1ml 1x BIORAD Bradford reagent, the OD values were read at 595nm (A_{595}).

2.10.3 SDS PAGE

Embryo lysates were separated by SDS PAGE. The glass plates were cleaned with 70% ethanol and assembled in the BIORAD apparatus. A 10% resolving gel was prepared and poured in between the glass plates, this was topped with 0.5ml isopropanol and left to set. The isopropranol was removed by blotting with Whatman paper. A 4% stacking gel was prepared and poured on top of the resolving gel, a well comb was inserted immediately and the gel was left to set. The gel was then assembled in the BIORAD mini PROTEAN® TETRA system and covered with running buffer. Protein loading buffer (2µl) was added to 50µg of each lysate, which were then loaded on to the gel. A protein marker

(Precision Plus Protein Standards, BIORAD) was loaded on the gel. Gel electrophoresis took place at 200V for 45 minutes.

2.10.4 Wet transfer

The gel was removed from the electrophoresis kit and placed into transfer buffer for 5 minutes. A piece of PVDF membrane was soaked in 100% methanol for approximately 30 seconds. The gel was transferred to the PVDF (BIORAD Immuno-Blot™ 0.2µm) membrane using the BIORAD mini PROTEAN II ™ kit in transfer buffer, at 100V for one hour.

2.10.5 Antibody treatment

After transfer the gels were blocked in 5% (w/v) skimmed milk powder in PBST for one hour, at room temperature with gentle agitation, then incubated in primary antibody overnight at 4℃, with gentle agitation. The gels were then rinsed in PBST three times for 5 minutes each, before 1 hour incubation in secondary antibody.

2.10.6 Antibody detection

The gels were rinsed in PBST, 3X5 minutes, again. The antibody was detected using enhanced chemiluminescence (ECL) and Fujifilm LAS 3000 Intelligent dark box.

Solutions

NP40; 150nM NaCl, 1% NP-40, 50nM Tris pH 8.0

Freon; 1,1,2, trichlorotrifluroethane 99.9%

Resolving gel (10%); Tris-HCl (1.5 M, pH 8.8), 3.33ml 30% Bis-acrylamide, 0.1ml 10% SDS, 0.05ml 10% APS (ammonium perrsulphate), 0.01ml TEMED, 4.01ml dH2O.

Stacking gel (4%); 2.5ml Tris-HCl (0.5 M, pH 6.8), 1.33ml Bis-acrylamide, 0.1ml 10% SDS, 0.05ml APS, 0.02ml TEMED, 6ml dH2O.

Running buffer; 10ml 10%SDS, 100ml 10X tris glycine, 890ml dH_2O

Transfer buffer; 100ml 10X tris gylcine, 700ml dH_2O, 200ml 100% methanol

10X tris gylcine; 25mM Tris, 192mM glycine pH 8.3, up to 1L dH_2O

Antibodies; primary - anti myc (9B11 New England Biolabs), diluted 1:1000 in 5% skimmed milk, secondary – polyclonal goat anti mouse immunoglobins HRP diluted 1:2000 in 5% skimmed milk, actin mouse monoclonal, Abcam.

ECL Solution 1; 200µl luminol (250mM), 88 µl p-coumaric acid (90mM), 2ml Tris (1M, pH 8.5), 17.7ml H_2O.

ECL Solution 2; 12 µl H_2O_2 (30%), 2ml Tris (1M, pH 8.5), 17.7ml H_2O

Chapter Three:

Cloning *X.laevis* SLC24A5

3.1 Background

As discussed earlier, SLC24A5 was first found as the gene responsible for the golden hypopigmented phenotype seen in zebrafish (Lamason et al., 2005). Human SLC24A5 carries a non synonymous SNP which correlates with lighter skin populations.

Due to its significant role in human skin pigmentation, SLC24A5 is of interest to the large international household product company Unilever. Here they have worked with SLC24A5 for over 6 years and collaborate with several labs. This project was developed to provide an in vivo dimension to their research. The Unilever team have analysed the intracellular expression of SLC24A5 and demonstrated its function as an ion exchanger in cell culture (Ginger et al., 2008). Unilever also conducted a genomewide association study of skin pigmentation, this included analysis of more than 1.6 million SNP's in a South Asian population, where they found that polymorphisms in SLC24A5, SLC45A2 and tyrosinase account for a large proportion of the natural variation of human skin pigmentation (Stokowski et al., 2007).

3.2 Introduction

The genome of *X.laevis* has not yet been sequenced. This is partly due to the pseudotetraploidy of the species. Some genes and expressed sequence tags have been published, but it is difficult to obtain some sequences of interest. *X.tropicalis (Xenopus tropicalis)* is more commonly used for genetic studies and does now have a published genome sequence (Hellsten et al., 2010). However, this was not available at the start of this project.

No previous work has been conducted on *X.laevis* SLC24A5; as such no sequence data was available. Therefore bioinfomatical approaches were employed to investigate the sequence information available from other species.

This included Ensembl and GenBank searches. The human and zebrafish sequence have been well characterised (Lamason et al., 2005), the mouse sequence was also found (Vogel et al., 2008), but of particular use was the *X.tropicalis* sequence, which was found in Ensembl. From this sequence primers were designed for PCR to be used with *X.laevis* cDNA. Alignment analysis using DNAstar software revealed approximately 68% similarity in the protein sequence across the different species (figure 24).

The pseudotetraploidy of *X.laevis* complicates the process of isolating a gene of interest by PCR, as there may be more than one paralog of the gene. Although primers were designed from highly conserved regions of the gene in other species, this is no guarantee that they will work with the *X.laevis* template. Thus a considerable amount of optimisation was required to yield even a fragment of *X.laevis* SLC24A5. Eventually RACE PCR was utilised to identify the 5' and 3' extremities of the sequence. Successful RACE PCR negated the need to screen a cDNA library. Template cDNA generated from stage 38 (Nieuwkoop and Faber, 1994) tadpoles was used for all PCR analyses as at this stage the tadpoles have developed their characteristic pigment pattern.

RACE PCR is based on oligo-capping and RNA-ligase mediated (RLM) techniques (Fehr et al., 1999). These methods involve replacing the cap structure of mRNA with a predefined oligonucleotide to label this region (Maruyama and Sugano, 1994) and using T4 RNA ligase to join endogenous RNA to a predefined ribonucleotide sequence respectively (Clepet et al., 2004; Volloch et al., 1994). In the RACE method used here unknown regions of DNA are amplified between primers in the known sequence and within 'tags' added to the 5' or 3' ends (Scotto-Lavino et al., 2006).

3.3 Results

In order to functionally characterise SLC24A5 in *X.laevis* we need the nucleotide sequence. Bioinfomatic searches using the NCBI BLAST and Ensembl programmes identified two transcripts for *X.tropicalis*, encoding 503 and 555 amino acid peptides. Figure 24 shows an alignment of these sequences with human, mouse and zebrafish SLC24A5. The transcript encoding a 555 amino acid peptide appeared to have extra sequence in the middle which is not homologous to any of the other species; therefore this sequence was not used for further analyses.

Several PCR primers were designed from the X.*tropicalis* 503 sequence (appendix). Primer3 software was used to assist primer design, factors such as; length, AT:GC content, annealing temperature and sequence repeats were considered to ensure optimum performance of the primers. The primers were tested and optimised on cDNA synthesised from X.*tropicalis* stage 38 tadpoles (kind gift from Lyle Zimmerman).

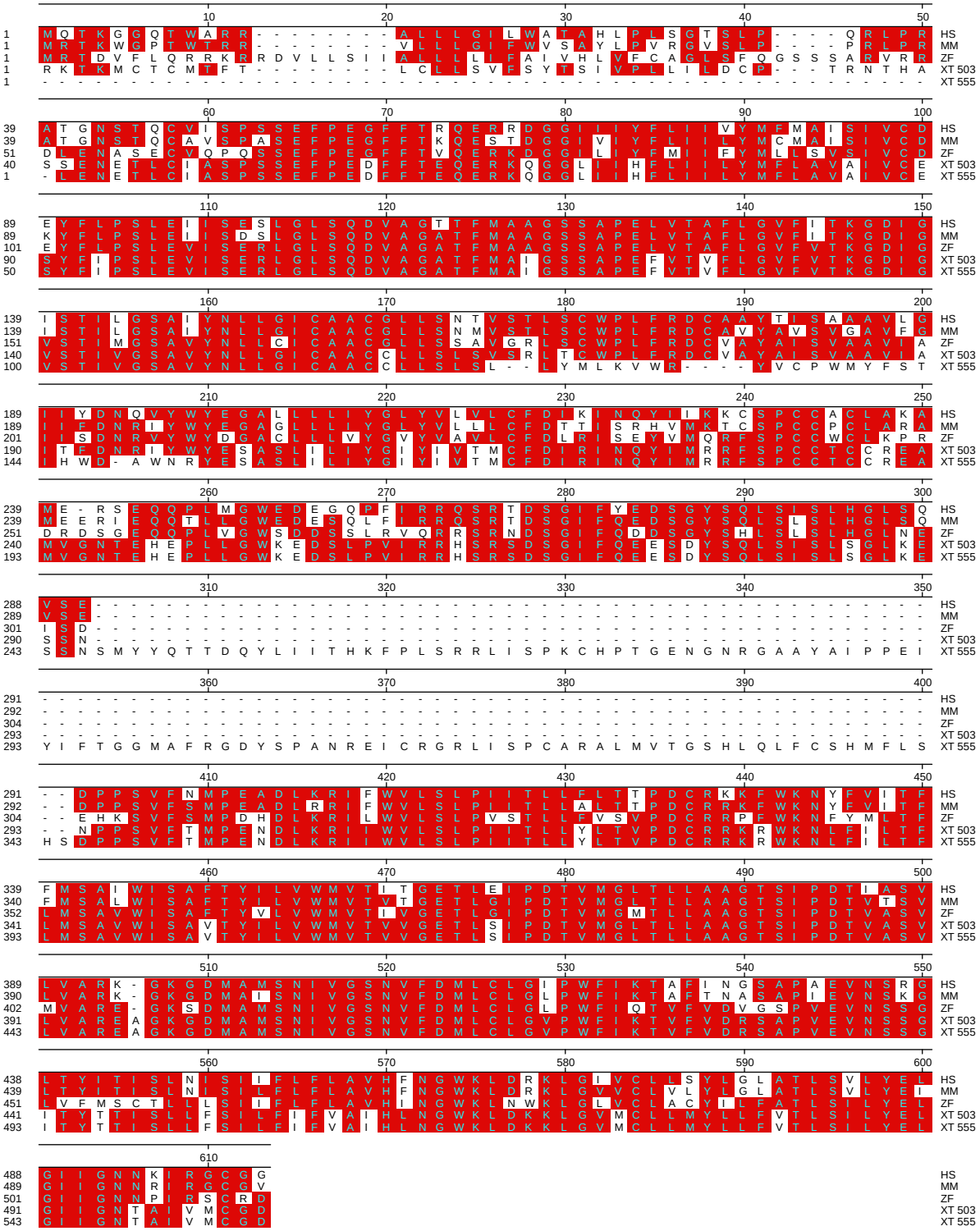

Figure 24
ClustalW alignment using DNAstar, of the *X.tropicalis* (39854) SLC24A5 protein sequences with human (283652), mouse (317759) and zebrafish (570312) reveals close similarity of 68.7% over the protein sequence across the selected species. GenBank numbers in brackets..

3.3.1. Initial PCR's yield a fragment of *X.laevis* SLC24A5

Primers XT I.P1F and XT I.P1R yielded a 400bp fragment of *X.tropicalis* SLC24A5 (figure 25A). XT I.P1F/I.P1R and XT I.P2F/I.P2R primers were then used on stage 38 *X.laevis* cDNA which yielded two separate overlapping 400bp fragments (figure 25B and C). The outer primers of these fragments (I.P1F and I.P2R) were then successfully used to create an 800bp fragment of SLC24A5 in *X.laevis* (figure 25 D). This was cloned into pGEM T easy and sequenced. The alignment data showed approximately 70% similarity of *X.laevis* SLC24A5 compared with human, mouse, zebrafish and *X.tropicalis* (figure 26).

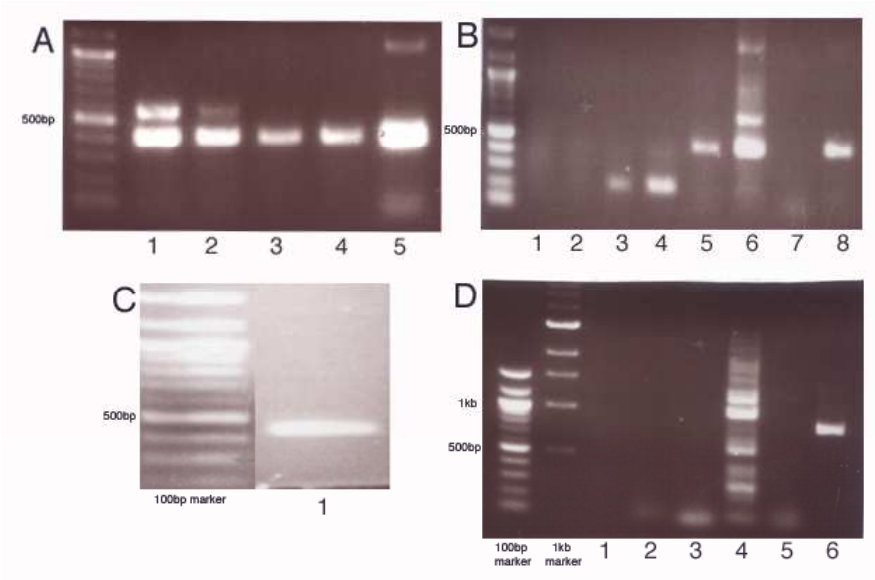

Figure 25
PCR results
A, PCR using primers IP1F/IP1R over a temperature gradient yields a 400bp fragment of *X.tropicalis*, lane 1 54℃, lane 2 56℃, lane 3 58℃, lane 4 60° C, lane 5 ODC control. The product in lane 4 was cloned and sequenced.
B, PCR using the same primers and temperature gradient yields a 400bp fragment of *X.laevis* SLC24A5. Lanes 1-4 H4 controls, lane 1 50℃, lane 2 53℃, lane 3 57℃, lane 4 60℃. Lanes 5-8 primers IP1F/IP1R, lane 5 50℃, lane 6 53℃, lane 7 57℃, lane 8 60℃. The product in lane 8 was cloned and sequenced.
C, PCR at 60℃ with primers IP2F/IP2R yields a seco nd 400bp fragment of *X.laevis* SLC24A5. This product was cloned and sequenced; it is just slightly downstream of the first 400bp fragment.
D, combinations of different primers were used to try to obtain further *X.laevis* sequence of SLC24A5. Lane 1 IP1F/SLCR, lane 2 SLCF/SLCR, lane 3 SLCF/IP1R, lane 4 IP2F/SLCR, lane 5 SLCF/IP2R, lane 6 IP1F/IP2R. Only lane 6 worked, this 800bp product was cloned and sequenced; this is effectively the two previous 400bp fragments together.

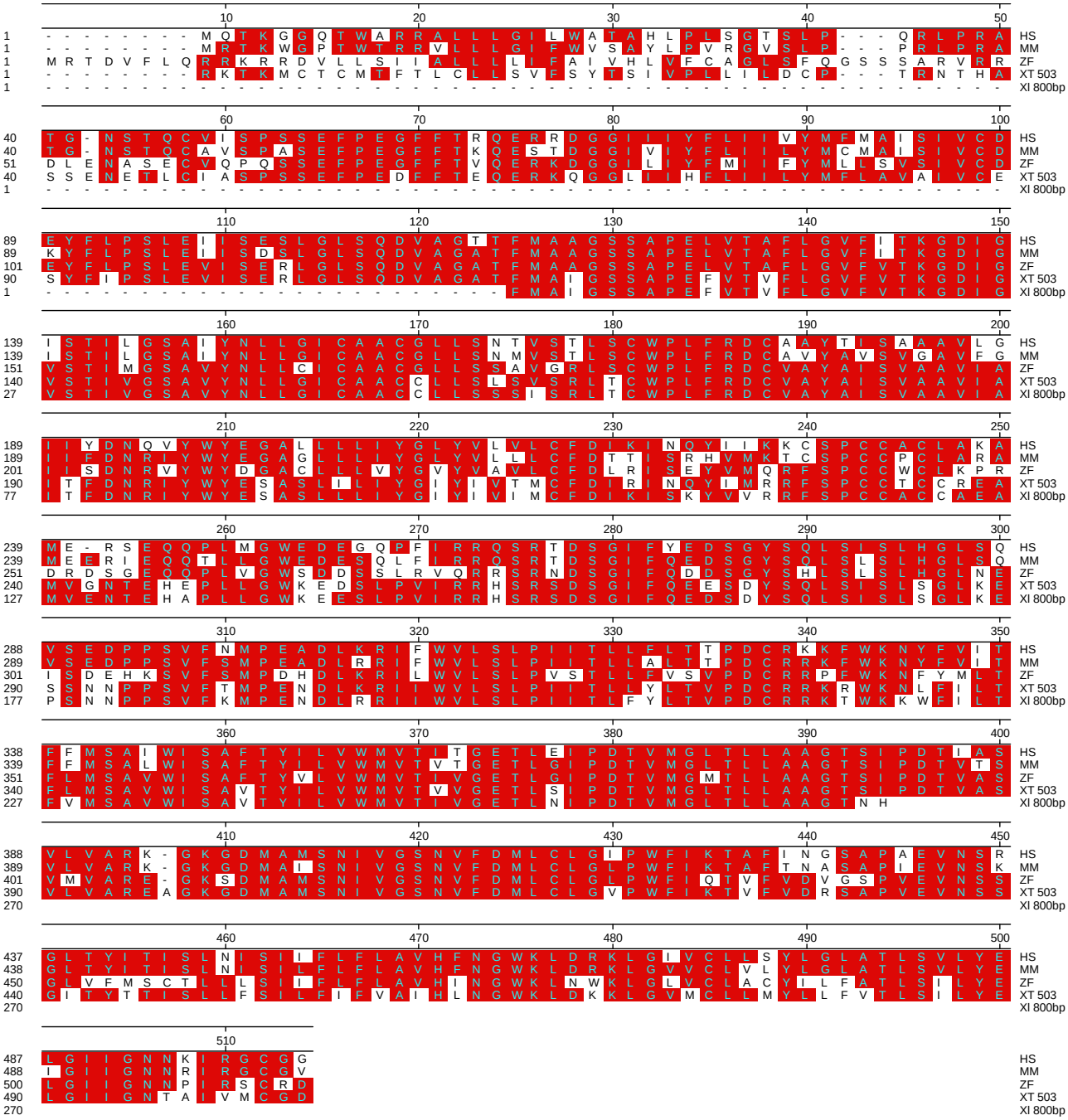

Figure 26
Alignment of the 800bp *X.laevis* sequence, showing the missing the 5' and 3' sequence.

3.3.2 5’ RACE

The 800bp fragment of *X laevis* SLC24A5 initially cloned was an internal fragment providing no sequence data for the 5’ or 3’ ends (figure 26). 5’ sequence is crucial for designing a morpholino, so other primers were designed and used to try to obtain the extremities of the sequence, however despite numerous PCR’s this sequence was not found, so RACE (rapid amplification of cDNA ends) was used. RACE PCR is a technique frequently used to facilitate the isolation of 5’ and 3’ end sequence data.

To perform 5’ RACE, total RNA was obtained from stage 38 *X.laevis* embryos. The RNA is treated as described in materials and methods to remove phosphate groups and the cap structure. After these reactions the specific oligo, provided in the kit, can be ligated, using T4 ligase, to the 5’ end, the oligo will only attach here as it needs the free phosphate group left after the de-capping reaction. The oligo contains the priming site for the RACE PCR primers also provided in the kit, this ensures polymerisation will only commence at the 5’ end. In conjunction with a 3’ gene specific primer (RACE 1*) designed from the 800bp sequence the 5’ end was amplified, (figure 27).

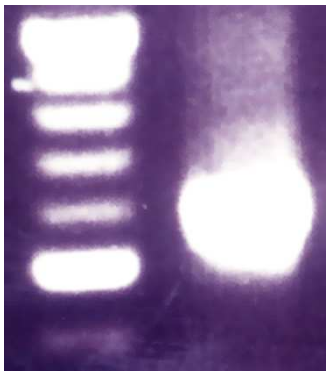

Figure 27
5’ RACE PCR product
This 5’ product was obtained using GeneRacer 5’ and RACE1* primers. This fragment is approximately 600bp, indicating ~480bp of new 5’ sequence is present; this correlates with the length of 5’ sequence of other species seen in figure 24.

This 5’ RACE product was cloned and sequenced and showed good similarity to human, mouse, zebrafish and *X.tropicalis* sequence (data not shown).

3.3.3. 3’ RACE

3’ RACE works by the same principle as 5’ RACE, except with 3’ RACE the endogenous polyA tail is used as a ligation site for the oligo provided. Again total RNA from stage 38 *X.laevis* embryos was used. The oligo contains the adapter primer sequence, which was used with 3’RACE 3 primer to yield the 3’ product, (figure 28).

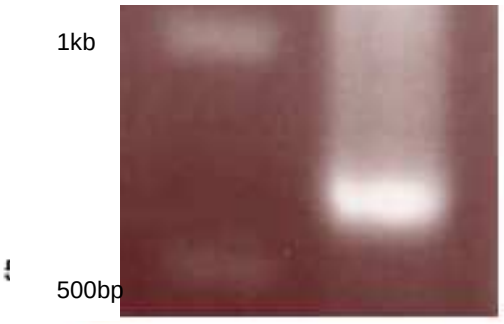

Figure 28
3’RACE PCR product.
The 3’ fragment is approximately 600bp, as expected when looking at the length of SLC24A5 from other species.

This product was also cloned and sequenced, the results of which suggest this is most likely SLC24A5 (data not shown).

3.3.4. Cloning the full length X.laevis SLC24A5

The 5' and 3' ends were now obtained, both overlapping into the previously cloned 800bp fragment, to obtain the full length sequence new primers were designed from the new 5' and 3' sequence, after some optimisation these yielded the full length *X.laevis* SLC24A5 1.5kb in length (figure 29).

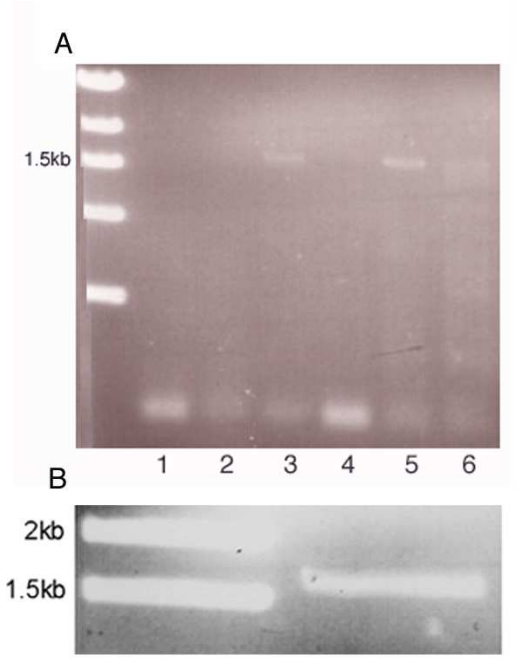

Figure 29
PCR to obtain the full length SLC24A5
A, primers FL5'* and FL3'* were used to obtain the full 1.5kb length SLC24A5. PCR was conducted over a temperature gradient, lane 1 58℃, lane 2 60℃, lane 3 62℃, lane 4 64℃, lane 5 66℃, lane 6 68℃. Only lane 3 and 5 gave a product which was cloned and sequenced. B, PCR product from A, lane 5, before gel extraction and subsequent cloning.

When analysing the sequence data following cloning of the full length product a frameshift was found. Further PCR analysis was conducted over this area to see if it was just a PCR error or if it potentially could be the other allele of SLC24A5. The PCR results in figure 30 B shows that the frameshift is not

present in the PCR over this area and thus it was most likely a PCR error in the original PCR. This was found to be due to a nucleotide insertion (green arrow in figure 30 A).

Figure 30
PCR analysis was conducted over a frameshift seen in sequencing data. A and B, the open reading frame is indicated by the red box. A sequencing data from full length clone showing a frameshift. B, sequence data following PCR over the frameshift region showing no frameshift.

A summary of the PCR/cloning process is presented in figure 31. Internal primers were used to obtain internal fragments of the gene, RACE PCR was then used to obtain the full length gene.

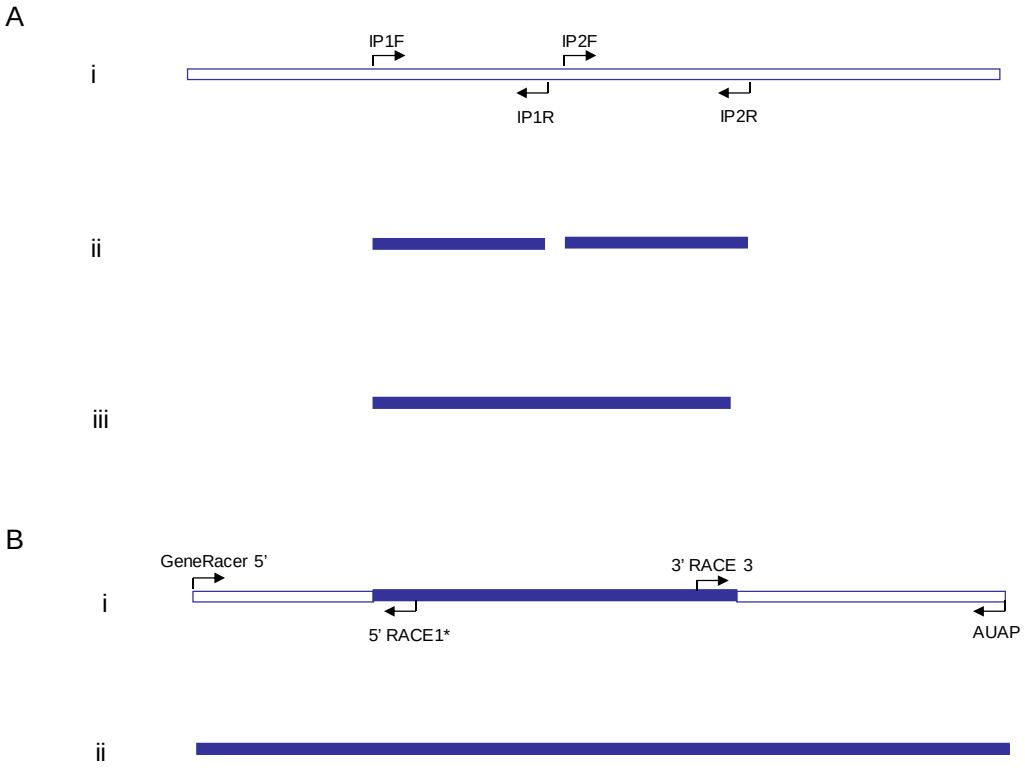

Figure 31
Schematic summary of PCR strategy.
Ai, primers (IP1F, IP1R, IP2F and IP2R) were designed from the full length *X,tropicalis* SLC24A5 sequence. Aii, these primers yielded two 400bp fragments of *X,tropicalis* SLC24A5, which were then also generated from *X.laevis*. Aiii the outer primers (IP1F and IP2R) of these two fragments yielded an 800bp fragment of *X.laevis* SLC24A5.
B, RACE PCR was used to obtain the 5' and 3' missing sequence. Bi, for RACE internal primers (RACE1* and 3'RACE3) were designed from the 800bp fragment. Bii, these primers were used in conjunction with the RACE kit primers (GeneRacer 5' and AUAP) to generate the full length sequence.

Once the full length gene was cloned and sequenced it was compared to the sequence data obtained from cloning the individual fragments of SLC24A5, which aligned at ~100% similarity. The full length sequence was also compared to the human and other species sequence, which revealed 64-84% similarity (as shown in figure 31). Also when used as the query sequence in a BLAST search *X.laevis* SLC24A5 protein sequence returns human SLC24A5, again reassuring that the cloned sequence is SLC24A5. When assembled on a phylogenetic tree with other SLC24 proteins from other species, it is clear that the sequence we have for *X.laevis* SLC24A5 is closer to SLC24A5 than any other SLC24 proteins and *X.laevis* SLC24A5 is most closely related to *X.tropicalis* SLC24A5 (figure 32).

A

Percent Identity

Divergence

	1	2	3	4	5		
1		84.8	66.6	67.6	65.8	**1**	HS
2	17.0		66.1	66.5	65.7	**2**	MM
3	44.1	45.0		64.7	63.9	**3**	ZF
4	42.3	44.3	44.9		84.7	**4**	XT 503
5	45.5	45.7	47.9	16.7		**5**	XL full length
	1	**2**	**3**	**4**	**5**		

B

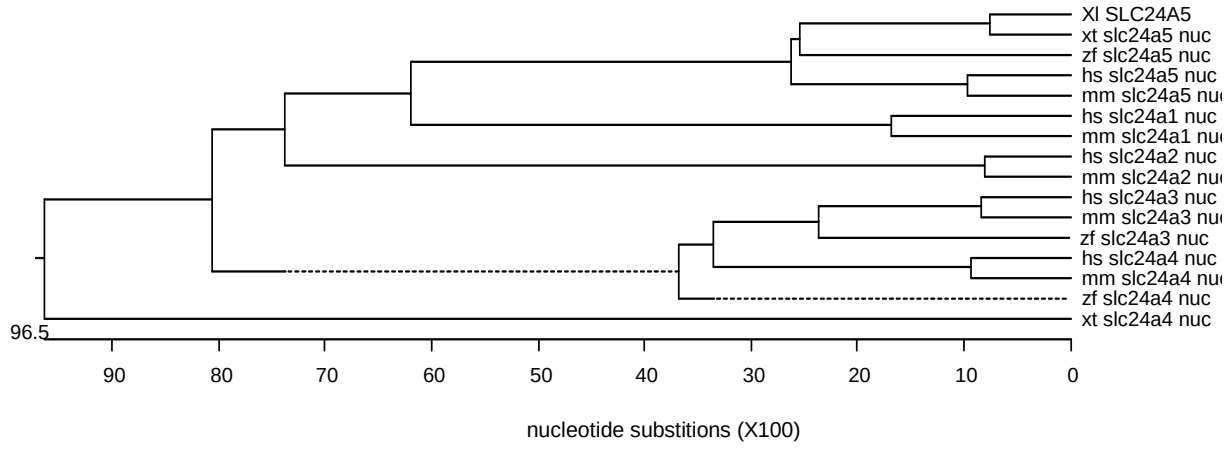

Figure 32
A, Sequence distances between full length X.laevis SLC24A5 and other species SLC24A5. B, Phylogenetic tree of SLC24A1, SLC24A2, SLC24A3, SLC24A4 and SLC24A5 across humans (hs), mouse (mm), zebrafish (zf), *X. tropicalis* (xt) and *X.laevis* (xl).

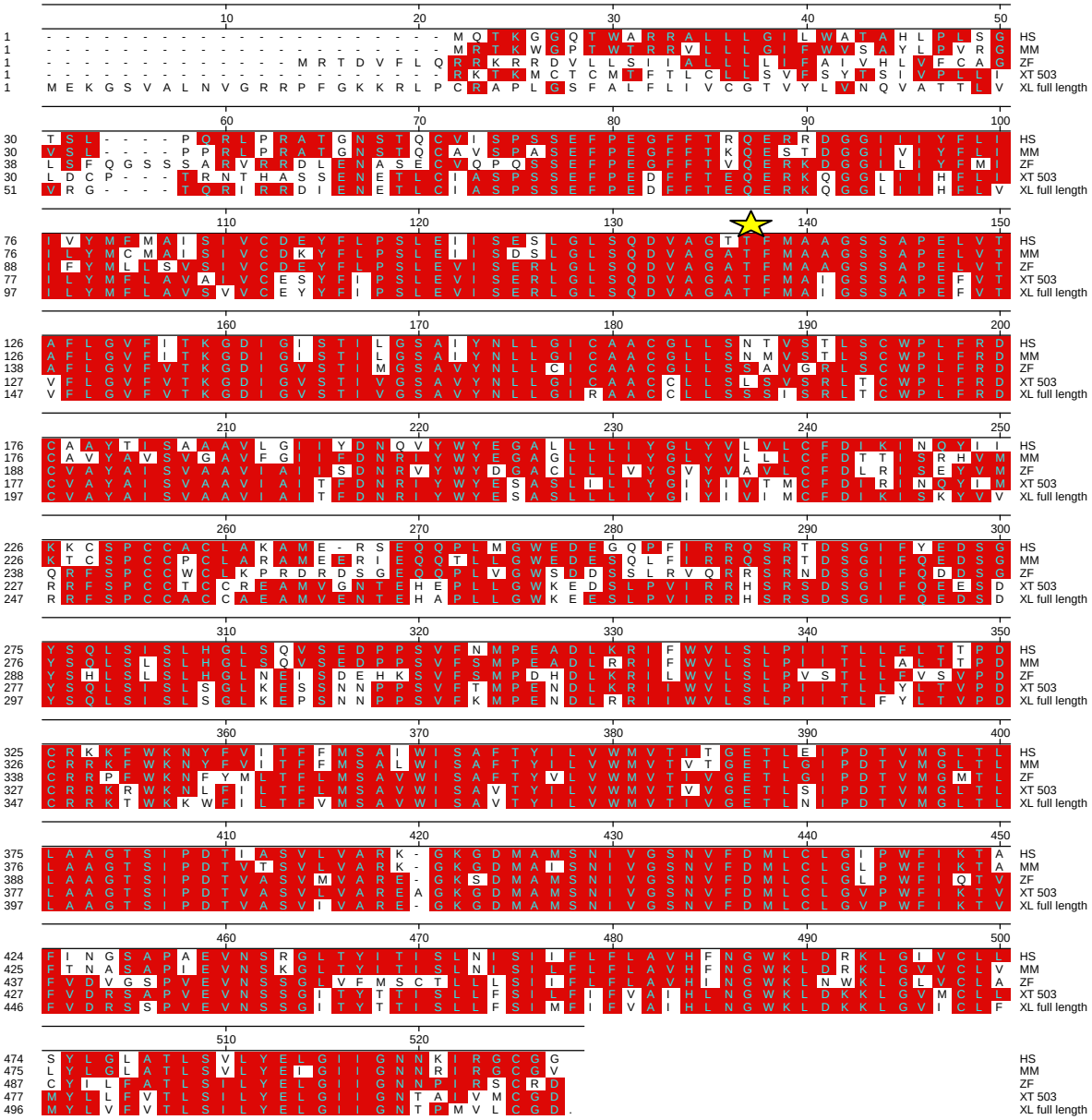

Figure 33
Alignment of newly cloned X.laevis SLC24A5.
Clustal W (DNAstar) was used to align the full length X.laevis SLC24A5 with SLC24A5 from human, mouse, zebrafish and *X.tropicalis* (amino acid sequences were used). Overall similarity is good, average ~70% similarity between *X.laevis* and other species. The 5' end and in the middle region show the least similarity. The yellow star indicates the 111 position of the human sequence, which in *X.laevis* and other species is an A.

The phylogenetic tree in figure 32 represents how the SLC24 family members have diverged over time into their respective groups, but ultimately sharing a common ancestor. *X.laevis* SLC24A5 is most closely related to *X.tropicalis* SLC24A5, showing less than 1000 nucleotide substitutions and then next closely related to SLC24A5 from other species. This provides further confidence that the gene cloned here is indeed *X.laevis* SLC24A5.

The newly cloned *X.laevis* SLC24A5 is 84.7% similar to the known *X.tropicalis* SLC24A5 sequence (at the protein level), this is 79% at the nucleotide level. The high level of similarity seen here indicates this gene is well conserved between these species, but also they are sufficiently dissimilar to offer confidence that the new clone is indeed *X.laevis* and there has not been a mix up with *X.tropicalis* material in the lab, as was seen earlier in the cloning process. The greatest region of divergence in the sequences is the 5' area of *X.laevis* SLC24A5. This did cause some concern, particularly as there is not a stop codon upstream of the start methionine, however further work using morpholinos targeted to this area have proved successful (see chapter five), thus suggesting this is the complete sequence.

3.4. Discussion

Using a combination of RT PCR and 5' and 3' RACE PCR we have cloned the full length open reading frame of *X.laevis* SLC24A5. This is approximately 1.5kb in length and encodes a protein of 523 amino acids.

BLAST and alignment analysis of the sequencing results strongly suggest the PCR products generated here are *X.laevis* SLC24A5. The sequence presented here also shows close similarity to the SLC24A5 sequence from other species, although there are some differences at the 5' region between all species. This region is thought to contain a cleavable signal peptide, it could be therefore that this region is not crucial to the function of the protein and thus displays less homology. The high similarity revealed by the alignment in figure 33 suggests SLC24A5 is an evolutionary conserved gene. Note at the equivalent 111 position of the human sequence (indicated by a yellow star), an alanine residue is present, indicating *X.laevis* does not carry the ns-SNP observed in humans. This also seems to be true for mouse, zebrafish and *X.tropicalis,* as these other

species also carry the ancestral alanine residue. This residue is found in a highly conserved region of the protein. It would be of interest to explore the genome of the other species to determine if they also have a divergent SNP at this position and if this correlates with population changes in pigmentation patterns.

As mentioned previously *X.laevis* is tetraploid, meaning there are 4 copies of chromosomes and thus potentially 4 copies of every gene. This is thought to be caused by a genome duplication event 21-41 million years ago (Chain and Evans, 2006). *X.laevis* has 36 chromosomes (Hughes and Hughes, 1993). Due to this it is not unusual to isolate more than one paralog of any one gene during identification experiments; however, here no such phenomenon was uncovered here. Only one PCR product was found, although this did have a frameshift in the sequence, this was found to be a PCR error and not to represent the presence of the other paralog (figure 30).

Closer analysis of the peptide sequence shows several features of the NCKX5 protein. *In silico* transmembrane domain predictions suggest 11 or 12 transmembrane domains, the first of which is assumed to be the cleaved signal peptide, the others form clusters of 4 and 6 or 5 and 6 (depending on software used), both show a large cytosolic loop (figure 34). This analysis is consistent with that of NCKX2 (Kinjo et al., 2003). One of the potential transmembrane domains (figure 34 *) actually appears to be too short to cross the membrane. It is possible that this region associates with the inside of the membrane, as has been proposed for NCKX2 (figure 55).

MEKGSVALNVGRRPFGKKRLPCRAPLGSFALFLIVCGTVYLVNQVATTLVVRGTQRIRRDIE

NETLCIASPSSEFPEDFFTEQERKQGGLIIHFLVILYMFLAVSVVCEYYFIPSLEVISERLGLSQ

DVAG**A**TFMAIGSSAPEFVTVFLGVFVTKGDIGVSTIVGSAVYNLLGICAACCLLSSSISRLTC

WPLFRDCVAYAISVAAVIAITFDNRIYWYESASLLLIYGIYIVIMCFDIKISKYVVRRFSPCCACC

AEAMVENTEHAPLLGWKEESLPVIRRHSRSDSGIFQEDSDYSQLSISLSGLKEPSNNPPSVF

KMPENDLRRIIWVLSLPIITLFYLTVPDCRRKTWKKWFILTFVMSAVWISAVTYXLVWMVTIVG

ETLNIPDTVMGLTLLAAGTSIPDTVASVIVAREGKGDMAMSNIVGSNVFDMLCLGVPWFIKTV

DRSSPVEVNSSGITYTTISLLFSIMFIFVAIHFNGWKLDRKLGVVCLLXYLGLATLSVLYELGIIG

NNXIRGCGD

*

Figure 34
Peptide sequence of *X. laevis* SLC24A5 showing predicted transmembrane domains (yellow) and the intracellular loop (green), as predicted by TMHMM, this differs slightly from the prediction by TMpred. The bold enlarged A is the equivalent residue to position 111 of the human sequence. Pink boxes indicate roughly where the alpha repeats are located, these are highly conserved regions between NCKX proteins and NCX proteins.

Functional analysis of NCXK5 has been hindered by its intracellular localisation. Despite many efforts the protein cannot be targeted to the plasma membrane to facilitate functional analyses. Massive over expression of human NCKX5 in insect high five cells has yielded the only functional data, although this showed much less activity compared with NCKX2, which does reside in the plasma membrane (figure 22).

Once sequence data for *X.laevis* SLC24A5 was available expression studies could commence followed by knockdown analysis once the 5' sequence was determined. These experiments will be discussed next.

Chapter Four:

Expression analysis

4.1. Introduction

In order to understand the function of any gene, it is essential to first determine its temporal and spatial expression pattern. In developmental biology this is commonly done using Whole mount In Situ Hybridisation (WISH). Here we use whole embryos at various stages of development, to determine at which stages expression of SLC24A5 can be detected. This also shows the exact cells and tissues that express SLC24A5.

In order to carry out WISH an RNA probe specific to the gene of interest must be generated. The probe must be the antisense sequence to the mRNA of interest such that they will bind by complementary base pairing. This is achieved by reverse transcribing the DNA sequence of the gene of interest. Nucleotides are the building blocks for this process, a mixture of nucleotides including UTP labelled with digoxigenin (DIG) are added to the reaction. DIG is one of several haptens isolated from plants. Haptens have high immunospecificity, their readily available antibodies have high affinity, and thus they are amenable to many molecular applications. Once generated the RNA probe is applied to the embryos, they are then treated with the anti-DIG antibody, following a series of washes (more details in materials and methods), the DIG labelled probe is detected by applying the substrate for an enzyme (typically alkaline phospatase) conjugated to the DIG antibody. This causes a colour change reaction which allows visualisation of the expression of the gene of interest.

RT PCR is another way of determining expression, although it only indicates the temporal pattern, but it does have the advantage of being semi quantitative.

4.2. Results

4.2.1. Whole Mount In Situ Hybridisation (WISH)

An RNA probe was generated from the 800bp fragment of *X.laevis* SLC24A5 (figure 26). This was used to detect expression of *X.laevis* SLC24A5 transcripts by whole mount in situ hybridisation, as described in materials and methods. A probe to the melanophore marker DCT was also synthesised and used alongside SLC24A5 to compare melanophore expression, (figure 35). Sense probes were also used as negative controls, no expression was seen with these (data not shown). A variety of stages of *X.laevis* embryos were used to determine the temporal expression of SLC24A5 during the course of embryogenesis. Albino embryos were used to give clearer background. These are heterozygous for albinism; the fathers are pigmented, so they still have pigment cells that produce melanin at tadpole stages. As a control, the in situ was also performed on homozygous pigmented embryos which following in situ hybridisation were bleached (see materials and methods) to remove the melanin pigment, this revealed the same pigment pattern as seen in the albino embryos (data not shown).

The expression pattern of SLC24A5 and DCT is shown in figure 35. Expression of SLC24A5 was first seen at stage 25 (Nieuwkoop and Faber, 1994) in the neural crest cells (or dorsal neural tube) and retinal pigmented epithelium (RPE). Expression continues in the developing melanoblasts and mature melanophores in the lateral stripe and tail pigment pattern. RPE expression also continues and increases, throughout development. This expression is generally consistent with that seen with the DCT probe, suggesting this expression is most likely in the pigment cells. However when comparing the expression patterns in figure 35B and F it looks like SLC24A5 is not expressed in migrating cells as DCT is. This suggests SLC24A5 is expressed in differentiated melanophores.

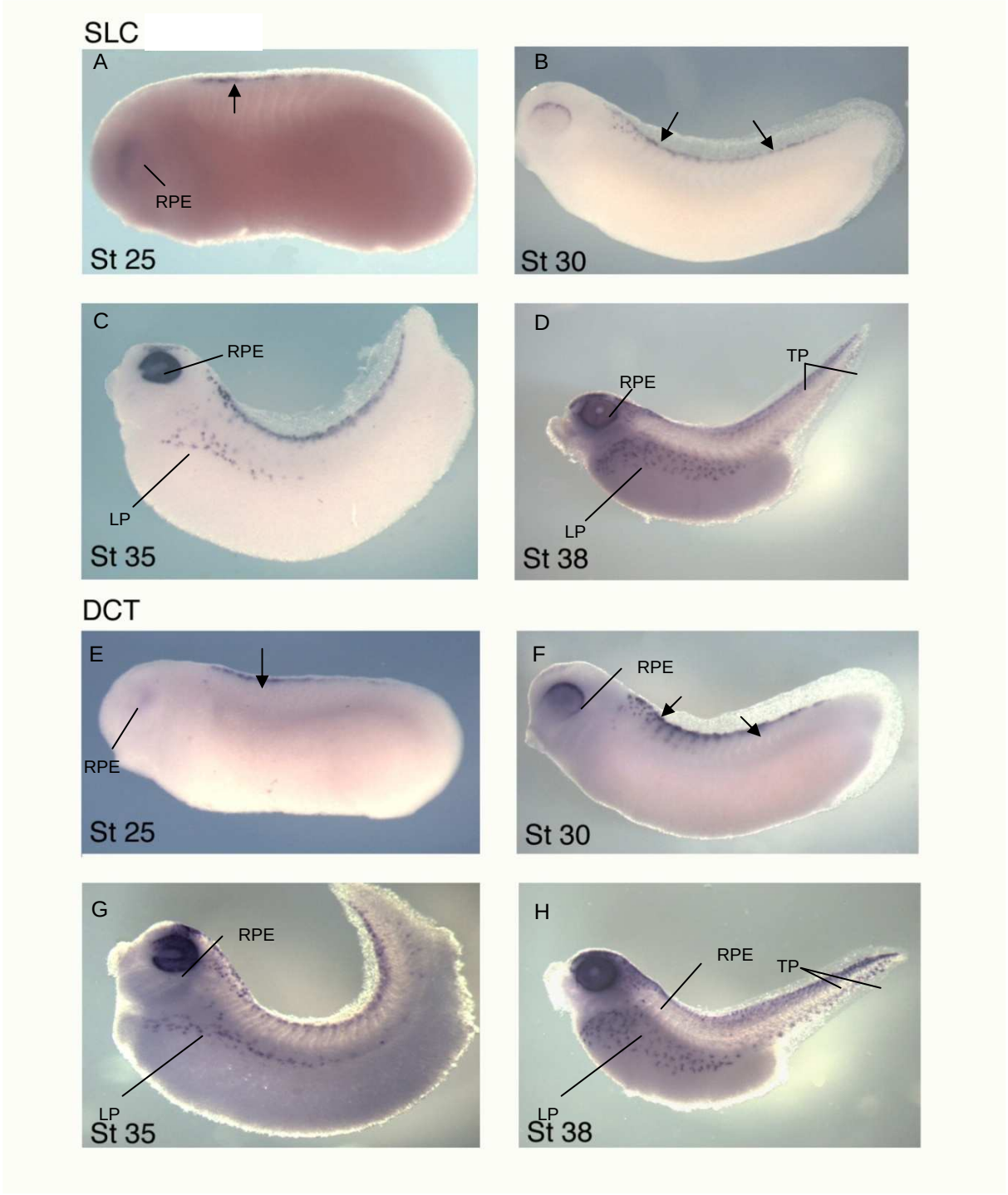

Figure 35
WISH analysis of SLC24A5 expression during *X.laevis* development. A, expression is first seen at st25 in the neural crest tissue and eye. B,stage 30 expression develops throughout the developing melanoblasts and further develops in the eye. C, D, expression continues in melanogenic neural crest cells along the dorso-lateral aspects. E-H, the same expression pattern is observed for DCT a known melanophore marker. RPE retinal pigmented epithelium, LP, lateral pigmentation, TP, tail pigmentation, arrow head in E points to neural crest cells, arrow heads in F point to migrating pigment cells.

To facilitate clearer observation of the in situ staining, some embryos were bleached following the in situ procedure. This process removes the endogenous brown melanin pigment while leaving the purple/blue of the in situ unaffected, figure 36.

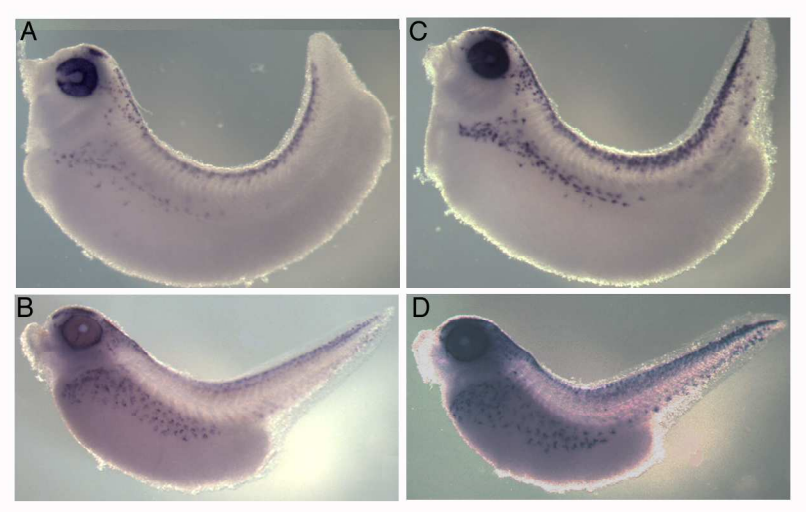

Figure 36
Following in situ hybridisation analysis of SLC24A5 expression, some older embryos were bleached to remove the pigment such that the blue staining of expression could be seen more clearly. This shows the expression is strong in the pigment cells and is unaffected by the bleaching procedure. A, SLC24A5 stage 35, B, SLC24A5 stage 38, C, DCT stage 35, D, DCT stage 38.

4.2.2. Histological analysis

To further investigate the expression pattern of SLC24A5 post hybridisation embryos were processed for cyrosectioning (figure 37).

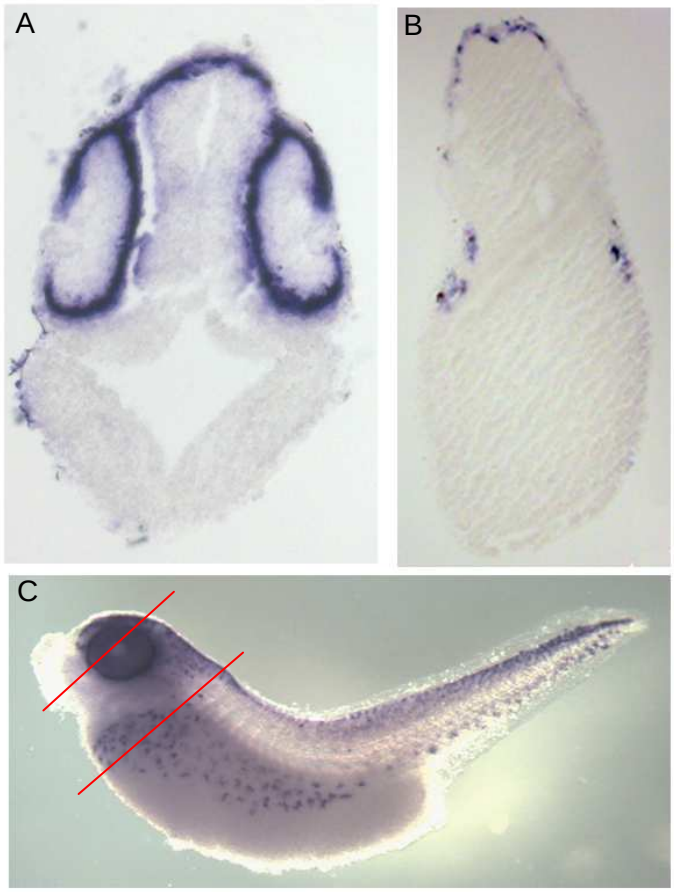

Figure 37
Histological analyses of SLC24A5 in situ expression.
Transverse sections through stage 38 tadpole following *in situ* for SLC24A5, (a) head and (b) body, locations of sections shown in C.

Sectioning through the embryo reveals no further expression of SLC24A5 inside the embryo. Expression is restricted to the RPE of the eye and lateral and head pigment cells. Also again expression is restricted to stationery melanophores, indicating no expression in migrating cells

4.2.3. RT PCR

Reverse transcription PCR was used to analyse the temporal expression pattern of SLC24A5, DCT was used as a melanogenic comparison. SLC24A5 expression is first seen at stage 28 and continues through to stage 38. Stages between 20 and 28 were tested but no expression was seen, this is probably due to the small amount of PCR product loaded on the gel (5µl of a 25µl reaction), as expression was seen at stage 25 in the in situ and PCR should be more sensitive. A similar pattern is observed for DCT, however this is also expressed in earlier stages, this is thought to be maternal (figure 38).

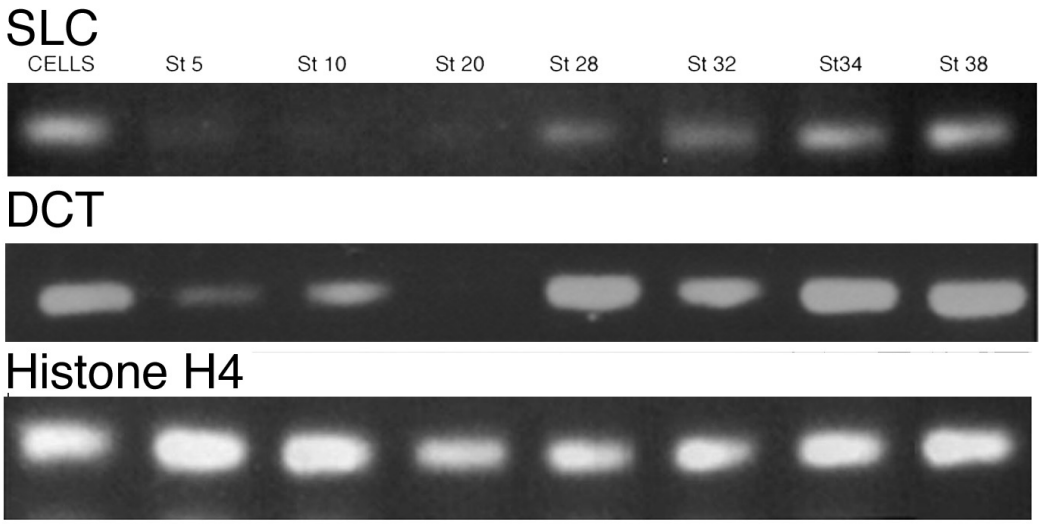

Figure 38
RT PCR analysis of SLC24A5 expression. The cells used were *X. laevis* melanophores (kind gift from Vladimir Gelfand). Histone H4 was used as a loading control.

4.3. Discussion

To analyse the expression pattern of SLC24A5 in the developing embryo, whole mount in situ hybridisation analysis was performed. An antisense RNA probe was generated from the 800bp fragment of SLC24A5; a sense probe was also made and used as a negative control (data not shown). As expected SLC24A5 expression is seen in the epidermal pigment cells and the RPE of the eye. Expression is first detected at stage 25, (earlier stages were analysed but no expression was seen, data not shown), in the melanocytes above the dorsal neural tube (figure 35 and 36) and becomes more intense as the embryo develops through stages 30 and onwards, as more pigment cells develop (figure 35 and 36). During this time expression is detected as the melanophores develop from the neural crest (figure 35 and 36) and is seen across the embryo in the lateral pigment stripe and pigmented areas of the tail (dorsal and ventral) (figure 35 and 36). The dendritic structure of the melanophores is clear. The SLC24A5 expression pattern mirrors that of DCT, a known melanophore marker, strongly suggesting the SLC24A5 expression is indeed in the melanophores. The curling up of some embryos in figure 35 is an artefact of the WISH protocol. This expression pattern is consistent with that seen in zebrafish embryos (figure 15), where both SLC24A5 and DCT are detected in the melanophores and RPE (Lamason et al., 2005). No expression was detected in other tissues such as pancreas, heart and lung, as seen by Lamason et al (2005) in mouse.

Cryosectioning of the embryos following WISH allows visualisation of any internal expression of SLC24A5. As expected all SLC24A5 expression was found in the epidermal tissue and eye. The sections clearly show high levels of expression in the eye, specifically the RPE. Sections further along the anterior-posterior axis show expression of SLC24A5 in the flank of the tadpole, this is the expression seen in the lateral strip on the whole animal (figure 37). This confirms, unlike other SLC24 genes that SLC24A5 is not expressed in the brain or other organs, and that unusually for this protein family its expression is quite restricted. Of the NCKX family, NCKX5 is the only protein expressed in non-excitatory tissue i.e. the melanophores, with the exception of a report where NCKX was found in platelet cells (Kimura et al., 1993).

The temporal expression of SLC24A5 detected by RT PCR is consistent with that seen by in situ analysis. Although the onset of expression detected by this method (RT PCR) was not until stage 28, this may be because so little of the gene is expressed at earlier stages it is not detectable in the volume of PCR visualised on the gel. Expression becomes stronger as the embryos get older which is consistent with the onset and increasing development of pigmentation across these stages. The timing of SLC24A5 expression is consistent with that of the melanophore marker DCT, although DCT is also expressed at early stages; this is thought to be maternal transcript. There also appears to be more DCT present than SLC24A5 at the later stages, and DCT comes on quite bold and remains constant, whereas SLC24A5 expression appears more gradually.

Chapter Five:

Loss of Function Analysis

5.1. Introduction

To further investigate the role of any given gene it is common practice to knockdown the expression of the gene and analyse the resulting phenotype, from which inferences can be made as to the function of the protein encoded by the gene.

In developmental biology morpholinos are used to repress the translation of a protein. Morpholinos are antisense oligonucleotides. They are non toxic synthetic nucleic acids which have a morpholine moiety (figure 39) in place of the ribose sugar group, this stabilises the oligo as well as making it more soluble. The morpholino groups are held together by phosphoramidate linkages, these linkages are less susceptible to damage than phosphodiester bonds because they are non-ionic. Also the morpholino backbone of the oligo is not recognised by any intracellular nucleases, therefore it is not degraded, and also does not initiate an immune response and related inflammation. Morpholinos can be designed to target either the ATG start codon to repress translation or a splice junction to interfere with normal mRNA splicing events. Morpholinos are generally 25 nucleotides in length and function by sterically blocking access to the transcript by molecular machinery needed for translation or splicing, thus inhibiting translation or splicing of the mRNA. Complementary base pairing facilitates morpholino targeting; they also show greater specificity and efficiency than ribonucleotides (Eisen and Smith, 2008).

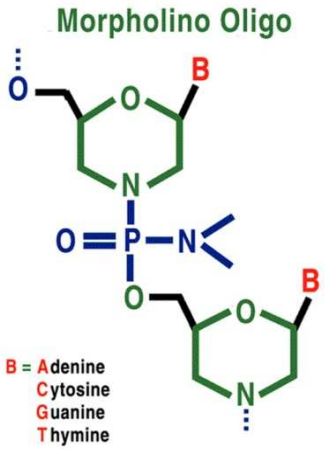

Figure 39
Morpholino structure. The morpholine moiety is shown in green these are joined by phosphorodiamidate linkages instead of phosphodiester linkages (GeneTools.com).

Once the 5' sequence of *X.laevis* SLC24A5 was known, a morpholino directed to the translational start site of this gene could be designed. This was done by GeneTools who also provided the morpholino, as was a splice site targeting morpholino. This is designed to inhibit splicing of the pre-mRNA such that the protein product should be truncated at the C terminal, this will be discussed in more detail below.

5.2. Results

5.2.1. Morpholino knockdown of SLC24A5

In order to confirm the ATG morpholino is indeed repressing translation of X.laevis SLC24A5 we carried out an in vitro translation (IVT) experiment. This revealed that the ATG morpholino does prevent translation of the target gene, SLC24A5, figure 40.

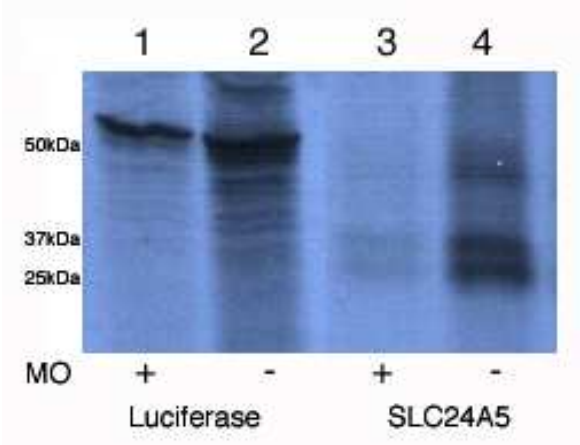

Figure 40
IVT analysis of ATG morpholino efficacy
Lanes 1 and 2 show the control luciferase is not affected by the morpholino. SLC24A5 protein expression is significantly reduced in the presence of the ATG morpholino, lanes 3 and 4. MO, morpholino.

X.laevis SLC24A5 was detected as a typical doublet band, of approximately 30kDa (figure 40). This is smaller than expected (40kDa by western analysis). This is possibly due to the in vitro environment in which the protein is translated, where post translational modification may differ. Luciferase is approximately 55kDa (figure 40), this is also slightly smaller than expected, 61kDa.

The morpholino was delivered to the embryo by microinjection in a final volume of 20nl; several concentrations were tested to determine the optimal concentration (figure 44). The target of microinjection was one cell at the two cell stage (figure 41a), although other more refined neural crest target sites (figure 41b) were tried, this proved to be the most effective and easiest to keep consistent. Injection into 1 cell of 2 cells or 1/2 cells at 8, 16, or 32 cell stages gave the same results. LacZ was co-injected to monitor targeting of injections (figure 42).

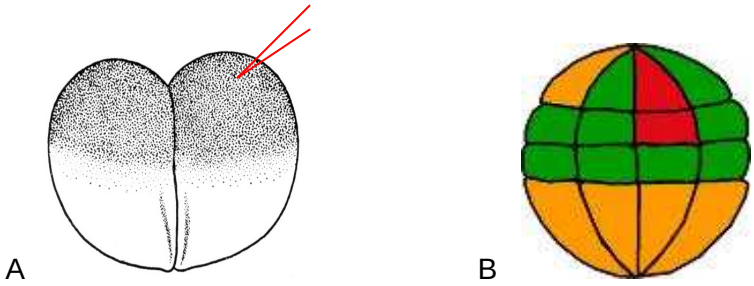

Figure 41
Target of morpholino injection.
A, 2 cell stage (~1.5hpf) *X.laevis* embryo, showing site of injection. B, 32 cell stage (~4hpf) *X.laevis* embryo. Historical fate mapping experiments have elucidated the fate of early blastomeres. Here the origin of neural crest cells is shown; red indicates the blastomeres from which the majority of neural crest cells are derived, green represents those blastomeres which offer less of a contribution to neural crest and orange indicates those blastomere which make no contribution. Ventral views, animal pole is at the top and vegetal pole is at the bottom, dorsal to the right and ventral to the left (www.Xenbase.com) (Bowes et al., 2008).

The red blastomeres were injected with morpholino, however precision of these injections proved difficult to maintain as obtaining embryos where the correct blastomeres could be identified was difficult.

Initially lacZ cRNA was injected alone into 1 cell at the 2 cell stage and analysed by detecting B-galactosidase activity at later stages by Red Gal staining (figure 42). This was to ensure targeting of the injections was accurate, as seen in figure 42, lacZ expression was only detected on the injected side of the embryo.

Figure 42
Tadpoles following injection with LacZ in to 1 cell at the 2 cell stage. The background red colour seen along the back of the non injected tadpole is simply the colour from the other side showing through as this area is transparent.

By injecting just one cell at the two cell stage just one lateral half of the developing embryo is affected, leaving the other half as an internal negative control. The embryos subjected to morpholino injection were raised to stage 38, counted and scored visually for a reduced pigmentation phenotype. Morpholino treatment resulted in a reduction in pigmentation. Varying degrees of effect were observed so a scale was devised to describe the different levels of morpholino effect (figure 43).

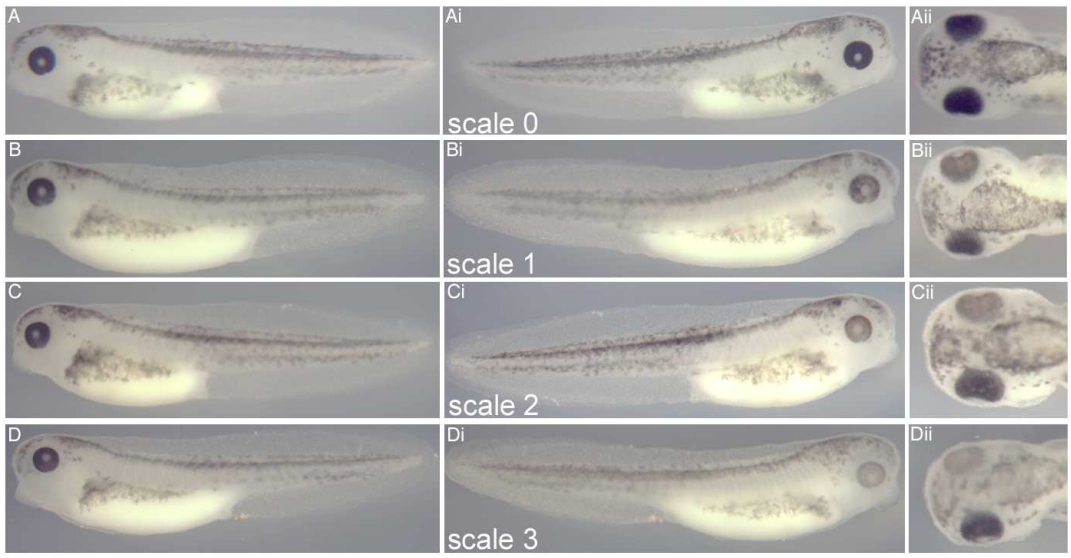

Figure 43
Scale of morpholino effect seen in morpholino treated embryos. Scale 0, no effect (wild type), scale 1, subtle effect, scale 2 clear effect, scale 3 obvious effect. The same tadpole is represented for each different scale, but photographed from different prospectives.

The reduction in pigmentation is most prominant in the RPE of the eye, although some reduction in lateral pigmentation is also observed, particulary in scale 3 tadpoles (figure 43). Head and tail pigmentation is generally not affected as much, as will be discussed below.

Following morpholino treatment embryos were raised to stage 38 and the phenotypes were scored according to the scale in figure 43, the relative percentages of each phenotype were then calculated and represented in graphs from here on (figure 44).

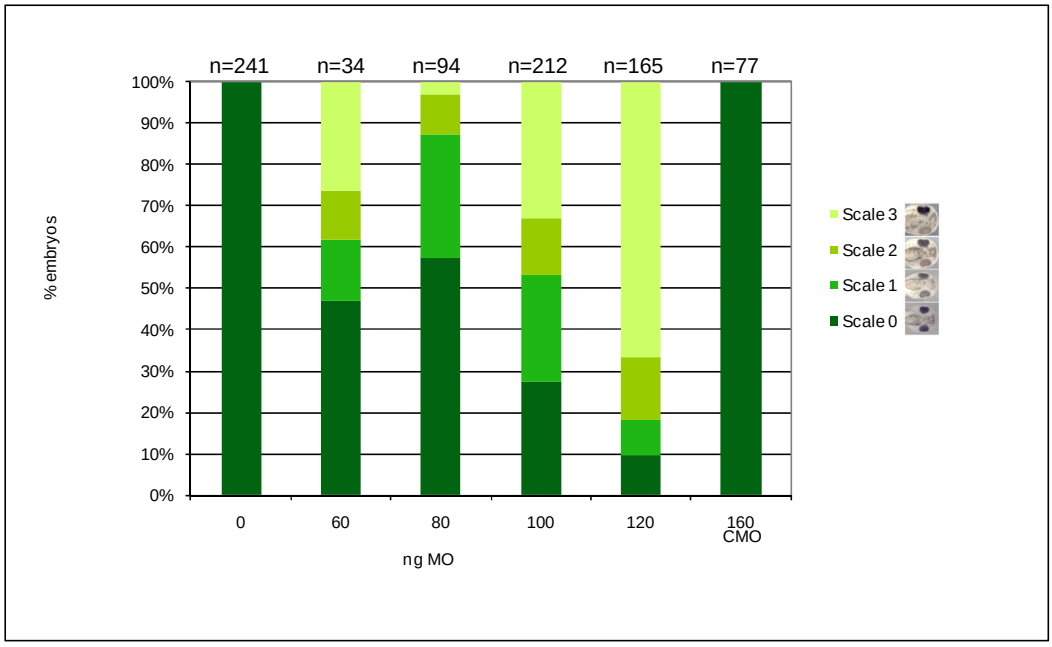

Figure 44
ATG morpholino knockdown of SLC24A5
Increasing concentration of morpholino results in more embryos of scale 3 phenotype. CMO is a control morpholino supplied by GeneTools (appendix). Numbers shown here reflect pooled data from 3 separate experiments.

No effect was seen in non injected embryos or with the control morpholino. Higher concentrations become toxic. Maximum reduction in pigmentation was 90%, as seen with 120ng morpholino. 60ng of morpholino was the lowest concentration to give any effect (figure 44).

5.2.2. Characterising the morpholino knockdown

5.2.2.1. Effects of SLC24A5 Knockdown on other Melanogenic Genes

Many other genes are involved in the complex process of melanogenesis. Key gene sequences in this pathway have been obtained from *X.laevis* and their expression pattern determined by in situ. These include; Tyr, Tyrp1, DCT (Kumasaka et al., 2003), and Mitf, (Kumasaka et al., 2004). The expression of these genes following morpholino knockdown of SLC24A5 was analysed by WISH to see firstly if the melanophores are present and morphologically normal and secondly to see if knockdown of SLC24A5 led to any change in expression of these different markers (figures 45, 46, 47).

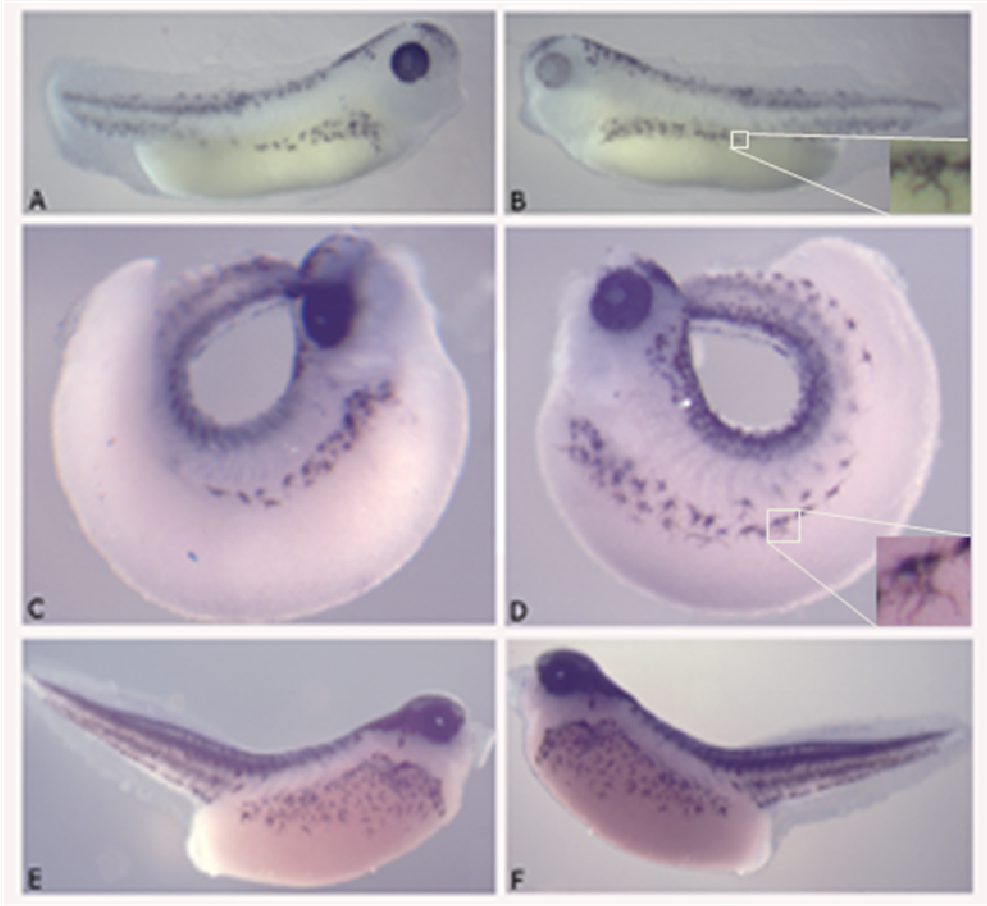

Figure 45
Expression of DCT following morpholino knockdown of SLC24A5. A, non injected side. B, 100ng morpholino injected side. C, A following DCT in situ. D, B following DCT in situ. E,F non injected controls following DCT in situ, n=19.

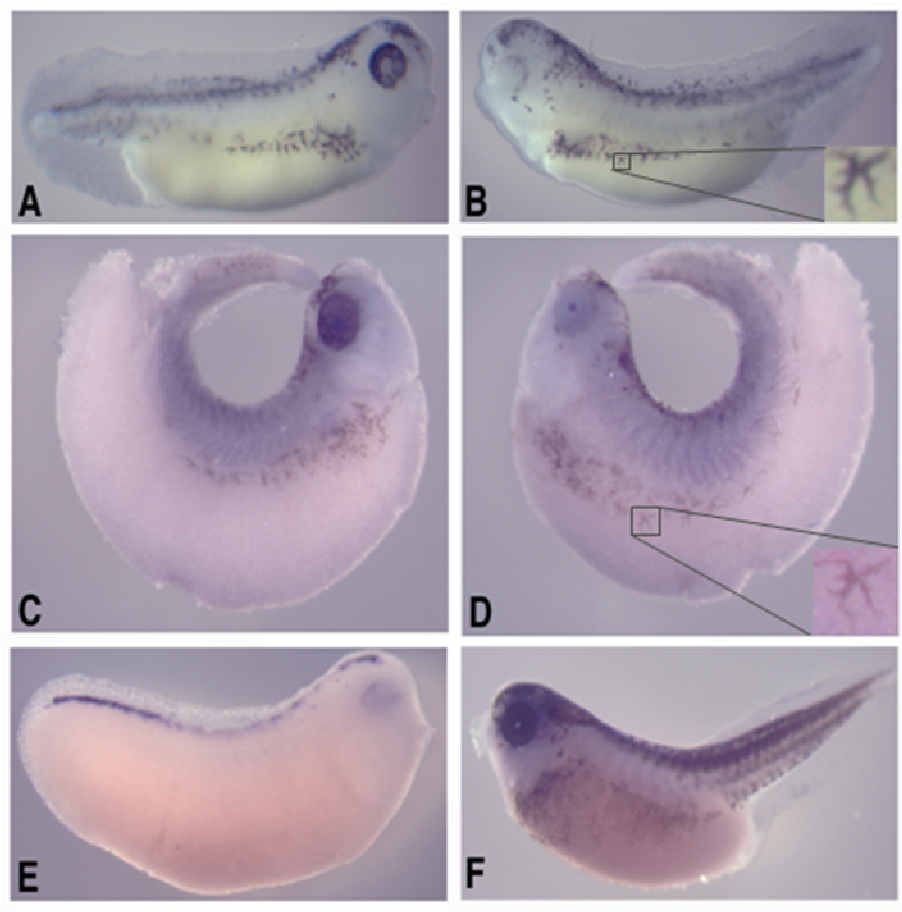

Figure 46
Expression of Mitf following morpholino knockdown of SLC24A5. A, non injected side. B, 100ng morpholino injected side. C, A following Mitf in situ. D, B following Mitf in situ. E,F non injected controls following Mitf in situ, n=15.

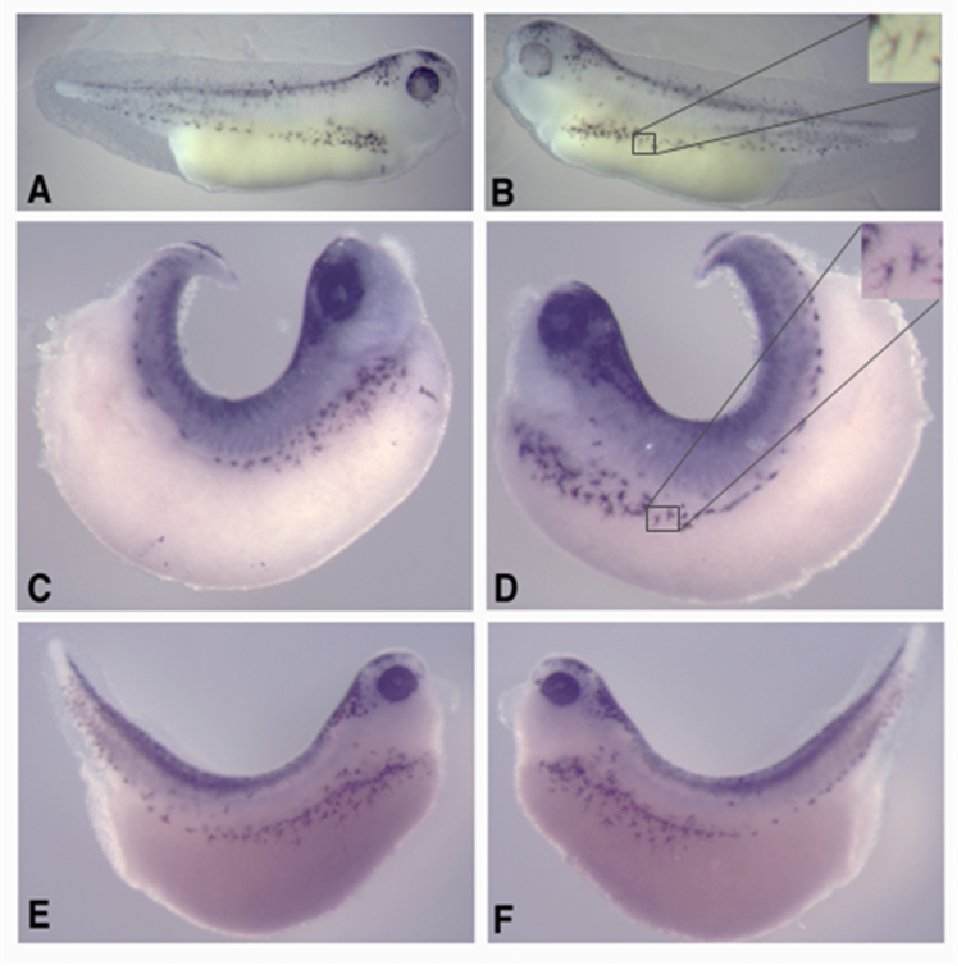

Figure 47
Expression of Tyr following morpholino knockdown of SLC24A5. A, non injected side. B, 100ng morpholino injected side. C, A following Tyr in situ. D, B following Tyr in situ. E,F non injected controls following Tyr in situ, n=14.

Figures 45 and 47 show that expression of DCT and tyrosinase is not effected by SLC24A5 knockdown. However, Mitf expression, as seen in figure 46 does appear to be slightly repressed in the eye, following SLC24A5 knockdown.

The same tadpoles are shown in A-D of each figure, E and F are positive controls for the *in situ.* These figures also highlight that the migration and morphology of the melanophores is normal.

5.2.2.2. Histological examination of morpholino knockdown

To further analyse the effects of the morpholino some embryos were processed for cyrosectioning. Figure 48 clearly shows a significant reduction in eye pigmentation. There appears to be fewer pigment cells and those present contain less melanin (figure 48).

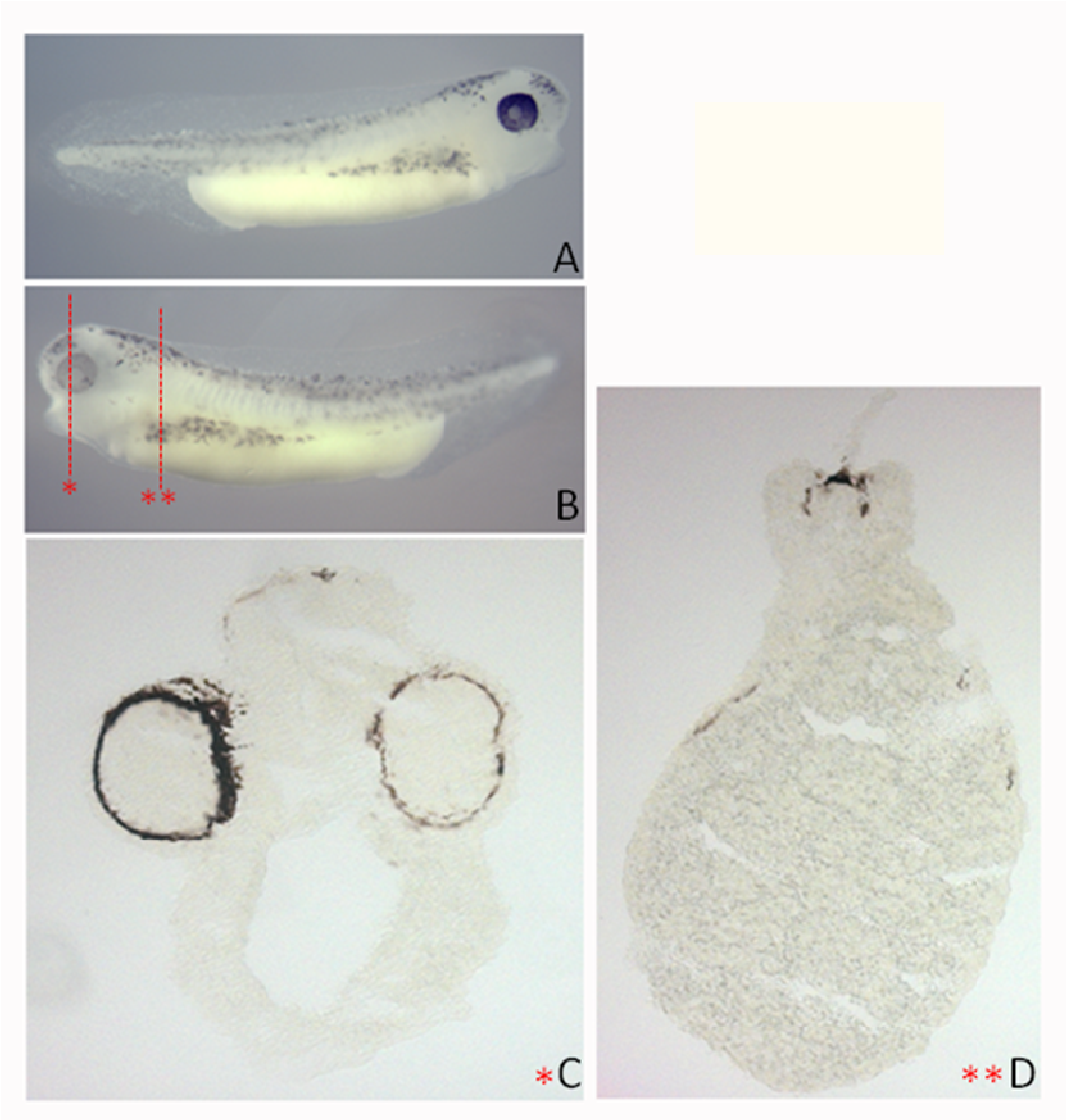

Figure 48
Transverse cyrosections through stage 38 tadpole injected on one side with 200ng morpholino. A, non injected side. B, injected side, C, transverse section through head, indicated on B by asterisk. D, transverse section through the body, indicated on B by double asterisk. Data shown here is representative of 25 embryos processed for sectioning.

It is clear from the section in figure 48C, that the morpholino causes a dramatic reduction in pigmentation in the eye, where there also appears to be fewer pigment producing cells. There is also a difference between the non injected and injected side in the lateral region (figure 48D). The head pigmentation does appear lighter in the injected side in the whole mount image (figure 48B), but this observation is not reflected in the sections (figure 48C and 48D). Again it can be seen that the melanophores are able to migrate normally (figure 48)

Morpholino to SLC24A5 was also injected into the two ventral blastomeres at the 4 cell stage to determine if the effect was cell autonomous or non cell autonomous. No effect on pigmentation was seen following these injections (data not shown), indicating that this is cell autonomous effect, i.e. cells injected with the morpholino do not have any influence on their surrounding cells.

5.2.3 Splice morpholino

When using morpholinos it is generally preferable to have more than one morpholino knockdown to show the effect is specific to the gene of interest. In order to confirm the morpholino knockdown phenotype is due to a reduction of SLC24A5 protein, and to see if a stronger knockdown could be achieved, a splice site morpholino was used. Splice morpholinos are different to ATG morpholinos because they prevent splice processing of the pre-mRNA in the nucleus, their effects can also be monitored by PCR (Draper et al., 2001; Morcos, 2007).

5.2.3.1. Obtaining splice morpholino sequence

To obtain a splice morpholino, sequence data over an intron/exon boundary is required, so further PCR analyses were conducted. The intron/exon boundary regions for the *X.tropicalis* sequence were already determined and available on Ensembl (figure 49), this was translated onto the *X.laevis* sequence, as these species often show close sequence similarity it was hoped the intron/exon structure would be similar. *X.tropicalis* SLC24A5 is comprised 9 exons which aligned reasonably well with the *X.laevis* sequence; however *X.laevis* appeared to have one extra exon at the end. As primers were already available over the

last intron/exon boundary of the *X.laevis* sequence, these were used in PCR on genomic *X.laevis* DNA to obtain the intronic sequence.

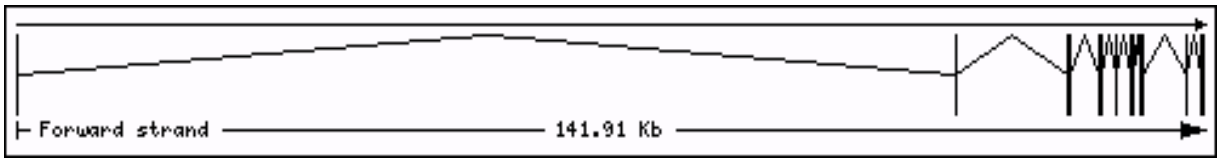

Figure 49
Intron/exon architecture of the *X.tropicalis* SLC24A5 gene (Ensembl).

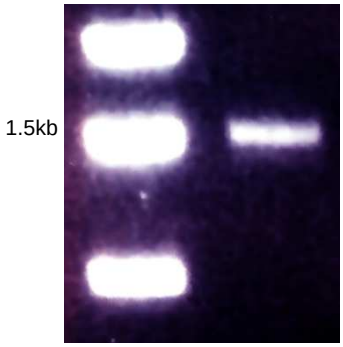

Figure 50
PCR product from primers SLC frameshift1 and full length 3'3* which cover the exon 9/intron 9 boundary.

Based on *X.tropicalis* sequence data a 2kb product was expected from the PCR. However a 1.5kb product (figure 50) was cloned and sequenced as there is likely to be some difference between *X.tropicalis* and *X.laevis*.

The sequencing results shown in figure 51, show the already known exonic sequence at the 5' and 3' ends of the PCR product and a large amount of unknown intronic sequence (represented by xxx in figure 51).

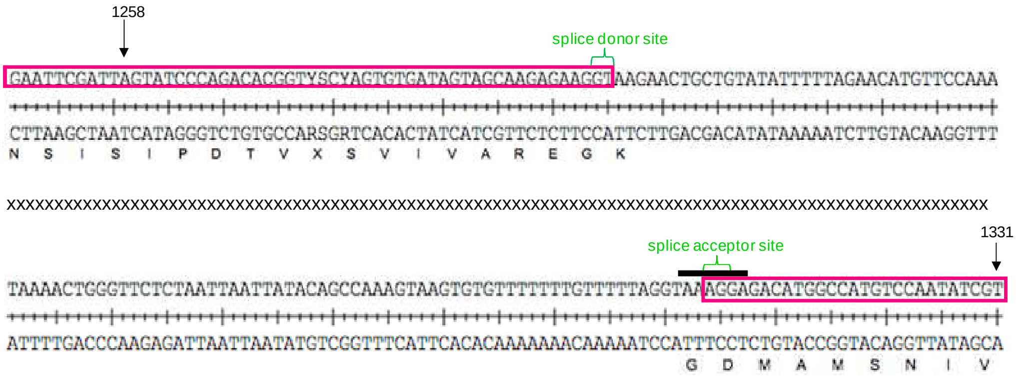

Figure 51
PCR over an intron/exon boundary.
Known exonic sequence is framed by pink boxes and the amino acid sequence they encode is also shown. Some nucleotide numbers are shown to orientate region of the gene. xxxxx represents previously unknown intronic sequence. The heavy black line indicates the target region of the splice morpholino. The splice donor and acceptor sites are also indicated.

Some of the sequence at the border of the new intron data and exon 10 was sent to GeneTools to design a morpholino.

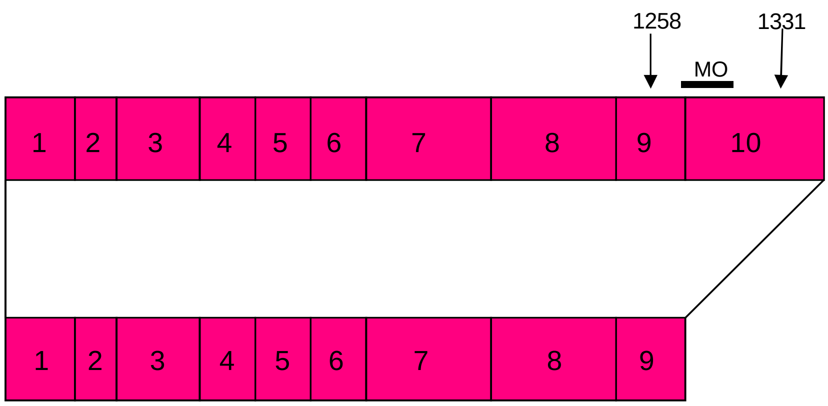

Figure 52
Schematic of *X.laevis* exon structure before and after morpholino treatment.
Pink boxes represent the exons of *X.laevis* SLC24A5, again some nucleotide numbers are indicated to offer some orientation, and the morpholino (MO) target sequence is represented as a black bar.

As shown in figure 52, the splice target morpholino should truncate the protein by removing the final exon. However it is also possible that the resulting transcript following splice morpholino treatment could be degraded by non-sense mediated RNA decay

5.2.3.2. Splice morpholino knockdown of SLC24A5

The splice morpholino was tested in embryo injections as for the ATG morpholino. As expected splice morpholino treated embryos display the same reduced pigment phenotype as that seen with the ATG morpholino, therefore tadpoles were scored to the same scale as that devised from the ATG morpholino results (figure 43). Various concentrations were used to establish a dose response; this showed that at lower concentrations the splice morpholino was more effective than the ATG morpholino, as shown in figure 53.

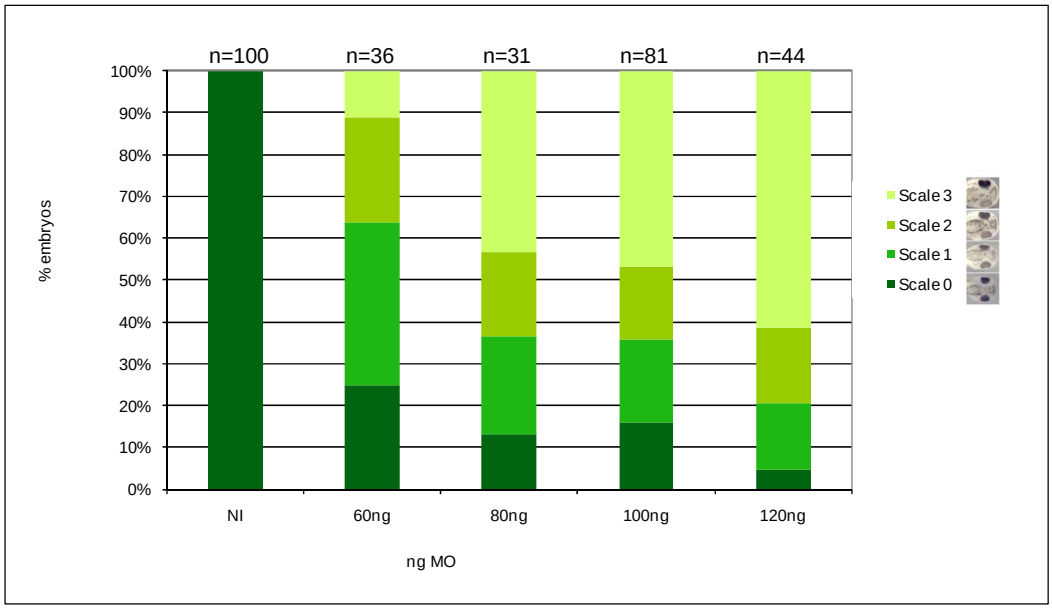

Figure 53
Splice morpholino knockdown
Increasing concentration of splice morpholino causes an increase in the amount of tadpoles with a scale 3 phenotype.

Lower concentrations of splice morpholino have a stronger effect than those of the ATG morpholino. 60ng of ATG morpholino causes approximately 55% of embryos to have a reduction in pigment, whereas with the same concentration of splice morpholino approximately 75% of embryos are affected. Similar patterns are seen with 80ng, 100ng and 120ng.

5.2.3.3 Determining the activity of the splice morpholino

Following splice morpholino treatment, some scale 3 tadpoles (the embryos used were injected at the 1 cell stage) were processed for PCR analysis over and around the intron/exon boundary target of the splice morpholino. To determine what affect the splice morpholino was having on the transcript.

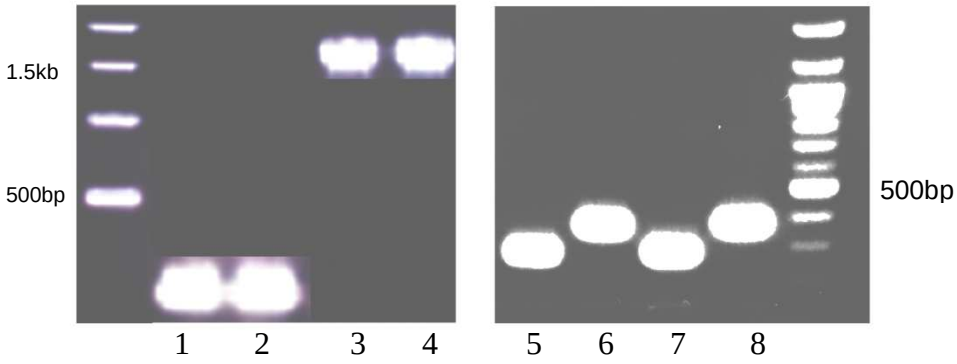

Figure 54
PCR analysis following splice morpholino treatment.
1 and 2 H4 controls, 3 and 4 full length primers (5'Xho1 and 3'Xba1 primers) , 1 and 3 NI embryos, 2 and 4 splice MO embryos, 5 and 6 NI embryos, 7 and 8 splice MO embryos, 5 and 7 FS2 and 3'Xba1 primers, 6 and 8 FS1 and 3'Xba1 primers (see appendix for primer information). NI; non injected, MO; morpholino.

Primers FS1 and 3'Xba1 cover the area over the splice morpholino target (400bp) and primers FS2 and 3'Xba1 cover a region following the splice morpholino target (300bp). The PCR results indicate that the splice morpholino is not affecting the exon structure for the SLC24A5 transcript (figure 54). This is also reflected in the full length PCR (1.5kb) where the splice morpholino treated sample would not be expected to work with these primers as the 3' priming site should be missing (1.1kb) (figure 54).

5.2.4. Double morpholino knockdown

Once both the ATG and splice morpholino had been shown to give a hypopigmented phenotype individually, they were used in combination to see if collectively they would give a stronger phenotype, particularly in the lateral pigmentation, where much of the pigmentation remains following individual morpholino treatment. The experiment was conducted as previously described for individual morpholinos, and the results are shown in figure 55.

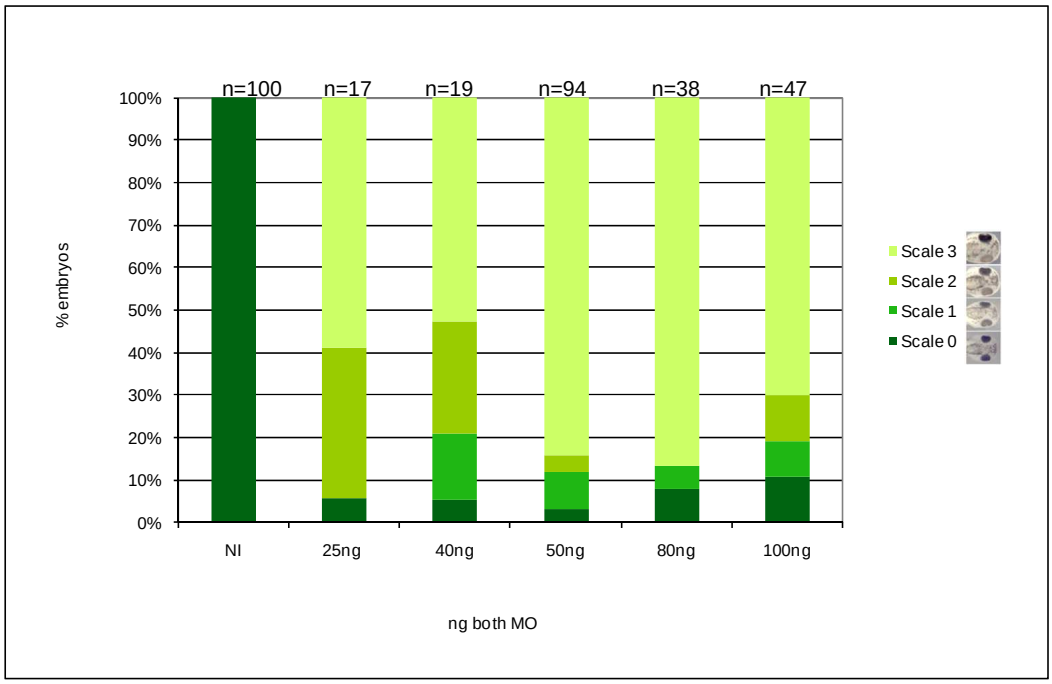

Figure 55
Double morpholino knockdown of SLC24A5.
Even at lower concentrations, combining the morpholinos has a stronger effect than individual treatment.

Treating embryos with both morpholinos causes a greater proportion of them to have a reduced pigment phenotype when compared to individual treatments. 40ng of each morpholino (total 80ng) causes a 95% knockdown, whereas 80ng of ATG morpholino alone causes 63% knockdown and 80ng of the splice morpholino alone causes 85% knockdown. The same result is seen with 50ng both morpholino (100ng total) and100ng of morpholinos individually (figure 55).

5.3. Discussion

Antisense morpholino oligos knockdown expression of target genes by complementarily base pairing to the gene transcript and thus repressing translation or splicing (Heasman, 2002).

Morpholino knockdown of SLC24A5 in *X.laevis* embryos causes a clear reduction in pigmentation (figure 43). This is most prominent in the RPE of the eye but also noticeable in the lateral pigmentation. The morpholino effect is proportional to the concentration of morpholino injected (figure 44, 53, 55). That is the proportion of embryos affected, rather than individual severity of effect, which is not seen to get any more severe than a scale 3 (figure 43). As varying degrees of effect were seen, a scale was devised to represent the phenotypes, by which all embryos could be visually scored and thus the phenotypes could be better qualified. Unaffected embryos were presented as scale 0, wild type. A subtle reduction in pigment was represented in scale 1. A clearer affect was represented as scale 2. Scale 3 was the most severe phenotype and corresponds to the golden phenotype in zebrafish larvae (figure 13). This kind of result where varying degrees of effect are seen is consistent with other *X.laevis* morpholino experiments (Afouda and Hoppler, 2011; Garcia-Morales et al., 2009). The lack of an all or nothing effect is presumably due to natural variations in the embryos, human error during injection or damaged morpholino. We see no non specific effects from either morpholino here suggesting that the morpholinos are specific, and other effects sometimes seen with morpholinos can be ruled out (Eisen and Smith, 2008).

60ng of ATG morpholino was the lowest concentration to give a reduced pigment phenotype although this was subtle. 80-120ng proved to be more effective, and gave a dose response (figure 44). Across these concentrations of the ATG morpholino, the percentage of scale 0 and scale 3 embryos changes considerably, whereas the percentages of scale 1 and 2 embryos remains quite similar. This could suggest that there is almost an all or nothing affect.

The splice morpholino gave a much stronger effect at lower concentrations. At 60ng the splice morpholino causes 75% of the embryos to have some pigmentation defect; this is 22% higher than that seen at the same concentration of ATG morpholino. At 80ng the difference between the 2 morpholinos is 44%, as here the ATG morpholino actually seems to have less of an effect, this is presumably due to some experimental variation. At higher concentrations, the difference in effect between the morpholinos is less significant; at 100ng and 120ng the difference is 11% and 5.2% respectively, indicating that at this range of concentration repression of SLC24A5 translation is maximal. Above 120ng gave similar phenotypes but also proved more toxic (data not shown). The PCR analysis shown in figure 53 suggests the splice morpholino is not affecting the transcript structure, as here the splice morpholino treated embryos have the same bands as the non injected controls. It is thought that as the splice morpholino cannot target all the transcript present the remaining transcript is being picked up in the PCR and as this is a sensitive technique no difference can be seen between the samples and controls. Quantitative PCR would be a better approach here, however this was not done due to time constraints.

When used in combination the morpholinos gave a stronger effect as seen in figure 54. Here just 25ng of each morpholino, (total 50ng morpholino), is sufficient to induce a reduction in pigmentation in a significant percentage of treated embryos (94%). 40ng, 50ng and 80ng also give a strong effect at 94.8%, 96.9% and 92.1% respectively. The double morpholino treatment also causes a larger proportion of the embryos to be scale 3 suggesting, as expected, that the morpholinos are stronger in conjunction than individually. However, a complete loss of pigment is still not achieved.

As discussed earlier, *X.laevis* is tetraploid, and only one SLC24A5 paralog was isolated in this study. Both morpholinos are targeted to this one gene, therefore it is possible that the other gene is sufficiently different in sequence that it is not targeted by the morpholinos, and as such is offering some redundancy to the function of the targeted protein.

The morpholino knockdown phenotype described here is consistent with that seen in the zebrafish, where morpholino knockdown of SLC24A5 phenocopies the golden phenotype (Lamason et al., 2005) (figure 56). The morpholino could be less effective in *X.laevis* due to the tetraploidy condition discussed above.

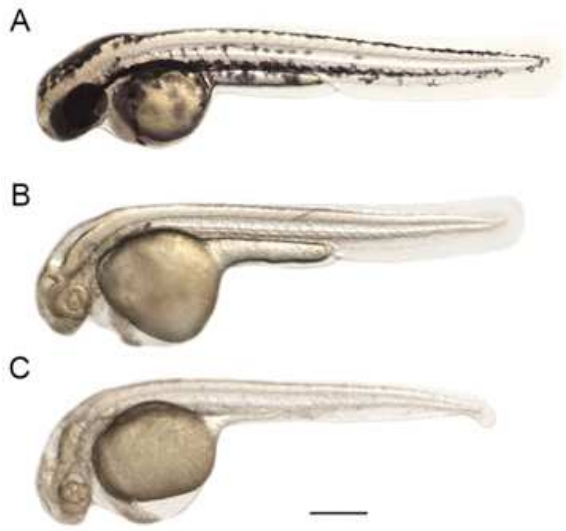

Figure 56
Morpholino knockdown of SLC24A5 in zebrafish.
As shown earlier, morpholino knockdown in zebrafish embryos reduces pigmentation. A, wild type 48hpf zebrafish embryo. B, golden 48hpf zebrafish embryo. C, wild type 48hpf embryo injected with morpholino targeted to SLC24A5 (Lamason et al., 2005).

The unilateral delivery of the morpholinos provides a good internal control, but it should also be noted that some neural crest cells do migrate from one lateral side of the developing tadpole to the other, thus pigment cells originating from the injected cell may be effected by the morpholino but move to the non injected side, and vice versa. This goes some way to explain the lack of pigment reduction in the lateral pigment stripe. As RPE cells do not originate from the neural crest there are no such issues with migration. Also as a dense population of cells a loss of pigmentation is more noticeable and thus easier to visually score with the eye.

Another issue regarding morpholino effectiveness is dilution. As the embryos have to be raised up to tadpole stages, ~3 days, to see the effect on pigmentation, the morpholino becomes diluted throughout the developing embryo and thus there is less available to saturate the pool of SLC24A5 transcript, which itself is not expressed until stage 25 at the earliest.

SLC24A5 expression is concentrated in one small cell population (the pigment cells), so overall SLC24A5 abundance throughout the whole embryo is relatively low, also when compared to other pigment genes SLC24A5 appears to be less prevalent (figure 38); therefore it is not surprising that relatively high concentrations of morpholino are needed to observe a phenotype.

As an ion exchanger protein, SLC24A5 was not expected to be directly involved in a signalling pathway. However, Ginger et al (2008) showed that siRNA mediated knockdown of SLC24A5 in human repigmented melanoblasts resulted in a significant decrease in protein expression of Pmel17, MART1, Tyr and Tyrp1, suggesting that SLC24A5 is important throughout melanosome development. Protein expression of the lysosome marker LAMP1 was found to be up-regulated following SLC24A5 knockdown (Ginger et al., 2008). In the absence of antibodies, *in situ* analysis was used here to detect any changes in the expression of key melanogenesis genes following SLC24A5 morpholino knockdown *in vivo*. As seen in figures 45 and 47 DCT and tyrosinase transcript expression is not affected by the SLC24A5 morpholino. This data also shows that the melanophores are able to migrate and have normal morphology following morpholino treatment.
Mitf expression however does seem to be reduced following SLC24A5 morpholino knockdown, this can be seen in the eye of the tadpole in figure 46D. This seems perverse as DCT and Tyr are targets of Mitf so if Mitf is affected then an effect on its targets would be expected. It would be of interest to analyse expression of these; and other targets of Mitf, at the protein level.

The presence of DCT and tyrosinase suggests that the melanophores do have the appropriate infrastructure to enable pigment production, but somehow the lack of SLC24A5 inhibits this to a degree. However, this analysis only shows any affect on the transcript of these genes, it is possible that translation is affected, but due to lack of antibodies this cannot be detected in this system.

Alternatively, SLC24A5 may be expressed after tyrosinase, DCT and Mitf and therefore its repression has no effect on their expression. Potentially, morpholino knockdown of one of these pigment genes could affect SLC24A5 expression, although at this time these gene functions are not thought to be inter linked.

The normal expression of transcripts of pigmentation genes seen here and the altered protein levels seen in human cell culture, and taking into account the TGN colocalisation of SLC24A5 suggest perhaps SLC24A5 is involved in the sorting and trafficking of these proteins. This fits with a model proposed by Ginger et al (2008) that NCXK5 plays a role in maintaining Ca^{2+} levels during membrane fusion events which are critical for melanosome biogenesis and are Ca^{2+} mediated (Ginger et al., 2008; Raposo et al., 2007; Raposo et al., 2001).

Histological analysis of morpholino treated tadpoles shows how severe the morpholino effect can be. This is particularly clear in the eye, which while remaining normal in size and shape appears to be lacking a layer of pigment cells thus giving a lighter phenotype (figure 48). It would be of interest to determine if this has any effect on visual acuity. This could be explored using a simple assay, where morpholino treated embryos are placed in a container which is half kept in darkness and half in light, if the embryos can see they would stay in the dark side, persistent presence of embryos in the light side would indicate some degree of blindness. (Viczian et al., 2009).

In summary, morpholino knockdown of SLC24A5 results in reduction of pigmentation. This supports a role for SLC24A5 in pigment production as seen already in human cell culture and zebrafish embryos. However this data alone does not provide any insight into the function of SLC24A5, thus further functional analyses were conducted.

Chapter Six:

Rescue analyses

6.1. Introduction

Currently it has been shown that SLC24A5 is important for pigmentation and that it likely encodes an NCKX protein; however the ion exchanger activity of this protein has not yet been linked to its role in pigmentation. To further analyse the role of NCKX5 in pigmentation a functional approach was undertaken. This involved rescue experiments with mutant clones of SLC24A5.

Previously, a significant amount of research has been conducted into the function of other NCKX proteins, including NCKX2. Much of this work has related to the biochemistry of the protein and has been done at the University of Calgary in the lab of Paul Schnetkamp (Altimimi et al., 2010; Altimimi and Schnetkamp, 2007a; Kang and Schnetkamp, 2003; Kang et al., 2005b; Kinjo et al., 2005; Kinjo et al., 2007; Kinjo et al., 2003; Kinjo et al., 2004; Shibukawa et al., 2007; Winkfein et al., 2004). This has revealed a number of residues within NCKX2 which are particularly important for various aspects of its function. As a plasma membrane protein it is relatively easy to perform functional assays on NCKX2, such as the reverse exchange assay used by Winkfein et al (2004), discussed earlier (figure 22.) and patch clamp experiments as used by Kang et al (2005). NCKX5 however, is found on an intracellular organelle membrane and therefore it is very difficult to examine in the same assays. We have collaborated with the Schnetkamp lab and they have provided several NCKX5 mutants, based on their findings in NCKX2. As proteins of the same family it is reasonable to infer that the crucial residues of NCKX2 are also crucial for NCKX5 function as some of these are conserved (figure 59). These mutant clones were used in rescue experiments to determine which residues of the protein are crucial for its role in pigmentation.

6.1.1. Mutant constructs

All the constructs used to rescue the morpholino effect were human sequences and had a myc tag added at the N terminal small intracellular loop to allow detection by western blot, location of a myc here in NCKX2 has been found not to interfere with the protein function (Kang and Schnetkamp, 2003). The wild type human gene was provided, along with the A111T variant allele, discussed earlier. The other mutants were; D383N, 4C and CH. The D383N mutant is the equivalent mutation to D548N in NCKX2 (Kang et al., 2005a) (figure 59), which has been shown to inhibit calcium transport function and thus render the protein non functional. In the 4C mutant, the 4 cysteines found in the large cytosolic loop have been replaced with glycine, and the CH mutant is missing the large cytosolic loop, this has been replaced with a spacer region (Kinjo et al., 2003). By sequence similarity, it was hypothesised that the human wild type clone should rescue or partially rescue the morpholino phenotype, as was also seen in the zebrafish (Lamason et al., 2005). It was also thought that the A111T may provide a partial rescue, although this may be less significant as it is a less functional protein. Based on the NCKX2 work the D383N mutant was not expected to rescue as this has impaired calcium transport. The Asp residue at this position is conserved in NCKX5, across the selected species (figure 59). The 4C and CH mutants were used to determine if the cysteines and cytosolic loop are important for function of the protein. Despite their common critical role in many proteins, it has been previously shown that cysteine residues are not important for NCXK2 function, here we can examine if this is also true for NCXK5 (Kinjo et al., 2004). The *X.laevis* clone was also used in rescue experiments, before this could be tested it had to be mutated in the morpholino target region to prevent it from being repressed by the morpholino and thus masking any rescue affect.

6.1.2. NCKX2 and chimeras

We also set out to test chimeras of NCKX2 and NCKX5 to determine crucial regions of the NCKX5 protein. NCKX2 is related to NCKX5, although they are expressed in different tissues and in different cellular locations; NCKX2 being plasma membrane bound and NCKX5 being intracellular. Human NCKX2 was used to rescue NCKX5 repression, although this was not expected to rescue, as it is does not have high similarity to NCKX5 and also although they are both potassium dependent sodium calcium exchangers they have different physiological roles. Also chimeric constructs of NCKX2 and NCKX5 were made and used in rescue analysis to test various parts of the protein. These were; NCKX5 with the large cytosolic loop of NCKX2 and NCKX5 with the signal sequence and N-terminal loop of NCKX2 (figure 58).

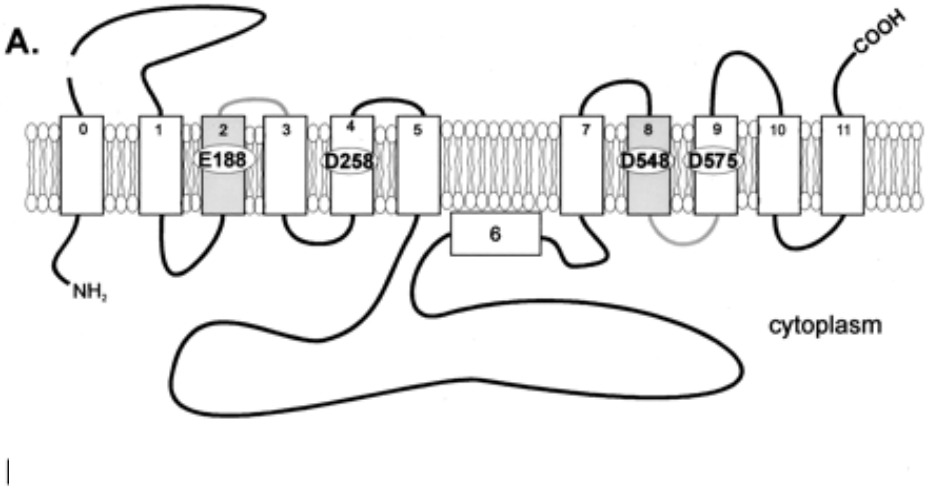

Figure 57
Schematic representation of the topology of NCKX2.
NCKX2 is comprised 12 transmembrane domains and a large cytosolic loop (Kang et al., 2005b).

Figure 57 shows the topology of NCKX2, Bioinfomatic analyses of NCKX5 suggest a similar topology (figure 34). Various areas of the SLC24A5 sequence have been substituted with the corresponding area of SLC24A2 sequence to encode chimera proteins.

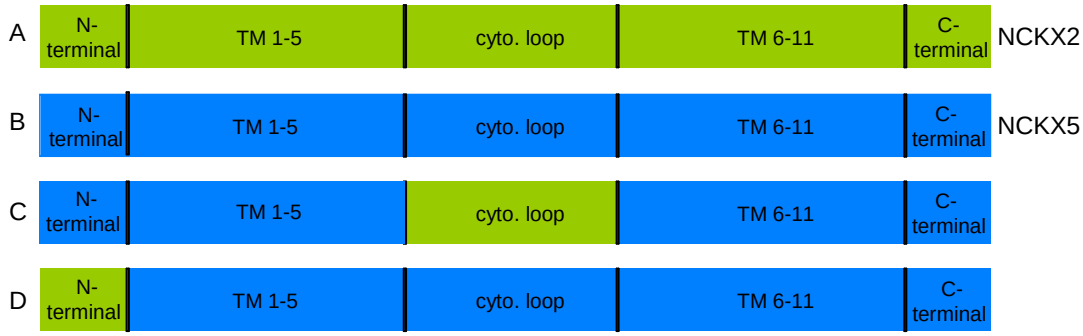

Figure 58
Schematic representation of the NCKX2/NCKX5 chimeras used in rescue analysis. Highlighting domains of the proteins. A, NCKX2, B, NCKX5, C, NCKX5 with cytosolic loop of NCKX2, D, NCKX5 with N-terminal domain of NCKX2. TM, transmembrane domains

Rescue from the first construct (figure 58C) would suggest that the cytosolic loop of NCKX5 is not crucial to its function, or that the loop from NCKX2 is similar enough to allow the protein to function. Conversely, no rescue would suggest the cytosolic loop is crucial for NCKX5 function. The loop of NCKX2 is approximately 170 amino acids in length (Winkfein et al., 2004); whereas the predicted cytosolic loop of NCKX5, based on sequence alignment is only 76 amino acids (figure 59).

With the second construct (figure 58D), (NCKX5 with signal peptide and N-terminal loop of NCKX2), a rescue would suggest this region is unimportant or functionally conserved between NCXK2 and NCKX5. It would be of interest to determine if this construct can target NCKX5 to the plasma membrane, in this system, and if from here it has any function in melanogenesis. The N terminal region of NCKX2 and NCKX5 is not well conserved (figure 59), so it would be surprising to see a rescue.

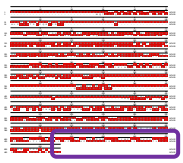

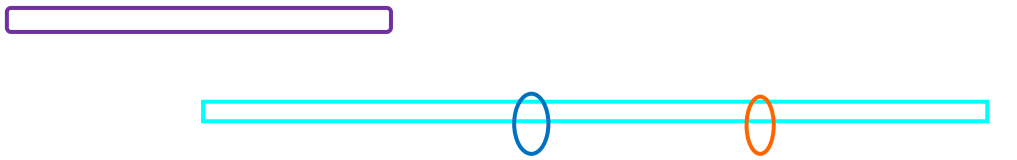

Figure 59
Conserved residues between NCKX2 and NCKX5.
Alignment of human NCKX2 and NCKX5. Showing residues mutated in the rescue constructs. Purple box; signal peptide sequence of NCKX2, green box; large cytosolic loop of NCKX2, blue circle; 111 position of the A to T switch, yellow circles; cysteines of the cytosolic loop, pink circle; D383N, orange circle; E188, light blue boxes; alpha repeats.

6.2. Results

6.2.1. Site Directed Mutagenesis of *X.laevis* SLC24A5

In order to use the *X.laevis* sequence in the rescue analysis it had to be mutated such that the morpholino would not recognise it. This was done by designing primers (SDM of SLC, full length 3'3*, see appendix), over this region with two nucleotide changes (figure 60), this should be sufficient to prevent the morpholino binding. Also the nucleotides chosen gave a BamH1 site (GGATCC), this was useful to ensure presence of the mutation as there are no other BamH1 sites in the full length sequence.

Figure 60
SDM of the *X.laevis* sequence showing the two nucleotide mismatches.

6.2.2. Rescuing the ATG morpholino phenotype

Synthetic capped RNA of the mutant constructs were combined with the morpholino and co-injected in the same way as the morpholino experiments. cRNA of the mutants was also injected alone as a control and also to see if there was any over expression affect. In each experiment some embryos were injected with just morpholino to provide a fair comparison of affect. Again all embryos were scored to the scale in figure 43. All the chimera constructs were tagged with GFP and myc to facilitate detection of the protein.

100ng of morpholino was felt to be the lowest concentration to give a strong consistent knockdown so this concentration was used in rescue experiments, as the threshold for the cRNA to rescue was thought to be achievable. Lower and higher concentrations of morpholino were tested, but 100ng seemed to be the best (data not shown). 1-5ng of cRNA was used to rescue 100ng morpholino (data not shown), only 4-5ng showed a rescue – depending on the construct, so 5ng was used for all constructs. 5ng of cRNA alone was not toxic and gave no phenotype (data not shown). The results are represented in the following figures.

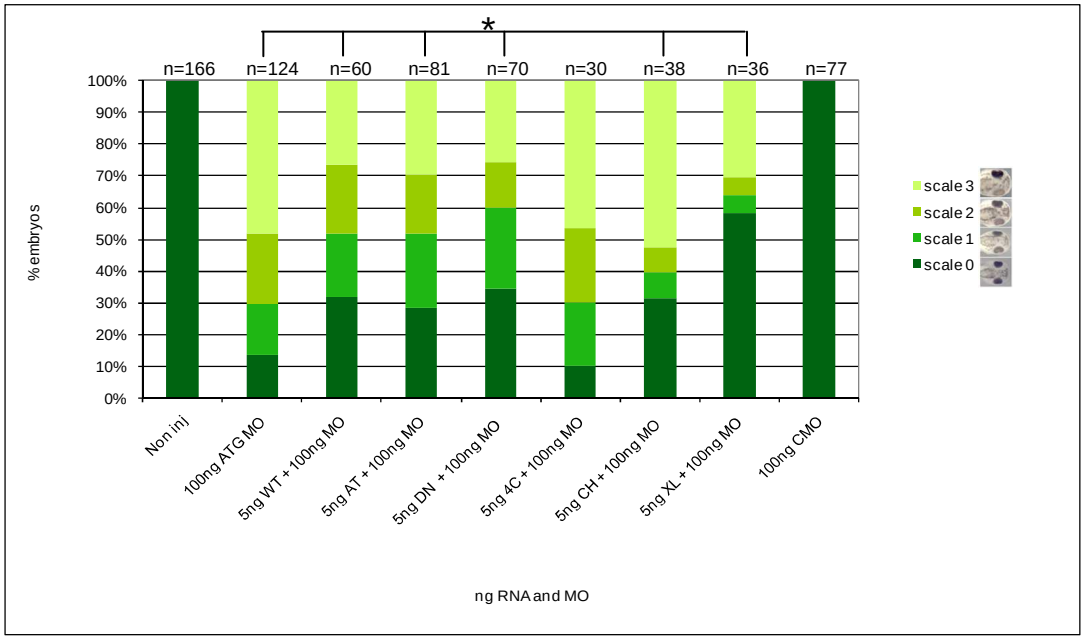

Figure 61
Rescuing the ATG morpholino.

Embryos injected with 100ng ATG morpholino and 5ng cRNA of the various constructs. Embryos were allowed to develop to stage 38 and then scored for effects in pigment pattern as the scale in figure 41.
NI non injected, WT wild type, AT A111T, DN D383N, XL *X.laevis,* mo morpholino, CMO control morpholino*.* Kruskal Wallis test revealed significant difference between 100ng ATG MO and the WT, AT, DN, CH and XL constructs, p=0.001 for all, but not 4C p=0.988, (for statistical analysis, see materials and methods 2.8.2).

In figure 61, following morpholino alone treatment 13.7% of embryos are wild type, however this increases to 31.6% when human wild type NCXK5 is co-injected with the morpholino. The percentage of embryos of the severe scale 3 phenotype is reduced from 48.3% to 26.6% with the human construct. Scales 1 and 2 remain largely unchanged (16.1% to 20% and 21.7% to- 21.6% respectively). This rescue also proved to be statistically significant where p=0.001*.

(* the statistical tests applied here and throughout further results, indicate a significant difference between the morpholino alone and WT rescue data, on analysing the percentages of different phenotypes one can conclude that this 'difference' suggests a rescue from this construct).

Addition of A111T with the morpholino caused an increase in wild type (scale 0) embryos from 13.7% (morpholino alone) to 28.4%. The percentage of scale 1 embryos was also increased, from 16.1% to 23.5% and scale 2 and 3 embryos were reduced by 3.3% and 18.75% respectively. This rescue is statistically significant, p=0.001.

D383N increased the amount of wild type embryos from 13.7% to 34.2% and scale 2 embryos from 16.1% to 25.7%. Scale 2 and 3 percentages were reduced by 7.4% and 22.7% respectively, p=0.01.

The percentages of embryos of the given phenotypes is largely unchanged with 4C, there does actually appear to be a slightly increased morpholino effect where the percentage of wild type embryos is 13.7% (MO alone) compared to 10% with 4C, this is not significant and is likely due to experimental variation. 20% of embryos are scale 1, compared with 16.1% in morpholino alone. Scale

2 is increased by 1.5% and scale 3 is reduced by 1.7%, but again this is insignificant, p=0.988 for 4C rescue.

Rescue with the CH mutant was a strong as wild type, indicating the loop region is not important for NCXK5 function. Scale 1 embryos were increased by 17.9%. Scale 1 and 2 were reduced by 8.2% and 13.9% respectively. Scale 3 actually increased slightly to 52.6% from 48.4%, but this is likely due to variation. This rescue is statistically significant p=0.001.

The mutated *X.laevis* construct can rescue, here scale 0 embryos were increased to 58.3% from 13.7%. Scale 1 and 2 embryos were reduced by 10.6% and 16.2% respectively. Scale 3 was reduced by 17.8%. This is statistically significant, p=0.001.

All constructs, except 4C, show a significant rescue (figure 60). This is particularly apparent in the percentage of scale 0 (wild type) embryos, which increases with the rescue constructs, compared to the morpholino alone data. Also the percentage of scale 3 embryos reduces significantly when treated with WT, A111T, D383N or Xl cRNA, this is less significant following CH or 4C treatment. The relative percentage of scale 1 and 2 embryos remains largely the same in the rescue treatments compared with the morpholino alone data, except CH and Xl where these phenotypes are significantly reduced.

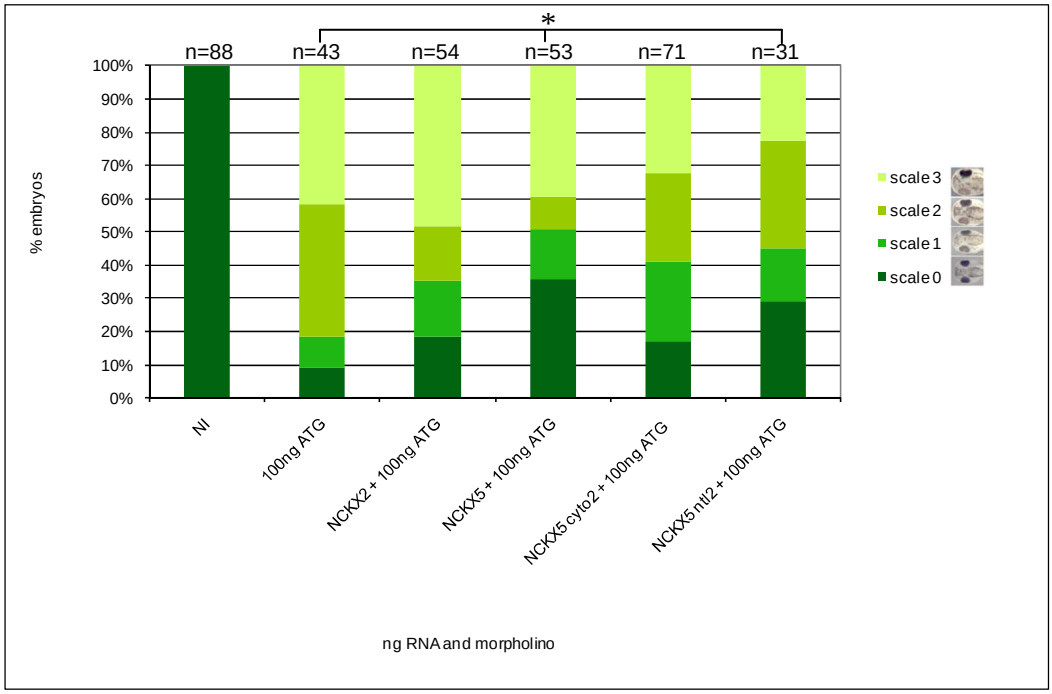

Figure 62
NCKX2/5 chimera rescues of the ATG morpholino.
NI non injected. NCKX2, NCKX5, NCKX5 cyto2, NCKX5 ntl2 are discussed in the text. Kruskal Wallis revealed a significant difference between 100ng ATG MO alone and the NCKX5 and NCKX5 ntl2 constructs, p=0.01 and p=0.022 respectively.

The NCKX2 construct and NCKX5 cyto2 chimeric constructs cannot rescue the 100ng ATG morpholino effect, the NCKX5 and NCKX5 ntl2 construct however can. This is consistent with previous data where the WT construct (effectively the same as NCKX5 here, although NCKX5 has a GFP tag) can rescue. Also earlier we saw that the 4C construct could not rescue, here the NCKX5 cyto2 construct cannot rescue either, these are both mutants/variants of the large loop

6.2.3. Rescuing the splice morpholino

As seen in figure 52, the splice morpholino gives a stronger effect at lower concentrations. However, 100ng of splice morpholino was used in the rescue experiments, consistent with the ATG morpholino rescues.

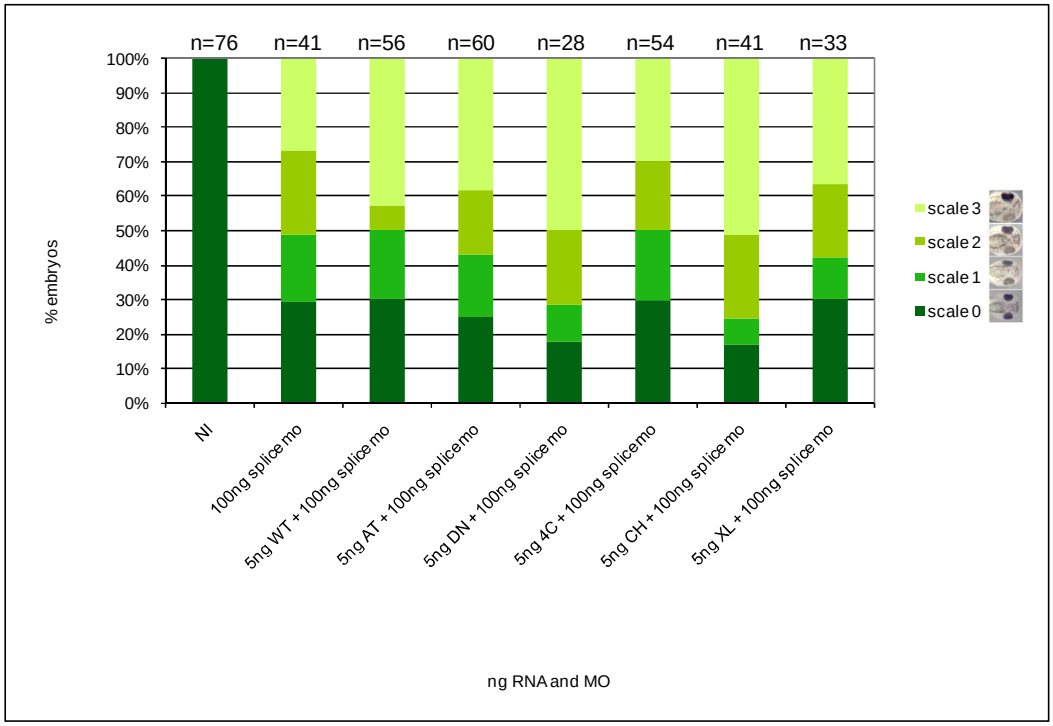

Figure 63
Rescuing the splice morpholino.
NI non injected, WT wild type, AT A111T, DN D383N, XL *X.laevis,* mo morpholino*.* Kruskal Wallis test showed no significant difference between morpholino alone and any of the rescue constructs.

Surprisingly the splice morpholino effect could not be rescued by any of the constructs tested (figure 63). Lower concentrations of splice morpholino were used to see if these could be rescued, but 80ng and 50ng splice morpholino still could not be rescued (data not shown). Increased concentrations of cRNA were not tried as 5ng is already the recommended maximum, and higher concentrations could lead to toxicity effects.

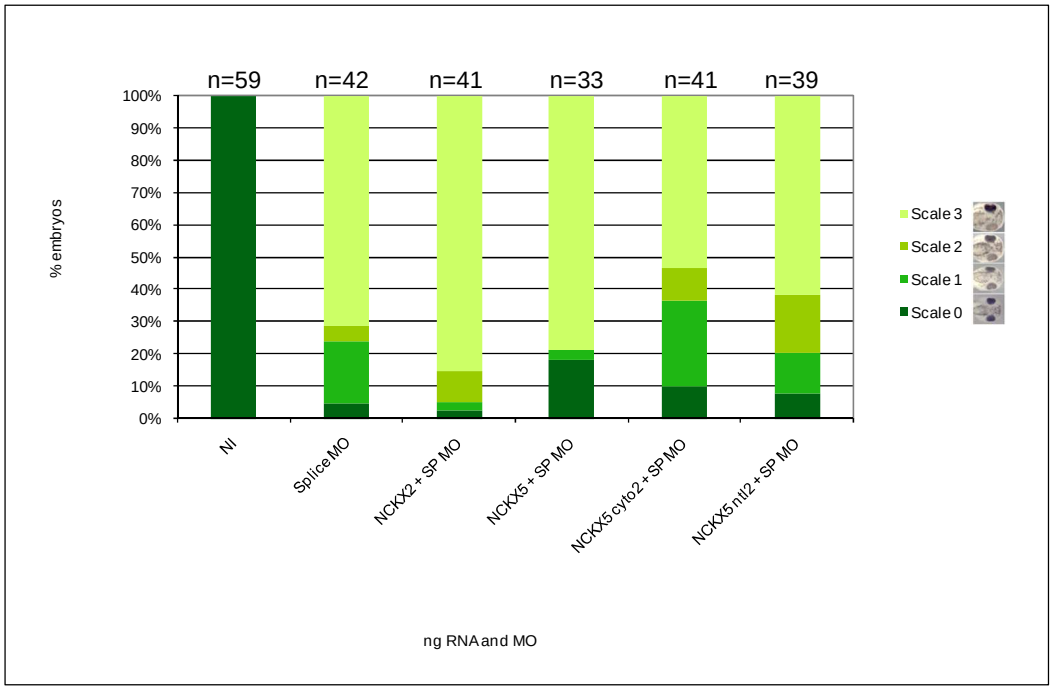

Figure 64
NCKX2 chimera rescues of splice morpholino
None of the chimera constructs can rescue the splice morpholino, there was no statistical significance. SP MO, splice morpholino.

Consistent with the other mutant constructs the chimera constructs cannot rescue the splice morpholino effect (figure 64). No statistical significance was observed.

6.2.4 Rescuing the double morpholino knockdown

To follow up the ATG and splice morpholino rescues we attempted to rescue the double morpholino knockdown. 50ng of both morpholino was the chosen concentration of morpholino, and again 5ng of cRNA was used.

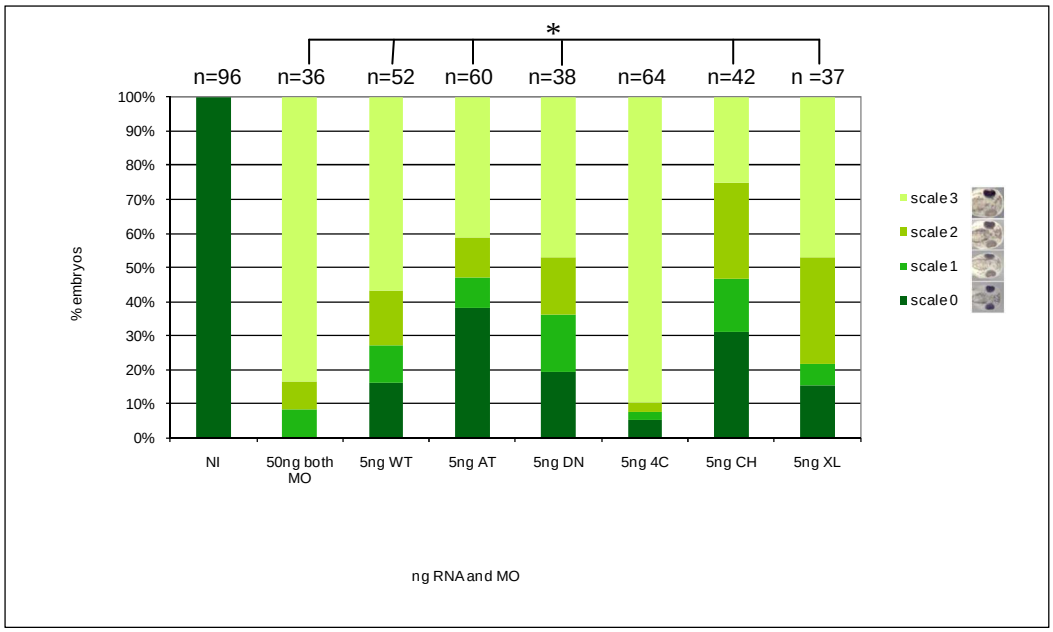

Figure 65
Double morpholino rescue
NI non injected, WT wild type, AT A111T, DN D383N, XL *X.laevis,* MO morpholino. Kruskal-Wallis test revealed significant differences between 50ng both MO and the WT, AT, DN, CH and XL constructs where p=0.029, 0.03, 0.001, 0.001, and 0.004 respectively, 4C p=0.123.

All constructs except 4C can rescue the double morpholino knockdown (figure 63). Surprisingly A111T seems to rescue better than wild type and *X.laevis.* Morpholino alone is having a strong effect, which is relatively consistent with the previous ATG morpholino alone data (figure 55). Lower concentrations of double morpholino could also be rescued (data not shown).

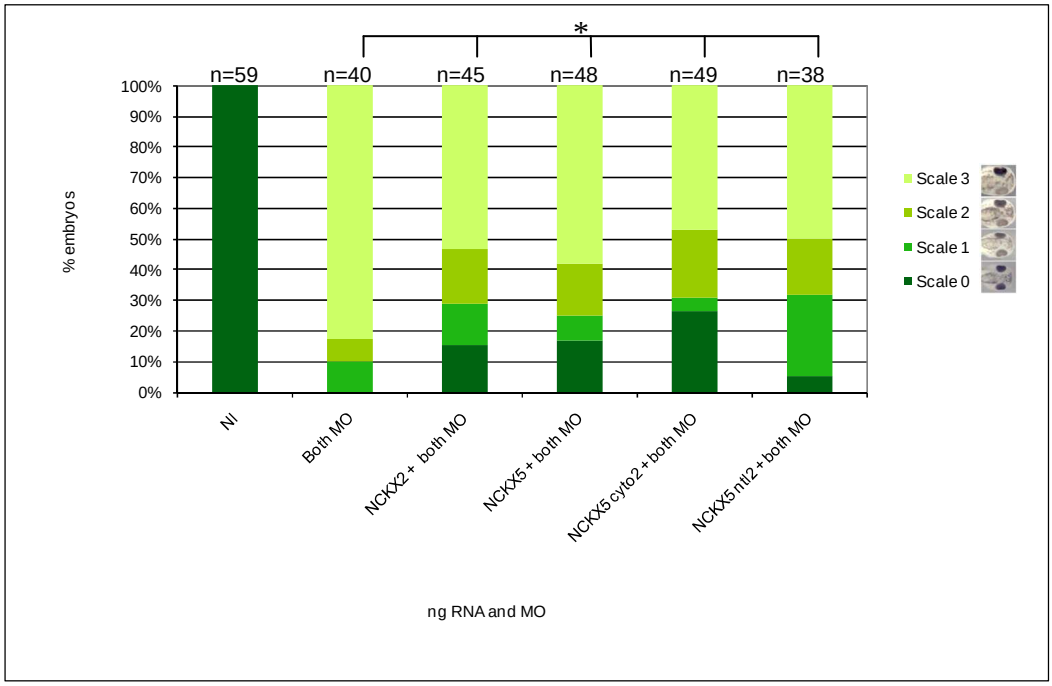

Figure 66
Rescue of the double knockdown with the chimera constructs.

Unexpectedly the NCKX2 construct appears to rescue the double morpholino knockdown, as can NCKX5. Also the NCKX5 cyto2 appears to rescue, this is inconsistent with the lack of rescue from the 4C construct seen earlier. The NCKX5 ntl2 construct rescue suggests this region of the protein is not functionally important, that or the NCKX2 region can perform here (figure 66). Statistical significance was detected in all constructs; p= 0.003, 0.01, 0.01 and 0.02 respectively. However the double morpholino effect here is so strong, no embryos were scale 0 (wild type), therefore any amount of wild type embryos in the rescue samples is potentially a rescue. Analysing the data it could be suggested that the NCKX5 ntl2 rescue is not real as there were only 2 wild type embryos.

6.2.5 Protein detection

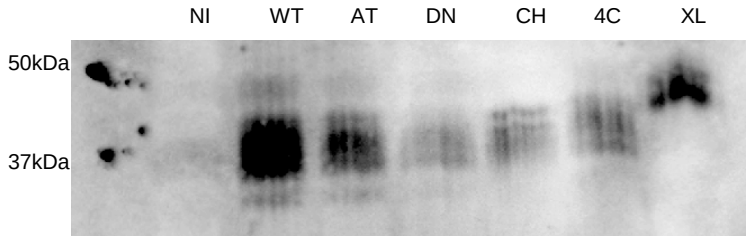

Figure 67
Western blot of embryo lysates following injection with the rescue constructs, using anti-myc antibody to the myc tag added to the constructs.

All rescue constructs could be detected by probing western blot with anti myc antibody. The proteins are ~40kDa and appear as a triplet, consistent with Ginger et al (2008). The *X.laevis* NCKX5 appears to be larger than the human.

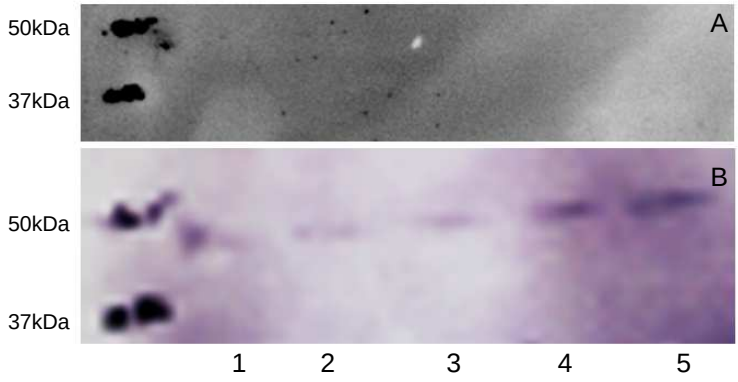

Figure 68
Western blot of embryo lysates following injection with the chimera constructs, using A; GFP antibody and B; actin loading control. 1, NCKX2, 2, NCKX5, 3, NCKX5 cyto2, 4, NCKX5 ntl2, 5, NI

Unfortunately the chimera constructs could not be detected by western blot, either with an anti GFP antibody (figure 68 A) or anti myc antibody (data not shown).

6.3 Discussion

6.3.1 Rescuing the Knockdown Phenotype

To further investigate the function of SLC24A5, mutant human NCKX5 constructs were used to attempt to rescue the morpholino induced pigmentation phenotype. These constructs carry mutations at equivalent residues, in NCKX5, known to be important for NCKX2 function, as well as one which carries the ancestral SNP at A111T, and two NCKX2/NCKX5 chimeras. The *X.laevis* construct was also used to rescue and to demonstrate the specificity of the ATG morpholino, this was mutated such that the morpholino wouldn't target it. These experiments were designed to elucidate key residues for NCKX5 function in melanogenesis.

6.3.1.1 Wild type human NCKX5 can rescue the ATG morpholino

The wild type human NCKX5 is 65.8% similar to the *X.laevis* sequence, at the amino acid level, (figure 33). In rescue experiments we found it could rescue the morpholino knockdown of *X.laevis* NCKX5. The rescue is assessed by the recovery of wild type embryos (scale 0). This was not as strong a rescue as the *X.laevis* clone provided though (figure 61), which is to be expected and fits with the hypothesis. This also fits with the zebrafish work, where human SLC24A5 could partially rescue the SLC24A5 morpholino which phenocopied the golden phenotype (Lamason et al., 2005)

6.3.1.2. A111T can rescue the ATG morpholino

The non synonymous SNP at position 111 of the human sequence causes an amino acid change, alanine to threonine. The alanine encoding allele was found to be prevalent in dark skin human populations, whereas the threonine encoding allele was found in lighter skin human populations. Switching alanine for threonine at position 111 of the human sequence causes the protein to be less active (Ginger et al., 2008). Thus it was rightly predicted that this protein would provide some rescue but not as much as the wild type human protein (figure 61). Although the rescue is stronger than anticipated. It may be worthwhile to

replace the alanine at the equivalent position of the *X.laevis* sequence (177), to determine if a switch here also affects *X.laevis* NCKX5 activity. This would be predicted to cause a similar reduction in function as this residue is thought to be conserved across species and the NCKX family. It has been shown that substituting the equivalent amino acid in NCKX2 also causes a reduction in protein activity (Ginger et al., 2008).

6.3.1.3 D383N can rescue the ATG morpholino

In NCKX2 aspartate 548 (383 in NCKX5) was found to be one of two crucial residues for calcium transport. Both these residues are conserved in NCXK5 (figure 59). This residue along with glutamate 188 is the central residue within the ion binding pocket of NCKX2. This binding pocket can hold 1 K^+ and 1 Ca^{2+} simultaneously and can alternate between an inward and outward facing conformation. Size conservative substitution of asp548 with asparagine eliminates the charge and results in a non functional NCKX2 protein. Whilst charge conservative D548E, affects the K^+ and Ca^{2+} concentration dependencies (Kang et al., 2005a). D548 and E188 are conserved residues in NCKX5, it would be of interest to use a E188N mutant to determine if this has the same effect.

The D383N mutant gave a strong rescue which is surprising because this mutant was predicted to have impaired calcium transport activity based on similar work in NCXK2 (Kang et al., 2005a). This suggests it is not the calcium transport function of NCKX5 which is important for its role in pigmentation, but that the protein may have some other function. Which is not uncommon for ion transporters, it has been demonstrated that NKCC1 (SLC12A2) $Na^+/K^+/Cl^-$ could induce secondary axis formation in *X.laevis*, independently of its co-transporter function (Walters et al., 2009). To this end *X.laevis* SLC24A5 was injected into the ventral marginal zone in 4 cell stage embryos (Garcia-Morales et al., 2009), to see if a duplicate axis could be induced (data not shown). No such effect was observed, ruling out this phenomenon from SLC24A5 function.

6.3.1.4 4C cannot rescue the ATG morpholino

Cysteine residues are known to be important in many proteins, particularly for enzymatic reactions and inter/intra molecular interactions (Leonard and Carroll, 2011).

The 4C cysteine mutant cannot rescue the morpholino knockdown; this suggests that these cysteine residues are important for NCKX5 function. Kinjo et al (2004) found that cysteine residues were not important for NCKX2 function. They developed a series of cys-mutants including a cys-less mutant, which did show some activity. However, their cysteine mutants did lose some transport activity, thus it is possible that the 4C mutant also loses some transport activity, and in NCKX5 in this system, the reduction is sufficient such that it cannot compensate for the reduction in NCXK5. Also the 4C mutant has lost cysteine residues within the cytosolic loop, whereas Kinjo et al (2004) substituted cysteines in the transmembrane domains. NCKX2 only has one cysteine in its cytosolic loop (C394), which has been shown to be particularly active (Kang et al., 2003). NCKX5 does not have a cysteine at this position, but does have 4 other cysteines in this loop region, which are conserved across selected species (figure 33), thus the cytosolic loop cysteines of NCXK5 may be equally as active and important for NCKX5 function. The cysteines in the 4C mutant have been replaced with glycine, previous analysis in NCKX2 have used serine or alanine (Cai et al., 2002; Kinjo et al., 2004) to replace the cysteines, it may be relevant to make cys-mutants with these residues as well to determine if the replacement amino acid is having an effect on the protein function. So it appears that perhaps structural effects are not important for transport function, but maybe they are involved in protein/protein interaction.

6.3.1.5 CH can rescue the ATG morpholino

The topology of NCKX2 has been shown to consist of a cleavable transmembrane signal peptide, followed by 2 groups of 5 transmembrane domains which are separated by a large hydrophilic cytoplasmic loop. Analysis of the NCKX5 sequence here suggests a similar topology (figure 34). The NCKX2 cytoplasmic loop is ~175 amino acids long, whereas the predicted loop of NCKX5 is just 76 amino acids long, and this is not a well conserved area. Previously, NCKX2 has been shown to form homodimers, and this is thought to

be stabilized by cys-395 in the large cytosolic loop (Cai et al., 2002). However this has not been demonstrated with NCKX5. In NCKX1 the large hydrophilic loop has been shown to not affect the transport activity of the protein (Kim et al., 1998), this could also be the case for NCKX5 here, however the D383N rescue indicates it is not the transport activity that is needed for NCKX5 function anyway. The CH mutant was used to test the importance of this loop in NCKX5 function. The significant rescue from the CH construct suggests the hydrophilic loop is not crucial for NCKX5 function, or the spacer region is somehow able to compensate. This result is surprising compared to the lack of rescue from the 4C mutant. In the 4C construct the 4 cysteines in the hydrophilic loop have been substituted and this does not rescue, in the CH construct the whole loop has been substituted, including the cysteines, there is only 1 cysteine in the spacer (Kinjo et al., 2003) so this is unlikely to have any effect, but it would be good to try a different spacer sequence to test this.

6.3.1.6 *X.laevis* SLC24A5 can rescue the ATG morpholino

As predicted, the strongest rescue was observed from the mutated *X.laevis* construct. This is mutated such that the morpholino would not target it. Primarily this confirms that the morpholino is specifically targeting SLC24A5. This also corresponds to morpholino rescue data seen in the zebrafish SLC24A5 work (figure 20) (Lamason et al., 2005). Unfortunately we have not had the opportunity to make other mutants in the *X.laevis* protein.

6.3.1.7 Chimera rescues

As expected, and consistent with the WT rescue seen earlier, the NCXK5 construct can rescue 100ng ATG morpholino effect. The NCKX5 ntl2 chimera can also rescue, this suggests the N-terminal region of NCKX5 is not crucial for its function, or the NCKX2 N-terminal region can substitute its function. NCKX2 was not expected to rescue as although it has the same core function it is normally expressed in different tissues. The lack of rescue from the NCKX5 cyto2 chimera is also consistent with the previous data where the 4C construct could not rescue. The 4C construct has had its loop cysteines replaced with glycine, the cytosolic loop of NCKX2 has no cysteines in it, so this chimera is

comparable with the 4C mutant. The rescues here also indicate that the GFP tag in these constructs does not affect protein function.
NCKX5 is a notoriously difficult protein to detect by western bloting. Human antibodies are available but are not very efficient and the results are difficult to reproduce. Here the mutant constructs were detected by western blot (figure 67), however this took at lot of optimisation and is difficult to reproduce. The chimera constructs could not be detected by western blot (figure 68).

6.3.2 Rescuing the splice morpholino

Very surprisingly none of the human or *X.laevis* constructs could rescue the splice morpholino phenotype, even at lower morpholino concentrations. This was not expected as these constructs (except 4C) can rescue the ATG morpholino and as the splice morpholino is targeting the same protein it is reasonable to assume it could also be rescued. It was considered that perhaps the splice morpholino was also targeting the sequence of the rescue constructs. This may be the case for the *X.laevis* construct as this has not been mutated in the splice morpholino region, but the human sequence has two nucleotide differences in the splice morpholino target region, so it is unlikely that the morpholino would target it. Consistently the chimera constructs are also unable to rescue the splice morpholino. None of the chimeras affect the splice morpholino target region of the gene, so this is not a factor. However this is not the only case where morpholino effects cannot be rescued, Haworth et al could not rescue their ATG or splice morpholino phenotypes (Haworth et al., 2008)

The splice morpholino was predicted to truncate the gene by removing the last exon (figure 52). According to the predicted trans membrane structure in figure 34, this truncation would include the last 3 trans membrane domains and part of the second alpha repeat.

It has been speculated that NCKX5, like NCKX2, could function as a homodimer or by interacting with another protein, it is possible that by truncating the protein it can no longer interact with its partner and thus cannot function in melanogenesis but equally cannot be rescued by the constructs. Conversely it could be that NCKX5 does not normally function as a dimer and truncation has caused it to interact with itself or something else.

It is also possible that the splice morpholino truncated protein acts as a dominant negative and thus the threshold of activity is too high for the constructs to rescue. It would be good to generate the truncated protein by PCR and inject this as mRNA alone to see if it has any dominant negative effect on the embryo.

It may also be prudent to generate further sequence data of intron/exon boundaries within *X.laevis* SLC24A5 and try morpholinos to these targets.

6.3.3 Rescuing the double morpholino

Similar to the ATG morpholino, the double morpholino can also be rescued by the mutant constructs. Presumably, due to the lack of rescue of the splice morpholino, the rescue seen here of the double knockdown is likely just representing rescue of the ATG morpholino, however this is not consistent with the dominant negative theory. Here again all constructs except 4C provided a statistically significant rescue. Surprisingly AT provides the strongest rescue, and CH rescues better than the XL or WT constructs. However the strength of the rescue (based on percentage of wild type embryos) from AT and CH is no greater with the double morpholino knockdown than the ATG morpholino, it is more a case that the other constructs give a weaker rescue.

It is very surprising to see that the NCKX2 construct can rescue the double knockdown. It is assumed that some of this protein gets into the melanosome/TGN membrane where it assumes the role of NCKX5, although it is then peculiar that this does not occur in the ATG or splice morpholino rescues. The rescue from NCKX5 is consistent with the rescue from the wild type construct and is expected. Rescue from the NCKX5 ntl2 construct is questionable as so few embryos here where recovered to scale 0, however if this constructs can rescue it indicates this region of the protein is not vital for its function, or that the NCKX2 equivalent region is redundant here.

NCKX5 cyto2 does not appear to rescue; this is consistent with our earlier finding that the 4C mutant could not rescue. Taken together this indicates the loop of NCKX5 is important for correct functioning in melanogenesis; however this theory is not supported by the rescue from the CH mutant.

6.3.4 Chimera rescues

Chimeric constructs of NCKX2/5 were made by the Schnetkamp lab and these were used here in rescue experiments.

Although members of the same protein family, NCKX2 and NCKX5 are only 36% similar in humans and human NCKX2 and *X.laevis* NCKX5 are only 27% similar. These proteins are thought to perform the same core function, as a potassium dependent sodium calcium exchanger, but their physiological roles are quite distinct. NCKX2 is predominantly found in the brain, where it has been shown to play a role in neuronal Ca^{2+} homeostasis (Li et al., 2006). NCKX2 is also found in retinal cone cells. The precise role of NCKX2 here is as yet undetermined; knockout of this gene surprisingly did not cause any significant retinal phenotype (Li et al., 2006). However the exchanger activity of NCKX2 has been demonstrated in retinal cone cells isolated from fish, this work also showed NCKX2 to be excusive in this cell type (Paillart et al., 2007). NCKX5 is found solely in pigment cells, where its role is as yet undetermined. Also NCKX5 is the only NCKX protein to be found on an intracellular membrane, which has hindered functional analysis of this protein.

By 'mix matching' regions of the NCKX2 and NCKX5 proteins it was hoped that important protein domains would be elucidated. However in this system these experiments are not conclusive. The rescue from NCKX5 ntl2 construct of the ATG morpholino could suggest that the N-terminal region (including the signal peptide) of NCKX5 is not vital to its function. In other NCKX proteins, this region is thought to be important for trafficking the protein to the plasma membrane (Kang and Schnetkamp, 2003), as NCKX5 does not translocate to the plasma membrane, this could explain its lack of importance to NCKX5 function. The other explanation is that this region of NCKX2 is able to perform the same role as the equivalent region of NCKX5, thus offering some redundancy of function. The lack of rescue from the NCKX5 cyto2 chimera indicates a fundamental importance of the large loop of NCKX5. In NCKX2 this loop is cytosolic, as NCKX5 is found on an organelle membrane it is thought this loop resides within the organelle. The sequence of the cytosolic loop is not well conserved across species, however a region of acidic residues is commonly found just before helix 6 (Paillart et al., 2007). NCKX1 has been shown to have a longer loop than

other NCKX proteins, and this has been suggested to play a role in protein-protein interactions (Poon et al., 2000).
The exact role of the large cytosolic loop of NCKX2 is not known, however the data presented here suggests its role is not conserved in NCKX5. The loop of NCKX2 is also approximately 100 amino acids longer than the equivalent region of NCKX5.
It would be interesting to develop chimeras of the alpha repeat region of NCKX2 and NCKX5 and test these in the rescue assay.

6.3.5 Overexpression analysis

All the constructs were injected alone, individually into embryos. This was to test for toxicity as well as identify any over expression phenotypes. No such phenotype was observed; however it would be difficult to detect visually an increase in pigmentation as the pigment cells are already black. No obvious increase in number of pigment cells was observed. A dominant negative effect was also considered but as no reduction in pigmentation observed this was ruled out. It may be worth analysing any effect on other pigmentation genes following over expression of NCKX5 constructs.

6.3.6 Constraints of the rescues

It must be acknowledged that not all *X.laevis* SLC24A5 is repressed by the morpholino, so there will always be some function, hence not complete knockdown and lower threshold for mutants to reach. Also as previously discussed there is likely a second paralog of SLC24A5 for which there is no sequence data and thus no morpholino, therefore this protein will be functioning normally and providing some redundancy to the morpholino knockdown.
All the rescue constructs used here are based on work conducted with NCKX2, although this is a related protein it is possible that some key residues differ in position and function. Also these human NCKX2 mutations were transferred into human NCKX5 and used to rescue. It could be that the human sequence is not similar enough to the *X.laevis* sequence to provide a clear interpretation of the function of the protein via rescue analysis. To better analyse the rescue capability of these mutants it would have been preferable to clone the mutations into the *X.laevis* sequence. This would have been advantageous as the rest of

the sequence would be wild type and thus more likely to behave normally within the embryo and would thus give a better reflection of the function of the protein. However, the human sequence was readily available for mutation and the transfer of mutations from human NCKX2 to human NCKX5 was quicker and easier.

Chapter Seven:

Final discussion

7.1 Summary

Over the past 6 years SLC24A5 has emerged as a key player in global skin pigmentation phenotypes. Research has predominantly focused on the ns SNP and how this correlates across population groups; however the function and mode of action of SLC24A5 in pigmentation is yet to be clarified. Ginger et al (2008) were the first to demonstrate a role for SLC24A5 in human melanogenesis in cell culture.

Here we have successfully cloned SLC24A5 from *X.laevis* and shown it to be expressed in pigment cells from their inception and throughout later stages of development. We have suppressed translation of SLC24A5 using antisense morpholinos and report that this causes a decrease in pigmentation in the RPE and epidermal pigmentation. The morpholino effect can be rescued by *X.laevis* SLC24A5 and some human mutant constructs, which indicate the role of SLC24A5 in pigmentation is not dependent on its ion exchanger function. A splice morpholino can also give a reduction in pigment, however this cannot be rescued.

Due to sequence homology SLC24A5 is suspected to encode NCKX5, but because of the intracellular location of this protein, functional analyses has been very tricky. Massive over expression of NCKX5 in insect high five cells does make some protein go to the plasma membrane and thus some functional assays have been performed (figure 22), but these are difficult to reproduce. Despite many other efforts including attaching signal peptides for plasma membrane targeting, NCKX5 cannot be persuaded to reside in the plasma membrane. This work provides some *in vivo* contribution to the functional analysis of NCKX5.

7.2 Potential roles for NCKX5

Morpholino knockdown of SLC24A5 does not appear to interfere with pigment cell development, morphology or migration (figures 45, 46, 47, 48), thus attention can be turned to the pigment producing organelle the melanosome.

7.2.1 NCKX5 and the melanosome

At the melansome level there are several potential roles for SLC24A5. Firstly a role in melanosome pH regulation is possible, and this has been shown to be important for melanosome function (Ancans et al., 2001b). Also, cholesterol metabolism has been suggested to be affected by SLC24A5 knockdown in cell culture (Wilson et al unpublished). Ca^{2+} signalling is also reported to be important for melanogenesis (Schallreuter, 2007). Despite the evidence presented here that the Ca^{2+} exchange function of NCKX5 may not be vital to its role in pigmentation, it cannot be ruled out, because we rescue *X.laevis* SLC24A5 knockdown with human SLC24A5 constructs which are based on NCKX2 mutations and these have not themselves been shown to be important.

It is possible that SLC24A5 is involved in the biogenesis or function of the melanosome. This is supported by the finding that the early melanosome marker and important structural protein Pmel17 is reduced following SLC24A5 siRNA knockdown in cell culture (Ginger et al., 2008). Electron microscopy was employed in the present study to analyse the melanosomes following morpholino knockdown, to see if they were still present, or whether they may be 'stuck' at an early developmental stage etc, but unfortunately the work was not completed. However the observation that later melanosome proteins such as tyrosinase and DCT are expressed following SLC24A5 knockdown suggest the melanosomes can develop normally. Although Mitf expression seems to be disrupted.

7.2.2 NCKX5 and the Trans Golgi network

The colocalisation of SLC24A5 with the trans Golgi network (TGN) (figure 19), implies the protein could be involved in the processing and trafficking of other proteins, potentially those of the melanosome. However, there is also expression of SLC24A5 throughout pigment cells (figure17 and 19), so direct expression within the melanosome cannot be ruled out. Furthermore, NCKX5 was enriched in melanosome fractions following proteomic analysis of fractionated melanocytes (Ginger et al., 2008). Also, the marker TGN-46, used in the colocalisation experiments can also be found in endosomes (Pfeffer, 2009), as melanosomes have been suggested to form from early endosomes it is possible that SLC24A5 has a role here.

The TGN can be regarded as the final sorting office of the Golgi network, distal from the Golgi cisternae stacks. It has a key role in sorting and transport of newly synthesised and recycled proteins and lipids. The TGN is particularly important for glycosylating proteins; TYRP-1 has to be extensively glycosylated before being transferred to the melanosome (Jimbow et al., 1997).

The TGN is distinct from the Golgi cisternae stacks as it forms different vesicles from the rest of the Golgi; the cisternae generate COPI (coat protein complex I) vesicles and the TGN produces clathrin coated vesicles. These domains also respond differently to brefeldin A (BFA, which disrupts ER/Golgi transport) treatment; the cisternae stacks tend to fuse with the endoplasmic reticulum whereas the TGN can fuse with endosomes (Nakano and Luini, 2010). BFA however does not affect cholesterol transport. It has recently been shown that the TGN localisation of SLC24A5 is robust enough to survive BFA treatment (Wilson et al unpublished data). This however does not rule out an endocytic localisation of SLC24A5. It was also shown nocodazole mediated disruption of the microtubule network did not affect SLC24A5 localisation. Nocodazole does however prevent the transport of cholesterol, via microtubule networks.

The Golgi is a known calcium store and fluctuations in calcium concentration can influence its function (Pinton et al., 1998). In this capacity the TGN also helps to regulate cellular calcium concentrations which are important to maintain homeostasis and for signalling pathways. As such it is possible that NCKX5 plays a role in regulating the calcium concentration of the TGN, and in this way contributes to the correct folding and processing of melanosomal proteins.

However, if this were the case one could reasonably expect more general phenotypes from knockdown of SLC24A5. The pH of the TGN also has to be carefully regulated to ensure correct folding of proteins, including tyrosinase (Wang and Hebert, 2006). A role here for NCKX5 would tie in with the model proposed by Lamason et al (2005), discussed below.

It has also been noted that tyrosinase activity is higher in melanocytes derived from black individuals than white melanocytes, this is thought to be due to the more acidic environment of white melanosomes. Na+/H+ exchangers (NHE's) have been found to be differentially expressed in black and white melanosomes. The vesicular ATPase was also found to be expressed in melanocytes, from both black and white backgrounds, highlighting the pH regulation system (Smith et al., 2004). This evidence correlates with the nsSNP in SLC24A5, where the SNP is present in white skinned populations, it reduces the activity of NCKX5 which in turn imbalances the electrochemical gradient resulting acidification of the TGN/ melanosome, and this impairs the activity of tyrosinase and thus the production of melanin.

Another model for NCKX5 function put forward by Ginger et al (2008) suggests NCKX5 may play a role in melanosome biogenesis. Here they hypothesise that NCKX5 is involved in protein trafficking and sorting at the endosome membrane. This is supported by their observation that Pmel17 is downregulated following SLC24A5 knockdown, indicating lack of endosomes, and the upregulation of Lamp1, a lysosome marker, following SLC24A5 knockdown, which indicates loss of SLC24A5 causes diversion of membrane proteins and lipids to the lysosome pathway (Ginger et al., 2008). Moreover the cleavage of Pmel17 into smaller fragments has been shown to be pH sensitive (McGlinchey et al., 2011; Pfefferkorn et al., 2010).

7.2.3 pH regulation

As discussed earlier (1.3.5) melanosome pH is an important factor for melanin synthesis. Lamason et al (2005) proposed a model for SLC24A5 in melanosome pH regulation, where proton exchange via a V-ATPase is coupled to SLC24A5 mediated calcium movement by a Na+/H+ exchanger (figure 69).

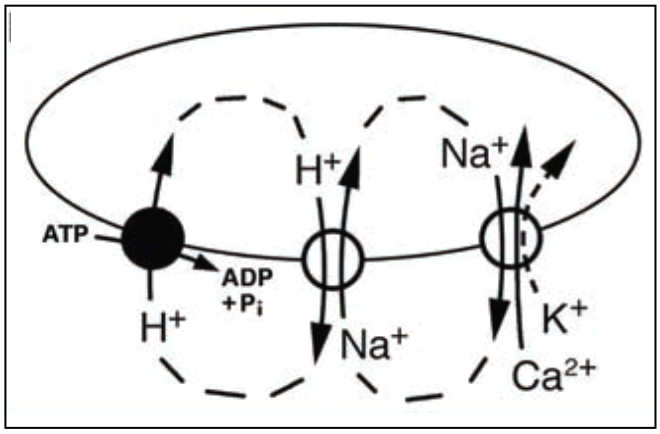

Figure 69
A potential role for SLC24A5 in melanosome pH regulation. The V-ATPase (left, dark circle) pumps protons into the melanosome, this drives Na+ movement into the melanosome via the Na+/H+ exchanger (middle), the Na+ gradient then stimulates Ca2+ uptake with K+ in exchange for Na+ by NCKX5 (right) (Lamason et al., 2005)

Figure 69 demonstrates the potential interplay between electrochemical gradients over the melanosome membrane. This model links together melanosome pH and calcium content both of which are important for regulation of melanogenesis. In this model Ca^{2+} is removed from the cytosol and accumulated in the melanosome, and the proton gradient is maintained. This model assumes that endogenous NCKX5 mediated ion exchange moves Ca^{2+} and K^{+} into the melanosome and Na^{+} out, *in vivo*, so far there is no experimental evidence that this is the case. According to this model, a reduction in activity of NCKX5 would cause a net acidification of the melanosome, which would hinder melanin synthesis due to the pH sensitivity of tyrosinase. The pH of early endosomes varies between discrete regions of the organelle (Jovic et al., 2010), this could be a niche for SLC24A5 function. The A111T and D383N mutants are both suspected to reduce the activity of NCKX5 and indeed, although these can

rescue the knockdown of SLC24A5 here, they cannot restore normal pigmentation to the same extent as the WT or XL clones (figure 61), suggesting a less active NCKX5 can hinder melanin synthesis, potentially via pH misregulation.

To further analyse the role of NCKX5 in pH regulation of melanosomes it would be useful to conduct cell culture experiments using acridine orange. This labels acidic organelles and could be used in conjunction with NCKX5 immunostaining, with and without siRNA to NCKX5, to see if there is any colocalisation.

The Lamason model also suggests that Ca^{2+} uptake into the melanosome is vital for the correct functioning of furin-like proteases which are important for processing Pmel17 (Lamason et al., 2005). This correlates with the observation by Ginger et al (2008) that Pmel17 protein levels are downregulated following siRNA knockdown of SLC24A5.

Despite finding alterations in protein expression of several melanogenic genes (Pmel17, Tyr, Tyrp1, Mart1 AND Lamp1), following siRNA knockdown of SLC24A5 no alterations in the corresponding mRNA levels (Wilson et al unpublished), this correlates with the findings here that following morpholino repression of SLC24A5, transcripts of Tyr and DCT are unaffected (figures 45, 47). However, figure 46 does suggest Mitf transcript is repressed by SLC24A5 knockdown, this has not been anaylsed at the protein level. This suggests SLC24A5 has more of a role in the post translational processing and trafficking of proteins. This has been analysed this in further detail by treating NHM with EndoH and PNGaseF, following siRNA knockdown of SLC24A5 (Wilson et al unpublished data). EndoH is an endogylcosidase which cleaves off oligosaccharides added to proteins in the ER and early stages in the Golgi. PNGaseF can cleave oligosaccharides added in the ER and throughout the Golgi. Western blot analysis of Tyr and Tyrp1 following such treatment revealed no differences between the control and SLC24A5 knockdown cells, suggesting that SLC24A5 has a role later in post translational processing, i.e. after the Golgi (Wilson et al unpublished).

In the same work, it was found that MC1R (melanocortin 1 receptor) mRNA levels were reduced following SLC24A5 knockdown, however the link here has not been established (Wilson et al unpublished data). MC1R is the receptor for αMSH and ASIP, αMSH has been shown to increase protein levels of NCKX5. They also found NCKX5 levels can be depleted by siRNA knockdown of Mitf. These findings highlight a role of SLC24A5/NCKX5 in the pigmentary system.

There has been no evidence, to date, to suggest that repression of NCKX5 causes an increase in any other NCKX or NCX protein, suggesting there is no redundancy among these families.

7.2.4 Acidic calcium stores

Based on data discussed so far, the melanosome can be considered as an acidic calcium store, which act as buffers to calcium fluctuations within the cell (Patel and Docampo, 2010). The Golgi, endosomes and lysosomes are well known acidic calcium stores. These organelles regulate their pH and Ca^{2+} levels through Ca^{2+} pumps and exchangers. These often use the proton gradient across the organelle membrane to move Ca^{2+} via calcium hydrogen exchangers (CAX), however this type of exchangers have not been found in mammals (Shigaki et al., 2006), thus other mechanisms for connecting proton and calcium gradients may be presence, this could be a role for NCKX5.

The accumulated Ca^{2+} in melanosomes can be absorbed by melanin which has been shown to play a role in Ca^{2+} homeostasis (Hoogduijn et al., 2003). Melanin binds Ca2+ via its carboxyl group (Bush and Simon, 2007) in a pH dependent manner (Drager, 1985). Although melanocytes are not excitory cells they do experience fluctuations in Ca^{2+} concentrations, similar to that seen in naive neurons, which is unsurprisingly due to their common origin (neural crest), also these calcium fluxes are thought to be associated with migration which again ties with their neural crest origin and thus extensive migration. Calcium is required in the skin to induce keratinocyte differentiation, this process is enhanced by the presence of vitamin D, which is synthesised in the keratinocytes and acts as an autocrine agent to increase keratinocyte sensitivity to Ca^{2+} (Bikle et al., 2001). Expression of NCKX5 in the keratinocytes has not been tested, this would be a worthy experiment as NCKX5 could play a role here once the melanosomes have been transferred.

The Golgi is a known calcium store, as are endosomes and lysosomes, although these are also acidic (Patel and Docampo, 2010), thus wherever NCKX5 may be expressed it could have a role in balancing pH and calcium concentration. Ca^{2+} is vital for a number of cellular functions including; migration and proliferation, it is also an important cofactor for many enzymes, notably phenylalanine hydroxylase (Schallreuter and Wood, 1999). It has also been shown to be

important for melanogenesis and melanosome transfer (Meyer zum Gottesberge, 1988). Hoogdujin et al (2003) described the dynamic nature of basal Ca^{2+} concentration in black and white melanocytes. Addition of exogenous Ca^{2+} to NHM results in a transient increase in intracellular Ca^{2+} concentration. The extent to which the Ca^{2+} concentration increases appears to be dependent on the endogenous melanin content, i.e. black and well melanised white melanocytes show less of an increase in cytosolic Ca^{2+} concentration than poorly melanised white melanocytes. This is thought to be due the Ca^{2+} binding capacity of melanin, whereby the more melanin that is present the more Ca^{2+} can be sequested and therefore the cytoplasmic Ca^{2+} concentration does not increase as much (Hoogduijn et al., 2003). In this way melanin acts as a reservoir for Ca^{2+}. NCKX5 could influence this phenomenon, less active NCKX5 in white melanocytes, will move less Ca^{2+} into the melanosome/TGN thus the cytoplasmic Ca^{2+} concentration goes up. So it would appear that while Ca^{2+} is important for melanogenesis and melanocyte behaviour, melanin is equally important for Ca^{2+} homeostasis. Salceda and Sanchez (2000) conducted Ca^{2+} uptake and release experiments of melanosome extracts from frog RPE cells. They noted that melanosomes are able to take up Ca^{2+} and this could not be interrupted by various inhibitors of plasma membrane or ER channels and pumps, including ATPase's. This is contrary to results using these inhibitors in other mammalian cell types, where they did inhibit Ca^{2+} uptake, leading to the suggestion that in these cells Ca^{2+}uptake is ATP dependent and partly driven by SERCA's (sacroplasmic endoplasmic reticulum Calcium ATPase) (Lopez et al., 2005). This suggests the melanosome has its own Ca^{2+} transport system, which may not be energy dependent, but may rely more on the proton gradient. This study was conducted in 2000, however here they implied this could be a job for Ca^{2+}-Na^{+}-K^{+} exchange, in light of more recent research this system is potentially run by NCKX5. It would be of interest to repeat these Ca^{2+} uptake and release experiments following siRNA knockdown of SLC24A5 to determine if this protein does have a role in this system. Of course all this accumulated Ca^{2+} needs to get out of the melanosome too, this is proposed to be conducted by IP3 and ryanodine receptors (Salceda and Sanchez-Chavez, 2000), but could NCXK5 be moving Ca^{2+} in the opposite direction or could it be bidirectional, like NCKX1 and NCKX2. We do know it is possible to reverse the direction of ion movement in vitro (figure 22). Defects in Ca^{2+} or pH regulation in melanosomes, or other endosomal/lysosomal organelles are thought to be partly responsible for the

pigmentation phenotype seen in Hermansky-Pudlak and Chediak-Higashi syndromes (Spritz, 1998). Mutations in secretory pathway Ca^{2+} ATPases (SPCA) have been found to be responsible for the keratinocyte disorder; Hailey-Hailey disease. SPCA's are a family of ATPases which regulate Ca^{2+} transport into the Golgi (Missiaen et al., 2007; Vanoevelen et al., 2007)

7.2.5 Cholesterol homeostasis

Cholesterol is an important component of cell membranes. It provides stability, fluidity, and permeability. 85% of cellular cholesterol is found in the plasma membrane, most organelle membranes contain very little cholesterol, except the TGN membrane which contains cholesterol at levels almost equivalent to that seen in the plasma membrane (Fielding and Fielding, 1997). Cholesterol is also the precursor for the synthesis of many steroid hormones and vitamin D, which have a role in melanogenesis (Rosenheim and Webster, 1927; Schallreuter et al., 2009). A role for cholesterol in pigmentation has been demonstrated (Hall et al., 2004; Jin et al., 2008; Schallreuter et al., 2009).

Cholesterol and related processing/biosynthesis proteins have been found to be expressed in melanocytes and melanoma cells, partially colocalises with a melanosome marker (NKI/beteb). Content of cholesterol was particularly high in amelanotic melanoma cells, indicating cholesterol may have a role in early melanosome biogenesis. Addition of exogenous cholesterol resulted in an increase in melanin content in melanocytes. The same study also found that cholesterol enhances cAMP, CREB, Mitf, THI, tyrosinase and estrogen receptors expression (Schallreuter et al., 2009), which are all important for melanogenesis. Taken together these results suggest that melanogenesis is regulated by cholesterol in melanocytes and melanoma cells. Hall et al (2004) found that by adding 25-hydroxy cholesterol (25HC) to melanocytes, pigmentation was reduced; this was found to be due to an increase in tyrosinase degradation (Hall et al., 2004). This correlates with the finding that cholesterol levels are high in amelanotic cells but not with the evidence that addition of cholesterol increases melanin content, however cholesterol and 25HC have previously been shown to function via different mechanisms (Adams et al., 2004). This adds another dimension to regulation of melanogenesis by cholesterol. Also 25HC mediated degradation of tyrosinase was found to take place in a Golgi compartment (Hall et al., 2004), this brings NCKX5 into the

picture. Recently NCKX5 has been proposed to play a role in cholesterol homeostasis since siRNA mediated reduction of NCKX5 causes an increase in cholesterol and ester levels (Wilson et al unpublished data). This observation was made in normal human melanocytes where following siRNA treatment micro array analysis of global mRNA profiles revealed altered expression levels of several cholesterol homeostasis genes, including; the ATP-binding cassette transporter A1 (ABCA1) and the low density lipoprotein receptor (LDLR). These both have well established functions in cholesterol metabolism (Chen et al., 2007; Zhou et al., 2009).

The current work can provide no additional evidence for a role of NCKX5 in cholesterol, nor can it contradict it. In future experiments *X.laevis* could provide an in vivo system to assess the effects of cholesterol on pigmentation and how this may be regulated by NCKX5. *X.laevis* has been shown to be a strong model for chemical genomic screening (Tomlinson et al., 2005; Tomlinson et al., 2009b), so it would seem reasonable to adopt a similar experimental paradigm to test cholesterol and its derivatives, in a medium-high throughput manner. Also cholesterol homeostasis components have been found to be expressed in *X.laevis* skin tissue (Tadjuidje and Hollemann, 2006).

It is clear from this work that NCKX5 has an important role in eye pigmentation. The expression seen here is thought to be in the RPE, however expression in the choroidal or iridial melanophores cannot be ruled out. Interaction between these cell types is known to be important for their respective functions, and this has been shown to involve calcium signalling (Smith-Thomas et al., 2001).

NCKX proteins were first discovered in the eye. NCKX1 is expressed in the rod photoreceptor cells and has been shown to be important for extruding calcium from the cells, following its entry via cGMP gated channels in response to light (Prinsen et al., 2000). It has been thought that NCKX1 was the only calcium extrusion mechanism in the rod photoreceptors, but perhaps NCKX5 is also playing a part in this system. NCKX2 is also expressed in the eye, specifically the cone photoreceptors, as well as broad expression in the brain (Winkfein et al., 2004). To date, most functional analyses has been conducted on NCKX1, due to its convenient location in the rod outer segments which can be easily isolated with intact plasma membranes, and NCKX2, in vitro studies suggest it plays a similar role to NCKX1 but in the cone photoreceptor cells (Altimimi and Schnetkamp, 2007b; Lytton, 2007). NCKX1 has been shown the form a dimer

(Schwarzer et al., 1997) and associate with the cGMP gated channel (Schwarzer et al., 2000), it would be of interest to determine if NCKX5 interacts with any other protein(s).

Calcium signalling is important for photo transduction, this is closely regulated by cGMP and calcium binding proteins within the cell (Koch et al., 2010). Ca^{2+} concentration within photoreceptor cells decreases dramatically following closure of cGMP cation channels, which stops Ca^{2+} getting in, this is initiated by the stimulation of light. NCKX1 is moving Ca^{2+} out of the cell during this process, contributing to the drop in cytosolic Ca^{2+}. Ca^{2+} levels also regulate retinal guanylate cyclases, which during the reduction in Ca^{2+} can synthesise GMP (Stephen et al., 2008). GMP is involved in a signalling cascade to pass on the photo transduction pathway (Koutalos et al., 1995), Ca^{2+} is important to restore equilibrium after photon excitation (Pugh and Lamb, 1990).
NCKX1 has recently been implicated in the eyesight disorder congenital stationery night blindness (Riazuddin et al., 2010). NCKX5 is yet to be associated with any disease state, although it is expressed in melanoma cells, weather it is enhancing the cancer is known.

7.3 Conclusion

A role for NCKX5 in pigmentation is now well established, in vitro and in vivo and across different species. The function of NCKX5 is likely to be as potassium dependent sodium calcium exchanger, although direct evidence of this is limited, due to the unusual intracellular location of NCKX5. Linking together ion exchange and pigmentation has proved challenging. Previous speculation has indicated a role for NCKX5 in pH maintenance, which is known to be important for melanin production, however how exactly NCKX5 links to proton exchange has not been determined experimentally. As an important signalling molecule for many processes, Ca^{2+} homeostasis has to be tightly regulated, as a $Na^{+}/Ca^{2+}/K^{+}$ exchanger it is acceptable to suggest a role for NCXK5 in Ca^{2+} regulation. It should also be taken into account that some ion exchangers do have secondary functions, this work has indicated that perhaps it is not the ion exchange activity of NCKX5 that is vital for its role in pigmentation, thus other functions should not be ruled out.

Appendix

Appendix 1 - Primer table

Primers are colour coded to the sequence map in the next figure.

Primer name	Sequence	Length	Tm ℃
XT SLC24A5 F + EcoR1	GAATTCATGTGTACGTGTATGACCTTTAC	29	63
XT SLC24A5 R+ HA + BamH1	CCTAGGTCAAGCGTAATCTGGAACATCGTATGGGTAGT CACCACACATCACGATAGC	57	76
XT SLC24A5 R+ BamH1	CCTAGGTTAGTCACCACACATCACGATAGC	30	68
XT SLC I.P1 F	TCATGGCAATTGGAAGTTCA	20	56
XT SLC I.P1 R	TGGCTCATGCTCTGTGTTTC	20	60
XT SLC I.P2 F	ACACAGAGCATGAGCCATTG	20	60
XT SLC I.P2 R	GTTCCAGCAGCGAGTAATG	20	60
XT ODC F (X.tropicalis cDNA control)	GCCAGTAAGACGGAAATCCA	20	60
XT ODC R (X.tropicalis cDNA control)	CCCATGTCAAAGACACATCG	20	60
T7 sense	CCAGTGAATACGACTCACTATAGG	24	62
SP6 antisense	CCAAGCTATTTAGGTGACACTATAG	25	61
RACE 1*	CCAACAACAGGCGGCACATATCCCAAGA	28	69
AUAP (3'RACE kit primer)	GGCCACGCGTCGACTAGTAC	20	66
AP (3'RACE kit primer)	GGCCACGCGTCGACTAGTACTTTTTTTTTTTTT	37	65
GeneRacer (5' kit primer)	CGACTGGAGCACGAGGACACTGA	23	68
GeneRacer 5' nested primer	GGACACTGACATGGACTGAAGGAGTA		
3' RACE 3	CAGACTGCAGGAGGAAAACATGG	23	64
DCT F	TGCTGGAAAGGGATCTTCAG	20	60
DCT R	TGTACATCTTCCACGGATGG	20	60
Full length 5' *	TCGA GAATTC CTGGCAGGGAGAGCAGAGTC	30	70
Full length 3' 3*	TCGACTCGAG TTAGTCACCACACAGTACCATAGG	34	70
SLC frameshift 1	AGTATCCCAGACACGGTTGC	20	54
SLC frameshift 2	GATATGCTGTGTTTGGGAGTCCCT	24	57
SDM of SLC	TCGA GAATTC ATGGAGAAAGGATCCGTTGC	30	62
EcoR1 F	GCATCACCATCATCAGAATTCCCTGAAG	28	60
EcoR1 R	CCGTGAAAAAATCTTCAGGGAATTCTGATGATGG	34	62
Myc R	GAATTC CAGATCCTCTTCTGAGATGAGCTTCTGTTC TGATGATGGTGATGCTATACAGAG	61	71
5' Xho1	TCGA CTCGAG GTGCATTTTAGCCATGGAG	29	63
3' Xba1 **	TATA TCTAGA TTAGTCACCACACAGTACC	29	57

Appendix 2 - Full length *X.laevis* SLC24A5

Full nucleotide sequence of *X.laevis* SLC24A5 showing morpholino target sites and primers, coloured coded with primer table.

GAATTCGATTTCGAGAATTCCTGGCAGGGAGAGCAGAGTCTGTGCATTTTAGCC**AT**
GGAGAAAGGTTCTGTTGCTCTGAATGTAGGAAGAAGGCCCTTTGGAAAGAAGAGA
TTGCCCTGCAGAGCTCCGCTGGGTTCATTCGCCCTGTTCTTGATTGTTTGCGGCAC
AGTCTATCTGGTCAACCAAGTGGCTACTACCCTGGTGGTGAGAGGCACGCAGAGA
ATCCGGAGGGATATAGAGAATGAGACTCTCTGTATAGCATCACCATCATCAGAATTT
CCTGAAGATTTTTTCACGGAACAGGAGAGGAAGCAAGGAGGCCTTATCATTCACTT
CCTAGTTATACTTTACATGTTCCTAGCGGTGTCCGTTGTATGCGAATACTATTTTATC
CCCTCATTAGAAGTCATTAGTGAACGTCTTGGTCTCTCCCAGGATGTCGCAGGGGC
AACATTTATGGCAATTGGAAGTTCAGCTCCAGAATTTGTCACTGTATTTCTAGGCGT
ATTTGTCACAAAGGGAGATATTGGTGTGAGCACTATTGTTGGATCAGCTGTCTACAA
TCTTCTTGGGATACGTGCCGCCTGTTGTTTGCTTTCATCATCGATTTCAAGGCTCAC
TTGCTGGCCTTTGTTTAGAGATTGTGTGGCGTATGCAATTAGTGTAGCAGCAGTAAT
TGCAATAACATTTGACAACAGGATATACTGGTATGAATCTGCATCTCTGCTTTTGAT
ATATGGCATATATATTGTTATAATGTGCTTCGACATTAAGATTAGCAAATATGTTGTA
AGGAGGTTCAGTCCTTGCTGTGCCTGTTGCGCTGAAGCAATGGTGGAAAACACAG
AGCACGCGCCATTGCTAGGTTGGAAAGAAGAGAGTTTGCCAGTTATTCGCCGCCA
CTCAAGATCAGACAGTGGGATTTTTTCAGGAAGATTCTGATTATTCTCAACTCTCAAT
AAGTCTGAGTGGGCTAAAGGAACCCTCTAATAACCCGCCAAGTGTCTTCAAGATGC
CAGAAAATGACCTGAGAAGGATTATTTGGGTATTGTCGCTGCCTATTATTACTTTGT
TTTATCTGACTGTGCCAGACTGCAGGAGGAAAACATGGAAAAAGTGGTTCATTCTC
ACATTTGTCATGTCAGCCGTTTGGATTTCTGCAGTGACTTACATTCTTGTATGGATG
GTGACGATTGTTGGTGAAACACTAAATATTCCAGACACAGTGATGGGACTGACATT
GCTTGCTGCTGGAACAAGTATCCCAGACACGGTTGCAAGTGTGATAGTAGCAA**GA**
GAAGGTAAAGGAGACATGGCCATGTCCAATATTGTGGGTTCCAACGTGTTTGATAT
GCTGTGTTTGGGAGTCCCTTGGTTTATTAAGACAGTCTTTGTCGACAGATCATCCCC
CGTGGAGGTTAATAGCAGCGGCATCACATACACCACAATTTCTCTCCTGTTCTCCAT
TATGTTCATCTTTGTGGCTATACATTTAAATGGCTGGAAACTTGATAAGAAGTTAGG
AGTTATTTGCCTATTTATGTATTTAGTATTTGTTACTTTATCGATATTGTATGAACTTG
GAATTATAGGGAACACTCCTATGGTACTGTGTGGTGACTAACTCGAGTGCAAAWCR
CTAGTGAATTC

BOLD = MO target

Colours = see primer table for code

Appendix 3

Map of pGEM-T Easy Vector

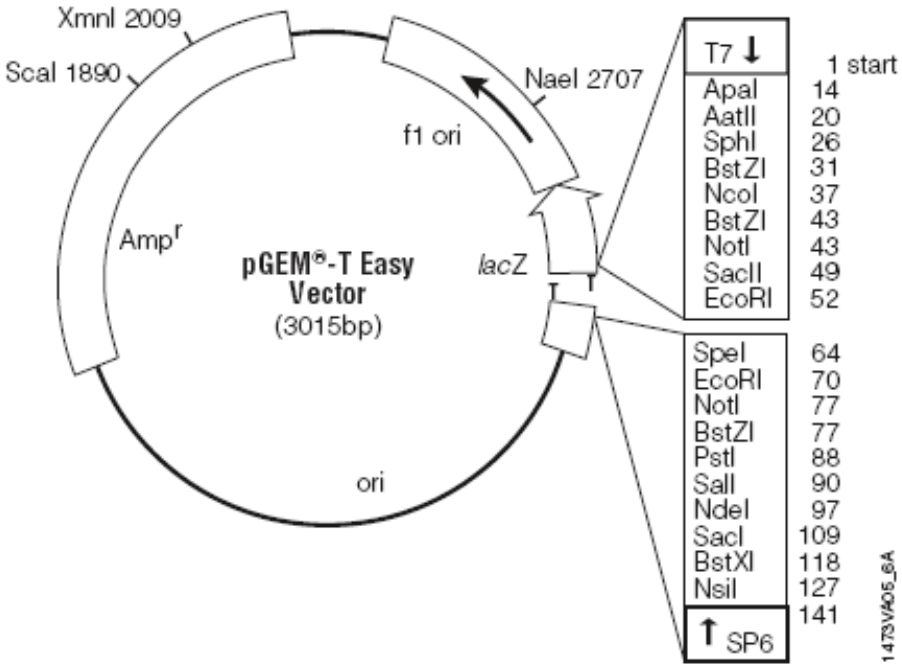

Appendix 4

Map of pCS2+ vector

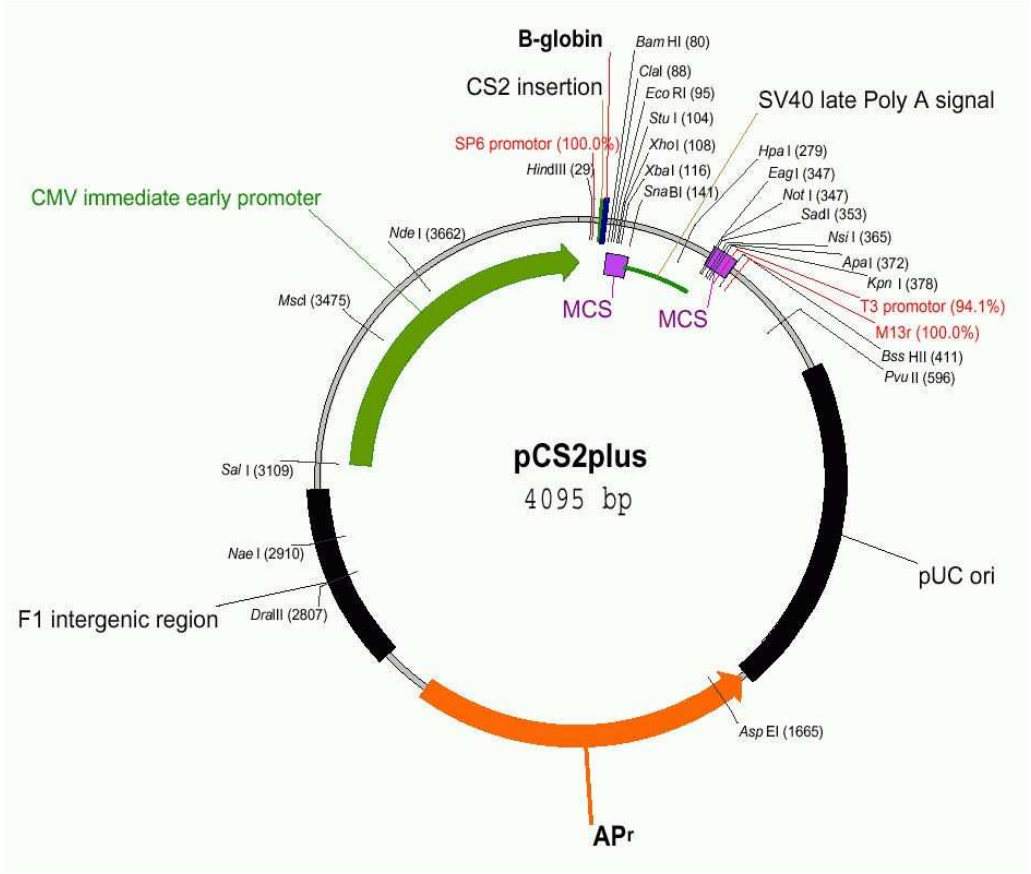

Appendix 5

Sequence of control morpholino

CCTCTTACCTCAGTTACAATTTATA

References

Abdel-Malek, Z. A., Kadekaro, A. L. and Swope, V. B. (2010). Stepping up melanocytes to the challenge of UV exposure. *Pigment Cell Melanoma Res* **23**, 171-86.

Abu-Elmagd, M., Garcia-Morales, C. and Wheeler, G. N. (2006). Frizzled7 mediates canonical Wnt signaling in neural crest induction. *Dev Biol* **298**, 285-98.

Adams, C. M., Reitz, J., De Brabander, J. K., Feramisco, J. D., Li, L., Brown, M. S. and Goldstein, J. L. (2004). Cholesterol and 25-hydroxycholesterol inhibit activation of SREBPs by different mechanisms, both involving SCAP and Insigs. *J Biol Chem* **279**, 52772-80.

Afouda, B. A. and Hoppler, S. (2011). Different requirements for GATA factors in cardiogenesis are mediated by non-canonical Wnt signaling. *Dev Dyn* **240**, 649-62.

Akira, E. and Ide, H. (1987). Differentiation of neural crest cells of Xenopus laevis in clonal culture. *Pigment Cell Res* **1**, 28-36.

Altimimi, H. F., Fung, E. H., Winkfein, R. J. and Schnetkamp, P. P. (2010). Residues contributing to the Na(+)-binding pocket of the SLC24 Na(+)/Ca(2+)-K(+) Exchanger NCKX2. *J Biol Chem* **285**, 15245-55.

Altimimi, H. F. and Schnetkamp, P. P. (2007a). Na+-dependent inactivation of the retinal cone/brain Na+/Ca2+-K+ exchanger NCKX2. *J Biol Chem* **282**, 3720-9.

Altimimi, H. F. and Schnetkamp, P. P. (2007b). Na+/Ca2+-K+ exchangers (NCKX): functional properties and physiological roles. *Channels (Austin)* **1**, 62-9.

Ancans, J., Hoogduijn, M. J. and Thody, A. J. (2001a). Melanosomal pH, pink locus protein and their roles in melanogenesis. *J Invest Dermatol* **117**, 158-9.

Ancans, J., Tobin, D. J., Hoogduijn, M. J., Smit, N. P., Wakamatsu, K. and Thody, A. J. (2001b). Melanosomal pH controls rate of melanogenesis, eumelanin/phaeomelanin ratio and melanosome maturation in melanocytes and melanoma cells. *Exp Cell Res* **268**, 26-35.

Aoki, H., Hara, A., Motohashi, T., Chem, H. and Kunisada, T. (2008). Iris as a recipient tissue for pigment cells: organized in vivo differentiation of melanocytes and pigmented epithelium derived from embryonic stem cells in vitro. *Dev Dyn* **237**, 2394-404.

April, C. S. and Barsh, G. S. (2007). Distinct pigmentary and melanocortin 1 receptor-dependent components of cutaneous defense against ultraviolet radiation. *PLoS Genet* **3**, e9.

Aspengren, S., Hedberg, D. and Wallin, M. (2006). Studies of pigment transfer between Xenopus laevis melanophores and fibroblasts in vitro and in vivo. *Pigment Cell Res* **19**, 136-45.

Baker, C. V., Bronner-Fraser, M., Le Douarin, N. M. and Teillet, M. A. (1997). Early- and late-migrating cranial neural crest cell populations have equivalent developmental potential in vivo. *Development* **124**, 3077-87.

Barral, D. C. and Seabra, M. C. (2004). The melanosome as a model to study organelle motility in mammals. *Pigment Cell Res* **17**, 111-8.

Basrur, V., Yang, F., Kushimoto, T., Higashimoto, Y., Yasumoto, K., Valencia, J., Muller, J., Vieira, W. D., Watabe, H., Shabanowitz, J. et al. (2003). Proteomic analysis of early melanosomes: identification of novel melanosomal proteins. *J Proteome Res* **2**, 69-79.

Baxter, L. L., Loftus, S. K. and Pavan, W. J. (2009). Networks and pathways in pigmentation, health, and disease. *Wiley Interdiscip Rev Syst Biol Med* **1**, 359-71.
Beaumont, K. A., Shekar, S. N., Newton, R. A., James, M. R., Stow, J. L., Duffy, D. L. and Sturm, R. A. (2007). Receptor function, dominant negative activity and phenotype correlations for MC1R variant alleles. *Hum Mol Genet* **16**, 2249-60.
Berson, J. F., Theos, A. C., Harper, D. C., Tenza, D., Raposo, G. and Marks, M. S. (2003). Proprotein convertase cleavage liberates a fibrillogenic fragment of a resident glycoprotein to initiate melanosome biogenesis. *J Cell Biol* **161**, 521-33.
Bharti, K., Nguyen, M. T., Skuntz, S., Bertuzzi, S. and Arnheiter, H. (2006). The other pigment cell: specification and development of the pigmented epithelium of the vertebrate eye. *Pigment Cell Res* **19**, 380-94.
Bhatnagar, V., Anjaiah, S., Puri, N., Darshanam, B. N. and Ramaiah, A. (1993). pH of melanosomes of B 16 murine melanoma is acidic: its physiological importance in the regulation of melanin biosynthesis. *Arch Biochem Biophys* **307**, 183-92.
Bikle, D. D., Ng, D., Tu, C. L., Oda, Y. and Xie, Z. (2001). Calcium- and vitamin D-regulated keratinocyte differentiation. *Mol Cell Endocrinol* **177**, 161-71.
Boissy, R. E. and Nordlund, J. J. (2011). Vitiligo: current medical and scientific understanding. *G Ital Dermatol Venereol* **146**, 69-75.
Boissy, R. E., Zhao, H., Oetting, W. S., Austin, L. M., Wildenberg, S. C., Boissy, Y. L., Zhao, Y., Sturm, R. A., Hearing, V. J., King, R. A. et al. (1996). Mutation in and lack of expression of tyrosinase-related protein-1 (TRP-1) in melanocytes from an individual with brown oculocutaneous albinism: a new subtype of albinism classified as "OCA3". *Am J Hum Genet* **58**, 1145-56.
Bondurand, N., Pingault, V., Goerich, D. E., Lemort, N., Sock, E., Le Caignec, C., Wegner, M. and Goossens, M. (2000). Interaction among SOX10, PAX3 and MITF, three genes altered in Waardenburg syndrome. *Hum Mol Genet* **9**, 1907-17.
Boulton, M. and Dayhaw-Barker, P. (2001). The role of the retinal pigment epithelium: topographical variation and ageing changes. *Eye (Lond)* **15**, 384-9.
Bowes, J. B., Snyder, K. A., Segerdell, E., Gibb, R., Jarabek, C., Noumen, E., Pollet, N. and Vize, P. D. (2008). Xenbase: a Xenopus biology and genomics resource. *Nucleic Acids Res* **36**, D761-7.
Brenner, M. and Hearing, V. J. (2008). The protective role of melanin against UV damage in human skin. *Photochem Photobiol* **84**, 539-49.
Brilliant, M. H. (2001). The mouse p (pink-eyed dilution) and human P genes, oculocutaneous albinism type 2 (OCA2), and melanosomal pH. *Pigment Cell Res* **14**, 86-93.
Burstyn-Cohen, T., Stanleigh, J., Sela-Donenfeld, D. and Kalcheim, C. (2004). Canonical Wnt activity regulates trunk neural crest delamination linking BMP/noggin signaling with G1/S transition. *Development* **131**, 5327-39.
Busca, R., Abbe, P., Mantoux, F., Aberdam, E., Peyssonnaux, C., Eychene, A., Ortonne, J. P. and Ballotti, R. (2000). Ras mediates the cAMP-dependent activation of extracellular signal-regulated kinases (ERKs) in melanocytes. *EMBO J* **19**, 2900-10.
Busca, R. and Ballotti, R. (2000). Cyclic AMP a key messenger in the regulation of skin pigmentation. *Pigment Cell Res* **13**, 60-9.
Bush, W. D. and Simon, J. D. (2007). Quantification of Ca(2+) binding to melanin supports the hypothesis that melanosomes serve a functional role in regulating calcium homeostasis. *Pigment Cell Res* **20**, 134-9.

Byers, H. R., Yaar, M., Eller, M. S., Jalbert, N. L. and Gilchrest, B. A. (2000). Role of cytoplasmic dynein in melanosome transport in human melanocytes. *J Invest Dermatol* **114**, 990-7.
Cai, X. and Lytton, J. (2004). Molecular cloning of a sixth member of the K+-dependent Na+/Ca2+ exchanger gene family, NCKX6. *J Biol Chem* **279**, 5867-76.
Cai, X., Zhang, K. and Lytton, J. (2002). A novel topology and redox regulation of the rat brain K+-dependent Na+/Ca2+ exchanger, NCKX2. *J Biol Chem* **277**, 48923-30.
Cano, A., Perez-Moreno, M. A., Rodrigo, I., Locascio, A., Blanco, M. J., del Barrio, M. G., Portillo, F. and Nieto, M. A. (2000). The transcription factor snail controls epithelial-mesenchymal transitions by repressing E-cadherin expression. *Nat Cell Biol* **2**, 76-83.
Cardinali, G., Ceccarelli, S., Kovacs, D., Aspite, N., Lotti, L. V., Torrisi, M. R. and Picardo, M. (2005). Keratinocyte growth factor promotes melanosome transfer to keratinocytes. *J Invest Dermatol* **125**, 1190-9.
Chain, F. J. and Evans, B. J. (2006). Multiple mechanisms promote the retained expression of gene duplicates in the tetraploid frog Xenopus laevis. *PLoS Genet* **2**, e56.
Chaplin, G. (2004). Geographic distribution of environmental factors influencing human skin coloration. *Am J Phys Anthropol* **125**, 292-302.
Cheli, Y., Luciani, F., Khaled, M., Beuret, L., Bille, K., Gounon, P., Ortonne, J. P., Bertolotto, C. and Ballotti, R. (2009). {alpha}MSH and Cyclic AMP elevating agents control melanosome pH through a protein kinase A-independent mechanism. *J Biol Chem* **284**, 18699-706.
Chen, Y., Ruan, X. Z., Li, Q., Huang, A., Moorhead, J. F., Powis, S. H. and Varghese, Z. (2007). Inflammatory cytokines disrupt LDL-receptor feedback regulation and cause statin resistance: a comparative study in human hepatic cells and mesangial cells. *Am J Physiol Renal Physiol* **293**, F680-7.
Chi, A., Valencia, J. C., Hu, Z. Z., Watabe, H., Yamaguchi, H., Mangini, N. J., Huang, H., Canfield, V. A., Cheng, K. C., Yang, F. et al. (2006). Proteomic and bioinformatic characterization of the biogenesis and function of melanosomes. *J Proteome Res* **5**, 3135-44.
Chiaverini, C., Beuret, L., Flori, E., Busca, R., Abbe, P., Bille, K., Bahadoran, P., Ortonne, J. P., Bertolotto, C. and Ballotti, R. (2008). Microphthalmia-associated transcription factor regulates RAB27A gene expression and controls melanosome transport. *J Biol Chem* **283**, 12635-42.
Chin, L., Tam, A., Pomerantz, J., Wong, M., Holash, J., Bardeesy, N., Shen, Q., O'Hagan, R., Pantginis, J., Zhou, H. et al. (1999). Essential role for oncogenic Ras in tumour maintenance. *Nature* **400**, 468-72.
Clepet, C., Le Clainche, I. and Caboche, M. (2004). Improved full-length cDNA production based on RNA tagging by T4 DNA ligase. *Nucleic Acids Res* **32**, e6.
Cohen, C., Zavala-Pompa, A., Sequeira, J. H., Shoji, M., Sexton, D. G., Cotsonis, G., Cerimele, F., Govindarajan, B., Macaron, N. and Arbiser, J. L. (2002). Mitogen-actived protein kinase activation is an early event in melanoma progression. *Clin Cancer Res* **8**, 3728-33.
Cooper, C. B., Winkfein, R. J., Szerencsei, R. T. and Schnetkamp, P. P. (1999). cDNA cloning and functional expression of the dolphin retinal rod Na-Ca+K exchanger NCKX1: comparison with the functionally silent bovine NCKX1. *Biochemistry* **38**, 6276-83.
Cooper, C. D. and Raible, D. W. (2009). Mechanisms for reaching the differentiated state: Insights from neural crest-derived melanocytes. *Semin Cell Dev Biol* **20**, 105-10.

Cui, R., Widlund, H. R., Feige, E., Lin, J. Y., Wilensky, D. L., Igras, V. E., D'Orazio, J., Fung, C. Y., Schanbacher, C. F., Granter, S. R. et al. (2007). Central role of p53 in the suntan response and pathologic hyperpigmentation. *Cell* **128**, 853-64.
Cuomo, O., Gala, R., Pignataro, G., Boscia, F., Secondo, A., Scorziello, A., Pannaccione, A., Viggiano, D., Adornetto, A., Molinaro, P. et al. (2008). A critical role for the potassium-dependent sodium-calcium exchanger NCKX2 in protection against focal ischemic brain damage. *J Neurosci* **28**, 2053-63.
Davies, H., Bignell, G. R., Cox, C., Stephens, P., Edkins, S., Clegg, S., Teague, J., Woffendin, H., Garnett, M. J., Bottomley, W. et al. (2002). Mutations of the BRAF gene in human cancer. *Nature* **417**, 949-54.
De Maziere, A. M., Muehlethaler, K., van Donselaar, E., Salvi, S., Davoust, J., Cerottini, J. C., Levy, F., Slot, J. W. and Rimoldi, D. (2002). The melanocytic protein Melan-A/MART-1 has a subcellular localization distinct from typical melanosomal proteins. *Traffic* **3**, 678-93.
Denvir, M. A., Tucker, C. S. and Mullins, J. J. (2008). Systolic and diastolic ventricular function in zebrafish embryos: influence of norepenephrine, MS-222 and temperature. *BMC Biotechnol* **8**, 21.
Derycke, L. D. and Bracke, M. E. (2004). N-cadherin in the spotlight of cell-cell adhesion, differentiation, embryogenesis, invasion and signalling. *Int J Dev Biol* **48**, 463-76.
Di Cristofano, A., Pesce, B., Cordon-Cardo, C. and Pandolfi, P. P. (1998). Pten is essential for embryonic development and tumour suppression. *Nat Genet* **19**, 348-55.
Dorsky, R. I., Moon, R. T. and Raible, D. W. (1998). Control of neural crest cell fate by the Wnt signalling pathway. *Nature* **396**, 370-3.
Drager, U. C. (1985). Calcium binding in pigmented and albino eyes. *Proc Natl Acad Sci U S A* **82**, 6716-20.
Draper, B. W., Morcos, P. A. and Kimmel, C. B. (2001). Inhibition of zebrafish fgf8 pre-mRNA splicing with morpholino oligos: a quantifiable method for gene knockdown. *Genesis* **30**, 154-6.
Du, J., Miller, A. J., Widlund, H. R., Horstmann, M. A., Ramaswamy, S. and Fisher, D. E. (2003). MLANA/MART1 and SILV/PMEL17/GP100 are transcriptionally regulated by MITF in melanocytes and melanoma. *Am J Pathol* **163**, 333-43.
Duffy, D. L., Zhao, Z. Z., Sturm, R. A., Hayward, N. K., Martin, N. G. and Montgomery, G. W. (2007). Multiple pigmentation gene polymorphisms account for a substantial proportion of risk of cutaneous malignant melanoma. *J Invest Dermatol* **130**, 520-8.
Dunn, K. J., Williams, B. O., Li, Y. and Pavan, W. J. (2000). Neural crest-directed gene transfer demonstrates Wnt1 role in melanocyte expansion and differentiation during mouse development. *Proc Natl Acad Sci U S A* **97**, 10050-5.
Dupin, E. and Le Douarin, N. M. (2003). Development of melanocyte precursors from the vertebrate neural crest. *Oncogene* **22**, 3016-23.
Eisen, J. S. and Smith, J. C. (2008). Controlling morpholino experiments: don't stop making antisense. *Development* **135**, 1735-43.
Erickson, C. A. (1993). From the crest to the periphery: control of pigment cell migration and lineage segregation. *Pigment Cell Res* **6**, 336-47.
Fehr, C., Fickova, M., Hiemke, C. and Dahmen, N. (1999). Rapid cloning of cDNA ends polymerase chain reaction of G-protein-coupled receptor kinase 6: an improved method to determine 5'- and 3'-cDNA ends. *Brain Res Brain Res Protoc* **3**, 242-51.

Fielding, C. J. and Fielding, P. E. (1997). Intracellular cholesterol transport. *J Lipid Res* **38**, 1503-21.
Fisher, G. J., Kang, S., Varani, J., Bata-Csorgo, Z., Wan, Y., Datta, S. and Voorhees, J. J. (2002). Mechanisms of photoaging and chronological skin aging. *Arch Dermatol* **138**, 1462-70.
Fistarol, S. K. and Itin, P. H. (2010). Disorders of pigmentation. *J Dtsch Dermatol Ges* **8**, 187-201; quiz 201-2.
Fuhrmann, S. (2010). Eye morphogenesis and patterning of the optic vesicle. *Curr Top Dev Biol* **93**, 61-84.
Fuhrmann, S., Levine, E. M. and Reh, T. A. (2000). Extraocular mesenchyme patterns the optic vesicle during early eye development in the embryonic chick. *Development* **127**, 4599-609.
Fuller, B. B., Spaulding, D. T. and Smith, D. R. (2001). Regulation of the catalytic activity of preexisting tyrosinase in black and Caucasian human melanocyte cell cultures. *Exp Cell Res* **262**, 197-208.
Futter, C. E. (2006). The molecular regulation of organelle transport in mammalian retinal pigment epithelial cells. *Pigment Cell Res* **19**, 104-11.
Gantz, I. and Fong, T. M. (2003). The melanocortin system. *Am J Physiol Endocrinol Metab* **284**, E468-74.
Garcia-Morales, C., Liu, C. H., Abu-Elmagd, M., Hajihosseini, M. K. and Wheeler, G. N. (2009). Frizzled-10 promotes sensory neuron development in Xenopus embryos. *Dev Biol* **335**, 143-55.
Garraway, L. A., Widlund, H. R., Rubin, M. A., Getz, G., Berger, A. J., Ramaswamy, S., Beroukhim, R., Milner, D. A., Granter, S. R., Du, J. et al. (2005). Integrative genomic analyses identify MITF as a lineage survival oncogene amplified in malignant melanoma. *Nature* **436**, 117-22.
Gennerich, A. and Vale, R. D. (2009). Walking the walk: how kinesin and dynein coordinate their steps. *Curr Opin Cell Biol* **21**, 59-67.
Gillbro, J. M., Marles, L. K., Hibberts, N. A. and Schallreuter, K. U. (2004). Autocrine catecholamine biosynthesis and the beta-adrenoceptor signal promote pigmentation in human epidermal melanocytes. *J Invest Dermatol* **123**, 346-53.
Ginger, R. S., Askew, S. E., Ogborne, R. M., Wilson, S., Ferdinando, D., Dadd, T., Smith, A. M., Kazi, S., Szerencsei, R. T., Winkfein, R. J. et al. (2008). SLC24A5 Encodes a trans-Golgi Network Protein with Potassium-dependent Sodium-Calcium Exchange Activity That Regulates Human Epidermal Melanogenesis. *J Biol Chem* **283**, 5486-95.
Goding, C. R. (2007). Melanocytes: the new Black. *Int J Biochem Cell Biol* **39**, 275-9.
Graf, J., Hodgson, R. and van Daal, A. (2005). Single nucleotide polymorphisms in the MATP gene are associated with normal human pigmentation variation. *Hum Mutat* **25**, 278-84.
Gray-Schopfer, V., Wellbrock, C. and Marais, R. (2007). Melanoma biology and new targeted therapy. *Nature* **445**, 851-7.
Gudbjartsson, D. F., Sulem, P., Stacey, S. N., Goldstein, A. M., Rafnar, T., Sigurgeirsson, B., Benediktsdottir, K. R., Thorisdottir, K., Ragnarsson, R., Sveinsdottir, S. G. et al. (2008). ASIP and TYR pigmentation variants associate with cutaneous melanoma and basal cell carcinoma. *Nat Genet* **40**, 886-91.
Gunn, T. M., Miller, K. A., He, L., Hyman, R. W., Davis, R. W., Azarani, A., Schlossman, S. F., Duke-Cohan, J. S. and Barsh, G. S. (1999). The mouse mahogany locus encodes a transmembrane form of human attractin. *Nature* **398**, 152-6.
Halaban, R., Langdon, R., Birchall, N., Cuono, C., Baird, A., Scott, G., Moellmann, G. and McGuire, J. (1988). Basic fibroblast growth factor from

human keratinocytes is a natural mitogen for melanocytes. *J Cell Biol* **107**, 1611-9.
Hall, A. M., Krishnamoorthy, L. and Orlow, S. J. (2004). 25-hydroxycholesterol acts in the Golgi compartment to induce degradation of tyrosinase. *Pigment Cell Res* **17**, 396-406.
Hammer, J. A. and Wu, X. S. (2007). Organelle motility: running on unleadened. *Curr Biol* **17**, R1017-9.
Hara, M., Yaar, M., Byers, H. R., Goukassian, D., Fine, R. E., Gonsalves, J. and Gilchrest, B. A. (2000). Kinesin participates in melanosomal movement along melanocyte dendrites. *J Invest Dermatol* **114**, 438-43.
Harding, R. M., Healy, E., Ray, A. J., Ellis, N. S., Flanagan, N., Todd, C., Dixon, C., Sajantila, A., Jackson, I. J., Birch-Machin, M. A. et al. (2000). Evidence for variable selective pressures at MC1R. *Am J Hum Genet* **66**, 1351-61.
Harland, R. M. (1991). In situ hybridization: an improved whole-mount method for Xenopus embryos. *Methods Cell Biol* **36**, 685-95.
Hattori, M., Hashimoto, H., Bubenshchikova, E. and Wakamatsu, Y. (2011). Nuclear Transfer of Embryonic Cell Nuclei to Non-enucleated Eggs in Zebrafish, Danio rerio. *Int J Biol Sci* **7**, 460-8.
Haug-Collet, K., Pearson, B., Webel, R., Szerencsei, R. T., Winkfein, R. J., Schnetkamp, P. P. and Colley, N. J. (1999). Cloning and characterization of a potassium-dependent sodium/calcium exchanger in Drosophila. *J Cell Biol* **147**, 659-70.
Haworth, K. E., Kotecha, S., Mohun, T. J. and Latinkic, B. V. (2008). GATA4 and GATA5 are essential for heart and liver development in Xenopus embryos. *BMC Dev Biol* **8**, 74.
Hearing, V. J. (2005). Biogenesis of pigment granules: a sensitive way to regulate melanocyte function. *J Dermatol Sci* **37**, 3-14.
Heasman, J. (2002). Morpholino oligos: making sense of antisense? *Dev Biol* **243**, 209-14.
Hellsten, U., Harland, R. M., Gilchrist, M. J., Hendrix, D., Jurka, J., Kapitonov, V., Ovcharenko, I., Putnam, N. H., Shu, S., Taher, L. et al. (2010). The genome of the Western clawed frog Xenopus tropicalis. *Science* **328**, 633-6.
Hemesath, T. J., Price, E. R., Takemoto, C., Badalian, T. and Fisher, D. E. (1998). MAP kinase links the transcription factor Microphthalmia to c-Kit signalling in melanocytes. *Nature* **391**, 298-301.
Hershkovitz, D. and Sprecher, E. (2008). Monogenic pigmentary skin disorders: genetics and pathophysiology. *Isr Med Assoc J* **10**, 713-7.
Hirobe, T. (2005). Role of keratinocyte-derived factors involved in regulating the proliferation and differentiation of mammalian epidermal melanocytes. *Pigment Cell Res* **18**, 2-12.
Hirobe, T. and Abe, H. (2006). The slaty mutation affects the morphology and maturation of melanosomes in the mouse melanocytes. *Pigment Cell Res* **19**, 454-9.
Hirobe, T., Ito, S. and Wakamatsu, K. (2011). The mouse pink-eyed dilution allele of the P-gene greatly inhibits eumelanin but not pheomelanin synthesis. *Pigment Cell Melanoma Res* **24**, 241-6.
Hirobe, T., Wakamatsu, K., Ito, S., Kawa, Y., Soma, Y. and Mizoguchi, M. (2006). The slaty mutation affects eumelanin and pheomelanin synthesis in mouse melanocytes. *Eur J Cell Biol* **85**, 537-49.
Hoashi, T., Watabe, H., Muller, J., Yamaguchi, Y., Vieira, W. D. and Hearing, V. J. (2005). MART-1 is required for the function of the melanosomal matrix

protein PMEL17/GP100 and the maturation of melanosomes. *J Biol Chem* **280**, 14006-16.
Hoek, K. S. (2010). MITF: the power and the glory. *Pigment Cell Melanoma Res* **24**, 262-3.
Hoogduijn, M. J., Cemeli, E., Ross, K., Anderson, D., Thody, A. J. and Wood, J. M. (2004). Melanin protects melanocytes and keratinocytes against H2O2-induced DNA strand breaks through its ability to bind Ca2+. *Exp Cell Res* **294**, 60-7.
Hoogduijn, M. J., Smit, N. P., van der Laarse, A., van Nieuwpoort, A. F., Wood, J. M. and Thody, A. J. (2003). Melanin has a role in Ca2+ homeostasis in human melanocytes. *Pigment Cell Res* **16**, 127-32.
Hughes, M. K. and Hughes, A. L. (1993). Evolution of duplicate genes in a tetraploid animal, Xenopus laevis. *Mol Biol Evol* **10**, 1360-9.
Hume, A. N., Collinson, L. M., Rapak, A., Gomes, A. Q., Hopkins, C. R. and Seabra, M. C. (2001). Rab27a regulates the peripheral distribution of melanosomes in melanocytes. *J Cell Biol* **152**, 795-808.
Ikeya, M., Lee, S. M., Johnson, J. E., McMahon, A. P. and Takada, S. (1997). Wnt signalling required for expansion of neural crest and CNS progenitors. *Nature* **389**, 966-70.
Imokawa, G., Yada, Y. and Miyagishi, M. (1992). Endothelins secreted from human keratinocytes are intrinsic mitogens for human melanocytes. *J Biol Chem* **267**, 24675-80.
Ito, S., Wakamatsu, K. and Ozeki, H. (2000). Chemical analysis of melanins and its application to the study of the regulation of melanogenesis. *Pigment Cell Res* **13 Suppl 8**, 103-9.
Jablonski, N. G. and Chaplin, G. (2000). The evolution of human skin coloration. *J Hum Evol* **39**, 57-106.
Jeffery, G. (1997). The albino retina: an abnormality that provides insight into normal retinal development. *Trends Neurosci* **20**, 165-9.
Jimbow, K., Gomez, P. F., Toyofuku, K., Chang, D., Miura, S., Tsujiya, H. and Park, J. S. (1997). Biological role of tyrosinase related protein and its biosynthesis and transport from TGN to stage I melanosome, late endosome, through gene transfection study. *Pigment Cell Res* **10**, 206-13.
Jin, S. H., Lee, Y. Y. and Kang, H. Y. (2008). Methyl-beta-cyclodextrin, a specific cholesterol-binding agent, inhibits melanogenesis in human melanocytes through activation of ERK. *Arch Dermatol Res* **300**, 451-4.
Jovic, M., Sharma, M., Rahajeng, J. and Caplan, S. (2010). The early endosome: a busy sorting station for proteins at the crossroads. *Histol Histopathol* **25**, 99-112.
Juzeniene, A., Setlow, R., Porojnicu, A., Steindal, A. H. and Moan, J. (2009). Development of different human skin colors: a review highlighting photobiological and photobiophysical aspects. *J Photochem Photobiol B* **96**, 93-100.
Kadekaro, A. L., Kavanagh, R., Kanto, H., Terzieva, S., Hauser, J., Kobayashi, N., Schwemberger, S., Cornelius, J., Babcock, G., Shertzer, H. G. et al. (2005). alpha-Melanocortin and endothelin-1 activate antiapoptotic pathways and reduce DNA damage in human melanocytes. *Cancer Res* **65**, 4292-9.
Kang, K., Bauer, P. J., Kinjo, T. G., Szerencsei, R. T., Bonigk, W., Winkfein, R. J. and Schnetkamp, P. P. (2003). Assembly of retinal rod or cone Na(+)/Ca(2+)-K(+) exchanger oligomers with cGMP-gated channel subunits as probed with heterologously expressed cDNAs. *Biochemistry* **42**, 4593-600.

Kang, K. and Schnetkamp, P. P. (2003). Signal sequence cleavage and plasma membrane targeting of the retinal rod NCKX1 and cone NCKX2 Na+/Ca2+ - K+ exchangers. *Biochemistry* **42**, 9438-45.
Kang, K. J., Kinjo, T. G., Szerencsei, R. T. and Schnetkamp, P. P. (2005a). Residues contributing to the Ca2+ and K+ binding pocket of the NCKX2 Na+/Ca2+-K+ exchanger. *J Biol Chem* **280**, 6823-33.
Kang, K. J., Shibukawa, Y., Szerencsei, R. T. and Schnetkamp, P. P. (2005b). Substitution of a single residue, Asp575, renders the NCKX2 K+-dependent Na+/Ca2+ exchanger independent of K+. *J Biol Chem* **280**, 6834-9.
Kanzler, B., Foreman, R. K., Labosky, P. A. and Mallo, M. (2000). BMP signaling is essential for development of skeletogenic and neurogenic cranial neural crest. *Development* **127**, 1095-104.
Kiedrowski, L. (2007). NCX and NCKX operation in ischemic neurons. *Ann N Y Acad Sci* **1099**, 383-95.
Kim, T. S., Reid, D. M. and Molday, R. S. (1998). Structure-function relationships and localization of the Na/Ca-K exchanger in rod photoreceptors. *J Biol Chem* **273**, 16561-7.
Kimura, M., Aviv, A. and Reeves, J. P. (1993). K(+)-dependent Na+/Ca2+ exchange in human platelets. *J Biol Chem* **268**, 6874-7.
King, R. A. (1993). Oculocutaneous Albinism Type 1.
Kinjo, T. G., Kang, K., Szerencsei, R. T., Winkfein, R. J. and Schnetkamp, P. P. (2005). Site-directed disulfide mapping of residues contributing to the Ca2+ and K+ binding pocket of the NCKX2 Na+/Ca2+-K+ exchanger. *Biochemistry* **44**, 7787-95.
Kinjo, T. G., Szerencsei, R. T. and Schnetkamp, P. P. (2007). Topologic investigation of the NCKX2 Na+/Ca2+-K+ exchanger alpha-repeats. *Ann N Y Acad Sci* **1099**, 34-9.
Kinjo, T. G., Szerencsei, R. T., Winkfein, R. J., Kang, K. and Schnetkamp, P. P. (2003). Topology of the retinal cone NCKX2 Na/Ca-K exchanger. *Biochemistry* **42**, 2485-91.
Kinjo, T. G., Szerencsei, R. T., Winkfein, R. J. and Schnetkamp, P. P. (2004). Role of cysteine residues in the NCKX2 Na+/Ca(2+)-K+ Exchanger: generation of a functional cysteine-free exchanger. *Biochemistry* **43**, 7940-7.
Klaus, S. N. (1969). Pigment transfer in mammalian epidermis. *Arch Dermatol* **100**, 756-62.
Kobayashi, T. and Hearing, V. J. (2007). Direct interaction of tyrosinase with Tyrp1 to form heterodimeric complexes in vivo. *J Cell Sci* **120**, 4261-8.
Kobayashi, T., Vieira, W. D., Potterf, B., Sakai, C., Imokawa, G. and Hearing, V. J. (1995). Modulation of melanogenic protein expression during the switch from eu- to pheomelanogenesis. *J Cell Sci* **108 (Pt 6)**, 2301-9.
Koch, K. W., Duda, T. and Sharma, R. K. (2010). Ca(2+)-modulated vision-linked ROS-GC guanylate cyclase transduction machinery. *Mol Cell Biochem* **334**, 105-15.
Koutalos, Y., Nakatani, K., Tamura, T. and Yau, K. W. (1995). Characterization of guanylate cyclase activity in single retinal rod outer segments. *J Gen Physiol* **106**, 863-90.
Kraev, A., Quednau, B. D., Leach, S., Li, X. F., Dong, H., Winkfein, R., Perizzolo, M., Cai, X., Yang, R., Philipson, K. D. et al. (2001). Molecular cloning of a third member of the potassium-dependent sodium-calcium exchanger gene family, NCKX3. *J Biol Chem* **276**, 23161-72.
Krizaj, D. and Copenhagen, D. R. (1998). Compartmentalization of calcium extrusion mechanisms in the outer and inner segments of photoreceptors. *Neuron* **21**, 249-56.

Kumasaka, M., Sato, H., Sato, S., Yajima, I. and Yamamoto, H. (2004). Isolation and developmental expression of Mitf in Xenopus laevis. *Dev Dyn* **230**, 107-13.
Kumasaka, M., Sato, S., Yajima, I. and Yamamoto, H. (2003). Isolation and developmental expression of tyrosinase family genes in Xenopus laevis. *Pigment Cell Res* **16**, 455-62.
Kuphal, S. and Bosserhoff, A. (2009). Recent progress in understanding the pathology of malignant melanoma. *J Pathol* **219**, 400-9.
Lahav, R., Dupin, E., Lecoin, L., Glavieux, C., Champeval, D., Ziller, C. and Le Douarin, N. M. (1998). Endothelin 3 selectively promotes survival and proliferation of neural crest-derived glial and melanocytic precursors in vitro. *Proc Natl Acad Sci U S A* **95**, 14214-9.
Lamason, R. L., Mohideen, M. A., Mest, J. R., Wong, A. C., Norton, H. L., Aros, M. C., Jurynec, M. J., Mao, X., Humphreville, V. R., Humbert, J. E. et al. (2005). SLC24A5, a putative cation exchanger, affects pigmentation in zebrafish and humans. *Science* **310**, 1782-6.
Lamoreux, M. L., Wakamatsu, K. and Ito, S. (2001). Interaction of major coat color gene functions in mice as studied by chemical analysis of eumelanin and pheomelanin. *Pigment Cell Res* **14**, 23-31.
Lang, D., Lu, M. M., Huang, L., Engleka, K. A., Zhang, M., Chu, E. Y., Lipner, S., Skoultchi, A., Millar, S. E. and Epstein, J. A. (2005). Pax3 functions at a nodal point in melanocyte stem cell differentiation. *Nature* **433**, 884-7.
Lao, O., de Gruijter, J. M., van Duijn, K., Navarro, A. and Kayser, M. (2007). Signatures of positive selection in genes associated with human skin pigmentation as revealed from analyses of single nucleotide polymorphisms. *Ann Hum Genet* **71**, 354-69.
Le Douarin, N. M. and Dupin, E. (2003). Multipotentiality of the neural crest. *Curr Opin Genet Dev* **13**, 529-36.
Le Pape, E., Passeron, T., Giubellino, A., Valencia, J. C., Wolber, R. and Hearing, V. J. (2009). Microarray analysis sheds light on the dedifferentiating role of agouti signal protein in murine melanocytes via the Mc1r. *Proc Natl Acad Sci U S A* **106**, 1802-7.
Le Pape, E., Wakamatsu, K., Ito, S., Wolber, R. and Hearing, V. J. (2008). Regulation of eumelanin/pheomelanin synthesis and visible pigmentation in melanocytes by ligands of the melanocortin 1 receptor. *Pigment Cell Melanoma Res* **21**, 477-86.
Leonard, S. E. and Carroll, K. S. (2011). Chemical 'omics' approaches for understanding protein cysteine oxidation in biology. *Curr Opin Chem Biol* **15**, 88-102.
Leonhardt, R. M., Vigneron, N., Rahner, C., Van den Eynde, B. J. and Cresswell, P. (2010). Endoplasmic reticulum export, subcellular distribution, and fibril formation by Pmel17 require an intact N-terminal domain junction. *J Biol Chem* **285**, 16166-83.
Levy, C., Khaled, M. and Fisher, D. E. (2006). MITF: master regulator of melanocyte development and melanoma oncogene. *Trends Mol Med* **12**, 406-14.
Li, X. F., Kiedrowski, L., Tremblay, F., Fernandez, F. R., Perizzolo, M., Winkfein, R. J., Turner, R. W., Bains, J. S., Rancourt, D. E. and Lytton, J. (2006). Importance of K+-dependent Na+/Ca2+-exchanger 2, NCKX2, in motor learning and memory. *J Biol Chem* **281**, 6273-82.
Li, X. F., Kraev, A. S. and Lytton, J. (2002). Molecular cloning of a fourth member of the potassium-dependent sodium-calcium exchanger gene family, NCKX4. *J Biol Chem* **277**, 48410-7.

Liao, H. K. and Essner, J. J. Use of RecA fusion proteins to induce genomic modifications in zebrafish. *Nucleic Acids Res*.
Lin, J. Y. and Fisher, D. E. (2007). Melanocyte biology and skin pigmentation. *Nature* **445**, 843-50.
Lister, J. A., Robertson, C. P., Lepage, T., Johnson, S. L. and Raible, D. W. (1999). nacre encodes a zebrafish microphthalmia-related protein that regulates neural-crest-derived pigment cell fate. *Development* **126**, 3757-67.
Liu, X. F., Luo, J., Hu, X. X., Yang, H., Lv, X. Q., Feng, C. G., Tong, J., Wang, Y. Q., Wang, S. H., Liu, X. J. et al. (2011). Repression of Slc24a5 can reduce pigmentation in chicken. *Front Biosci (Elite Ed)* **3**, 158-65.
Lopez, J. J., Camello-Almaraz, C., Pariente, J. A., Salido, G. M. and Rosado, J. A. (2005). Ca2+ accumulation into acidic organelles mediated by Ca2+- and vacuolar H+-ATPases in human platelets. *Biochem J* **390**, 243-52.
Lytton, J. (2007). Na+/Ca2+ exchangers: three mammalian gene families control Ca2+ transport. *Biochem J* **406**, 365-82.
Martinez-Morales, J. R., Rodrigo, I. and Bovolenta, P. (2004). Eye development: a view from the retina pigmented epithelium. *Bioessays* **26**, 766-77.
Maruyama, K. and Sugano, S. (1994). Oligo-capping: a simple method to replace the cap structure of eukaryotic mRNAs with oligoribonucleotides. *Gene* **138**, 171-4.
McGill, G. G., Horstmann, M., Widlund, H. R., Du, J., Motyckova, G., Nishimura, E. K., Lin, Y. L., Ramaswamy, S., Avery, W., Ding, H. F. et al. (2002). Bcl2 regulation by the melanocyte master regulator Mitf modulates lineage survival and melanoma cell viability. *Cell* **109**, 707-18.
McGlinchey, R. P., Shewmaker, F., Hu, K. N., McPhie, P., Tycko, R. and Wickner, R. B. (2011). Repeat domains of melanosome matrix protein Pmel17 orthologs form amyloid fibrils at the acidic melanosomal pH. *J Biol Chem* **286**, 8385-93.
Meyer zum Gottesberge, A. M. (1988). Physiology and pathophysiology of inner ear melanin. *Pigment Cell Res* **1**, 238-49.
Missiaen, L., Dode, L., Vanoevelen, J., Raeymaekers, L. and Wuytack, F. (2007). Calcium in the Golgi apparatus. *Cell Calcium* **41**, 405-16.
Moore, J., Wood, J. M. and Schallreuter, K. U. (1999). Evidence for specific complex formation between alpha-melanocyte stimulating hormone and 6(R)-L-erythro-5,6,7,8-tetrahydrobiopterin using near infrared Fourier transform Raman spectroscopy. *Biochemistry* **38**, 15317-24.
Moore, J. L., Rush, L. M., Breneman, C., Mohideen, M. A. and Cheng, K. C. (2006). Zebrafish genomic instability mutants and cancer susceptibility. *Genetics* **174**, 585-600.
Morcos, P. A. (2007). Achieving targeted and quantifiable alteration of mRNA splicing with Morpholino oligos. *Biochem Biophys Res Commun* **358**, 521-7.
Mottaz, J. H. and Zelickson, A. S. (1967). Melanin transfer: a possible phagocytic process. *J Invest Dermatol* **49**, 605-10.
Nadeau, N. J., Minvielle, F., Ito, S., Inoue-Murayama, M., Gourichon, D., Follett, S. A., Burke, T. and Mundy, N. I. (2008). Characterization of Japanese quail yellow as a genomic deletion upstream of the avian homolog of the mammalian ASIP (agouti) gene. *Genetics* **178**, 777-86.
Nakano, A. and Luini, A. (2010). Passage through the Golgi. *Curr Opin Cell Biol* **22**, 471-8.
Nan, H., Kraft, P., Hunter, D. J. and Han, J. (2009). Genetic variants in pigmentation genes, pigmentary phenotypes, and risk of skin cancer in Caucasians. *Int J Cancer* **125**, 909-17.

Newton, R. A., Roberts, D. W., Leonard, J. H. and Sturm, R. A. (2007). Human melanocytes expressing MC1R variant alleles show impaired activation of multiple signaling pathways. *Peptides* **28**, 2387-96.
Nieuwkoop, P. and Faber, J. (1994). Normal Table of Xenopus laevis. New York: Garlan Publishing
Nishimura, E. K., Granter, S. R. and Fisher, D. E. (2005). Mechanisms of hair graying: incomplete melanocyte stem cell maintenance in the niche. *Science* **307**, 720-4.
Oetting, W. S. and King, R. A. (1999). Molecular basis of albinism: mutations and polymorphisms of pigmentation genes associated with albinism. *Hum Mutat* **13**, 99-115.
Olivares, C. and Solano, F. (2009). New insights into the active site structure and catalytic mechanism of tyrosinase and its related proteins. *Pigment Cell Melanoma Res* **22**, 750-60.
Ono, H., Kawa, Y., Asano, M., Ito, M., Takano, A., Kubota, Y., Matsumoto, J. and Mizoguchi, M. (1998). Development of melanocyte progenitors in murine Steel mutant neural crest explants cultured with stem cell factor, endothelin-3, or TPA. *Pigment Cell Res* **11**, 291-8.
Paillart, C., Winkfein, R. J., Schnetkamp, P. P. and Korenbrot, J. I. (2007). Functional characterization and molecular cloning of the K+-dependent Na+/Ca2+ exchanger in intact retinal cone photoreceptors. *J Gen Physiol* **129**, 1-16.
Park, H. Y., Kosmadaki, M., Yaar, M. and Gilchrest, B. A. (2009). Cellular mechanisms regulating human melanogenesis. *Cell Mol Life Sci* **66**, 1493-506.
Park, H. Y., Perez, J. M., Laursen, R., Hara, M. and Gilchrest, B. A. (1999). Protein kinase C-beta activates tyrosinase by phosphorylating serine residues in its cytoplasmic domain. *J Biol Chem* **274**, 16470-8.
Parra, E. J. (2007). Human pigmentation variation: evolution, genetic basis, and implications for public health. *Am J Phys Anthropol* **Suppl 45**, 85-105.
Passeron, T., Namiki, T., Passeron, H. J., Le Pape, E. and Hearing, V. J. (2009). Forskolin protects keratinocytes from UVB-induced apoptosis and increases DNA repair independent of its effects on melanogenesis. *J Invest Dermatol* **129**, 162-6.
Passeron, T., Valencia, J. C., Bertolotto, C., Hoashi, T., Le Pape, E., Takahashi, K., Ballotti, R. and Hearing, V. J. (2007). SOX9 is a key player in ultraviolet B-induced melanocyte differentiation and pigmentation. *Proc Natl Acad Sci U S A* **104**, 13984-9.
Patel, S. and Docampo, R. (2010). Acidic calcium stores open for business: expanding the potential for intracellular Ca2+ signaling. *Trends Cell Biol* **20**, 277-86.
Peters, E. M., Tobin, D. J., Botchkareva, N., Maurer, M. and Paus, R. (2002). Migration of melanoblasts into the developing murine hair follicle is accompanied by transient c-Kit expression. *J Histochem Cytochem* **50**, 751-66.
Peters, E. M., Tobin, D. J., Seidah, N. G. and Schallreuter, K. U. (2000). Pro-opiomelanocortin-related peptides, prohormone convertases 1 and 2 and the regulatory peptide 7B2 are present in melanosomes of human melanocytes. *J Invest Dermatol* **114**, 430-7.
Pfeffer, S. R. (2009). Multiple routes of protein transport from endosomes to the trans Golgi network. *FEBS Lett* **583**, 3811-6.
Pfefferkorn, C. M., McGlinchey, R. P. and Lee, J. C. (2010). Effects of pH on aggregation kinetics of the repeat domain of a functional amyloid, Pmel17. *Proc Natl Acad Sci U S A* **107**, 21447-52.

Pinon, P. and Wehrle-Haller, B. (2011). Integrins: versatile receptors controlling melanocyte adhesion, migration and proliferation. *Pigment Cell Melanoma Res*.
Pinton, P., Pozzan, T. and Rizzuto, R. (1998). The Golgi apparatus is an inositol 1,4,5-trisphosphate-sensitive Ca2+ store, with functional properties distinct from those of the endoplasmic reticulum. *EMBO J* **17**, 5298-308.
Podsypanina, K., Ellenson, L. H., Nemes, A., Gu, J., Tamura, M., Yamada, K. M., Cordon-Cardo, C., Catoretti, G., Fisher, P. E. and Parsons, R. (1999). Mutation of Pten/Mmac1 in mice causes neoplasia in multiple organ systems. *Proc Natl Acad Sci U S A* **96**, 1563-8.
Poon, S., Leach, S., Li, X. F., Tucker, J. E., Schnetkamp, P. P. and Lytton, J. (2000). Alternatively spliced isoforms of the rat eye sodium/calcium+potassium exchanger NCKX1. *Am J Physiol Cell Physiol* **278**, C651-60.
Potterf, S. B., Mollaaghababa, R., Hou, L., Southard-Smith, E. M., Hornyak, T. J., Arnheiter, H. and Pavan, W. J. (2001). Analysis of SOX10 function in neural crest-derived melanocyte development: SOX10-dependent transcriptional control of dopachrome tautomerase. *Dev Biol* **237**, 245-57.
Price, E. R., Horstmann, M. A., Wells, A. G., Weilbaecher, K. N., Takemoto, C. M., Landis, M. W. and Fisher, D. E. (1998). alpha-Melanocyte-stimulating hormone signaling regulates expression of microphthalmia, a gene deficient in Waardenburg syndrome. *J Biol Chem* **273**, 33042-7.
Prinsen, C. F., Szerencsei, R. T. and Schnetkamp, P. P. (2000). Molecular cloning and functional expression of the potassium-dependent sodium-calcium exchanger from human and chicken retinal cone photoreceptors. *J Neurosci* **20**, 1424-34.
Pugh, E. N., Jr. and Lamb, T. D. (1990). Cyclic GMP and calcium: the internal messengers of excitation and adaptation in vertebrate photoreceptors. *Vision Res* **30**, 1923-48.
Puri, N., Gardner, J. M. and Brilliant, M. H. (2000). Aberrant pH of melanosomes in pink-eyed dilution (p) mutant melanocytes. *J Invest Dermatol* **115**, 607-13.
Raposo, G. and Marks, M. S. (2007). Melanosomes--dark organelles enlighten endosomal membrane transport. *Nat Rev Mol Cell Biol* **8**, 786-97.
Raposo, G., Marks, M. S. and Cutler, D. F. (2007). Lysosome-related organelles: driving post-Golgi compartments into specialisation. *Curr Opin Cell Biol* **19**, 394-401.
Raposo, G., Tenza, D., Murphy, D. M., Berson, J. F. and Marks, M. S. (2001). Distinct protein sorting and localization to premelanosomes, melanosomes, and lysosomes in pigmented melanocytic cells. *J Cell Biol* **152**, 809-24.
Rees, J. L. (2000). The melanocortin 1 receptor (MC1R): more than just red hair. *Pigment Cell Res* **13**, 135-40.
Reilander, H., Achilles, A., Friedel, U., Maul, G., Lottspeich, F. and Cook, N. J. (1992). Primary structure and functional expression of the Na/Ca,K-exchanger from bovine rod photoreceptors. *EMBO J* **11**, 1689-95.
Riazuddin, S. A., Shahzadi, A., Zeitz, C., Ahmed, Z. M., Ayyagari, R., Chavali, V. R., Ponferrada, V. G., Audo, I., Michiels, C., Lancelot, M. E. et al. (2010). A mutation in SLC24A1 implicated in autosomal-recessive congenital stationary night blindness. *Am J Hum Genet* **87**, 523-31.
Rinchik, E. M., Bultman, S. J., Horsthemke, B., Lee, S. T., Strunk, K. M., Spritz, R. A., Avidano, K. M., Jong, M. T. and Nicholls, R. D. (1993). A gene for the mouse pink-eyed dilution locus and for human type II oculocutaneous albinism. *Nature* **361**, 72-6.
Robinson, K. C. and Fisher, D. E. (2009). Specification and loss of melanocyte stem cells. *Semin Cell Dev Biol* **20**, 111-6.

Rosenheim, O. and Webster, T. A. (1927). The Relation of Cholesterol to Vitamin D. *Biochem J* **21**, 127-9.
Saito, H., Yasumoto, K., Takeda, K., Takahashi, K., Fukuzaki, A., Orikasa, S. and Shibahara, S. (2002). Melanocyte-specific microphthalmia-associated transcription factor isoform activates its own gene promoter through physical interaction with lymphoid-enhancing factor 1. *J Biol Chem* **277**, 28787-94.
Salceda, R. and Sanchez-Chavez, G. (2000). Calcium uptake, release and ryanodine binding in melanosomes from retinal pigment epithelium. *Cell Calcium* **27**, 223-9.
Saldana-Caboverde, A. and Kos, L. (2010). Roles of endothelin signaling in melanocyte development and melanoma. *Pigment Cell Melanoma Res* **23**, 160-70.
Schallreuter, K. U. (2007). Advances in melanocyte basic science research. *Dermatol Clin* **25**, 283-91, vii.
Schallreuter, K. U., Hasse, S., Rokos, H., Chavan, B., Shalbaf, M., Spencer, J. D. and Wood, J. M. (2009). Cholesterol regulates melanogenesis in human epidermal melanocytes and melanoma cells. *Exp Dermatol* **18**, 680-8.
Schallreuter, K. U., Kothari, S., Chavan, B. and Spencer, J. D. (2007). Regulation of melanogenesis - controversies and new concepts. *Exp Dermatol*.
Schallreuter, K. U. and Wood, J. M. (1999). The importance of L-phenylalanine transport and its autocrine turnover to L-tyrosine for melanogenesis in human epidermal melanocytes. *Biochem Biophys Res Commun* **262**, 423-8.
Schepsky, A., Bruser, K., Gunnarsson, G. J., Goodall, J., Hallsson, J. H., Goding, C. R., Steingrimsson, E. and Hecht, A. (2006). The microphthalmia-associated transcription factor Mitf interacts with beta-catenin to determine target gene expression. *Mol Cell Biol* **26**, 8914-27.
Scherer, D. and Kumar, R. (2010). Genetics of pigmentation in skin cancer--a review. *Mutat Res* **705**, 141-53.
Scherer, D., Nagore, E., Bermejo, J. L., Figl, A., Botella-Estrada, R., Thirumaran, R. K., Angelini, S., Hemminki, K., Schadendorf, D. and Kumar, R. (2009). Melanocortin receptor 1 variants and melanoma risk: a study of 2 European populations. *Int J Cancer* **125**, 1868-75.
Schiaffino, M. V. (2010). Signaling pathways in melanosome biogenesis and pathology. *Int J Biochem Cell Biol* **42**, 1094-104.
Schiaffino, M. V., Baschirotto, C., Pellegrini, G., Montalti, S., Tacchetti, C., De Luca, M. and Ballabio, A. (1996). The ocular albinism type 1 gene product is a membrane glycoprotein localized to melanosomes. *Proc Natl Acad Sci U S A* **93**, 9055-60.
Schnetkamp, P. P. (2004). The SLC24 Na+/Ca2+-K+ exchanger family: vision and beyond. *Pflugers Arch* **447**, 683-8.
Schnetkamp, P. P., Szerencsei, R. T. and Basu, D. K. (1991). Unidirectional Na+, Ca2+, and K+ fluxes through the bovine rod outer segment Na-Ca-K exchanger. *J Biol Chem* **266**, 198-206.
Schwarzer, A., Kim, T. S., Hagen, V., Molday, R. S. and Bauer, P. J. (1997). The Na/Ca-K exchanger of rod photoreceptor exists as dimer in the plasma membrane. *Biochemistry* **36**, 13667-76.
Schwarzer, A., Schauf, H. and Bauer, P. J. (2000). Binding of the cGMP-gated channel to the Na/Ca-K exchanger in rod photoreceptors. *J Biol Chem* **275**, 13448-54.
Scott, G., Leopardi, S., Parker, L., Babiarz, L., Seiberg, M. and Han, R. (2003). The proteinase-activated receptor-2 mediates phagocytosis in a Rho-dependent manner in human keratinocytes. *J Invest Dermatol* **121**, 529-41.
Scott, G., Leopardi, S., Printup, S. and Madden, B. C. (2002). Filopodia are conduits for melanosome transfer to keratinocytes. *J Cell Sci* **115**, 1441-51.

Scotto-Lavino, E., Du, G. and Frohman, M. A. (2006). Amplification of 5' end cDNA with 'new RACE'. *Nat Protoc* **1**, 3056-61.
Seiberg, M. (2001). Keratinocyte-melanocyte interactions during melanosome transfer. *Pigment Cell Res* **14**, 236-42.
Shibahara, S., Takeda, K., Yasumoto, K., Udono, T., Watanabe, K., Saito, H. and Takahashi, K. (2001). Microphthalmia-associated transcription factor (MITF): multiplicity in structure, function, and regulation. *J Investig Dermatol Symp Proc* **6**, 99-104.
Shibukawa, Y., Kang, K. J., Kinjo, T. G., Szerencsei, R. T., Altimimi, H. F., Pratikhya, P., Winkfein, R. J. and Schnetkamp, P. P. (2007). Structure-function relationships of the NCKX2 Na+/Ca2+-K+ exchanger. *Ann N Y Acad Sci* **1099**, 16-28.
Shigaki, T., Rees, I., Nakhleh, L. and Hirschi, K. D. (2006). Identification of three distinct phylogenetic groups of CAX cation/proton antiporters. *J Mol Evol* **63**, 815-25.
Silver, D. L., Hou, L. and Pavan, W. J. (2006). The genetic regulation of pigment cell development. *Adv Exp Med Biol* **589**, 155-69.
Slominski, A., Paus, R., Plonka, P., Chakraborty, A., Maurer, M., Pruski, D. and Lukiewicz, S. (1994). Melanogenesis during the anagen-catagen-telogen transformation of the murine hair cycle. *J Invest Dermatol* **102**, 862-9.
Slominski, A., Zbytek, B., Pisarchik, A., Slominski, R. M., Zmijewski, M. A. and Wortsman, J. (2006). CRH functions as a growth factor/cytokine in the skin. *J Cell Physiol* **206**, 780-91.
Smith-Thomas, L. C., Moustafa, M., Dawson, R. A., Wagner, M., Balafa, C., Haycock, J. W., Krauss, A. H., Woodward, D. F. and MacNeil, S. (2001). Cellular and hormonal regulation of pigmentation in human ocular melanocytes. *Pigment Cell Res* **14**, 298-309.
Smith, D. R., Spaulding, D. T., Glenn, H. M. and Fuller, B. B. (2004). The relationship between Na(+)/H(+) exchanger expression and tyrosinase activity in human melanocytes. *Exp Cell Res* **298**, 521-34.
Soejima, M. and Koda, Y. (2007). Population differences of two coding SNPs in pigmentation-related genes SLC24A5 and SLC45A2. *Int J Legal Med* **121**, 36-9.
Soengas, M. S. and Lowe, S. W. (2003). Apoptosis and melanoma chemoresistance. *Oncogene* **22**, 3138-51.
Song, X., Mosby, N., Yang, J., Xu, A., Abdel-Malek, Z. and Kadekaro, A. L. (2009). alpha-MSH activates immediate defense responses to UV-induced oxidative stress in human melanocytes. *Pigment Cell Melanoma Res* **22**, 809-18.
Spritz, R. A. (1998). Molecular genetics of the Hermansky-Pudlak and Chediak-Higashi syndromes. *Platelets* **9**, 21-9.
Stambolic, V., Suzuki, A., de la Pompa, J. L., Brothers, G. M., Mirtsos, C., Sasaki, T., Ruland, J., Penninger, J. M., Siderovski, D. P. and Mak, T. W. (1998). Negative regulation of PKB/Akt-dependent cell survival by the tumor suppressor PTEN. *Cell* **95**, 29-39.
Steingrimsson, E., Copeland, N. G. and Jenkins, N. A. (2005). Melanocyte stem cell maintenance and hair graying. *Cell* **121**, 9-12.
Steingrimsson, E., Copeland, N. G. and Jenkins, N. A. (2006). Mouse coat color mutations: from fancy mice to functional genomics. *Dev Dyn* **235**, 2401-11.
Stephen, R., Filipek, S., Palczewski, K. and Sousa, M. C. (2008). Ca2+ -dependent regulation of phototransduction. *Photochem Photobiol* **84**, 903-10.
Steventon, B., Carmona-Fontaine, C. and Mayor, R. (2005). Genetic network during neural crest induction: from cell specification to cell survival. *Semin Cell Dev Biol* **16**, 647-54.

Stokowski, R. P., Pant, P. V., Dadd, T., Fereday, A., Hinds, D. A., Jarman, C., Filsell, W., Ginger, R. S., Green, M. R., van der Ouderaa, F. J. et al. (2007). A genomewide association study of skin pigmentation in a South Asian population. *Am J Hum Genet* **81**, 1119-32.
Strauss, O. (2005). The retinal pigment epithelium in visual function. *Physiol Rev* **85**, 845-81.
Strom, M., Hume, A. N., Tarafder, A. K., Barkagianni, E. and Seabra, M. C. (2002). A family of Rab27-binding proteins. Melanophilin links Rab27a and myosin Va function in melanosome transport. *J Biol Chem* **277**, 25423-30.
Sturm, R. A. (2006). A golden age of human pigmentation genetics. *Trends Genet* **22**, 464-8.
Su, Y. H. and Vacquier, V. D. (2002). A flagellar K(+)-dependent Na(+)/Ca(2+) exchanger keeps Ca(2+) low in sea urchin spermatozoa. *Proc Natl Acad Sci U S A* **99**, 6743-8.
Szerencsei, R. T., Tucker, J. E., Cooper, C. B., Winkfein, R. J., Farrell, P. J., Iatrou, K. and Schnetkamp, P. P. (2000). Minimal domain requirement for cation transport by the potassium-dependent Na/Ca-K exchanger. Comparison with an NCKX paralog from Caenorhabditis elegans. *J Biol Chem* **275**, 669-76.
Tachibana, M. (2000). MITF: a stream flowing for pigment cells. *Pigment Cell Res* **13**, 230-40.
Tadjuidje, E. and Hollemann, T. (2006). Cholesterol homeostasis in development: the role of Xenopus 7-dehydrocholesterol reductase (Xdhcr7) in neural development. *Dev Dyn* **235**, 2095-110.
Tanaka, T. (2005). [International HapMap project]. *Nippon Rinsho* **63 Suppl 12**, 29-34.
Taneyhill, L. A. (2008). To adhere or not to adhere: the role of Cadherins in neural crest development. *Cell Adh Migr* **2**, 223-30.
Theos, A. C., Berson, J. F., Theos, S. C., Herman, K. E., Harper, D. C., Tenza, D., Sviderskaya, E. V., Lamoreux, M. L., Bennett, D. C., Raposo, G. et al. (2006). Dual loss of ER export and endocytic signals with altered melanosome morphology in the silver mutation of Pmel17. *Mol Biol Cell* **17**, 3598-612.
Thomas, A. J. and Erickson, C. A. (2008). The making of a melanocyte: the specification of melanoblasts from the neural crest. *Pigment Cell Melanoma Res* **21**, 598-610.
Thomas, G. (2002). Furin at the cutting edge: from protein traffic to embryogenesis and disease. *Nat Rev Mol Cell Biol* **3**, 753-66.
Tobin, D. J. (2008). Human hair pigmentation--biological aspects. *Int J Cosmet Sci* **30**, 233-57.
Tobin, D. J. (2009). Aging of the hair follicle pigmentation system. *Int J Trichology* **1**, 83-93.
Tobin, D. J. and Bystryn, J. C. (1996). Different populations of melanocytes are present in hair follicles and epidermis. *Pigment Cell Res* **9**, 304-10.
Tomlinson, M. L., Field, R. A. and Wheeler, G. N. (2005). Xenopus as a model organism in developmental chemical genetic screens. *Mol Biosyst* **1**, 223-8.
Tomlinson, M. L., Guan, P., Morris, R. J., Fidock, M. D., Rejzek, M., Garcia-Morales, C., Field, R. A. and Wheeler, G. N. (2009a). A chemical genomic approach identifies matrix metalloproteinases as playing an essential and specific role in Xenopus melanophore migration. *Chem Biol* **16**, 93-104.
Tomlinson, M. L., Rejzek, M., Fidock, M., Field, R. A. and Wheeler, G. N. (2009b). Chemical genomics identifies compounds affecting Xenopus laevis pigment cell development. *Mol Biosyst* **5**, 376-84.

Tsoi, M., Rhee, K. H., Bungard, D., Li, X. F., Lee, S. L., Auer, R. N. and Lytton, J. (1998). Molecular cloning of a novel potassium-dependent sodium-calcium exchanger from rat brain. *J Biol Chem* **273**, 4155-62.
Tully, G. (2007). Genotype versus phenotype: human pigmentation. *Forensic Sci Int Genet* **1**, 105-10.
Uong, A. and Zon, L. I. (2010). Melanocytes in development and cancer. *J Cell Physiol* **222**, 38-41.
Van Den Bossche, K., Naeyaert, J. M. and Lambert, J. (2006). The quest for the mechanism of melanin transfer. *Traffic* **7**, 769-78.
Vanoevelen, J., Dode, L., Raeymaekers, L., Wuytack, F. and Missiaen, L. (2007). Diseases involving the Golgi calcium pump. *Subcell Biochem* **45**, 385-404.
Viczian, A. S., Solessio, E. C., Lyou, Y. and Zuber, M. E. (2009). Generation of functional eyes from pluripotent cells. *PLoS Biol* **7**, e1000174.
Virador, V. M., Muller, J., Wu, X., Abdel-Malek, Z. A., Yu, Z. X., Ferrans, V. J., Kobayashi, N., Wakamatsu, K., Ito, S., Hammer, J. A. et al. (2002). Influence of alpha-melanocyte-stimulating hormone and ultraviolet radiation on the transfer of melanosomes to keratinocytes. *Faseb J* **16**, 105-7.
Vogel, P., Read, R. W., Vance, R. B., Platt, K. A., Troughton, K. and Rice, D. S. (2008). Ocular albinism and hypopigmentation defects in Slc24a5-/- mice. *Vet Pathol* **45**, 264-79.
Voisey, J., Gomez-Cabrera Mdel, C., Smit, D. J., Leonard, J. H., Sturm, R. A. and van Daal, A. (2006). A polymorphism in the agouti signalling protein (ASIP) is associated with decreased levels of mRNA. *Pigment Cell Res* **19**, 226-31.
Volloch, V., Schweitzer, B. and Rits, S. (1994). Ligation-mediated amplification of RNA from murine erythroid cells reveals a novel class of beta globin mRNA with an extended 5'-untranslated region. *Nucleic Acids Res* **22**, 2507-11.
Walters, Z. S., Haworth, K. E. and Latinkic, B. V. (2009). NKCC1 (SLC12a2) induces a secondary axis in Xenopus laevis embryos independently of its co-transporter function. *J Physiol* **587**, 521-9.
Wang, N. and Hebert, D. N. (2006). Tyrosinase maturation through the mammalian secretory pathway: bringing color to life. *Pigment Cell Res* **19**, 3-18.
Watabe, H., Valencia, J. C., Yasumoto, K., Kushimoto, T., Ando, H., Muller, J., Vieira, W. D., Mizoguchi, M., Appella, E. and Hearing, V. J. (2004). Regulation of tyrosinase processing and trafficking by organellar pH and by proteasome activity. *J Biol Chem* **279**, 7971-81.
Webel, R., Haug-Collet, K., Pearson, B., Szerencsei, R. T., Winkfein, R. J., Schnetkamp, P. P. and Colley, N. J. (2002). Potassium-dependent sodium-calcium exchange through the eye of the fly. *Ann N Y Acad Sci* **976**, 300-14.
Wehrle-Haller, B., Meller, M. and Weston, J. A. (2001). Analysis of melanocyte precursors in Nf1 mutants reveals that MGF/KIT signaling promotes directed cell migration independent of its function in cell survival. *Dev Biol* **232**, 471-83.
Wehrle-Haller, B. and Weston, J. A. (1995). Soluble and cell-bound forms of steel factor activity play distinct roles in melanocyte precursor dispersal and survival on the lateral neural crest migration pathway. *Development* **121**, 731-42.
Wehrle-Haller, B. and Weston, J. A. (1997). Receptor tyrosine kinase-dependent neural crest migration in response to differentially localized growth factors. *Bioessays* **19**, 337-45.
Weiner, L., Han, R., Scicchitano, B. M., Li, J., Hasegawa, K., Grossi, M., Lee, D. and Brissette, J. L. (2007). Dedicated epithelial recipient cells determine pigmentation patterns. *Cell* **130**, 932-42.

White, R. M., Cech, J., Ratanasirintrawoot, S., Lin, C. Y., Rahl, P. B., Burke, C. J., Langdon, E., Tomlinson, M. L., Mosher, J., Kaufman, C. et al. (2011). DHODH modulates transcriptional elongation in the neural crest and melanoma. *Nature* **471**, 518-22.
Williams, D. E., de Vries, P., Namen, A. E., Widmer, M. B. and Lyman, S. D. (1992). The Steel factor. *Dev Biol* **151**, 368-76.
Wilson S., S. M., Dadd T., Gunn D., Lim F-L., Ferdinando D., Abraham K. H., Askew S. E., Ginger R., Green M. R. (unpublished data). SLC24A5 / NCKX5 EXPRESSION IS REGULATED BY MC1R AND ALPHA-MSH AND ALTERS CHOLESTEROL HOMEOSTASIS IN NORMAL HUMAN MELANOCYTES (ed.: Unilever Discover.
Wilson, S. M., Yip, R., Swing, D. A., O'Sullivan, T. N., Zhang, Y., Novak, E. K., Swank, R. T., Russell, L. B., Copeland, N. G. and Jenkins, N. A. (2000). A mutation in Rab27a causes the vesicle transport defects observed in ashen mice. *Proc Natl Acad Sci U S A* **97**, 7933-8.
Winkfein, R. J., Pearson, B., Ward, R., Szerencsei, R. T., Colley, N. J. and Schnetkamp, P. P. (2004). Molecular characterization, functional expression and tissue distribution of a second NCKX Na+/Ca2+ -K+ exchanger from Drosophila. *Cell Calcium* **36**, 147-55.
Wu, H., Goel, V. and Haluska, F. G. (2003). PTEN signaling pathways in melanoma. *Oncogene* **22**, 3113-22.
Wu, M., Hemesath, T. J., Takemoto, C. M., Horstmann, M. A., Wells, A. G., Price, E. R., Fisher, D. Z. and Fisher, D. E. (2000). c-Kit triggers dual phosphorylations, which couple activation and degradation of the essential melanocyte factor Mi. *Genes Dev* **14**, 301-12.
Yamaguchi, Y. and Hearing, V. J. (2009). Physiological factors that regulate skin pigmentation. *Biofactors* **35**, 193-9.
Yamamoto, O. and Bhawan, J. (1994). Three modes of melanosome transfers in Caucasian facial skin: hypothesis based on an ultrastructural study. *Pigment Cell Res* **7**, 158-69.
Yasumoto, K., Takeda, K., Saito, H., Watanabe, K., Takahashi, K. and Shibahara, S. (2002). Microphthalmia-associated transcription factor interacts with LEF-1, a mediator of Wnt signaling. *EMBO J* **21**, 2703-14.
Zhou, L., Choi, H. Y., Li, W. P., Xu, F. and Herz, J. (2009). LRP1 controls cPLA2 phosphorylation, ABCA1 expression and cellular cholesterol export. *PLoS One* **4**, e6853.

www.pg.com

www.xenbase.org